

Heat and Mass Transfer*

James G. Knudsen, Ph.D., *Professor Emeritus of Chemical Engineering, Oregon State University; Member, American Institute of Chemical Engineers, American Chemical Society; Registered Professional Engineer (Oregon). (Conduction and Convection; Condensation, Boiling; Section Coeditor)*

Hoyt C. Hottel, S.M., *Professor Emeritus of Chemical Engineering, Massachusetts Institute of Technology; Member, National Academy of Sciences, American Academy of Arts and Sciences, American Institute of Chemical Engineers, American Chemical Society, Combustion Institute. (Radiation)*

Adel F. Sarofim, Sc.D., *Lamot du Pont Professor of Chemical Engineering and Assistant Director, Fuels Research Laboratory, Massachusetts Institute of Technology; Member, American Institute of Chemical Engineers, American Chemical Society, Combustion Institute. (Radiation)*

Phillip C. Wankat, Ph.D., *Professor of Chemical Engineering, Purdue University; Member, American Institute of Chemical Engineers, American Chemical Society, International Adsorption Society. (Mass Transfer Section Coeditor)*

Kent S. Knaebel, Ph.D., *President, Adsorption Research, Inc.; Member, American Institute of Chemical Engineers, American Chemical Society, International Adsorption Society, Professional Engineer (Ohio). (Mass Transfer Section Coeditor)*

HEAT TRANSFER

Modes of Heat Transfer 5-8

HEAT TRANSFER BY CONDUCTION

Fourier's Law 5-8
 Three-Dimensional Conduction Equation 5-8
 Thermal Conductivity 5-9
 Steady-State Conduction 5-9
 One-Dimensional Conduction 5-9
 Conduction through Several Bodies in Series 5-9
 Conduction through Several Bodies in Parallel 5-10
 Several Bodies in Series with Heat Generation 5-10
 Example 1. Steady-State Conduction with Heat Generation 5-10
 Two-Dimensional Conduction 5-10
 Unsteady-State Conduction 5-10
 One-Dimensional Conduction 5-10
 Two-Dimensional Conduction 5-11
 Conduction with Change of Phase 5-11

HEAT TRANSFER BY CONVECTION

Coefficient of Heat Transfer 5-12
 The Energy Equation 5-12
 Individual Coefficient of Heat Transfer 5-12
 Overall Coefficient of Heat Transfer 5-12
 Representation of Heat-Transfer Film Coefficients 5-12
 Natural Convection 5-12
 Nusselt Equation for Various Geometries 5-12
 Simplified Dimensional Equations 5-12
 Simultaneous Loss by Radiation 5-12
 Enclosed Spaces 5-12
 Forced Convection 5-14
 Analogy between Momentum and Heat Transfer 5-14
 Laminar Flow 5-15
 Transition Region 5-16
 Turbulent Flow 5-16
 Example 2. Calculation of f Factors in an Annulus 5-17
 Jackets and Coils of Agitated Vessels 5-19

* The contribution to the section on Interphase Mass Transfer of Mr. William M. Edwards (editor of Sec. 14), who was an author for the sixth edition, is acknowledged.

5-2 HEAT AND MASS TRANSFER

Nonnewtonian Fluids	5-19
Liquid Metals	5-19

HEAT TRANSFER WITH CHANGE OF PHASE

Condensation	5-20
Condensation Mechanisms	5-20
Condensation Coefficients	5-20
Boiling (Vaporization) of Liquids	5-22
Boiling Mechanisms	5-22
Boiling Coefficients	5-22

HEAT TRANSFER BY RADIATION

General References	5-23
Nomenclature for Radiative Transfer	5-23
Nature of Thermal Radiation	5-24
Blackbody Radiation	5-24
Radiative Exchange between Surfaces and Solids	5-25
Emissance and Absorptance	5-25
Black-Surface Enclosures	5-27
Example 3: Calculation of View Factor	5-29
Example 4: Calculation of Exchange Area	5-29
Non-Black Surface Enclosures	5-29
Example 5: Radiation in a Furnace Chamber	5-31
Emissivities of Combustion Products	5-32
Gaseous Combustion Products	5-33
Example 6: Calculation of Gas Emissivity and Absorptivity	5-34
Flames and Particle Clouds	5-35
Radiative Exchange between Gases or Suspended Matter and a Boundary	5-36
Example 7: Radiation in Gases	5-36
Single-Gas-Zone/Two-Surface-Zone Systems	5-37
The Effect of Nongrayness of Gas on Total-Exchange Area	5-37
Example 8: Effective Gas Emissivity	5-38
Treatment of Refractory Walls Partially Enclosing a Radiating Gas	5-39
Combustion Chamber Heat Transfer	5-40
Example 9: Radiation in a Furnace	5-41

MASS TRANSFER

General References	5-42
Introduction	5-42
Fick's First Law	5-42
Mutual Diffusivity, Mass Diffusivity, Interdiffusion Coefficient	5-46

Self Diffusivity	5-46
Tracer Diffusivity	5-46
Mass-Transfer Coefficient	5-46
Problem Solving Methods	5-46
Continuity and Flux Expressions	5-46
Material Balances	5-46
Flux Expressions: Simple Integrated Forms of Fick's First Law	5-47
Stefan-Maxwell Equations	5-47
Diffusivity Estimation—Gases	5-48
Binary Mixtures—Low Pressure—Nonpolar Components	5-48
Binary Mixtures—Low Pressure—Polar Components	5-49
Self-Diffusivity—High Pressure	5-49
Supercritical Mixtures	5-49
Low-Pressure/Multicomponent Mixtures	5-50
Diffusivity Estimation—Liquids	5-50
Stokes-Einstein and Free-Volume Theories	5-50
Dilute Binary Nonelectrolytes: General Mixtures	5-50
Binary Mixtures of Gases in Low-Viscosity, Nonelectrolyte Liquids	5-51
Dilute Binary Mixtures of a Nonelectrolyte in Water	5-52
Dilute Binary Hydrocarbon Mixtures	5-52
Dilute Binary Mixtures of Nonelectrolytes with Water as the Solvent	5-52
Dilute Dispersions of Macromolecules in Nonelectrolytes	5-52
Concentrated, Binary Mixtures of Nonelectrolytes	5-52
Binary Electrolyte Mixtures	5-53
Multicomponent Mixtures	5-54
Diffusion of Fluids in Porous Solids	5-54
Interphase Mass Transfer	5-54
Mass-Transfer Principles: Dilute Systems	5-54
Mass-Transfer Principles: Concentrated Systems	5-56
HTU (Height Equivalent to One Transfer Unit)	5-57
NTU (Number of Transfer Units)	5-57
Definitions of Mass-Transfer Coefficients \hat{k}_C and \hat{k}_L	5-57
Simplified Mass-Transfer Theories	5-57
Mass-Transfer Correlations	5-58
Effects of Total Pressure on \hat{k}_C and \hat{k}_L	5-61
Effects of Temperature on \hat{k}_C and \hat{k}_L	5-64
Effects of System Physical Properties on \hat{k}_C and \hat{k}_L	5-66
Effects of High Solute Concentrations on \hat{k}_C and \hat{k}_L	5-69
Influence of Chemical Reactions on \hat{k}_C and \hat{k}_L	5-69
Effective Interfacial Mass-Transfer Area a	5-74
Volumetric Mass-Transfer Coefficients \hat{K}_{Ca} and \hat{K}_{La}	5-78
Chilton-Colburn Analogy	5-79

Nomenclature and Units

Specialized heat transfer nomenclature used for radiative heat transfer is defined in the subsection "Heat Transmission by Radiation." Nomenclature for mass transfer is defined in the subsection "Mass Transfer."

Symbol	Definition	SI units	U.S. customary units
a	Proportionality coefficient	Dimensionless	Dimensionless
a_x	Cross-sectional area of a fin	m^2	ft^2
a'	Proportionality factor		
A	Area of heat transfer surface; A_i for inside; A_o for outside; A_m for mean; A_{avg} for average; A_1 , A_2 , and A_3 for points 1, 2, and 3 respectively; A_B for bare surface of finned tube; A_f for finned portion of tube; A_{of} for external area of unfinned portion of finned tube; A_{of} for external area of finned tube before fins are attached, equals A_o ; A_w for effective area of finned surface; A_T for total external area of finned tube; A_d for surface area of dirt (scale) deposit	m^2	ft^2
b	Proportionality coefficient		
b'	Proportionality factor		
b_f	Height of fin	m	ft
B	Material constant = $5D^{-0.5}$		
$c_1, c_2, \text{etc.}$	Constants of integration		
c, c_p	Specific heat at constant pressure; c_s for specific heat of solid; c_g for specific heat of gas	$J/(kg \cdot K)$	$Btu/(lb \cdot ^\circ F)$
C	Thermal conductance, equals kA/x , hA , or UA ; C_1 , C_2 , C_3 , C_n , thermal conductance of sections 1, 2, 3, and n respectively of a composite body	$J/(s \cdot K)$	$Btu/(h \cdot ^\circ F)$
C_r	Correlating constant; proportionality coefficient	Dimensionless	Dimensionless
d_m	Depth of divided solids bed	m	ft
D	Diameter; D_o for outside; D_i for inside; D_r for root diameter of finned tube	m	ft
D_c	Diameter of a coil or helix	m	ft
D_e	Equivalent diameter of a cross section, usually 4 times free area divided by wetted perimeter; D_w for equivalent diameter of window	m	ft
D_j	Diameter of a jacketed cylindrical vessel	m	ft
D_{ol}	Outside diameter of tube bundle	m	ft
D_p	Diameter of packing in a packed tube	m	ft
D_s	Inside diameter of heat-exchanger shell	m	ft
D_t	Solids-processing vessel diameter	m	ft
D_1, D_2	Diameter at points 1 and 2 respectively; inner and outer diameter of annulus respectively	m	ft
E_H	Eddy conductivity of heat	$J/(s \cdot m \cdot K)$	$Btu/(h \cdot ft \cdot ^\circ F)$
E_M	Eddy viscosity	Pa-s	$lb/(ft \cdot h)$
f	Fanning friction factor; f_1 for inner wall and f_2 for outer wall of annulus; f_i for ideal tube bank; skin friction drag coefficient	Dimensionless	Dimensionless
F	Entrance factors		
F_a	Dry solids feed rate	$kg/(s \cdot m^2)$	$lb/(h \cdot ft^2)$
F_g	Gas volumetric flow rate	$m^3 (s \cdot m^2 \text{ of bed area})$	$ft^3/(h \cdot ft^2 \text{ of bed area})$
F_c	Fraction of total tubes in cross-flow; F_{bp} for fraction of cross-flow area available for bypass flow		
F_t	Factor, ratio of temperature difference across tube-side film to overall mean temperature difference	Dimensionless	Dimensionless
F_s	Factor, ratio of temperature difference across shell-side film to overall mean temperature difference	Dimensionless	Dimensionless
F_w	Factor, ratio of temperature difference across retaining wall to overall mean temperature difference between bulk fluids	Dimensionless	Dimensionless
F_D	Factor, ratio of temperature difference across combined dirt or scale films to overall mean temperature difference between bulk fluids	Dimensionless	Dimensionless
F_T	Temperature-difference correction factor		
g, g_L	Acceleration due to gravity	$981 m/s^2$	$(4.18)(10^8) ft/h^2$
g_c	Conversion factor	$1.0 (kg \cdot m)/(N \cdot s^2)$	$(4.17)(10^8) (lb \cdot ft)/(lbf \cdot h^2)$
G	Mass velocity, equals $V\rho$ or W/S ; G_v for vapor mass velocity	$kg/(m^2 \cdot s)$	$lb/(h \cdot ft^2)$
G_{max}	Mass velocity through minimum free area between rows of tubes normal to the fluid stream	$kg/(m^2 \cdot s)$	$lb/(h \cdot ft^2)$
G_{mf}	Minimum fluidizing mass velocity	$kg/(m^2 \cdot s)$	$lb/(h \cdot ft^2)$
h	Local individual coefficient of heat transfer, equals $dq/(dA)(\Delta T)$	$J/(m^2 \cdot s \cdot K)$	$Btu/(h \cdot ft^2 \cdot ^\circ F)$
h_{am}, h_{lm}	Film coefficient based on arithmetic-mean temperature difference and logarithmic-mean temperature difference respectively	$J/(m^2 \cdot s \cdot K)$	$Btu/(h \cdot ft^2 \cdot ^\circ F)$
h_b	Film coefficient delivered at base of fin	$J/(m^2 \cdot s \cdot K)$	$Btu/(h \cdot ft^2 \cdot ^\circ F)$
h_{og}	Effective combined coefficient for simultaneous gas-vapor cooling and vapor condensation	$J/(m^2 \cdot s \cdot K)$	$Btu/(h \cdot ft^2 \cdot ^\circ F)$
$h_c + h_r$	Combined coefficient for conduction, convection, and radiation between surface and surroundings	$J/(m^2 \cdot s \cdot K)$	$Btu/(h \cdot ft^2 \cdot ^\circ F)$

5-4 HEAT AND MASS TRANSFER

Nomenclature and Units (Continued)

Symbol	Definition	SI units	U.S. customary units
h_{do}, h_{di}	Film coefficient for dirt or scale on outside or inside respectively of a surface	$J/(m^2 \cdot s \cdot K)$	Btu/(h-ft ² ·°F)
h_f	Film coefficient for finned-tube exchangers based on total external surface	$J/(m^2 \cdot s \cdot K)$	Btu/(h-ft ² ·°F)
h_{fi}	Effective outside film coefficient of a finned tube based on inside area	$J/(m^2 \cdot s \cdot K)$	Btu/(h-ft ² ·°F)
h_{fo}	Film coefficient for air film of an air-cooled finned-tube exchanger based on external bare surface	$J/(m^2 \cdot s \cdot K)$	Btu/(h-ft ² ·°F)
h_f, h_s	Effective film coefficient for dirt or scale on heat-transfer surface	$J/(m^2 \cdot s \cdot K)$	Btu/(h-ft ² ·°F)
h_i, h_o	Film coefficient for heat transfer for inside and outside surface respectively	$J/(m^2 \cdot s \cdot K)$	Btu/(h-ft ² ·°F)
h_k	Film coefficient for ideal tube bank; h_s for shell side of baffled exchanger; h_{sw} for coefficient at liquid-vapor interface	$J/(m^2 \cdot s \cdot K)$	Btu/(h-ft ² ·°F)
h_1	Condensing coefficient on top tube; h_N coefficient for N tubes in a vertical row	$J/(m^2 \cdot s \cdot K)$	Btu/(h-ft ² ·°F)
h'	Film coefficient for enclosed spaces	$J/(m^2 \cdot s \cdot K)$	Btu/(h-ft ² ·°F)
h_{lm}	Film coefficient based on log-mean temperature difference	$J/(m^2 \cdot s \cdot K)$	Btu/(h-ft ² ·°F)
h_r	Heat-transfer coefficient for radiation	$J/(m^2 \cdot s \cdot K)$	Btu/(h-ft ² ·°F)
h_T	Coefficient of total heat transfer by conduction, convection, and radiation between the surroundings and the surface of a body subject to unsteady-state heat transfer	$J/(m^2 \cdot s \cdot K)$	Btu/(h-ft ² ·°F)
h_w	Equivalent coefficient of retaining wall, equals k/x	$J/(m^2 \cdot s \cdot K)$	Btu/(h-ft ² ·°F)
j	Ordinate, Colburn j factor, equals $f/2$; j_H for heat transfer; j_{H1} for inner wall of annulus; j_{H2} for outer wall of annulus; j_k for heat transfer for ideal tube bank	Dimensionless	Dimensionless
J	Mechanical equivalent of heat	1.0(N·m)/J	778(ft·lbf)/Btu
J_b, J_c, J_l, J_r	Correction factors for baffle bypassing, baffle configuration, baffle leakage, and adverse temperature gradient respectively		
k	Thermal conductivity; k_1, k_2, k_3 , thermal conductivities of bodies 1, 2, and 3	$J/(m \cdot s \cdot K)$	(Btu-ft)/(h-ft ² ·°F)
k_v	Thermal conductivity of vapor; k_l for liquid thermal conductivity; k_s for thermal conductivity of solid	$J/(m \cdot s \cdot K)$	(Btu-ft)/(h-ft ² ·°F)
k_{avg}, k_m	Mean thermal conductivity	$J/(m \cdot s \cdot K)$	(Btu-ft)/(h-ft ² ·°F)
k_f	Thermal conductivity of fluid at film temperature	$J/(m \cdot s \cdot K)$	(Btu-ft)/(h-ft ² ·°F)
k_w	Thermal conductivity of retaining-wall material	$J/(m \cdot s \cdot K)$	(Btu-ft)/(h-ft ² ·°F)
K'	Property of non-Newtonian fluid		
l_c	Baffle cut; l_s for baffle spacing	m	ft
L	Length of heat-transfer surface	m	ft
L_o	Flow rate	kg/s	lb/h
L_u	Undisturbed length of path of fluid flow	m	ft
L_F	Thickness of dirt or scale deposit	m	ft
L_{fl}	Depth of fluidized bed	m	ft
L_p	Diameter of agitator blade	m	ft
m	Ratio, term, or exponent as defined where used		
M	Molecular weight	kg/mol	lb/mol
M	Weight of fluid	kg	lb
n	Position ratio or number	Dimensionless	Dimensionless
n_t	Number of tubes in parallel in a heat exchanger		
n_r	Number of rows in a vertical plane		
n'	Flow-behavior index for nonnewtonian fluids		
n_b	Number of baffle-type coils		
N_r	Speed of agitator	rad/s	r/h
N	Number of tubes in a vertical row; or number of tubes in a bundle; N_b for number of baffles; N_T for total number of tubes in exchanger; N_c for number of tubes in one cross-flow section; N_{ac} for number of cross-flow rows in each window		
N_B	Biot number, $h_T \Delta x/k$		
N_d	Proportionality coefficient, dimensionless group	Dimensionless	Dimensionless
N_{Gr}	Grashof number, $L^3 \rho^2 g \beta \Delta t / \mu^2$		
N_{Nu}	Nusselt number, hD/k or hL/k		
N_{Pe}	Peclet number, DGc/k		
N_{Pr}	Prandtl number, $c\mu/k$		
N_{Re}	Reynolds number, DG/μ		
N_{St}	Stanton number, $N_{Nu}/N_{Re}N_{Pr}$		
N_{ss}	Number of sealing strips		
p	Pressure	kPa	lbf/ft ² abs
p_f	Perimeter of a fin	m	ft
p, p'	Center-to-center spacing of tubes in tube bundle (tube pitch); p_n for tube pitch normal to flow; p_p for tube pitch parallel to flow	m	ft

Nomenclature and Units (Continued)

Symbol	Definition	SI units	U.S. customary units
Δp	Pressure of the vapor in a bubble minus saturation pressure of a flat liquid surface	kPa	lb/ft ² abs
P	Absolute pressure; P_c for critical pressure	kPa	lb/ft ²
P'	Spacing between adjacent baffles on shell side of a heat exchanger (baffle pitch)	m	ft
$\Delta P_{bk}, \Delta P_{uk}$	Pressure drop for ideal-tube-bank cross-flow and ideal window respectively; ΔP_s for shell side of baffled exchanger	kPa	lb/ft ²
q	Rate of heat flow, equals Q/θ	W, J/s	Btu/h
q'	Rate of heat generation	J/(s·m ³)	Btu/(h·ft ³)
$(q/A)_{\max}$	Maximum heat flux in nucleate boiling	J/(s·m ²)	Btu/(h·ft ²)
Q	Quantity of heat; rate of heat transfer	J/s	Btu/h
Q	Quantity of heat; Q_T for total quantity	J	Btu
r	Radius; cylindrical and spherical coordinate; distance from midplane to a point in a body; r_1 for inner wall of annulus; r_2 for outer wall of annulus; r_i for inside radius of tube; r_m for distance from midplane or center of a body to the exterior surface of the body	m	ft
r_j	Inside radius	Dimensionless	Dimensionless
R	Thermal resistance, equals x/kA , $1/UA$, $1/hA$; R_1 , R_2 , R_3 , R_n for thermal resistance of sections 1, 2, 3, and n of a composite body; R_T for sum of individual resistances of several resistances in series or parallel; R_{di} and R_{do} for dirt or scale resistance on inner and outer surface respectively	(s·K)/J	(h·°F)/Btu
R_j	Ratio of total outside surface of finned tube to area of tube having same root diameter		
S	Cross-sectional area; S_m for minimum cross-sectional area between rows of tubes, flow normal to tubes; S_{tb} for tube-to-baffle leakage area for one baffle; S_{db} for shell-to-baffle area for one baffle; S_w for area for flow through window; S_{wg} for gross window area; S_{wt} for window area occupied by tubes	m ²	ft ²
S_r	Slope of rotary shell		
s	Specific gravity of fluid referred to liquid water		
t	Bulk temperature; temperature at a given point in a body at time θ	K	°F
t_1, t_2, t_n	Temperature at points 1, 2, and n in a system through which heat is being transferred	K	°F
t'	Temperature of surroundings	K	°F
t'_1, t'_2	Inlet and outlet temperature respectively of hotter fluid	K	°F
t''_1, t''_2	Inlet and outlet temperature respectively of colder fluid	K	°F
t_b	Initial uniform bulk temperature of a body; bulk temperature of a flowing fluid	K	°F
t_H, t_L	High and low temperature respectively on tube side of a heat exchanger	K	°F
t_s	Surface temperature	K	°F
t_w	Saturated-vapor temperature	K	°F
t_w	Wall temperature	K	°F
t_∞	Temperature of undisturbed flowing stream	K	°F
T_H, T_L	High and low temperature respectively on shell side of a heat exchanger	K	°F
T	Absolute temperature; T_b for bulk temperature; T_w for wall temperature; T_v for vapor temperature; T_c for coolant temperature; T_e for temperature of emitter; T_r for temperature of receiver	K	°R
$\Delta T, \Delta t$	Temperature difference; Δt_1 , Δt_2 , and Δt_3 temperature difference across bodies 1, 2, and 3 or at points 1, 2, and 3; ΔT_{ov} , ΔT_o for overall temperature difference; Δt_b for temperature difference between surface and boiling liquid	K	°F, °R
$\Delta t_{am}, \Delta t_{lm}$	Arithmetic- and logarithmic-mean temperature difference respectively	K	°F
Δt_{em}	Mean effective overall temperature difference	K	°F
$\Delta T_H, \Delta t_H$	Greater terminal temperature difference	K	°F
$\Delta T_L, \Delta t_L$	Lesser terminal temperature difference	K	°F
$\Delta T_m, \Delta t_m$	Mean temperature difference	K	°F
u	Velocity in x direction	m/s	ft/h
u°	Friction velocity	m/s	ft/h
U	Overall coefficient of heat transfer; U_o for outside surface basis; U' for overall coefficient between liquid-vapor interface and coolant	J/(s·m ² ·K)	Btu/(h·ft ² ·°F)
U_1, U_2	Overall coefficient of heat transfer at points 1 and 2 respectively	J/(s·m ² ·K)	Btu/(h·ft ² ·°F)
$U_{co}, U_{cc}, U_{ct}, U_{ra}$	Overall coefficients for divided solids processing by conduction, convection, contact, and radiation mechanism respectively	J/(s·m ² ·K)	Btu/(h·ft ² ·°F)
U_m	Mean overall coefficient of heat transfer	J/(s·m ² ·K)	Btu/(h·ft ² ·°F)
v	Velocity in y direction	m/s	ft/h
V_r	Volume of rotating shell	m ³	ft ³

Nomenclature and Units (Concluded)

Symbol	Definition	SI units	U.S. customary units
V	Velocity	m/s	ft/h
V', V_s	Velocity	m/s	ft/s
V_F	Face velocity of a fluid approaching a bank of finned tubes	m/s	ft/h
V_g, V_l	Specific volume of gas, liquid	m ³ /kg	ft ³ /lb
V'_{max}	Maximum velocity through minimum free area between rows of tubes normal to the fluid stream	m/s	ft/h
w	Velocity in z direction	m/s	ft/h
w	Flow rate	kg/s	lb/h
W	Total mass rate of flow; mass rate of vapor generated; W_f for total rate of vapor condensation in one tube	kg/s	lb/h
W_f	Weight rate of flow	kg/(s·tube)	lb/(h·tube)
W_1, W_o	Total mass rate of flow on tube side and shell side respectively of a heat exchanger	kg/s	lb/h
x_q	Vapor quality, x_i for inlet quality, x_o for outlet quality	kg/s	lb/h
x	Coordinate direction; length of conduction path; x for thickness of scale; $x_1, x_2,$ and x_3 at positions 1, 2, and 3 in a body through which heat is being transferred	m	ft
X	Factor	Dimensionless	Dimensionless
y	Coordinate direction	m	ft
y^+	Wall distance	Dimensionless	Dimensionless
Y	Factor	Dimensionless	Dimensionless
Z	Coordinate direction	m	ft
z_p	Distance (perimeter) traveled by fluid across fin	m	ft
Z_H	Ratio of sensible heat removed from vapor to total heat transferred	Dimensionless	Dimensionless
Greek symbols			
α	Thermal diffusivity, equals $k/\rho c$; α_e for effective thermal diffusivity of powdered solids	m ² /s	ft ² /h
β	Volumetric coefficient of thermal expansion	K ⁻¹	°F ⁻¹
β'	Contact angle of a bubble	°	°
γ	Fluid consistency	kg/(s ^{3-n'} ·m)	lb/(ft·s ^{2-n'})
Γ	Mass rate of flow of a falling film from a tube or surface per unit perimeter, equals $w/\pi D$ for vertical tube, $w/2L$ for horizontal tube	kg/(s·m)	lb/(h·ft)
δ_s	Correction factor, ratio of nonnewtonian to newtonian shear rates		
δ	Cell width	m	ft
δ_{db}	Diametral shell-to-baffle clearance	m	ft
ϵ	Eddy diffusivity; ϵ_M for eddy diffusivity of momentum; ϵ_H for eddy diffusivity of heat	m ² /s	ft ² /h
ϵ_v	Fraction of voids in porous bed		
η	Fluidization efficiency		
θ	Time	s	h
θ_b	Baffle cut		
λ	Latent heat (enthalpy) of vaporization (condensation)	J/kg	Btu/lb
λ_m	Radius of maximum velocity	m	ft
μ	Viscosity; μ_w for viscosity at wall temperature; μ_b for viscosity at bulk temperature; μ_f for viscosity at film temperature; $\mu_G, \mu_g,$ and μ_v for viscosity of gas or vapor; μ_L, μ_l for viscosity of liquid; μ_w for viscosity at wall; μ_i for viscosity of fluid at inner wall of annulus	Pa·s	lb/(h·ft)
ν	Kinematic viscosity	m ² /s	ft ² /h
ρ	Density; ρ_L, ρ_l for density of liquid; ρ_G, ρ_g, ρ_v for density of gas or vapor; ρ_s for density of solid	kg/m ³	lb/ft ³
σ	Surface tension between a liquid and its vapor	N/m	lb/ft
Σ	Term indicating summation of variables		
τ	Shear stress τ_w for shear stress at the wall	N/m ²	lb/ft ²
ϕ	Velocity-potential function		
ϕ_p	Particle sphericity		
Φ	Viscous-dissipation function		
ω	Angle of repose of powdered solid	rad	rad
Ω	Fin efficiency	Dimensionless	Dimensionless

GENERAL REFERENCES: Becker, *Heat Transfer*, Plenum, New York, 1986. Bejan, *Convection Heat Transfer*, Wiley, New York, 1984. Bird, Stewart, and Lightfoot, *Transport Phenomena*, Wiley, New York, 1960. Carslaw and Jaeger, *Conduction of Heat in Solids*, Clarendon Press, Oxford, 1959. Chapman, *Heat Transfer*, 2d ed., Macmillan, New York, 1967. Drew and Hoopes, *Advances in Chemical Engineering*, Academic, New York, vol. 1, 1956; vol. 2, 1958; vol. 5, 1964; vol. 6, 1966; vol. 7, 1968. Dusinberre, *Heat Transfer Calculations by Finite Differences*, International Textbook, Scranton, Pa., 1961. Eckert and Drake, *Heat and Mass Transfer*, 2d ed., McGraw-Hill, New York, 1959. Gebhart, *Heat Transfer*, McGraw-Hill, New York, 1961. Irvine and Hartnett, *Advances in Heat Transfer*, Academic, New York, vol. 2, 1965; vol. 3, 1966. Grigull and Sandner, *Heat Conduction*, Hemisphere Publishing, 1984. Jakob, *Heat Transfer*, Wiley, New York, vol. 1, 1949; vol. 2, 1957. Jakob and Hawkins, *Elements of Heat Transfer*, 3d ed., Wiley, New York, 1957. Kakac, Bergles, and Mayinger, *Heat Exchangers: Thermal Hydraulic Fundamentals and Design*, Hemisphere Publishing, Washington, 1981. Kakac and Yener, *Convective Heat Transfer*, Hemisphere Publishing, Washington, 1980. Kay, *An Introduction to Fluid Mechanics and Heat Transfer*, 2d ed., Cambridge University Press, Cambridge, England, 1963. Kays, *Convective Heat and Mass Transfer*, McGraw-Hill, New York, 1966. Kays and London, *Compact Heat Exchangers*, 3d ed., McGraw-Hill, New York, 1984. Kern, *Process Heat Transfer*, McGraw-Hill, New York, 1950. Knudsen and Katz, *Fluid Dynamics and Heat Transfer*, McGraw-Hill, New York, 1958. Kraus, *Analysis and Evaluation of Extended Surface Thermal Systems*, Hemisphere Publishing, Washington, 1982. Kutateladze, *A Concise Encyclopedia of Heat Transfer*, 1st English ed., Pergamon, New York, 1966. Lykov, *Heat and Mass Transfer in Capillary Porous Bodies*, translated from Russian, Pergamon, New York, 1966. McAdams, *Heat Transmission*, 3d ed., McGraw-Hill, New York, 1954. Mickle, Sherwood, and Reed, *Applied Mathematics in Chemical Engineering*, 2d ed., McGraw-Hill, New York, 1957. Rohsenow and Choi, *Heat, Mass, and Momentum Transfer*, Prentice-Hall, Englewood Cliffs, N.J., 1961. Schlinder (ed.), *Heat Exchanger Design Handbook*, Hemisphere Publishing, Washington, 1983 (Book 2; Chapter 2.4 [Conduction], Chapter 2.5 [Convection], Chapter 2.6 [Condensation], Chapter 2.7 [Boiling]). Skelland, *Non-Newtonian Flow and Heat Transfer*, Wiley, New York, 1967. Taborek and Bell, *Process Heat Exchanger Design*, Hemisphere Publishing, Washington, 1984. Taborek, Hewitt, and Afghan, *Heat Exchangers: Theory and Practice*, Hemisphere Publishing, Washington, 1983. TSederberg, *Thermal Conductivity of Liquids and Gases*, M.I.T., Cambridge, Mass., 1965. Welty, Wicks, and Wilson, *Fundamentals of Momentum, Heat and Mass Transfer*, 3d ed., Wiley, New York, 1984. Zenz and Othmer, *Fluidization and Fluid Particle Systems*, Reinhold, New York, 1960.

REFERENCES FOR DIFFUSIVITIES

1. Akita, *Ind. Eng. Chem. Fundam.*, **10**, 89 (1981).
2. Asfour and Dullien, *Chem. Eng. Sci.*, **41**, 1891 (1986).
3. Blanc, *J. Phys.*, **7**, 825 (1908).
4. Brokaw, *Ind. Eng. Chem. Process Des. and Dev.*, **8**, 2, 240 (1969).
5. Caldwell and Babb, *J. Phys. Chem.*, **60**, 51 (1956).
6. Catchpole and King, *Ind. Eng. Chem. Res.*, **33**, 1828 (1994).
7. Chen and Chen, *Chem. Eng. Sci.*, **40**, 1735 (1985).
8. Chung, Ajlan, Lee and Starling, *Ind. Eng. Chem. Res.*, **27**, 671 (1988).
9. Condon and Craven, *Aust. J. Chem.*, **25**, 695 (1972).
10. Cullinan, *AIChE J.*, **31**, 1740–1741 (1985).
11. Cullinan, *Can. J. Chem. Eng.*, **45**, 377–381 (1967).
12. Cussler, *AIChE J.*, **26**, 1 (1980).
13. Darken, *Trans. Am. Inst. Mining Met. Eng.*, **175**, 184 (1948).
14. Debenedetti and Reid, *AIChE J.*, **32**, 2034 (1986); see errata: *AIChE J.*, **33**, 496 (1987).
15. Elliott, R. W. and H. Watts, *Can. J. Chem.*, **50**, 31 (1972).
16. Erkey and Akgerman, *AIChE J.*, **35**, 443 (1989).
17. Ertl, Ghai, and Dullien, *AIChE J.*, **20**, 1, 1 (1974).
18. Fairbanks and Wilke, *Ind. Eng. Chem.*, **42**, 471 (1950).
19. Fuller, Schettler and Giddings, *Ind. Eng. Chem.*, **58**, 18 (1966).
20. Ghai, Ertl, and Dullien, *AIChE J.*, **19**, 5, 881 (1973).
21. Gordon, *J. Chem. Phys.*, **5**, 522 (1937).
22. Graham and Dranooff, *Ind. Eng. Chem. Fundam.*, **21**, 360–365 (1982).
23. Graham and Dranooff, *Ind. Eng. Chem. Fundam.*, **21**, 365–369 (1982).
24. Gurkan, *AIChE J.*, **33**, 175–176 (1987).
25. Hayduk and Laudie, *AIChE J.*, **20**, 3, 611 (1974).
26. Hayduk and Minhas, *Can. J. Chem. Eng.*, **60**, 195 (1982).
27. Hildebrand, *Science*, **174**, 490 (1971).
28. Hiss and Cussler, *AIChE J.*, **19**, 4, 698 (1973).
29. Jossi, Stiel, and Thodos, *AIChE J.*, **8**, 59 (1962).
30. Krishnamurthy and Taylor, *Chem. Eng. J.*, **25**, 47 (1982).

31. Lee and Thodos, *Ind. Eng. Chem. Fundam.*, **22**, 17–26 (1983).
32. Lee and Thodos, *Ind. Eng. Chem. Res.*, **27**, 992–997 (1988).
33. Lees and Sarraz, *J. Chem. Eng. Data*, **16**, 1, 41 (1971).
34. Leffler and Cullinan, *Ind. Eng. Chem. Fundam.*, **9**, 84, 88 (1970).
35. Lugg, *Anal. Chem.*, **40**, 1072 (1968).
36. Marrero and Mason, *AIChE J.*, **19**, 498 (1973).
37. Mathur and Thodos, *AIChE J.*, **11**, 613 (1965).
38. Matthews and Akgerman, *AIChE J.*, **33**, 881 (1987).
39. Matthews, Rodden and Akgerman, *J. Chem. Eng. Data*, **32**, 317 (1987).
40. Olander, *AIChE J.*, **7**, 175 (1961).
41. Passut and Danner, *Chem. Eng. Prog. Symp. Ser.*, **140**, 30 (1974).
42. Perkins and Geankoplis, *Chem. Eng. Sci.*, **24**, 1035–1042 (1969).
43. Pinto and Graham, *AIChE J.*, **32**, 291 (1986).
44. Pinto and Graham, *AIChE J.*, **33**, 436 (1987).
45. Quale, *Chem. Rev.*, **53**, 439 (1953).
46. Rathbun and Babb, *Ind. Eng. Chem. Proc. Des. Dev.*, **5**, 273 (1966).
47. Reddy and Doraiswamy, *Ind. Eng. Chem. Fundam.*, **6**, 77 (1967).
48. Riazi and Whitson, *Ind. Eng. Chem. Res.*, **32**, 3081 (1993).
49. Robinson, Edmister, and Dullien, *Ind. Eng. Chem. Fundam.*, **5**, 75 (1966).
50. Rollins and Knaebel, *AIChE J.*, **37**, 470 (1991).
51. Siddiqi, Krahn, and Lucas, *J. Chem. Eng. Data*, **32**, 48 (1987).
52. Siddiqi and Lucas, *Can. J. Chem. Eng.*, **64**, 839 (1986).
53. Smith and Taylor, *Ind. Eng. Chem. Fundam.*, **22**, 97 (1983).
54. Sridhar and Potter, *AIChE J.*, **23**, 4, 590 (1977).
55. Stiel and Thodos, *AIChE J.*, **7**, 234 (1961).
56. Sun and Chen, *Ind. Eng. Chem. Res.*, **26**, 815 (1987).
57. Tanford, *Phys. Chem. of Macromolecule*, Wiley, New York, NY (1961).
58. Taylor and Webb, *Comput. Chem. Eng.*, **5**, 61 (1981).
59. Tyn and Calus, *J. Chem. Eng. Data*, **20**, 310 (1975).
60. Úmesi and Danner, *Ind. Eng. Chem. Process Des. Dev.*, **20**, 662 (1981).
61. Van Geet and Adamson, *J. Phys. Chem.*, **68**, 2, 238 (1964).
62. Vignes, *Ind. Eng. Chem. Fundam.*, **5**, 184 (1966).
63. Wilke, *Chem. Eng. Prog.*, **46**, 2, 95 (1950).
64. Wilke and Chang, *AIChE J.*, **1**, 164 (1955).
65. Wilke and Lee, *Ind. Eng. Chem.*, **47**, 1253 (1955).

REFERENCES FOR DIFFUSIVITIES IN POROUS SOLIDS, TABLE 5-20

66. Ruthven, *Principles of Adsorption & Adsorption Processes*, Wiley, 1984.
67. Satterfield, *Mass Transfer in Heterogeneous Catalysis*, MIT Press, 1970.
68. Suzuki, *Adsorption Engineering*, Kodansha—Elsevier, 1990.
69. Yang, *Gas Separation by Adsorption Processes*, Butterworths, 1987.

REFERENCES FOR TABLES 5-21 TO 5-28

70. Bahmanyar, Chang-Kakoti, Garro, Liang, and Slater, *Chem. Engr. Rsch. Des.*, **68**, 74 (1990).
71. Beenackers and van Swaaij, *Chem. Engr. Sci.*, **48**, 3109 (1993).
72. Bird, Stewart and Lightfoot, *Transport Phenomena*, Wiley, 1960.
73. Blatt, Dravid, Michaels, and Nelson in Flinn (ed.), *Membrane Science and Technology*, **47**, Plenum, 1970.
74. Bolles and Fair, *Institution Chem. Eng. Symp. Ser.*, **56**, 3/35 (1979).
75. Bolles and Fair, *Chem. Eng.*, **89**(14), 109 (July 12, 1982).
76. Bravo and Fair, *Ind. Eng. Chem. Process Des. Dev.*, **21**, 162 (1982).
77. Bravo, Rocha and Fair, *Hydrocarbon Processing*, 91 (Jan. 1985).
78. Brian and Hales, *AIChE J.*, **15**, 419 (1969).
79. Calderbank and Moo-Young, *Chem. Eng. Sci.*, **16**, 39 (1961).
80. Chilton and Colburn, *Ind. Eng. Chem.*, **26**, 1183 (1934).
81. Cornell, Knapp, and Fair, *Chem. Engr. Prog.*, **56**(7), 68 (1960).
82. Cornet and Kaloo, *Proc. 3rd Int'l. Congr. Metallic Corrosion—Moscow*, **3**, 83 (1966).
83. Cussler, *Diffusion: Mass Transfer in Fluid Systems*, Cambridge, 1984.
84. Dividedi and Upadhyay, *Ind. Eng. Chem. Process Des. Develop.*, **16**, 1657 (1977).
85. Eisenberg, Tobias, and Wilke, *Chem. Engr. Prog. Symp. Sec.*, **51**(16), 1 (1955).
86. Elzinga and Banchemo, *Chem. Engr. Progr. Symp. Ser.*, **55**(29), 149 (1959).
87. Fair, "Distillation" in Rousseau (ed.), *Handbook of Separation Process Technology*, Wiley, 1987.
88. Faust, Wenzel, Clump, Maus, and Andersen, *Principles of Unit Operations*, 2d ed., Wiley, 1980.
89. Frossling, *Gerlands Beitr. Geophys.*, **52**, 170 (1938).
90. Garner and Suckling, *AIChE J.*, **4**, 114 (1958).
91. Geankoplis, *Transport Processes and Unit Operations*, 3d ed., Prentice Hall, 1993.

92. Gibilaro, Davies, Cooke, Lynch, and Middleton, *Chem. Engr. Sci.*, **40**, 1811 (1985).
93. Gilliland and Sherwood, *Ind. Engr. Chem.*, **26**, 516 (1934).
94. Griffith, *Chem. Engr. Sci.*, **12**, 198 (1960).
95. Gupta and Thodos, *AIChE J.*, **9**, 751 (1963).
96. Gupta and Thodos, *Ind. Eng. Chem. Fundam.*, **3**, 218 (1964).
97. Harriott, *AIChE J.*, **8**, 93 (1962).
98. Hausen, *Verfahrenstech. Beih. Z. Ver. Dtsch. Ing.*, **4**, 91 (1943).
99. Heertjes, Holve, and Talsma, *Chem. Engr. Sci.*, **3**, 122 (1954).
100. Hines and Maddox, *Mass Transfer: Fundamentals and Applications*, Prentice Hall, 1985.
101. Hsiung and Thodos, *Int. J. Heat Mass Transfer*, **20**, 331 (1977).
102. Hsu, Sato, and Sage, *Ind. Engr. Chem.*, **46**, 870 (1954).
103. Hughmark, *Ind. Eng. Chem. Fundam.*, **6**, 408 (1967).
104. Johnson, Besic, and Hamielec, *Can. J. Chem. Engr.*, **47**, 559 (1969).
105. Johnstone and Pigford, *Trans. AIChE*, **38**, 25 (1942).
106. Kafesjian, Plank, and Gerhard, *AIChE J.*, **7**, 463 (1961).
107. Kelly and Swenson, *Chem. Engr. Prog.*, **52**, 263 (1956).
108. King, *Separation Processes*, 2d ed., McGraw-Hill (1980).
109. Kirwan, "Mass Transfer Principles" in Rousseau, *Handbook of Separation Process Technology*, Wiley, 1987.
110. Klein, Ward, and Lacey, "Membrane Processes—Dialysis and Electro-Dialysis" in Rousseau, *Handbook of Separation Process Technology*, Wiley, 1987.
111. Kohl, "Absorption and Stripping" in Rousseau, *Handbook of Separation Process Technology*, Wiley, 1987.
112. Kojima, Uchida, Ohsawa, and Iguchi, *J. Chem. Engrg. Japan*, **20**, 104 (1987).
113. Koloimi, Sopic, and Zumer, *Chem. Engr. Sci.*, **32**, 637 (1977).
114. Lee, *Biochemical Engineering*, Prentice Hall, 1992.
115. Lee and Foster, *Appl. Catal.*, **63**, 1 (1990).
116. Lee and Holder, *Ind. Engr. Chem. Res.*, **34**, 906 (1995).
117. Levich, *Physicochemical Hydrodynamics*, Prentice Hall, 1962.
118. Levins and Gastonbury, *Trans. Inst. Chem. Engr.*, **50**, 32, 132 (1972).
119. Lim, Holder, and Shah, *J. Supercrit. Fluids*, **3**, 186 (1990).
120. Linton and Sherwood, *Chem. Engr. Prog.*, **46**, 258 (1950).
121. Ludwig, *Applied Process Design for Chemical and Petrochemical Plants*, 2d ed., vol. 2, Gulf Pub. Co., 1977.
122. McCabe, Smith, and Harriott, *Unit Operations of Chemical Engineering*, 5th ed., McGraw-Hill, 1993.
123. Nelson and Galloway, *Chem. Engr. Sci.*, **30**, 7 (1975).
124. Nottter and Sleichner, *Chem. Eng. Sci.*, **26**, 161 (1971).
125. Ohashi, Sugawara, Kikuchi, and Konno, *J. Chem. Engr. Japan*, **14**, 433 (1981).
126. Onda, Takeuchi, and Okumoto, *J. Chem. Engr. Japan*, **1**, 56 (1968).
127. Pasternak and Gauvin, *AIChE J.*, **7**, 254 (1961).
128. Pasternak and Gauvin, *Can. J. Chem. Engr.*, **38**, 35 (April 1960).
129. Perez and Sandall, *AIChE J.*, **20**, 770 (1974).
130. Petrovic and Thodos, *Ind. Eng. Chem. Fundam.*, **7**, 274 (1968).
131. Pinczewski and Sideman, *Chem. Engr. Sci.*, **29**, 1969 (1974).
132. Prandtl, *Phys. Zeit.*, **29**, 487 (1928).
133. Prasad and Sirkar, *AIChE J.*, **34**, 177 (1988).
134. Rahman and Streat, *Chem. Engr. Sci.*, **36**, 293 (1981).
135. Ranz and Marshall, *Chem. Engr. Prog.*, **48**, 141, 173 (1952).
136. Reiss, *Ind. Eng. Chem. Process Des. Develop.*, **6**, 486 (1967).
137. Riet, *Ind. Eng. Chem. Process Des. Dev.*, **18**, 357 (1979).
138. Rowe, *Chem. Engr. Sci.*, **30**, 7 (1975).
139. Rowe, Claxton, and Lewis, *Trans. Inst. Chem. Engr. London*, **43**, 14 (1965).
140. Ruckenstein and Rajagopalan, *Chem. Engr. Commun.*, **4**, 15 (1980).
141. Ruthven, *Principles of Adsorption & Adsorption Processes*, Wiley, 1984.
142. Satterfield, *AIChE J.*, **21**, 209 (1975).
143. Schluter and Deckwer, *Chem. Engr. Sci.*, **47**, 2357 (1992).
144. Schmitz, Steiff, and Weinspach, *Chem. Engrg. Technol.*, **10**, 204 (1987).
145. Sherwood, Brian, Fisher, and Dresner, *Ind. Eng. Chem. Fundam.*, **4**, 113 (1965).
146. Sherwood, Pigford, and Wilke, *Mass Transfer*, McGraw-Hill, 1975.
147. Shulman, Ullich, Proulx, and Zimmerman, *AIChE J.*, **1**, 253 (1955).
148. Shulman and Margolis, *AIChE J.*, **3**, 157 (1957).
149. Siegel, Sparrow, and Hallman, *Appl. Sci. Res. Sec. A.*, **7**, 386 (1958).
150. Sissom and Pitts, *Elements of Transport Phenomena*, McGraw-Hill, 1972.
151. Skelland, *Diffusional Mass Transfer*, Wiley (1974).
152. Skelland and Cornish, *AIChE J.*, **9**, 73 (1963).
153. Skelland and Moeti, *Ind. Eng. Chem. Res.*, **29**, 2258 (1990).
154. Skelland and Tedder, "Extraction—Organic Chemicals Processing" in Rousseau, *Handbook of Separation Process Technology*, Wiley, 1987, pp. 405–466.
155. Skelland and Wellek, *AIChE J.*, **10**, 491, 789 (1964).
156. Slater, "Rate Coefficients in Liquid-Liquid Extraction Systems" in Godfrey and Slater, *Liquid-Liquid Extraction Equipment*, Wiley, 1994, pp. 45–94.
157. Steinberger and Treybal, *AIChE J.*, **6**, 227 (1960).
158. Steiner, L., *Chem. Eng. Sci.*, **41**, 1979 (1986).
159. Taylor and Krishna, *Multicomponent Mass Transfer*, Wiley, 1993.
160. Tourmie, Laguerie, and Couderc, *Chem. Engr. Sci.*, **34**, 1247 (1979).
161. Treybal, *Mass Transfer Operations*, 3d ed., McGraw-Hill, 1980.
162. Von Karman, *Trans. ASME*, **61**, 705 (1939).
163. Wakao and Funazkri, *Chem. Engr. Sci.*, **33**, 1375 (1978).
164. Wankat, *Equilibrium-Stage Separations*, Prentice Hall, 1988.
165. Wankat, *Rate-Controlled Separations*, Chapman-Hall, 1990.
166. Wilson and Geankoplis, *Ind. Eng. Chem. Fundam.*, **5**, 9 (1966).
167. Yagi and Yoshida, *Ind. Eng. Chem. Process Des. Dev.*, **14**, 488 (1975).
168. Yang, *Gas Separation by Adsorption Processes*, Butterworths, 1987.
169. Yoshida, Ramaswami, and Hougen, *AIChE J.*, **8**, 5 (1962).

HEAT TRANSFER

MODES OF HEAT TRANSFER

There are three fundamental types of heat transfer: conduction, convection, and radiation. All three types may occur at the same time, and it is advisable to consider the heat transfer by each type in any particular case.

Conduction is the transfer of heat from one part of a body to another part of the same body, or from one body to another in physical contact with it, without appreciable displacement of the particles of the body.

Convection is the transfer of heat from one point to another within a fluid, gas, or liquid by the mixing of one portion of the fluid with another. In natural convection, the motion of the fluid is entirely the result of differences in density resulting from temperature differences; in forced convection, the motion is produced by mechanical means. When the forced velocity is relatively low, it should be realized that "free-convection" factors, such as density and temperature difference, may have an important influence.

Radiation is the transfer of heat from one body to another, not in contact with it, by means of wave motion through space.

HEAT TRANSFER BY CONDUCTION

FOURIER'S LAW

Fourier's law is the fundamental differential equation for heat transfer by conduction:

$$dQ/d\theta = -kA(dt/dx) \quad (5-1)$$

where $dQ/d\theta$ (quantity per unit time) is the rate of flow of heat, A is the area at right angles to the direction in which the heat flows, and $-dt/dx$ is the rate of change of temperature with the distance in the

direction of the flow of heat, i.e., the temperature gradient. The factor k is called the thermal conductivity; it is a characteristic property of the material through which the heat is flowing and varies with temperature.

THREE-DIMENSIONAL CONDUCTION EQUATION

Equation (5-1) is used as a basis for derivation of the unsteady-state three-dimensional energy equation for **solids or static fluids**:

$$c\rho \frac{\partial t}{\partial \theta} = \frac{\partial}{\partial x} \left(k \frac{\partial t}{\partial x} \right) + \frac{\partial}{\partial y} \left(k \frac{\partial t}{\partial y} \right) + \frac{\partial}{\partial z} \left(k \frac{\partial t}{\partial z} \right) + q' \quad (5-2)$$

where x, y, z are distances in the rectangular coordinate system and q' is the rate of heat generation (by chemical reaction, nuclear reaction, or electric current) in the solid per unit of volume. Solution of Eq. (5-2) with appropriate boundary and initial conditions will give the temperature as a function of time and location in the material. Equation (5-2) may be transformed into spherical or cylindrical coordinates to conform more closely to the physical shape of the system.

THERMAL CONDUCTIVITY

Thermal conductivity varies with temperature but not always in the same direction. The thermal conductivities for many materials, as a function of temperature, are given in Sec. 2. Additional and more comprehensive information may often be obtained from suppliers of the materials. Impurities, especially in metals, can give rise to variations in thermal conductivity of from 50 to 75 percent. In using thermal conductivities, engineers should remember that conduction is not the sole method of transferring heat and that, particularly with liquids and gases, radiation and convection may be much more important.

The thermal conductivity at a given temperature is a function of the apparent, or bulk, density. Thus, at 0°C (32°F), k for asbestos wool is 0.09 J/(m·s·K) [0.052 Btu/(hr·ft·°F)] when the bulk density is 400 kg/m³ (24.9 lb/ft³) and is 0.19 (0.111) for a density of 700 (43.6).

In determining the apparent thermal conductivities of **granular solids**, such as granulated cork or charcoal grains, Griffiths (Spec. Rep. 5, Food Investigation Board, H. M. Stationery Office, 1921) found that air circulates within the mass of granular solid. Under a certain set of conditions, the apparent thermal conductivity of a charcoal was 9 percent greater when the test section was vertical than when it was horizontal. When the apparent conductivity of a mixture of cellular or porous nonhomogeneous solid is determined, the observed temperature coefficient may be much larger than for the homogeneous solid alone, because heat is transferred not only by the mechanism of conduction but also by convection in the gas pockets and by radiation from surface to surface of the individual particles. If internal radiation is an important factor, a plot of the apparent conductivity as ordinate versus temperature should show a curve concave upward, since radiation increases with the fourth power of the absolute temperature. Griffiths noted that cork, slag, wool, charcoal, and wood fibers, when of good quality and dry, have thermal conductivities about 2.2 times that of still air, whereas a highly cellular form of rubber, 112 kg/m³ (7 lb/ft³), had a thermal conductivity only 1.6 times that of still air. In measuring the apparent thermal conductivity of diathermanous substances such as quartz (especially when exposed to radiation emitted at high temperatures), it should be remembered that a part of the heat is transmitted by radiation.

Bridgman [*Proc. Am. Acad. Arts Sci.*, **59**, 141 (1923)] showed that the thermal conductivity of **liquids** is increased by only a few percent under a pressure of 100,330 kPa (1000 atm). The thermal conductivity of some liquids varies with temperature through a maximum. It is often necessary for the engineer to estimate thermal conductivities; methods are indicated in Sec. 2.

Equation (5-2) considers the thermal conductivity to be variable. If k is expressed as a function of temperature, Eq. (5-2) is nonlinear and difficult to solve analytically except for certain special cases. Usually in complicated systems numerical solution by means of computer is possible. A complete review of heat conduction has been given by Davis and Akers [*Chem. Eng.*, **67**(4), 187, (5), 151 (1960)] and by Davis [*Chem. Eng.*, **67**(6), 213, (7), 135 (8), 137 (1960)].

STEADY-STATE CONDUCTION

For steady flow of heat, the term $dQ/d\theta$ in Eq. (5-1) is constant and may be replaced by Q/θ or q . Likewise, in Eq. (5-2) the term $\partial t/\partial \theta$ is zero. Hence, for constant thermal conductivity, Eq. (5-2) may be expressed as

$$\nabla^2 t = (q'/k) \quad (5-3)$$

One-Dimensional Conduction Many heat-conduction problems may be formulated into a one-dimensional or pseudo-one-dimensional form in which only one space variable is involved. Forms of the conduction equation for rectangular, cylindrical, and spherical coordinates are, respectively,

$$\frac{\partial^2 t}{\partial x^2} = -\frac{q'}{k} \quad (5-4a)$$

$$\frac{1}{r} \frac{d}{dr} \left(r \frac{dt}{dr} \right) = -\frac{q'}{k} \quad (5-4b)$$

$$\frac{1}{r^2} \frac{d}{dr} \left(r^2 \frac{dt}{dr} \right) = -\frac{q'}{k} \quad (5-4c)$$

These are second-order differential equations which upon integration become, respectively,

$$t = -(q'x^2/2k) + c_1x + c_2 \quad (5-5a)$$

$$t = -(q'r^2/4k) + c_1 \ln r + c_2 \quad (5-5b)$$

$$t = -(q'r^2/6k) - (c_1/r) + c_2 \quad (5-5c)$$

Constants of integration c_1 and c_2 are determined by the boundary conditions, i.e., temperatures and temperature gradients at known locations in the system.

For the case of a solid surface exposed to surroundings at a different temperature and for a finite surface coefficient, the **boundary condition** is expressed as

$$h_T(t_s - t') = -k(dt/dx)_{\text{surf}} \quad (5-6)$$

Inspection of Eqs. (5-5a), (5-5b), and (5-5c) indicates the form of temperature profile for various conditions and geometries and also reveals the effect of the heat-generation term q' upon the temperature distributions.

In the **absence of heat generation**, one-dimensional steady-state conduction may be expressed by integrating Eq. (5-1):

$$q \int_{x_1}^{x_2} \frac{dx}{A} = -\int_{t_1}^{t_2} k dt \quad (5-7)$$

Area A must be known as a function of x . If k is constant, Eq. (5-7) is expressed in the integrated form

$$q = kA_{\text{avg}}(t_1 - t_2)/(x_2 - x_1) \quad (5-8)$$

where

$$A_{\text{avg}} = \frac{1}{x_2 - x_1} \int_{x_1}^{x_2} \frac{dx}{A} \quad (5-9)$$

Examples of values of A_{avg} for various functions of x are shown in the following table.

Area proportional to	A_{avg}
Constant	$A_1 = A_2$
x	$\frac{A_2 - A_1}{\ln(A_2/A_1)}$
x^2	$\sqrt{A_2 A_1}$

Usually, thermal conductivity k is not constant but is a function of temperature. In most cases, over the ranges of values used the relation is linear. Integration of Eq. (5-7), with k linear in t , gives

$$q \int_{x_1}^{x_2} \frac{dx}{A} = k_{\text{avg}}(t_1 - t_2) \quad (5-10)$$

where k_{avg} is the arithmetic-average thermal conductivity between temperatures t_1 and t_2 . This average probably gives results which are correct within the precision of the data in the majority of cases, though a special integration can be made whenever k is known to be greatly different from linear in temperature.

Conduction through Several Bodies in Series Figure 5-1 illustrates diagrammatically the temperature gradients accompanying the steady conduction of heat in series through three solids.

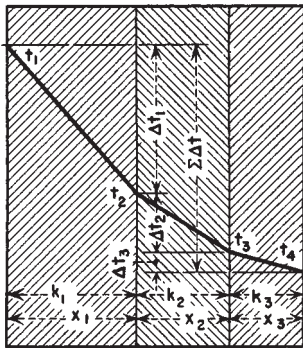


FIG. 5-1 Temperature gradients for steady heat conduction in series through three solids.

Since the heat flow through each of the three walls must be the same,

$$q = (k_1 A_1 \Delta t_1 / x_1) = (k_2 A_2 \Delta t_2 / x_2) = (k_3 A_3 \Delta t_3 / x_3) \quad (5-11)$$

Since, by definition, individual thermal resistance

$$R = x/kA \quad (5-12)$$

$$\text{then} \quad \Delta t_1 = qR_1 \quad \Delta t_2 = qR_2 \quad \Delta t_3 = qR_3 \quad (5-13)$$

Adding the individual temperature drops, noting that q is uniform,

$$q(R_1 + R_2 + R_3) = \Delta t_1 + \Delta t_2 + \Delta t_3 = \sum \Delta t \quad (5-14)$$

$$\text{or} \quad q = \sum \Delta t / R_T = (t_1 - t_4) / R_T \quad (5-15)$$

where R_T is the overall resistance and is the sum of the individual resistances in series, then

$$R_T = R_1 + R_2 + \cdots + R_n \quad (5-16)$$

When a wall is constructed of several layers of solids, the joints at adjacent layers may not perfectly exclude air spaces, and these additional resistances should not be overlooked.

Conduction through Several Bodies in Parallel For n resistances in parallel, the rates of heat flow are additive:

$$q = \Delta t / R_1 + \Delta t / R_2 + \cdots + \Delta t / R_n \quad (5-17a)$$

$$q = \left(\frac{1}{R_1} + \frac{1}{R_2} + \cdots + \frac{1}{R_n} \right) \Delta t \quad (5-17b)$$

$$q = (C_1 + C_2 + \cdots + C_n) \Delta t = \sum C \Delta t \quad (5-17c)$$

where R_1 to R_n are the individual resistances and C_1 to C_n are the individual conductances; $C = kA/x$.

Several Bodies in Series with Heat Generation The simple Fourier type of equation indicated by Eq. (5-15) may not be used when heat generation occurs in one of the bodies in the series. In this case, Eq. (5-5a), (5-5b), or (5-5c) must be solved with appropriate boundary conditions.

Example 1: Steady-State Conduction with Heat Generation A plate-type nuclear fuel element, consisting of a uranium-zirconium alloy $(3.2)(10^{-3})$ m (0.125 in) thick clad on each side with a $(6.4)(10^{-4})$ -m (0.025-in) thick layer of zirconium, is cooled by water under pressure at 200°C (400°F), the heat-transfer coefficient being $42,600$ J/(m²·s·K) [7500 Btu/(h·ft²·°F)]. If the temperature at the center of the fuel must not exceed 570°C (1050°F), determine the maximum rate of heat generation in the fuel. The zirconium and zirconium alloy have a thermal conductivity of 21 J/(m·s·K) [12 Btu/(h·ft²·°F/ft)].

Solution. Equation (5-4a) may be integrated for each material. The heat generation is zero in the cladding, and its value for the fuel may be determined from the integrated equations. Let $x = 0$ at the midplane of the fuel. Then $x_1 = (1.6)(10^{-3})$ m (0.0625 in) at the cladding-fuel interface and $x_2 = (2.2)(10^{-2})$ m (0.0875 in) at the cladding-water interface. Let the subscripts c, f refer to cladding and fuel respectively.

The boundary conditions are:

For fuel, at $x = 0$, $t = 570^\circ\text{C}$ (1050°F), $dt/dx = 0$ (this follows if the temperature is finite at the midplane).

For fuel and cladding, at $x = x_1$, $t_f = t_c$,

$$k_f(dt/dx) = k_c(dt/dx)$$

For cladding, at $x = x_2$,

$$t_c - 400 = -(k_c/42,600)(dt/dx)$$

For the fuel, the first integration of Eq. (10-4a) gives

$$dt_f/dx = -(q'/k_f)x + c_1$$

which gives $c_1 = 0$ when the boundary condition is applied. Thus the second integration gives

$$t_f = -(q'/2k_f)x^2 + c_2$$

from which c_2 is determined to be 570 (1050) upon application of the boundary condition. Thus the temperature profile in the fuel is

$$t_f = -(q'/2k_f)x^2 + 570$$

The temperature profile in the cladding is obtained by integrating Eq. (10-4a) twice with $q' = 0$. Hence

$$(dt_c/dx) = c_1 \quad \text{and} \quad t_c = c_1x + c_2$$

There are now three unknowns, c_1 , c_2 , and q' , and three boundary conditions by which they can be determined.

At $x = x_1$,

$$q'x_1^2/2k_f + 570 = c_1x_1 + c_2 - k_fq'x_1/k_f = k_c c_1$$

At $x = x_2$,

$$c_1x_2 + c_2 - 200 = -(k_c/42,600)c_1$$

$$\text{From which} \quad q' = (2.53)(10^9) \text{ J/(m}^3\cdot\text{s)} [(2.38)(10^8) \text{ Btu/(h}\cdot\text{ft}^3)] \\ c_1 = -(1.92)(10^5) \\ c_2 = 724$$

Two-Dimensional Conduction If the temperature of a material is a function of two space variables, the two-dimensional conduction equation is (assuming constant k)

$$\partial^2 t / \partial x^2 + \partial^2 t / \partial y^2 = -q'/k \quad (5-18)$$

When q' is zero, Eq. (5-18) reduces to the familiar Laplace equation. The analytical solution of Eq. (10-18) as well as of Laplace's equation is possible for only a few boundary conditions and geometric shapes. Carslaw and Jaeger (*Conduction of Heat in Solids*, Clarendon Press, Oxford, 1959) have presented a large number of analytical solutions of differential equations applicable to heat-conduction problems. Generally, graphical or numerical **finite-difference methods** are most frequently used. Other numerical and relaxation methods may be found in the general references in the "Introduction." The methods may also be extended to three-dimensional problems.

UNSTEADY-STATE CONDUCTION

When temperatures of materials are a function of both time and space variables, more complicated equations result. Equation (5-2) is the three-dimensional unsteady-state conduction equation. It involves the rate of change of temperature with respect to time $\partial t / \partial \theta$. Solutions to most practical problems must be obtained through the use of digital computers. Numerous articles have been published on a wide variety of transient conduction problems involving various geometrical shapes and boundary conditions.

One-Dimensional Conduction The one-dimensional transient conduction equations are (for constant physical properties)

$$\partial t / \partial \theta = \alpha (\partial^2 t / \partial x^2) + q'/c\rho \quad (\text{rectangular coordinates}) \quad (5-19a)$$

$$\frac{\partial t}{\partial \theta} = \frac{\alpha}{r} \frac{\partial}{\partial r} \left(r \frac{\partial t}{\partial r} \right) + \frac{q'}{c\rho} \quad (\text{cylindrical coordinates}) \quad (5-19b)$$

$$\frac{\partial t}{\partial \theta} = \frac{\alpha}{r^2} \frac{\partial}{\partial r} \left(r^2 \frac{\partial t}{\partial r} \right) + \frac{q'}{c\rho} \quad (\text{spherical coordinates}) \quad (5-19c)$$

These equations have been solved analytically for solid slabs, cylinders, and spheres. The solutions are in the form of infinite series, and usually the results are plotted as curves involving four ratios [Gurney and Lurie, *Ind. Eng. Chem.*, **15**, 1170 (1923)] defined as follows with $q' = 0$:

$$Y = (t' - t)/(t' - t_i) \quad X = k\theta/\rho c_p r_m^2 \quad (5-20a,b)$$

$$m = k/h_T r_m \quad n = r/r_m \quad (5-20c,d)$$

Since each ratio is dimensionless, any consistent units may be employed in any ratio. The significance of the symbols is as follows: t' = temperature of the surroundings; t_i = initial uniform temperature of the body; t = temperature at a given point in the body at the time θ measured from the start of the heating or cooling operations; k = uniform thermal conductivity of the body; ρ = uniform density of the body; c = specific heat of the body; h_T = coefficient of total heat transfer between the surroundings and the surface expressed as heat transferred per unit time per unit area of the surface per unit difference in temperature between surroundings and surface; r = distance, in the direction of heat conduction, from the midpoint or midplane of the body to the point under consideration; r_m = radius of a sphere or cylinder, one-half of the thickness of a slab heated from both faces, the total thickness of a slab heated from one face and insulated perfectly at the other; and x = distance, in the direction of heat conduction, from the surface of a semi-infinite body (such as the surface of the earth) to the point under consideration. In making the integrations which lead to the curves shown, the following factors were assumed constant: c , h_T , k , r , r_m , t' , x , and ρ .

The working curves are shown in Figs. 5-2 to 5-5 for **cylinders of infinite length, spheres, slabs of infinite faces, and semi-infinite solids** respectively, with Y plotted as ordinates on a logarithmic scale versus X as abscissas to an arithmetic scale, for various values of the ratios m and n . To facilitate calculations involving instantaneous rates of cooling or heating of the semi-infinite body, Fig. 5-5 shows also a curve of dY/dX versus X . Similar plots to a larger scale are given in McAdams,

Brown and Marco, Schack, and Stoeber (see "Introduction: General References"). For a solid of infinite thickness (Fig. 5-5) and with $m = 0$,

$$Y = \frac{2}{\sqrt{\pi}} \int_0^z \exp(-z^2) dz \quad (5-21)$$

where $z = 1/\sqrt{2}X$ and the "error integral" may be evaluated from standard mathematical tables.

Various numerical and graphical methods are used for unsteady-state conduction problems, in particular the Schmidt graphical method (*Foppls Festschrift*, Springer-Verlag, Berlin, 1924). These methods are very useful because any form of initial temperature distribution may be used.

Two-Dimensional Conduction The governing differential equation for two-dimensional transient conduction is

$$\frac{\partial t}{\partial \theta} = \alpha \left(\frac{\partial^2 t}{\partial x^2} + \frac{\partial^2 t}{\partial y^2} \right) + \frac{q'}{cp} \quad (5-22)$$

McAdams (*Heat Transmission*, 3d ed., McGraw-Hill, New York, 1954) gives various forms of transient difference equations and methods of solving transient conduction problems. The availability of computers and a wide variety of computer programs permits virtually routine solution of complicated conduction problems.

Conduction with Change of Phase A special type of transient problem (the Stefan problem) involves conduction of heat in a material when freezing or melting occurs. The liquid-solid interface moves with time, and in addition to conduction, latent heat is either generated or absorbed at the interface. Various problems of this type are discussed by Bankoff [in Drew et al. (eds.), *Advances in Chemical Engineering*, vol. 5, Academic, New York, 1964].

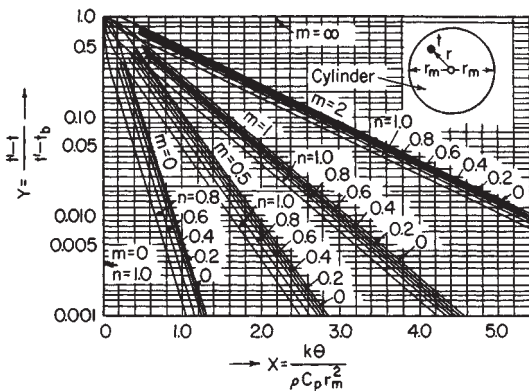


FIG. 5-2 Heating and cooling of a solid cylinder having an infinite ratio of length to diameter.

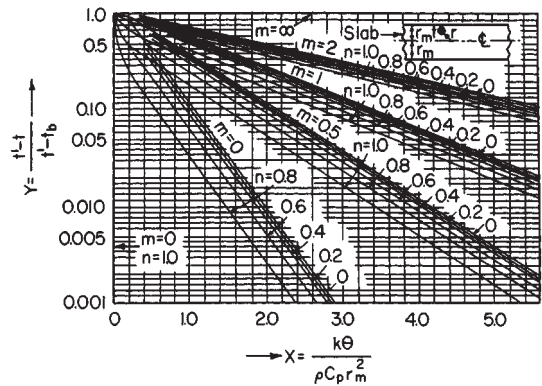


FIG. 5-4 Heating and cooling of a solid slab having a large face area relative to the area of the edges.

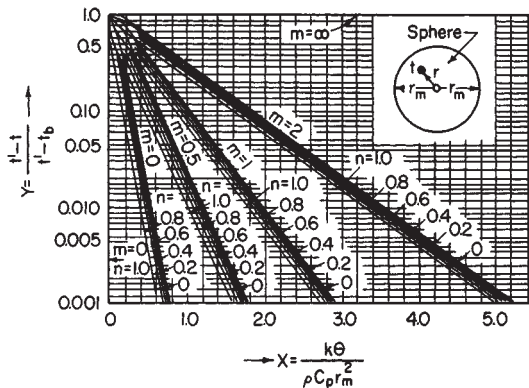


FIG. 5-3 Heating and cooling of a solid sphere.

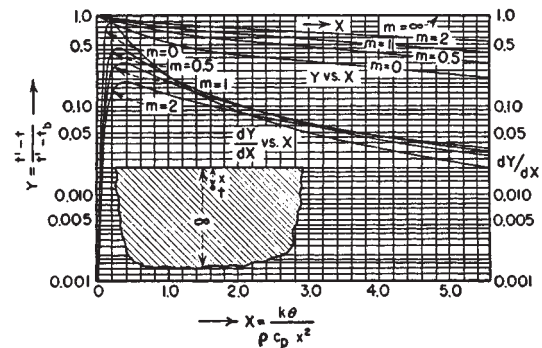


FIG. 5-5 Heating and cooling of a solid of infinite thickness, neglecting edge effects. (This may be used as an approximation in the zone near the surface of a body of finite thickness.)

HEAT TRANSFER BY CONVECTION

COEFFICIENT OF HEAT TRANSFER

In many cases of heat transfer involving either a liquid or a gas, convection is an important factor. In the majority of heat-transfer cases met in industrial practice, heat is being transferred from one fluid through a solid wall to another fluid. Assume a hot fluid at a temperature t_1 flowing past one side of a metal wall and a cold fluid at t_7 flowing past the other side to which a scale of thickness x_s adheres. In such a case, the conditions obtaining at a given section are illustrated diagrammatically in Fig. 5-6.

For turbulent flow of a fluid past a solid, it has long been known that, in the immediate neighborhood of the surface, there exists a relatively quiet zone of fluid, commonly called the **film**. As one approaches the wall from the body of the flowing fluid, the flow tends to become less turbulent and develops into laminar flow immediately adjacent to the wall. The film consists of that portion of the flow which is essentially in laminar motion (the laminar sublayer) and through which heat is transferred by molecular conduction. The resistance of the laminar layer to heat flow will vary according to its thickness and can range from 95 percent of the total resistance for some fluids to about 1 percent for other fluids (liquid metals). The turbulent core and the buffer layer between the laminar sublayer and turbulent core each offer a **resistance to heat transfer** which is a function of the turbulence and the thermal properties of the flowing fluid. The relative temperature difference across each of the layers is dependent upon their resistance to heat flow.

The Energy Equation A complete energy balance on a flowing fluid through which heat is being transferred results in the energy equation (assuming constant physical properties):

$$cp \left(\frac{\partial t}{\partial \theta} + u \frac{\partial t}{\partial x} + v \frac{\partial t}{\partial y} + w \frac{\partial t}{\partial z} \right) = k \left(\frac{\partial^2 t}{\partial x^2} + \frac{\partial^2 t}{\partial y^2} + \frac{\partial^2 t}{\partial z^2} \right) + q' + \Phi \quad (5-23)$$

where Φ is the term accounting for energy dissipation due to fluid viscosity and is significant in high-speed gas flow and in the flow of highly viscous liquids. Except for the time term, the left-hand terms of Eq. (5-23) are the so-called **convective terms** involving the energy carried by the fluid by virtue of its velocity. Therefore, the solution of the equation is dependent upon the solution of the momentum equations of flow. Solutions of Eq. (5-23) exist only for several simple flow cases and geometries and mainly for laminar flow. For turbulent flow the difficulties of expressing the fluid velocity as a function of space and time coordinates and of obtaining reliable values of the effective thermal conductivity of the flowing fluid have prevented solution of the equation unless simplifying assumptions and approximations are made.

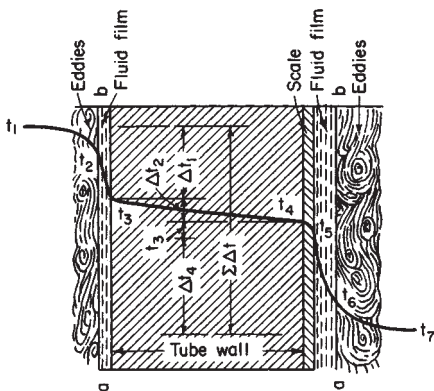


FIG. 5-6 Temperature gradients for a steady flow of heat by conduction and convection from a warmer to a colder fluid separated by a solid wall.

Individual Coefficient of Heat Transfer Because of the complicated structure of a turbulent flowing stream and the impracticability of measuring thicknesses of the several layers and their temperatures, the **local rate of heat transfer** between fluid and solid is defined by the equations

$$dq = h_i dA_i (t_1 - t_3) = h_o dA_o (t_5 - t_7) \quad (5-24)$$

where h_i and h_o are the local heat-transfer coefficients inside and outside the wall, respectively, and temperatures are defined by Fig. 5-6.

The definition of the heat-transfer coefficient is arbitrary, depending on whether *bulk-fluid temperature*, *centerline temperature*, or *some other reference temperature* is used for t_1 or t_7 . Equation (5-24) is an expression of Newton's law of cooling and incorporates all the complexities involved in the solution of Eq. (5-23). The **temperature gradients** in both the fluid and the adjacent solid at the fluid-solid interface may also be related to the heat-transfer coefficient:

$$dq = h_i dA_i (t_1 - t_3) = \left(-k \frac{dt}{dx} \right)_{\text{fluid}} = \left(-k \frac{dt}{dx} \right)_{\text{solid}} \quad (5-25)$$

Equation (5-25) holds for the liquid *only* if laminar flow exists immediately adjacent to the solid surface. The integration of Eq. (5-24) will give

$$A_i = \int_{\text{in}}^{\text{out}} \frac{dq}{h_i \Delta t_i} \quad \text{or} \quad A_o = \int_{\text{in}}^{\text{out}} \frac{dq}{h_o \Delta t_o} \quad (5-26)$$

which may be evaluated only if the quantities under the integral can be expressed in terms of a single variable. If q is a linear function of Δt and h is constant, then Eq. (5-26) gives

$$q = \frac{hA(\Delta t_{\text{in}} - \Delta t_{\text{out}})}{\ln(\Delta t_{\text{in}}/\Delta t_{\text{out}})} \quad (5-27)$$

where the Δt factor is the **logarithmic-mean temperature difference** between the wall and the fluid.

Frequently experimental data report average heat-transfer coefficients based upon an arbitrarily defined temperature difference, the two most common being

$$q = \frac{h_{lm}A(\Delta t_{\text{in}} - \Delta t_{\text{out}})}{\ln(\Delta t_{\text{in}}/\Delta t_{\text{out}})} \quad (5-28a)$$

$$q = \frac{h_{am}A(\Delta t_{\text{in}} + \Delta t_{\text{out}})}{2} \quad (5-28b)$$

where h_{lm} and h_{am} are average heat-transfer coefficients based upon the logarithmic-mean temperature difference and the arithmetic-average temperature difference, respectively.

Overall Coefficient of Heat Transfer In testing commercial heat-transfer equipment, it is not convenient to measure tube temperatures (t_3 or t_4 in Fig. 5-6), and hence the overall performance is expressed as an overall coefficient of heat transfer U based on a convenient area dA , which may be dA_i , dA_o , or an average of dA_i and dA_o ; whence, by definition,

$$dq = U dA (t_1 - t_7) \quad (5-29)$$

U is called the "overall coefficient of heat transfer," or merely the "overall coefficient." The rate of conduction through the tube wall and scale deposit is given by

$$dq = \frac{k dA_{\text{avg}}(t_3 - t_4)}{x} = h_d dA_d (t_4 - t_5) \quad (5-30)$$

Upon eliminating t_3 , t_4 , t_5 from Eqs. (5-24), (5-29), and (5-30), the complete expression for the **steady rate of heat flow** from one fluid through the wall and scale to a second fluid, as illustrated in Fig. 5-6, is

$$dq = \frac{t_1 - t_7}{\frac{1}{h_i dA_i} + \frac{x}{k dA_{\text{avg}}} + \frac{1}{h_d dA_d} + \frac{1}{h_o dA_o}} = U dA (t_1 - t_7) \quad (5-31)^{\circ}$$

^o Normally, dirt and scale resistance must be considered on both sides of the tube wall. The area dA is any convenient reference area.

Representation of Heat-Transfer Film Coefficients There are two general methods of expressing film coefficients: (1) dimensionless relations and (2) dimensional equations.

The dimensionless relations are usually indicated in either of two forms, each yielding identical results. The preferred form is that suggested by Colburn [*Trans. Am. Inst. Chem. Eng.*, **29**, 174–210 (1933)]. It relates, primarily, three dimensionless groups: the Stanton number h/cG , the Prandtl number $c\mu/k$, and the Reynolds number DG/μ . For more accurate correlation of data (at Reynolds number $<10,000$), two additional dimensionless groups are used: ratio of length to diameter L/D and ratio of viscosity at wall (or surface) temperature to viscosity at bulk temperature. Colburn showed that the product of the Stanton number and the two-thirds power of the Prandtl number (and, in addition, power functions of L/D and μ_w/μ for Reynolds number $<10,000$) is approximately equal to half of the Fanning friction factor $f/2$. This product is called the **Colburn j factor**. Since the Colburn type of equation relates heat transfer and fluid friction, it has greater utility than other expressions for the heat-transfer coefficient.

The classical (and perhaps more familiar) form of dimensionless expressions relates, primarily, the Nusselt number hD/k , the Prandtl number $c\mu/k$, and the Reynolds number DG/μ . The L/D and viscosity-ratio modifications (for Reynolds number $<10,000$) also apply.

The **dimensional equations** are usually expansions of the dimensionless expressions in which the terms are in more convenient units and in which all numerical factors are grouped together into a single numerical constant. In some instances, the combined physical properties are represented as a linear function of temperature, and the dimensional equation resolves into an equation containing only one or two variables.

NATURAL CONVECTION

Natural convection occurs when a solid surface is in contact with a fluid of different temperature from the surface. Density differences provide the body force required to move the fluid. Theoretical analyses of natural convection require the simultaneous solution of the coupled equations of motion and energy. Details of theoretical studies are available in several general references (Brown and Marco, *Introduction to Heat Transfer*, 3d ed., McGraw-Hill, New York, 1958; and Jakob, *Heat Transfer*; Wiley, New York, vol. 1, 1949; vol. 2, 1957) but have generally been applied successfully to the simple case of a vertical plate. Solution of the motion and energy equations gives temperature and velocity fields from which heat-transfer coefficients may be derived. The general type of equation obtained is the so-called **Nusselt equation**:

$$\frac{hL}{k} = a \left(\frac{L^3 \rho^2 g \beta \Delta t}{\mu^2} \frac{c\mu}{k} \right)^m \quad (5-32a)$$

$$N_{Nu} = a(N_{Gr} N_{Pr})^m \quad (5-32b)$$

Nusselt Equation for Various Geometries Natural-convection coefficients for various bodies may be predicted from Eq. (5-32). The various numerical values of a and m have been determined experimen-

tally and are given in Table 5-1. Fluid properties are evaluated at $t_f = (t_s + t')/2$. For **vertical plates and cylinders** and $1 < N_{Pr} < 40$, Kato, Nishiwaki, and Hirata [*Int. J. Heat Mass Transfer*, **11**, 1117 (1968)] recommend the relations

$$N_{Nu} = 0.138 N_{Gr}^{0.36} (N_{Pr}^{0.175} - 0.55) \quad (5-33a)$$

for $N_{Gr} > 10^9$, and

$$N_{Nu} = 0.683 N_{Gr}^{0.25} N_{Pr}^{0.25} [N_{Pr}/(0.861 + N_{Pr})]^{0.25} \quad (5-33b)$$

for $N_{Gr} < 10^9$.

Simplified Dimensional Equations Equation (5-32) is a dimensionless equation, and any consistent set of units may be used. Simplified dimensional equations have been derived for air, water, and organic liquids by rearranging Eq. (5-32) into the following form by collecting the fluid properties into a single factor:

$$h = b(\Delta t)^m L^{3m-1} \quad (5-34)$$

Values of b in SI and U.S. customary units are given in Table 5-1 for air, water, and organic liquids.

Simultaneous Loss by Radiation The heat transferred by radiation is often of significant magnitude in the loss of heat from surfaces to the surroundings because of the diathermanous nature of atmospheric gases (air). It is convenient to represent radiant-heat transfer, for this case, as a **radiation film coefficient** which is added to the film coefficient for convection, giving the combined coefficient for convection and radiation ($h_c + h_r$). In Fig. 5-7 values of the film coefficient for radiation h_r are plotted against the two surface temperatures for emissivity = 1.0.

Table 5-2 shows values of ($h_c + h_r$) from single horizontal oxidized pipe surfaces.

Enclosed Spaces The rate of heat transfer across an enclosed space is calculated from a special coefficient h' based upon the temperature difference between the two surfaces, where $h' = (q/A)/(t_{s1} - t_{s2})$. The value of $h'L/k$ may be predicted from Eq. (5-32) by using the values of a and m given in Table 5-3.

For **vertical enclosed cells** 10 in high and up to 2-in gap width, Landis and Yanowitz (*Proc. Third Int. Heat Transfer Conf.*, Chicago, 1966, vol. II, p. 139) give

$$\left(\frac{q}{A} \right) \frac{\delta}{k \Delta t} = 0.123 (\delta/L)^{0.84} (N_{Gr} N_{Pr})^{0.28} \quad (5-35)$$

for $2 \times 10^3 < N_{Gr} N_{Pr} (\delta/L)^3 < 10^7$, where q/A is the uniform heat flux and Δt is the temperature difference at $L/2$. Equation (5-35) is applicable for air, water, and silicone oils.

For **horizontal annuli** Grugel and Hauf (*Proc. Third Int. Heat Transfer Conf.*, Chicago, 1966, vol. II, p. 182) report

$$\frac{h\delta}{k} = \left(0.2 + 0.145 \frac{\delta}{D_1} N_{Gr} \right)^{0.25} \exp \left(-0.02 \frac{\delta}{D_1} \right) \quad (5-36)$$

for $0.55 < \delta/D_1 < 2.65$, where N_{Gr} is based upon gap width δ and D_1 is the core diameter of the annulus.

TABLE 5-1 Values of a , m , and b for Eqs. (5-32) and (5-34)

Configuration	$Y = N_{Gr} N_{Pr}$	a	m	b , air at		b , water at		b , organic liquid at	
				21°C	70°F	21°C	70°F	21°C	70°F
				Vertical surfaces	$<10^4$	1.36	1/5		
$L =$ vertical dimension < 3 ft	$10^4 < Y < 10^9$	0.59	1/4	1.37	0.28	127	26	59	12
	$>10^9$	0.13	1/5	1.24	0.18				
Horizontal cylinder	$<10^{-5}$	0.49	0						
	$10^{-5} < Y < 10^{-3}$	0.71	1/25						
	$10^{-3} < Y < 1$	1.09	1/10						
	$1 < Y < 10^4$	1.09	1/5						
	$10^4 < Y < 10^9$	0.53	1/4	1.32	0.27				
Horizontal flat surface	$>10^9$	0.13	1/5	1.24	0.18				
	$10^5 < Y < 2 \times 10^7$ (FU)	0.54	1/4	1.86	0.38				
	$2 \times 10^7 < Y < 3 \times 10^{10}$ (FU)	0.14	1/5						
	$3 \times 10^5 < Y < 3 \times 10^{10}$ (FD)	0.27	1/4	0.88	0.18				

NOTE: FU = facing upward; FD = facing downward. b in SI units is given in °C column; b in U.S. customary units, in °F column.

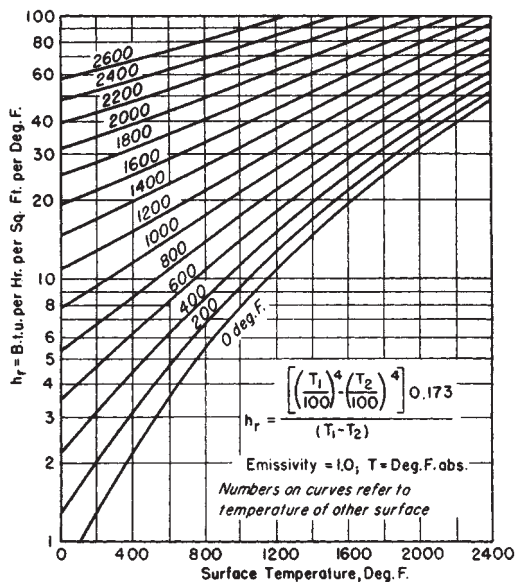


FIG. 5-7 Radiation coefficients of heat transfer h_r . To convert British thermal units per hour-square foot-degrees Fahrenheit to joules per square meter-second-kelvins, multiply by 5.6783; $^{\circ}\text{C} = (^{\circ}\text{F} - 32)/1.8$.

FORCED CONVECTION

Forced-convection heat transfer is the most frequently employed mode of heat transfer in the process industries. Hot and cold fluids, separated by a solid boundary, are pumped through the heat-transfer equipment, the rate of heat transfer being a function of the physical properties of the fluids, the flow rates, and the geometry of the system. Flow is generally turbulent, and the flow duct varies in complexity from circular tubes to baffled and extended-surface heat exchangers. Theoretical analyses of forced-convection heat transfer have been limited to relatively simple geometries and laminar flow. Analyses of turbulent-flow heat transfer have been based upon some mechanistic model and have not generally yielded relationships which were suitable for design purposes. Usually for complicated geometries only empirical relationships are available, and frequently these are based upon limited data and special operating conditions. Heat-transfer coefficients are strongly influenced by the mechanics of flow occurring during forced-convection heat transfer. Intensity of turbulence, entrance conditions, and wall conditions are some of the factors which must be considered in detail as greater accuracy in prediction of coefficients is required.

Analogy between Momentum and Heat Transfer The inter-relationship of momentum transfer and heat transfer is obvious from examining the equations of motion and energy. For constant fluid properties, the equations of motion must be solved before the energy equation is solved. If fluid properties are not constant, the equations are coupled, and their solutions must proceed simultaneously. Con-

siderable effort has been directed toward deriving some simple relationship between momentum and heat transfer. The methodology has been to use easily observed velocity profiles to obtain a measure of the diffusivity of momentum in the flowing stream. The analogy between heat and momentum is invoked by assuming that diffusion of heat and diffusion of momentum occur by essentially the same mechanism so that a relatively simple relationship exists between the diffusion coefficients. Thus, the diffusivity of momentum is used to predict temperature profiles and thence by Eq. (10-25) to predict the heat-transfer coefficient.

The analogy has been reasonably successful for simple geometries and for fluids of very low Prandtl number (liquid metals). For high-Prandtl-number fluids the **empirical analogy of Colburn** [Trans. Am. Inst. Chem. Eng., 29, 174 (1933)] has been very successful. A j factor for momentum transfer is defined as $j = f/2$, where f is the friction factor for the flow. The j factor for heat transfer is assumed to be equal to the j factor for momentum transfer

$$j = h/cG(c\mu/k)^{2/3} \tag{5-37}$$

More involved analyses for **circular tubes** reduce the equations of motion and energy to the form

$$\frac{\tau_{yz}}{\rho} = -\frac{(v + \epsilon_M)du}{dy} \tag{5-38a}$$

$$\frac{q/A}{c\rho} = -\frac{(\alpha + \epsilon_H)dt}{dy} \tag{5-38b}$$

where ϵ_H is the eddy diffusivity of heat and ϵ_M is the eddy diffusivity of momentum. The units of diffusivity are L^2/θ . The eddy viscosity is $E_M = \rho\epsilon_M$, and the eddy conductivity of heat is $E_H = \epsilon_H c\rho$. Values of ϵ_M are determined via Eq. (5-38a) from experimental velocity-distribution data. By assuming $\epsilon_H/\epsilon_M = \text{constant}$ (usually unity), Eq. (10-38b) is solved to give the temperature distribution from which the heat-transfer coefficient may be determined. The major difficulties in solving Eq. (5-38b) are in accurately defining the thickness of the various flow layers (laminar sublayer and buffer layer) and in obtaining a suitable relationship for prediction of the eddy diffusivities. For assistance in predicting eddy diffusivities, see Reichardt (NACA Tech. Memo 1408, 1957) and Strunk and Chao [Am. Inst. Chem. Eng. J., 10, 269 (1964)].

Internal and External Flow Two main types of flow are considered in this subsection: internal or conduit flow, in which the fluid completely fills a closed stationary duct, and external or immersed flow, in which the fluid flows past a stationary immersed solid. With **internal flow**, the heat-transfer coefficient is theoretically infinite at the location where heat transfer begins. The local heat-transfer coefficient rapidly decreases and becomes constant, so that after a certain length the average coefficient in the conduit is independent of the length. The local coefficient may follow an irregular pattern, however, if obstructions or turbulence promoters are present in the duct. For **immersed flow**, the local coefficient is again infinite at the point where heating begins, after which it decreases and may show various irregularities depending upon the configuration of the body. Usually in this instance the local coefficient never becomes constant as flow proceeds downstream over the body.

When heat transfer occurs during immersed flow, the rate is dependent upon the configuration of the body, the position of the body, the proximity of other bodies, and the flow rate and turbulence of the

TABLE 5-2 Values of $(h_c + h_r)^*$

Btu/(h-ft²- $^{\circ}$ F from pipe to room)
For horizontal bare standard steel pipe of various sizes in a room at 80 $^{\circ}$ F

Nominal pipe diameter, in	Temperature difference, $^{\circ}$ F														
	30	50	100	150	200	250	300	350	400	450	500	550	600	650	700
1	2.16	2.26	2.50	2.73	3.00	3.29	3.60	3.95	4.34	4.73	5.16	5.60	6.05	6.51	6.98
3	1.97	2.05	2.25	2.47	2.73	3.00	3.31	3.69	4.03	4.43	4.85	5.26	5.71	6.19	6.66
5		1.95	2.15	2.36	2.61	2.90	3.20	3.54	3.90						
10	1.80	1.87	2.07	2.29	2.54	2.82	3.12	3.47	3.84						

*Bailey and Lyell [Engineering, 147, 60 (1939)] give values for $(h_c + h_r)$ up to Δt_c of 1000 $^{\circ}$ F. $^{\circ}\text{C} = (^{\circ}\text{F} - 32)/1.8$; 5.6783 Btu/(h-ft²- $^{\circ}$ F) = J/(m²-s-K).

TABLE 5-3 Values of a and m for Eq. (5-32)

Configuration	$N_{Gr}N_{Pr}(\delta/L)^3$	a	m
Vertical spaces	2×10^4 to 2×10^5	$0.20 (\delta/L)^{-5/6}$	$1/4$
	2×10^5 to 10^7	$0.071 (\delta/L)^{1/9}$	$1/3$
Horizontal spaces	10^4 to 3×10^5	$0.21 (\delta/L)^{-1/4}$	$1/4$
	3×10^5 to 10^7	0.075	$1/3$

δ = cell width, L = cell length.

stream. The heat-transfer coefficient varies over the immersed body, since both the thermal and the momentum boundary layers vary in thickness. Relatively simple relationships are available for simple configurations immersed in an infinite flowing fluid. For complicated configurations and assemblages of bodies such as are found on the shell side of a heat exchanger, little is known about the local heat-transfer coefficient; empirical relationships giving average coefficients are all that are usually available. Research that has been conducted on local coefficients in complicated geometries has not been extensive enough to extrapolate into useful design relationships.

Laminar Flow Normally, laminar flow occurs in closed ducts when $N_{Re} < 2100$ (based on equivalent diameter $D_e = 4 \times \text{free area} \div \text{perimeter}$). Laminar-flow heat transfer has been subjected to extensive theoretical study. The energy equation has been solved for a variety of boundary conditions and geometrical configurations. However, true laminar-flow heat transfer very rarely occurs. Natural-convection effects are almost always present, so that the assumption that molecular conduction alone occurs is not valid. Therefore, empirically derived equations are most reliable.

Data are most frequently correlated by the Nusselt number $(N_{Nu})_{lm}$ or $(N_{Nu})_{am}$, the Graetz number $N_{Gz} = (N_{Re}N_{Pr}D/L)$, and the Grashof (natural-convection effects) number N_{Gr} . Some correlations consider only the variation of viscosity with temperature, while others also consider density variation. Theoretical analyses indicate that for very long tubes $(N_{Nu})_{lm}$ approaches a limiting value. Limiting Nusselt numbers for various closed ducts are shown in Table 5-4.

Circular Tubes For horizontal tubes and constant wall temperature, several relationships are available, depending on the Graetz number. For $0.1 < N_{Gz} < 10^4$, Hausen's [Allg. Waermetech., 9, 75 (1959)], the following equation is recommended.

$$(N_{Nu})_{lm} = 3.66 + \frac{0.19N_{Gz}^{0.8}}{1 + 0.117N_{Gz}^{0.467}} \left(\frac{\mu_b}{\mu_w} \right)^{0.14} \quad (5-39)$$

For $N_{Gz} > 100$, the Sieder-Tate relationship [Ind. Eng. Chem., 28, 1429 (1936)] is satisfactory for small diameters and Δt 's:

$$(N_{Nu})_{am} = 1.86N_{Gz}^{1/3} (\mu_b/\mu_w)^{0.14} \quad (5-40)$$

A more general expression covering all diameters and Δt 's is obtained by including an additional factor $0.87(1 + 0.015N_{Gz}^{1/3})$ on the right side of Eq. (5-40). The diameter should be used in evaluating N_{Gr} . An equation published by Oliver [Chem. Eng. Sci., 17, 335 (1962)] is also recommended.

TABLE 5-4 Values of Limiting Nusselt Number in Laminar Flow in Closed Ducts

Configuration	Limiting Nusselt number $N_{Gr} < 4.0$	
	Constant wall temperature	Constant heat flux
Circular tube	3.66	4.36
Concentric annulus		Eq. (10-42)
Equilateral triangle		3.00
Rectangles		
Aspect ratio:		
1.0 (square)	2.89	3.63
0.713		3.78
0.500	3.39	4.11
0.333		4.77
0.25		5.35
0 (parallel planes)	7.60	8.24

For laminar flow in vertical tubes a series of charts developed by Pigford [Chem. Eng. Prog. Symp. Ser. 17, 51, 79 (1955)] may be used to predict values of h_{ann} .

Annuli Approximate heat-transfer coefficients for laminar flow in annuli may be predicted by the equation of Chen, Hawkins, and Solberg [Trans. Am. Soc. Mech. Eng., 68, 99 (1946)]:

$$(N_{Nu})_{am} = 1.02N_{Re}^{0.45}N_{Pr}^{0.5} \left(\frac{D_c}{L} \right)^{0.4} \left(\frac{D_2}{D_1} \right)^{0.8} \left(\frac{\mu_b}{\mu_1} \right)^{0.14} N_{Gr}^{0.05} \quad (5-41)$$

Limiting Nusselt numbers for slug-flow annuli may be predicted (for constant heat flux) from Trefethen (General Discussions on Heat Transfer, London, ASME, New York, 1951, p. 436):

$$(N_{Nu})_{lm} = \frac{8(m-1)(m^2-1)^2}{4m^4 \ln m - 3m^4 + 4m^2 - 1} \quad (5-42)$$

where $m = D_2/D_1$. The Nusselt and Reynolds numbers are based on the equivalent diameter, $D_2 - D_1$.

Limiting Nusselt numbers for laminar flow in annuli have been calculated by Dwyer [Nucl. Sci. Eng., 17, 336 (1963)]. In addition, theoretical analyses of laminar-flow heat transfer in concentric and eccentric annuli have been published by Reynolds, Lundberg, and McCuen [Int. J. Heat Mass Transfer, 6, 483, 495 (1963)]. Lee [Int. J. Heat Mass Transfer, 11, 509 (1968)] presented an analysis of turbulent heat transfer in entrance regions of concentric annuli. Fully developed local Nusselt numbers were generally attained within a region of 30 equivalent diameters for $0.1 < N_{Pr} < 30$, $10^4 < N_{Re} < 2 \times 10^5$, $1.01 < D_2/D_1 < 5.0$.

Parallel Plates and Rectangular Ducts The limiting Nusselt number for parallel plates and flat rectangular ducts is given in Table 5-4. Norris and Streid [Trans. Am. Soc. Mech. Eng., 62, 525 (1940)] report for constant wall temperature

$$(N_{Nu})_{lm} = 1.85N_{Gz}^{1/3} \quad (5-43)$$

for $N_{Gz} > 70$. Both Nusselt number and Graetz numbers are based on equivalent diameter. For large temperature differences it is advisable to apply the correction factor $(\mu_b/\mu_w)^{0.14}$ to the right side of Eq. (5-43).

For rectangular ducts Kays and Clark (Stanford Univ., Dept. Mech. Eng. Tech. Rep. 14, Aug. 6, 1953) published relationships for heating and cooling of air in rectangular ducts of various aspect ratios. For most noncircular ducts Eqs. (5-39) and (5-40) may be used if the equivalent diameter ($= 4 \times \text{free area} / \text{wetted perimeter}$) is used as the characteristic length. See also Kays and London, Compact Heat Exchangers, 3d ed., McGraw-Hill, New York, 1984.

Immersed Bodies When flow occurs over immersed bodies such that the boundary layer is completely laminar over the whole body, laminar flow is said to exist even though the flow in the mainstream is turbulent. The following relationships are applicable to single bodies immersed in an infinite fluid and are not valid for assemblages of bodies.

In general, the average heat-transfer coefficient on immersed bodies is predicted by

$$N_{Nu} = C_r(N_{Re})^m(N_{Pr})^{1/3} \quad (5-44)$$

Values of C_r and m for various configurations are listed in Table 5-5. The characteristic length is used in both the Nusselt and the Reynolds numbers, and the properties are evaluated at the film temperature $= (t_w + t_\infty)/2$. The velocity in the Reynolds number is the undisturbed free-stream velocity.

Heat transfer from immersed bodies is discussed in detail by Eckert and Drake, Jakob, and Knudsen and Katz (see "Introduction: General References"), where equations for local coefficients and the effects of unheated starting length are presented. Equation (5-44) may also be expressed as

$$N_{St}N_{Pr}^{2/3} = C_rN_{Re}^{m-1} = f/2 \quad (5-45)$$

where f is the skin-friction drag coefficient (not the form drag coefficient).

Falling Films When a liquid is distributed uniformly around the periphery at the top of a vertical tube (either inside or outside) and allowed to fall down the tube wall by the influence of gravity, the fluid

TABLE 5-5 Laminar-Flow Heat Transfer over Immersed Bodies [Eq. (5-44)]

Configuration	Characteristic length	N_{Re}	N_{Pr}	C_r	m
Flat plate parallel to flow Circular cylinder axes perpendicular to flow	Plate length Cylinder diameter	10^3 to 3×10^5	>0.6	0.648	0.50
		1 - 4		0.989	0.330
		4 - 40	>0.6	0.911	0.385
		40 - 4000		0.683	0.466
Non-circular cylinder, axis Perpendicular to flow, characteristic Length perpendicular to flow	Square, short diameter Square, long diameter Hexagon, short diameter Hexagon, long diameter	$4 \times 10^3 - 4 \times 10^4$	>0.6	0.193	0.618
		$4 \times 10^4 - 2.5 \times 10^5$		0.0266	0.805
		$5 \times 10^3 - 10^5$		0.104	0.675
		$5 \times 10^3 - 10^5$		0.250	0.588
		$5 \times 10^3 - 10^5$		0.155	0.638
		$5 \times 10^3 - 2 \times 10^4$		0.162	0.638
Sphere*	Diameter	$2 \times 10^4 - 10^5$	0.6 - 400	0.0391	0.782
		$1 - 7 \times 10^4$		0.6	0.50

*Replace N_{Nu} by $N_{Nu} - 2.0$ in Eq. (5-44).

does not fill the tube but rather flows as a thin layer. Similarly, when a liquid is applied uniformly to the outside and top of a horizontal tube, it flows in layer form around the periphery and falls off the bottom. In both these cases the mechanism is called gravity flow of liquid layers or falling films.

For the turbulent flow of water in layer form down the walls of vertical tubes the dimensional equation of McAdams, Drew, and Bays [Trans. Am. Soc. Mech. Eng., 62, 627 (1940)] is recommended:

$$h_{lm} = b\Gamma^{1/3} \quad (5-46)$$

where $b = 9150$ (SI) or 120 (U.S. customary) and is based on values of $\Gamma = W_p/\pi D$ ranging from 0.25 to 6.2 kg/(m·s) [600 to 15,000 lb/(h·ft)] of wetted perimeter. This type of water flow is used in vertical vapor-in-shell ammonia condensers, acid coolers, cycle water coolers, and other process-fluid coolers.

The following dimensional equations may be used for any liquid flowing in layer form down vertical surfaces:

$$\text{For } \frac{4\Gamma}{\mu} > 2100 \quad h_{lm} = 0.01 \left(\frac{k^3 \rho^2 g}{\mu^2} \right)^{1/3} \left(\frac{c\mu}{k} \right)^{1/3} \left(\frac{4\Gamma}{\mu} \right)^{1/3} \quad (5-47a)$$

$$\text{For } \frac{4\Gamma}{\mu} < 2100 \quad h_{am} = 0.50 \left(\frac{k^3 \rho^{4/3} c g^{2/3}}{L\mu^{1/3}} \right)^{1/3} \left(\frac{\mu}{\mu_w} \right)^{1/4} \left(\frac{4\Gamma}{\mu} \right)^{1/9} \quad (5-47b)$$

Equation (5-47b) is based on the work of Bays and McAdams [Ind. Eng. Chem., 29, 1240 (1937)]. The significance of the term L is not clear. When $L = 0$, the coefficient is definitely not infinite. When L is large and the fluid temperature has not yet closely approached the wall temperature, it does not appear that the coefficient should necessarily decrease. Within the finite limits of 0.12 to 1.8 m (0.4 to 6 ft), this equation should give results of the proper order of magnitude.

For falling films applied to the outside of horizontal tubes, the Reynolds number rarely exceeds 2100. Equations may be used for falling films on the outside of the tubes by substituting $\pi D/2$ for L .

For water flowing over a horizontal tube, data for several sizes of pipe are roughly correlated by the dimensional equation of McAdams, Drew, and Bays [Trans. Am. Soc. Mech. Eng., 62, 627 (1940)].

$$h_{am} = b (\Gamma/D_0)^{1/3} \quad (5-48)$$

where $b = 3360$ (SI) or 65.6 (U.S. customary) and Γ ranges from 0.94 to 4 kg/(m·s) [100 to 1000 lb/(h·ft)].

Falling films are also used for evaporation in which the film is both entirely or partially evaporated (juice concentration). This principle is also used in crystallization (freezing).

The advantage of high coefficient in falling-film exchangers is partially offset by the difficulties involved in distribution of the film, maintaining complete wettability of the tube, and pumping costs required to lift the liquid to the top of the exchanger.

Transition Region Turbulent-flow equations for predicting heat transfer coefficients are usually valid only at Reynolds numbers greater than 10,000. The transition region lies in the range $2000 < N_{Re} < 10,000$. No simple equation exists for accomplishing a smooth mathematical transition from laminar flow to turbulent flow. Of the relationships proposed, Hausen's equation [Z. Ver. Dtsch. Ing. Beih. Verfahrenstech., No.

4, 91 (1934)] fits both the laminar extreme and the fully turbulent extreme quite well.

$$(N_{Nu})_{lam} = 0.116(N_{Re}^{2/3} - 125)N_{Pr}^{1/3} \left[1 + \left(\frac{D}{L} \right)^{2/3} \right] \left(\frac{\mu_b}{\mu_w} \right)^{0.14} \quad (5-49)$$

between 2100 and 10,000. It is customary to represent the probable magnitude of coefficients in this region by hand-drawn curves (Fig. 5-8). Equation (5-40) is plotted as a series of curves (j factor versus Reynolds number with L/D as parameters) terminating at Reynolds number = 2100. Continuous curves for various values of L/D are then hand-drawn from these terminal points to coincide tangentially with the curve for forced-convection, fully turbulent flow [Eq. (5-50c)].

Turbulent Flow

Circular Tubes Numerous relationships have been proposed for predicting turbulent flow in tubes. For high-Prandtl-number fluids, relationships derived from the equations of motion and energy through the momentum-heat-transfer analogy are more complicated and no more accurate than many of the empirical relationships that have been developed.

For $N_{Re} > 10,000$, $0.7 < N_{Pr} < 170$, for properties based on the bulk temperature and for heating, the Dittus-Boelter equation [Boelter, Cherry, Johnson and Martinelli, Heat Transfer Notes, McGraw-Hill, New York (1965)] may be used:

$$N_{Nu} = 0.0243 N_{Re}^{0.8} N_{Pr}^{0.4} (\mu_b/\mu_w)^{0.14} \quad (5-50a)$$

For cooling, the relationship is

$$N_{Nu} = 0.0265 N_{Re}^{0.8} N_{Pr}^{0.3} (\mu_b/\mu_w)^{0.14} \quad (5-50b)$$

The Colburn correlation is

$$j_H = N_{St} N_{Pr}^{2/3} (\mu_w/\mu_b)^{0.14} = 0.023 N_{Re}^{-0.2} \quad (5-50c)$$

In Eq. (5-50c), the viscosity-ratio factor may be neglected if properties are evaluated at the film temperature $(t_b + t_w)/2$.

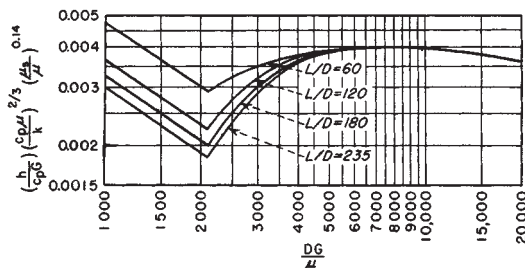


FIG. 5-8 Graphical representation of the Colburn j factor for the heating and cooling of fluids inside tubes. The curves for N_{Re} below 2100 are based on Eq. (5-40). L is the length of each pass in feet. The curve for N_{Re} above 10,000 is represented by Eq. (5-50c).

For the **transition and turbulent regions, including diameter to length effects**, Gnielinski [*Int. Chem. Eng.*, **16**, 359 (1976)] recommends a modification of an equation suggested by Petukhov and Popov [*High Temp.*, **1**, 69 (1963)]. This equation applies in the regions $0 < D/L < 1$, $0.6 < N_{Pr} < 2000$, $2300 < N_{Re} < 10^6$.

$$N_{Nu} = \frac{(f/2)(N_{Re} - 1000) N_{Pr}}{1 + 12.7(f/2)^{0.5}(N_{Pr}^{2/3} - 1)} \left(1 + \left(\frac{D}{L} \right)^{2/3} \right) \left(\frac{\mu_b}{\mu_w} \right)^{0.14} \quad (5-51a)$$

The Fanning friction f is determined by an equation recommended by Filonenko [*Teploenergetika*, **1**, 40 (1954)]

$$f = 0.25 (1.82 \log_{10} N_{Re} - 1.64)^{-2} \quad (5-51b)$$

Any other appropriate friction factor equation for smooth tubes may be used.

Approximate predictions for **rough pipes** may be obtained from Eq. (5-50c) if the right-hand term is replaced by $f/2$ for the rough pipe. For air, Nunner [*Z. Ver. Dtsch. Ing. Forsch.*, 1956, p. 455] obtains

$$\frac{(N_{Nu})_{rough}}{(N_{Nu})_{smooth}} = \frac{f_{rough}}{f_{smooth}} \quad (5-52)$$

Dippyery and Sabersky [*Int. J. Heat Mass Transfer*, **6**, 329 (1963)] present a complete discussion of the influence of roughness on heat transfer in tubes.

Dimensional Equations for Various Conditions For gases at ordinary pressures and temperatures based on $c\mu/k = 0.78$ and $\mu = (1.76)(10^{-75})$ Pa·s [0.0426 lb/(ft·h)]

$$h = bcp^{0.8}(V^{0.8}/D^{0.2}) \quad (5-53)$$

where $b = (3.04)(10^{-3})$ (SI) or $(1.44)(10^{-2})$ (U.S. customary). For air at atmospheric pressure

$$h = b(V^{0.8}/D^{0.2}) \quad (5-54)$$

where $b = 3.52$ (SI) or $(4.35)(10^{-4})$ (U.S. customary). For water [based on a temperature range of 5 to 104°C (40 to 220°F)]

$$h = 1057 (1.352 + 0.02t) (V^{0.8}/D^{0.2}) \quad (5-55a)$$

in SI units with $t = ^\circ\text{C}$, or

$$h = 0.13(1 + 0.011t)(V^{0.8}/D^{0.2}) \quad (5-55b)$$

in U.S. customary units with $t = ^\circ\text{F}$.

For organic liquids, based on $c = 2.092$ J/kg·K [0.5 Btu/(lb·°F)], $k = 0.14$ J/(m·s·K) [0.08 Btu/(h·ft·°F)], $\mu_b = (1)(10^{-3})$ Pa·s (1.0 cP), and $\rho = 810$ kg/m³ (50 lb/ft³),

$$h = b(V^{0.8}/D^{0.2}) \quad (5-56)$$

where $b = 423$ (SI) or $(5.22)(10^{-2})$ (U.S. customary). Within reasonable limits, coefficients for organic liquids are about one-third of the values obtained for water.

Entrance effects are usually not significant industrially if $L/D > 60$. Below this limit Nusselt recommended the conservative equation for $10 < L/D < 400$ and properties evaluated at bulk temperature

$$N_{Nu} = 0.036 N_{Re}^{0.8} N_{Pr}^{1/3} (L/D)^{-0.054} \quad (5-57)$$

It is common to correlate entrance effects by the equation

$$h_m/h = 1 + F(D/L) \quad (5-58)$$

where h is predicted by Eq. (5-50a) or (5-50b), and h_m is the mean coefficient for the pipe in question. Values of F are reported by Boelter, Young, and Iverson [NACA Tech. Note 1451, 1948] and tabulated by Kays and Knudsen and Katz (see "Introduction: General References"). Selected values of F are as follows:

Fully developed velocity profile	1.4
Abrupt contraction entrance	6
90° right-angle bend	7
180° round bend	6

* Equation (5-62) predicts the point of maximum velocity for laminar flow in annuli and is only an approximate equation for turbulent flow. Brighton and Jones [*Am. Soc. Mech. Eng. Basic Eng.*, **86**, 835 (1964)] and Macagno and McDougall [*Am. Inst. Chem. Eng. J.*, **12**, 437 (1966)] give more accurate equations for predicting the point of maximum velocity for turbulent flow.

For **large temperature differences** different equations are necessary and usually are specifically applicable to either gases or liquids. Gambill [*Chem. Eng.*, Aug. 28, 1967, p. 147] provides a detailed review of high-flux heat transfers to gases. He recommends

$$N_{Nu} = \frac{0.021 N_{Re}^{0.8} N_{Pr}^{0.4}}{(T_w/T_b)^{0.29 + 0.0019(L/D)}} \quad (5-59)$$

for $10 < L/D < 240$, $110 < T_b < 1560$ K ($200 < T_b < 2800^\circ\text{R}$), $1.1 < (T_w/T_b) < 8.0$, and properties evaluated at T_b . For liquids, Eq. (5-50c) is generally satisfactory.

Annuli For diameter ratios $D_2/D_1 > 0.2$, Monrad and Pelton's equation [*Trans. Am. Inst. Chem. Eng.*, **38**, 593 (1942)] is recommended for either or both the inner and outer tube:

$$N_{Nu} = 0.020 N_{Re}^{0.8} N_{Pr}^{1/3} (D_2/D_1)^{0.53} \quad (5-60a)$$

Equation (5-51a) may also be used for **smooth annuli** as follows:

$$\frac{(N_{Nu})_{ann}}{(N_{Nu})_{tube}} = \phi \left(\frac{D_1}{D_2} \right) \quad (5-60b)$$

The hydraulic diameter $D_2 - D_1$ is used in N_{Nu} , N_{Re} , and D/L is used for the annulus. The function on the right of Eq. (5-60b) is given by Petukhov and Roizen [*High Temp.*, **2**, 65 (1964)] as follows:

$$\begin{aligned} \text{Inner tube heated} & \quad 0.86 (D_1/D_2)^{-0.16} \\ \text{Outer tube heated} & \quad 1 - 0.14 (D_1/D_2)^{0.6} \end{aligned}$$

If both tubes are heated, the function is the sum of the above two functions divided by $1 + D_1/D_2$ [Stephan, *Chem. Ing. Tech.*, **34**, 207 (1962)]. The Colburn form of relationship may be employed for the individual walls of the annulus by using the individual friction factor for each wall [see Knudsen, *Am. Inst. Chem. Eng. J.*, **8**, 566 (1962)]:

$$j_{m1} = (N_{St})_1 N_{Pr}^{2/3} = f_1/2 \quad (5-61a)$$

$$j_{m2} = (N_{St})_2 N_{Pr}^{2/3} = f_2/2 \quad (5-61b)$$

Rothfus, Monrad, Sikchi, and Heideger [*Ind. Eng. Chem.*, **47**, 913 (1955)] report that the friction factor f_2 for the outer wall bears the same relation to the Reynolds number for the outer portion of the annular stream $2(r_2^2 - \lambda_m)V_0/r_2\mu$ as the friction factor for circular tubes does to the Reynolds number for circular tubes, where r_2 is the radius of the outer tube and λ_m is the position of maximum velocity in the annulus, estimated from

$$\lambda_m = \frac{r_2^2 - r_1^2}{\ln(r_2/r_1)} \quad (5-62)^*$$

To calculate the friction factor f_1 for the inner tube use the relation

$$f_1 = \frac{f_2 r_2 (\lambda_m - r_1^2)}{r_1 (r_2^2 - \lambda_m)} \quad (5-63)$$

There have been several analyses of turbulent heat transfer in annuli: for example, Deissler and Taylor (NACA Tech. Note 3451, 1955), Kays and Leung [*Int. J. Heat Mass Transfer*, **6**, 537 (1963)], Lee [*Int. J. Heat Transfer*, **11**, 509 (1968)], Sparrow, Hallman and Siegel [*Appl. Sci. Res.*, **7A**, 37 (1958)], and Johnson and Sparrow [*Am. Soc. Mech. Eng. J. Heat Transfer*, **88**, 502 (1966)]. The reader is referred to these for details of the analyses.

For **annuli containing externally finned tubes** the heat-transfer coefficients are a function of the fin configurations. Knudsen and Katz (*Fluid Dynamics and Heat Transfer*, McGraw-Hill, New York, 1958) present relationships for transverse finned tubes, spined tubes, and longitudinal finned tubes in annuli.

Noncircular Ducts Equations (5-50a) and (5-50b) may be employed for noncircular ducts by using the equivalent diameter $D_e = 4 \times$ free area per wetted perimeter. Kays and London (*Compact Heat Exchangers*, 3rd ed., McGraw-Hill, New York, 1984) give charts for various noncircular ducts encountered in compact heat exchangers.

Vibrations and pulsations generally tend to increase heat-transfer coefficients.

Example 2: Calculation of j Factors in an Annulus Calculate the heat-transfer j factors for both walls of an annulus for the following condi-

tions: $D_1 = 0.0254$ m (1.0 in); $D_2 = 0.0635$ m (2.5 in); water at 15.6°C (60°F); $\mu\rho = (1.124)(10^{-6})$ m^2/s [$(1.21)(10^{-5})$ ft^2/s]; velocity = 1.22 m/s (4 ft/s).

$$\lambda_m = \frac{0.0635^2 - 0.0254^2}{4 \ln(0.0635/0.0254)^2} = (4.621)(10^{-4}) \text{ m}^2 (0.716 \text{ in}^2)$$

$$\text{Re}_2 = \frac{2(r_2^2 - \lambda_m)V\rho}{r_2\mu} = \frac{2[(0.0318^2 - (4.621)(10^{-4})(1.22)]}{(0.0318)(1.124)(10^{-6})} = (3.74)(10^4)$$

From Eq. (5-51b), $f_2 = 0.0055$. Hence

$$j_{H2} = (N_{St})_2 N_{Pr}^{2/3} = 0.00275$$

From Eq. (5-63),

$$f_1 = \frac{(0.0055)(0.0318)[(4.621)(10^{-4}) - 0.0127^2]}{(0.0127)[(0.0318^2 - (4.621)(10^{-4})]} = 0.00754$$

from which $j_{H1} = (N_{St})_1 N_{Pr}^{2/3} = 0.00377$.

These results indicate that for this system the heat-transfer coefficient on the inner tube is about 40 percent greater than on the outer tube.

Coils For flow *inside helical coils*, Reynolds number above 10,000, multiply the value of the film coefficient obtained from the applicable equation for straight tubes by the term $(1 + 3.5 D_i/D_c)$.

For flow *inside helical coils*, Reynolds number less than 10,000, substitute the term $(D_c/D_i)^{1/2}$ for (L/D_i) where the latter appears in the applicable equation for straight tubes (frequently as part of the Graetz number).

For **flat spiral (pancake) coils**, in which the ratio D_c/D_i varies for each turn, a different value of coefficient will be obtained for each turn; a weighted average based on length per turn is used.

For flow *outside helical coils* use the equation for flow normal to a bank of tubes, in-line flow.

Finned Tubes (Extended Surface) When the film coefficient on the outside of a metal tube is much lower than that on the inside, as when steam condensing in a pipe is being used to heat air, externally finned (or extended) heating surfaces are of value in increasing substantially the rate of heat transfer per unit length of tube. The data on extended heating surfaces, for the case of air flowing outside and at right angles to the axes of a bank of finned pipes, can be represented approximately by the dimensional equation derived from

$$h_f = b \frac{V_f^{0.6}}{D_o^{0.4}} \left(\frac{p'}{p' - D_o} \right)^{0.6} \quad (5-64)$$

where $b = 5.29$ (SI) or $(5.39)(10^{-3})$ (U.S. customary); h_f is the film coefficient of heat transfer on the air side; V_f is the face velocity of the air; p' is the center-to-center spacing, m, of the tubes in a row; and D_o is the outside diameter, m, of the bare tube (diameter at the root of the fins).

In atmospheric air-cooled finned tube exchangers, the air-film coefficient from Eq. (5-64) is sometimes converted to a value based on outside bare surface as follows:

$$h_{fo} = h_f \frac{A_f + A_{uf}}{A_{of}} = h_f \frac{A_f}{A_o} \quad (5-65)$$

in which h_{fo} is the air-film coefficient based on external bare surface; h_f is the air-film coefficient based on total external surface; A_f is total external surface, and A_o is external bare surface of the unfinned tube; A_f is the area of the fins; A_{uf} is the external area of the unfinned portion of the tube; and A_{of} is area of tube before fins are attached.

Fin efficiency is defined as the ratio of the mean temperature difference from surface to fluid divided by the temperature difference from fin to fluid at the base or root of the fin. Graphs of fin efficiency for extended surfaces of various types are given by Gardner [*Trans. Am. Soc. Mech. Eng.*, **67**, 621 (1945)].

Heat-transfer coefficients for finned tubes of various types are given in a series of papers [*Trans. Am. Soc. Mech. Eng.*, **67**, 601 (1945)].

For flow of air normal to fins in the form of **short strips or pins**, Norris and Spofford [*Trans. Am. Soc. Mech. Eng.*, **64**, 489 (1942)] correlate their results for air by the dimensionless equation of Pohlhausen:

$$\frac{h_m}{c_p G_{\max}} \left(\frac{c_p \mu}{k} \right)^{2/3} = 1.0 \left(\frac{z_p G_{\max}}{\mu} \right)^{-0.5} \quad (5-66)$$

for values of $z_p G_{\max}/\mu$ ranging from 2700 to 10,000.

For the general case, the treatment suggested by Kern (*Process Heat Transfer*, McGraw-Hill, New York, 1950, p. 512) is recommended. Because of the wide variations in fin-tube construction, it is convenient to convert all film coefficients to values based on the inside bare surface of the tube. Thus to convert the film coefficient based on outside area (finned side) to a value based on inside area Kern gives the following relationship:

$$h_{fi} = (\Omega A_f + A_o)(h_f/A_i) \quad (5-67)$$

in which h_{fi} is the effective outside film coefficient based on the inside area, h_f is the outside film coefficient calculated from the applicable equation for bare tubes, A_f is the surface area of the fins, A_o is the surface area on the outside of the tube which is not finned, A_i is the inside area of the tube, and Ω is the fin efficiency defined as

$$\Omega = (\tanh mb_f)/mb_f \quad (5-68)$$

in which

$$m = (h_f p_f / ka_s)^{1/2} \text{ m}^{-1} (\text{ft}^{-1}) \quad (5-69)$$

and b_f = height of fin. The other symbols are defined as follows: p_f is the perimeter of the fin, a_s is the cross-sectional area of the fin, and k is the thermal conductivity of the material from which the fin is made.

Fin efficiencies and fin dimensions are available from manufacturers. Ratios of finned to inside surface are usually available so that the terms A_f , A_o , and A_i may be obtained from these ratios rather than from the total surface areas of the heat exchangers.

Banks of Tubes For heating and cooling of fluids flowing normal to a bank of circular tubes at least 10 rows deep the following equations are applicable:

Colburn type:

$$\frac{h}{c G_{\max}} \left(\frac{c \mu}{k} \right)^{2/3} = \frac{a}{(D_o G_{\max} / \mu)^{0.4}} = j \quad (5-70)$$

Nusselt type:

$$\frac{hD}{k} = a \left(\frac{D_o G_{\max}}{\mu} \right)^{0.6} \left(\frac{c \mu}{k} \right)^{1/3} \quad (5-71)$$

The dimensionless constant a in these equations varies depending upon conditions.

Conditions, Reynolds number > 3000	Value of a
Flow normal to apex of diamond, staggered arrangement	
No leakage	0.330
Normal leakage in baffled exchanger	0.198
Flow normal to flat side of diamond, not staggered (in-line) arrangement	
No leakage	0.260
Normal leakage in baffled exchanger	0.156

For Reynolds number less than 3000, Eq. (5-70) would give conservative results, but greater accuracy (if desired) may be obtained by using the following equation.

$$\frac{h}{c G_{\max}} \left(\frac{c \mu}{k} \right)^{2/3} = \frac{a}{(D_o G_{\max} / \mu)^m} = j \quad (5-72)$$

in which the constant a and exponent m are as follows:

Reynolds number	m	Tube pitch	Leakage	a
100–300	0.492	Staggered	None	0.695
			Normal	0.416
		In-line	None	0.548
1–100	0.590	Staggered	Normal	0.329
			None	1.086
		In-line	Normal	0.650
			None	0.855
		Normal	0.513	

The following **dimensional equations** (5-73 to 5-77) are based on flow normal to a bank of staggered tubes without leakage. Multiply the values obtained for h by 0.6 for normal leakage and, in addition, by 0.79 for in-line (not staggered) tube arrangement.

$$h = b \frac{c^{1/3} k^{2/3} \rho^{0.6} \mu^{0.6} v_{\max}^{0.6}}{\mu^{0.267} D_0^{0.4}} \quad (5-73)$$

where $b = 0.33$ (SI) or 0.261 (U.S. customary). For gases at ordinary pressures and temperatures, based on $c\mu/k = 0.78$; $\mu = (1.76)(10^{-5})$ Pa·s [0.0426 lb/(ft·h)],

$$h = bc \frac{C_{\max}^{0.6}}{D_0^{0.4}} \quad (5-74)$$

where $b = (4.82)(10^{-3})$ (SI) or 0.109 (U.S. customary). For air at atmospheric pressure

$$h = b \frac{V_{\max}^{0.6}}{D_0^{0.4}} \quad (5-75)$$

where $b = 5.33$ (SI) or $(5.44)(10^{-3})$ (U.S. customary). For water based on a temperature range 7 to 104°C (40 to 220°F)

$$h = 986(1.21 + 0.0121t) \frac{V_{\max}^{0.6}}{D_0^{0.4}} \quad (5-76a)$$

in SI units and t in °C.

$$h = 1.01(1 + 0.0067t) \frac{V_{\max}^{0.6}}{D_0^{0.4}} \quad (5-76b)$$

in U.S. customary units and t in °F. For organic liquids, based on $c = 2.22$ J/(kg·K) [0.53 Btu/(lb·°F)], $k = 0.14$ J/(m·s·K) [0.08 Btu/(h·ft·°F)], $\mu_b = (1)(10^{-3})$ Pa·s (1.0 cP), $\rho = 810$ kg/m³ (50 lb/ft³),

$$h = b \frac{V_{\max}^{0.6}}{D_0^{0.4}} \quad (5-77)$$

where $b = 400$ (SI) or 0.408 (U.S. customary).

JACKETS AND COILS OF AGITATED VESSELS

See Sec. 18.

NONNEWTONIAN FLUIDS

A wide variety of nonnewtonian fluids are encountered industrially. They may exhibit Bingham-plastic, pseudoplastic, or dilatant behavior and may or may not be thixotropic. For design of equipment to handle or process nonnewtonian fluids, the properties must usually be measured experimentally, since no generalized relationships exist to predict the properties or behavior of the fluids. Details of handling nonnewtonian fluids are described completely by Skelland (*Non-Newtonian Flow and Heat Transfer*, Wiley, New York, 1967). The generalized shear-stress rate-of-strain relationship for nonnewtonian fluids is given as

$$n' = \frac{d \ln(D \Delta P/4L)}{d \ln(8V/D)} \quad (5-78)$$

as determined from a plot of shear stress versus velocity gradient.

For **circular tubes**, $N_{Gz} > 100$, $n' > 0.1$, and laminar flow

$$(N_{Nu})_{lm} = 1.75 \delta_s^{1/3} N_{Gz}^{1/3} \quad (5-79)$$

where $\delta_s = (3n' + 1)/4n'$. When natural-convection effects are considered, Metzger and Gluck [*Chem. Eng. Sci.*, **12**, 185 (1960)] obtained the following for **horizontal tubes**:

$$(N_{Nu})_{lm} = 1.75 \delta_s^{1/3} \left[N_{Gz} + 12.6 \left(\frac{N_{Pr} N_{Cr} D}{L} \right)^{0.4} \right]^{1/3} \left(\frac{\gamma_b}{\gamma_w} \right)^{0.14} \quad (5-80)$$

where, properties are evaluated at the wall temperature, i.e., $\gamma = \rho_w K' 8^{n'-1}$ and $\tau_w = K'(8V/D)^{n'}$.

Metzner and Friend [*Ind. Eng. Chem.*, **51**, 879 (1959)] present relationships for turbulent heat transfer with nonnewtonian fluids. Relationships for heat transfer by natural convection and through laminar boundary layers are available in Skelland's book (op. cit.).

LIQUID METALS

Liquid metals constitute a class of heat-transfer media having Prandtl numbers generally below 0.01. Heat-transfer coefficients for liquid metals cannot be predicted by the usual design equations applicable to gases, water, and more viscous fluids with Prandtl numbers greater than 0.6. Relationships for predicting heat-transfer coefficients for liquid metals have been derived from solution of Eqs. (5-38a) and (5-38b). By the momentum-transfer-heat-transfer analogy, the eddy conductivity of heat is $kN_{Pr}(E_M/\mu) \approx k$ for small N_{Pr} . Thus in the solution of Eqs. (5-38a) and (5-38b) the knowledge of the thickness of various layers of flow is not critical. In fact, assumption of slug flow and constant conductivity ($=k$) across the duct gives reasonable values of heat-transfer coefficients for liquid metals.

For **constant heat flux**:

$$N_{Nu} = 5 + 0.025(N_{Re} N_{Pr})^{0.8} \quad (5-81)$$

For **constant wall temperature**:

$$N_{Nu} = 7 + 0.025(N_{Re} N_{Pr})^{0.8} \quad (5-82)$$

For $0.003 < N_{Pr} < 0.05$ and constant heat flux, Sleicher and Rouse [*Int. J. Heat Mass Transfer*, **18**, 677 (1975)] obtained the correlation

$$N_{Nu} = 6.3 + 0.0167 N_{Re}^{0.85} N_{Pr}^{0.93} \quad (5-83)$$

For **parallel plates and annuli** with $D_2/D_1 < 1.4$ and uniform heat flux, Seban [*Trans. Am. Soc. Mech. Eng.*, **72**, 789 (1950)] obtained the equation

$$N_{Nu} = 5.8 + 0.020(N_{Re} N_{Pr})^{0.8} \quad (5-84)$$

For annuli only, application of a factor of $0.70(D_2/D_1)^{0.53}$ is recommended for Eqs. (5-81) and (5-82). For more accurate semiempirical relationships for tubes, annuli, and rod bundles, refer to Dwyer [*Am. Inst. Chem. Eng. J.*, **9**, 261 (1963)].

Hsu [*Int. J. Heat Mass Transfer*, **7**, 431 (1964)] and Kalish and Dwyer [*Int. J. Heat Mass Transfer*, **10**, 1533 (1967)] discuss heat transfer to liquid metals flowing across **banks of tubes**. Hsu recommends the equations

$$N_{Nu} = 0.81 N_{Re} N_{Pr} (\phi/D)^{1/2} \quad (\text{for uniform heat flux}) \quad (5-85)$$

$$N_{Nu} = 0.096 N_{Re} N_{Pr} (\phi/D)^{1/2} \quad (\text{for cosine surface temperature}) \quad (5-86)$$

where the heat-transfer coefficient is based on the average circumferential temperature around the tubes, the Reynolds number is based on the superficial velocity through the tube bank, D is the tube outside diameter, and ϕ is a velocity potential function having the following values:

D/p'	ϕ/D square pitch	ϕ/D equilateral triangular pitch
0	2.00	2.00
0.1	2.02	2.02
0.2	2.07	2.06
0.3	2.16	2.15
0.4	2.30	2.27
0.5	2.52	2.45
0.6	2.84	2.71
0.7	3.34	3.11
0.8	4.23	3.80

Equations (5-85) and (5-86) are useful in calculating tube-surface temperatures.

Further information on liquid-metal heat transfer in tube banks is given by Hsu for spheres and elliptical rod bundles [*Int. J. Heat Mass Transfer*, **8**, 303 (1965)] and by Kalish and Dwyer for oblique flow across tube banks [*Int. J. Heat Mass Transfer*, **10**, 1533 (1967)]. For additional details of heat transfer with liquid metals for various systems see Dwyer (1968 ed., Na and Nak supplement to *Liquid Metals Handbook*) and Stein ("Liquid Metal Heat Transfer," in *Advances in Heat Transfer*, vol. 3, Academic, New York, 1966).

HEAT TRANSFER WITH CHANGE OF PHASE

In any operation in which a material undergoes a change of phase, provision must be made for the addition or removal of heat to provide for the latent heat of the change of phase plus any other sensible heating or cooling that occurs in the process. Heat may be transferred by any one or a combination of the three modes—conduction, convection, and radiation. The process involving change of phase involves mass transfer simultaneous with heat transfer.

CONDENSATION

Condensation Mechanisms Condensation occurs when a saturated vapor comes in contact with a surface whose temperature is below the saturation temperature. Normally a film of condensate is formed on the surface, and the thickness of this film, per unit of breadth, increases with increase in extent of the surface. This is called **film-type condensation**.

Another type of condensation, called **dropwise**, occurs when the wall is not uniformly wetted by the condensate, with the result that the condensate appears in many small droplets at various points on the surface. There is a growth of individual droplets, a coalescence of adjacent droplets, and finally a formation of a rivulet. Adhesive force is overcome by gravitational force, and the rivulet flows quickly to the bottom of the surface, capturing and absorbing all droplets in its path and leaving dry surface in its wake.

Film-type condensation is more common and more dependable. Dropwise condensation normally needs to be promoted by introducing an impurity into the vapor stream. Substantially higher (6 to 18 times) coefficients are obtained for dropwise condensation of steam, but design methods are not available. Therefore, the development of equations for condensation will be for the film type only.

The physical properties of the liquid, rather than those of the vapor, are used for determining the film coefficient for condensation. Nusselt [Z. Ver. Dtsch. Ing., 60, 541, 569 (1916)] derived theoretical relationships for predicting the film coefficient of heat transfer for condensation of a pure saturated vapor. A number of simplifying assumptions were used in the derivation.

The **Reynolds number** of the condensate film (falling film) is $4\Gamma/\mu$, where Γ is the weight rate of flow (loading rate) of condensate per unit perimeter $\text{kg}/(\text{s}\cdot\text{m})$ [$\text{lb}/(\text{h}\cdot\text{ft})$]. The thickness of the condensate film for Reynolds number less than 2100 is $(3\mu\Gamma/\rho^2g)^{1/3}$.

Condensation Coefficients

Vertical Tubes For the following cases Reynolds number < 2100 and is calculated by using $\Gamma = W_F/\pi D$. The **Nusselt equation** for the heat-transfer coefficient for condensate films may be written in the following ways (using liquid physical properties and where L is the cooled length and Δt is $t_{sv} - t_s$):

Colburn type:

$$\frac{h}{cG} \frac{c\mu}{k} = \frac{5.35}{4\Gamma/\mu} \quad (5-87)$$

$$\text{where } G = \frac{\Gamma}{(3\mu\Gamma/\rho^2g)^{1/3}} = \left(\frac{W_F^2 \rho^2 g}{29.6 D^2 \mu} \right)^{1/3} \text{ kg}/(\text{s}\cdot\text{m}^2) \text{ [lb}/(\text{h}\cdot\text{ft}^2)]$$

Nusselt type:

$$\frac{hL}{k} = 0.943 \left(\frac{L^3 \rho^2 g \lambda}{k\mu \Delta t} \right)^{1/4} = 0.925 \left(\frac{L^3 \rho^2 g}{\mu\Gamma} \right)^{1/3} \quad (5-88)$$

Dimensional:

$$h = b(k^3 \rho^2 D / \mu_b W_F)^{1/3} \quad (5-89)$$

where $b = 127$ (SI) or 756 (U.S. customary). For steam at atmospheric pressure, $k = 0.682 \text{ J}/(\text{m}\cdot\text{s}\cdot\text{K})$ [$0.394 \text{ Btu}/(\text{h}\cdot\text{ft}\cdot^\circ\text{F})$], $\rho = 960 \text{ kg}/\text{m}^3$ ($60 \text{ lb}/\text{ft}^3$), $\mu_b = (0.28)(10^{-3}) \text{ Pa}\cdot\text{s}$ (0.28 cP),

$$h = b(D/W_F)^{1/3} \quad (5-90)$$

where $b = 2954$ (SI) or 6978 (U.S. customary). For organic vapors at normal boiling point, $k = 0.138 \text{ J}/(\text{m}\cdot\text{s}\cdot\text{K})$ [$0.08 \text{ Btu}/(\text{h}\cdot\text{ft}\cdot^\circ\text{F})$], $\rho = 720 \text{ kg}/\text{m}^3$ ($45 \text{ lb}/\text{ft}^3$), $\mu_b = (0.35)(10^{-3}) \text{ Pa}\cdot\text{s}$ (0.35 cP),

$$h = b(D/W_F)^{1/3} \quad (5-91)$$

where $b = 457$ (SI) or 1080 (U.S. customary).

Horizontal Tubes For the following cases Reynolds number < 2100 and is calculated by using $\Gamma = W_F/2L$.

Colburn type:

$$\frac{h}{cG} \frac{c\mu}{k} = \frac{4.4}{4\Gamma/\mu} \quad (5-92)$$

$$G = \frac{\Gamma}{(3\mu\Gamma/\rho^2g)^{1/3}} = \left(\frac{W_F^2 \rho^2 g}{12L^2 \mu} \right)^{1/3} \text{ kg}/(\text{s}\cdot\text{m}^2) \text{ [lb}/(\text{h}\cdot\text{ft}^2)]$$

Nusselt type:

$$\frac{hD}{k} = 0.73 \left(\frac{D^3 \rho^2 g \lambda}{k\mu \Delta t} \right)^{1/4} = 0.76 \left(\frac{D^3 \rho^2 g}{\mu\Gamma} \right)^{1/3} \quad (5-93)^*$$

Dimensional:

$$h = b(k^3 \rho^2 L / \mu_b W_F)^{1/3} \quad (5-94)$$

where $b = 205.4$ (SI) or 534 (U.S. customary). For steam at atmospheric pressure

$$h = b(L/W_F)^{1/3} \quad (5-95)$$

where $b = 2080$ (SI) or 4920 (U.S. customary). For organic vapors at normal boiling point

$$h = b(L/W_F)^{1/3} \quad (5-96)$$

where $b = 324$ (SI) or 766 (U.S. customary).

Figure 5-9 is a nomograph for determining coefficients of heat transfer for condensation of pure vapors.

Banks of Horizontal Tubes ($N_{Re} < 2100$) In the idealized case of N tubes in a vertical row where the total condensate flows smoothly from one tube to the one beneath it, without splashing, and still in laminar flow on the tube, the mean condensing coefficient h_N for the entire row of N tubes is related to the condensing coefficient for the top tube h_1 by

$$h_N = h_1 N^{-1/4} \quad (5-97)$$

Dukler Theory The preceding expressions for condensation are based on the classical Nusselt theory. It is generally known and conceded that the film coefficients for steam and organic vapors calculated by the Nusselt theory are conservatively low. Dukler [Chem. Eng. Prog., 55, 62 (1959)] developed equations for velocity and temperature distribution in thin films on vertical walls based on expressions of Deissler (NACA Tech. Notes 2129, 1950; 2138, 1952; 3145, 1959) for the eddy viscosity and thermal conductivity near the solid boundary. According to the Dukler theory, three fixed factors must be known to establish the value of the average film coefficient: the terminal Reynolds number, the Prandtl number of the condensed phase, and a dimensionless group N_d defined as follows:

$$N_d = (0.250\mu_L^{1.173} \mu_C^{0.16} / (g^{2/3} D^2 \rho_L^{0.553} \rho_C^{0.78})) \quad (5-98)$$

Graphical relationships of these variables are available in Document 6058, ADI Auxiliary Publications Project, Library of Congress, Washington. If rigorous values for condensing-film coefficients are desired, especially if the value of N_d in Eq. (5-98) exceeds $(1)(10^{-5})$, it is suggested that these graphs be used. For the case in which interfacial shear is zero, Fig. 5-10 may be used. It is interesting to note that, according to the Dukler development, there is no definite transition Reynolds number; deviation from Nusselt theory is less at low Reynolds numbers; and when the Prandtl number of a fluid is less

* If the vapor density is significant, replace ρ^2 with $\rho(\rho_l - \rho_v)$.

No.	Substance
10	Acetic Acid
6	Acetone
1	Ammonia
5	Aniline
12	Benzene
8	Carbon Disulfide
14	Carbon Tetrachloride
9	Ethyl Acetate
4	Ethyl Alcohol
13	Ethyl Ether
3	Methyl Alcohol
11	Nitrobenzene
7	n-Propyl Alcohol
2	Water

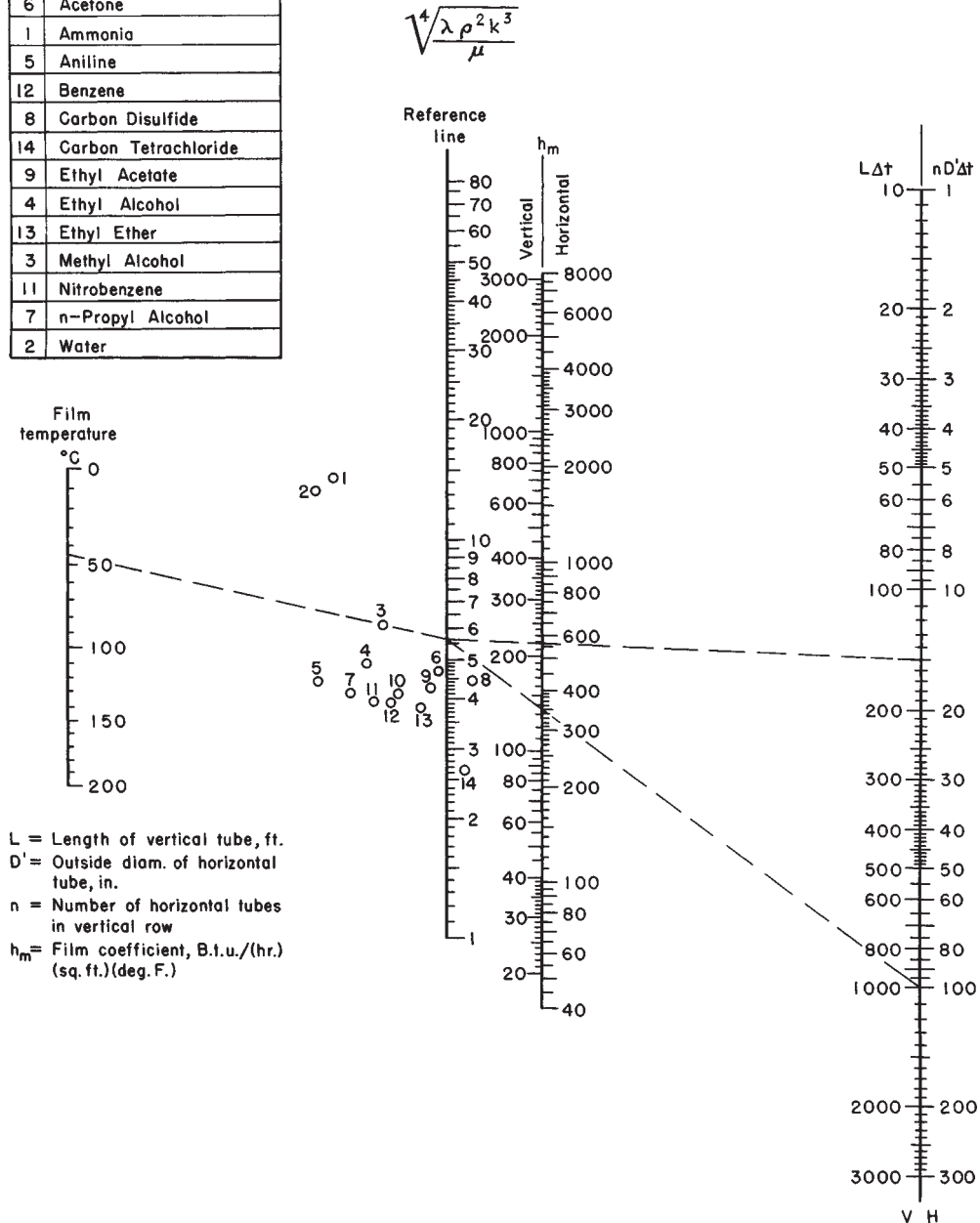


FIG. 5-9 Chart for determining film coefficient h_m for film-type condensation of pure vapor, based on Eqs. 5-88 and 5-93. For vertical tubes multiply h_m by 1.2. If $4\Gamma/\mu_f$ exceeds 2100, use Fig. 5-10. $\sqrt[4]{\lambda \rho^2 k^3 / \mu}$ is in U.S. customary units; to convert feet to meters, multiply by 0.3048; to convert inches to centimeters, multiply by 2.54; and to convert British thermal units per hour-square foot-degrees Fahrenheit to watts per square meter-kelvins, multiply by 5.6780.

than 0.4 (at Reynolds number above 1000), the predicted values for film coefficient are lower than those predicted by the Nusselt theory.

The Dukler theory is applicable for condensate films on horizontal tubes and also for falling films, in general, i.e., those not associated with condensation or vaporization processes.

Vapor Shear Controlling For vertical in-tube condensation with vapor and liquid flowing cocurrently downward, if gravity controls, Figs. 5-9 and 5-10 may be used. If vapor shear controls, the Carpenter-Colburn correlation (*General Discussion on Heat Transfer*, London, 1951, ASME, New York, p. 20) is applicable:

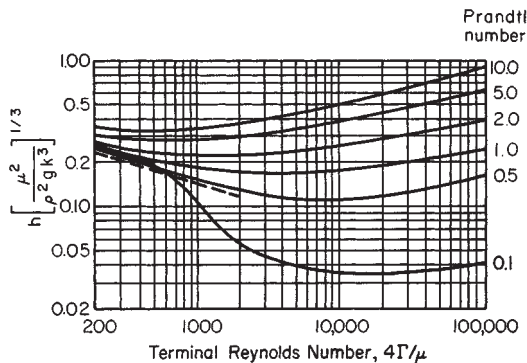


FIG. 5-10 Dukler plot showing average condensing-film coefficient as a function of physical properties of the condensate film and the terminal Reynolds number. (Dotted line indicates Nusselt theory for Reynolds number < 2100.) [Reproduced by permission from Chem. Eng. Prog., 55, 64 (1959).]

$$h\mu_l/k_l\rho_l^{1/2} = 0.065(N_{Pr})^{1/2}F_{cc}^{1/2} \quad (5-99a)$$

where $F_{cc} = fG_{vm}^2/2\rho_v$ (5-99b)

$$G_{vm} = \left(\frac{G_{vi}^2 + G_{vi}G_{vo} + G_{vo}^2}{3} \right)^{1/2} \quad (5-99c)$$

and f is the Fanning friction factor evaluated at

$$(N_{Re})_{vm} = D_i G_{vm} / \mu_v \quad (5-99d)$$

and the subscripts vi and vo refer to the vapor inlet and outlet, respectively. An alternative formulation, directly in terms of the friction factor, is

$$h = 0.065 (c\rho k f / 2\mu\rho_v)^{1/2} G_{vm} \quad (5-99e)$$

expressed in consistent units.

Another correlation for vapor-shear-controlled condensation is the Boyko-Kruzhilin correlation [Int. J. Heat Mass Transfer, 10, 361 (1967)], which gives the mean condensing coefficient for a stream between inlet quality x_i and outlet quality x_o :

$$\frac{hD_i}{k_l} = 0.024 \left(\frac{D_i G_T}{\mu_l} \right)^{0.8} (N_{Pr})_l^{0.43} \frac{\sqrt{(\rho/\rho_m)_i} + \sqrt{(\rho/\rho_m)_o}}{2} \quad (5-100a)$$

where G_T = total mass velocity in consistent units

$$\left(\frac{\rho}{\rho_m} \right)_i = 1 + \frac{\rho_l - \rho_v}{\rho_v} x_i \quad (5-100b)$$

and $\left(\frac{\rho}{\rho_m} \right)_o = 1 + \frac{\rho_l - \rho_v}{\rho_v} x_o$ (5-100c)

For horizontal in-tube condensation at low flow rates Kern's modification (Process Heat Transfer, McGraw-Hill, New York, 1950) of the Nusselt equation is valid:

$$h_m = 0.761 \left[\frac{Lk_l^3 \rho_l (\rho_l - \rho_v) g}{W_F \mu_l} \right]^{1/3} = 0.815 \left[\frac{k_l^3 \rho_l (\rho_l - \rho_v) g \lambda}{\pi \mu_l D_i \Delta t} \right]^{1/4} \quad (5-101)$$

where W_F is the total vapor condensed in one tube and Δt is $t_{wv} - t_s$. A more rigorous correlation has been proposed by Chaddock [Refriger. Eng., 65(4), 36 (1957)]. Use consistent units.

At high condensing loads, with vapor shear dominating, tube orientation has no effect, and Eq. (5-100a) may also be used for horizontal tubes.

Condensation of pure vapors under laminar conditions in the presence of noncondensable gases, interfacial resistance, superheating, variable properties, and diffusion has been analyzed by Minkowicz and Sparrow [Int. J. Heat Mass Transfer, 9, 1125 (1966)].

BOILING (VAPORIZATION) OF LIQUIDS

Boiling Mechanisms Vaporization of liquids may result from various mechanisms of heat transfer, singly or combinations thereof.

For example, vaporization may occur as a result of heat absorbed, by radiation and convection, at the surface of a pool of liquid; or as a result of heat absorbed by natural convection from a hot wall beneath the disengaging surface, in which case the vaporization takes place when the superheated liquid reaches the pool surface. Vaporization also occurs from falling films (the reverse of condensation) or from the flashing of liquids superheated by forced convection under pressure.

Pool boiling refers to the type of boiling experienced when the heating surface is surrounded by a relatively large body of fluid which is not flowing at any appreciable velocity and is agitated only by the motion of the bubbles and by natural-convection currents. Two types of pool boiling are possible: subcooled pool boiling, in which the bulk fluid temperature is below the saturation temperature, resulting in collapse of the bubbles before they reach the surface, and saturated pool boiling, with bulk temperature equal to saturation temperature, resulting in net vapor generation.

The general shape of the curve relating the heat-transfer coefficient to Δt_{fb} , the temperature driving force (difference between the wall temperature and the bulk fluid temperature) is one of the few parametric relations that are reasonably well understood. The familiar boiling curve was originally demonstrated experimentally by Nukiyama [J. Soc. Mech. Eng. (Japan), 37, 367 (1934)]. This curve points out one of the great dilemmas for boiling-equipment designers. They are faced with at least six heat-transfer regimes in pool boiling: natural convection (+), incipient nucleate boiling (+), nucleate boiling (+), transition to film boiling (-), stable film boiling (+), and film boiling with increasing radiation (+). The signs indicate the sign of the derivative $d(q/A)/d\Delta t_{fb}$. In the transition to film boiling, heat-transfer rate decreases with driving force. The regimes of greatest commercial interest are the nucleate-boiling and stable-film-boiling regimes.

Heat transfer by **nucleate boiling** is an important mechanism in the vaporization of liquids. It occurs in the vaporization of liquids in kettle-type and natural-circulation reboilers commonly used in the process industries. High rates of heat transfer per unit of area (heat flux) are obtained as a result of bubble formation at the liquid-solid interface rather than from mechanical devices external to the heat exchanger. There are available several expressions from which reasonable values of the film coefficients may be obtained.

The boiling curve, particularly in the nucleate-boiling region, is significantly affected by the temperature driving force, the total system pressure, the nature of the boiling surface, the geometry of the system, and the properties of the boiling material. In the nucleate-boiling regime, heat flux is approximately proportional to the cube of the temperature driving force. Designers in addition must know the minimum Δt (the point at which nucleate boiling begins), the critical Δt (the Δt above which transition boiling begins), and the maximum heat flux (the heat flux corresponding to the critical Δt). For designers who do not have experimental data available, the following equations may be used.

Boiling Coefficients For the nucleate-boiling coefficient the Mostinski equation [Teplenergetika, 4, 66 (1963)] may be used:

$$h = bP_c^{0.69} \left(\frac{q}{A} \right)^{0.7} \left[1.8 \left(\frac{P}{P_c} \right)^{0.17} + 4 \left(\frac{P}{P_c} \right)^{1.2} + 10 \left(\frac{P}{P_c} \right)^{10} \right] \quad (5-102)$$

where $b = (3.75)(10^{-5})(SI)$ or $(2.13)(10^{-4})$ (U.S. customary), P_c is the critical pressure and P the system pressure, q/A is the heat flux, and h is the nucleate-boiling coefficient. The McNelly equation [J. Imp. Coll. Chem. Eng. Soc., 7(18), (1953)] may also be used:

$$h = 0.225 \left(\frac{q c_l}{A \lambda} \right)^{0.69} \left(\frac{P k_l}{\sigma} \right)^{0.31} \left(\frac{\rho_l}{\rho_v} - 1 \right)^{0.33} \quad (5-103)$$

where c_l is the liquid heat capacity, λ is the latent heat, P is the system pressure, k_l is the thermal conductivity of the liquid, and σ is the surface tension.

An equation of the Nusselt type has been suggested by Rohsenow [Trans. Am. Soc. Mech. Eng., 74, 969 (1952)].

$$hD/k = C_s (DG/\mu)^{2/3} (c\mu/k)^{-0.7} \quad (5-104a)$$

in which the variables assume the following form:

$$\frac{h\beta'}{k} \left[\frac{g_c \sigma}{g(\rho_l - \rho_v)} \right]^{1/2} = C_s \left[\frac{\beta'}{\mu} \left(\frac{g_c \sigma}{g(\rho_l - \rho_v)} \right)^{1/2} \frac{W}{A} \right]^{2/3} \left(\frac{c\mu}{k} \right)^{-0.7} \quad (5-104b)$$

The coefficient C_r is not truly constant but varies from 0.006 to 0.015.^{*} It is possible that the nature of the surface is partly responsible for the variation in the constant. The only factor in Eq. (5-104b) not readily available is the value of the contact angle β' .

Another Nusselt-type equation has been proposed by Forster and Zuber:[†]

$$N_{Nu} = 0.0015 N_{Re}^{0.62} N_{Pr}^{1/3} \quad (5-105)$$

which takes the following form:

$$\frac{c\rho_L \sqrt{\pi\alpha}}{k\rho_c} \frac{W}{A} \left(\frac{2\sigma}{\Delta p}\right)^{1/2} \left(\frac{\rho_L}{\Delta p g_c}\right)^{1/4} = 0.0015 \left[\frac{\rho_L}{\mu} \left(\frac{c\rho_L \Delta T \sqrt{\pi\alpha}}{\lambda\rho_c} \right)^2 \right]^{0.62} \left(\frac{c\mu}{k}\right)^{1/2} \quad (5-106)$$

where $\alpha = k/\rho c$ (all liquid properties)

Δp = pressure of the vapor in a bubble minus saturation pressure of a flat liquid surface

Equations (5-104b) and (5-106) have been arranged in dimensional form by Westwater.

The numerical constant may be adjusted to suit any particular set of data if one desires to use a certain criterion. However, surface conditions vary so greatly that deviations may be as large as ± 25 percent from results obtained.

The **maximum heat flux** may be predicted by the Kutateladse-Zuber [*Trans. Am. Soc. Mech. Eng.*, **80**, 711 (1958)] relationship, using consistent units:

$$\left(\frac{q}{A}\right)_{\max} = 0.18 g_c^{1/4} \rho_c \lambda \left[\frac{(\rho_l - \rho_v) \sigma g_c}{\rho_v^2} \right]^{1/4} \quad (5-107)$$

Alternatively, Mostinski presented an equation which approximately represents the Cichelli-Bonilla [*Trans. Am. Inst. Chem. Eng.*, **41**, 755 (1945)] correlation:

$$\frac{(q/A)_{\max}}{P_c} = b \left(\frac{P}{P_c}\right)^{0.35} \left(1 - \frac{P}{P_c}\right)^{0.9} \quad (5-108)$$

where $b = 0.368$ (SI) or 5.58 (U.S. customary); P_c is the critical pressure, Pa absolute; P is the system pressure; and $(q/A)_{\max}$ is the maximum heat flux.

The lower limit of applicability of the nucleate-boiling equations is from 0.1 to 0.2 of the maximum limit and depends upon the magnitude of natural-convection heat transfer for the liquid. The best method of determining the lower limit is to plot two curves: one of h versus Δt for natural convection, the other of h versus Δt for nucleate boiling. The intersection of these two curves may be considered the lower limit of applicability of the equations.

These equations apply to single tubes or to flat surfaces in a large pool. In tube bundles the equations are only approximate, and designers must rely upon experiment. Palen and Small [*Hydrocarbon Process.*, **43**(11), 199 (1964)] have shown the effect of tube-bundle size on maximum heat flux.

$$\left(\frac{q}{A}\right)_{\max} = b \frac{p}{D_o \sqrt{N_T}} \rho_c \lambda \left[\frac{g\sigma(\rho_l - \rho_v)}{\rho_v^2} \right]^{1/4} \quad (5-109)$$

where $b = 0.43$ (SI) or 61.6 (U.S. customary), p is the tube pitch, D_o is the tube outside diameter, and N_T is the number of tubes (twice the number of complete tubes for U-tube bundles).

For **film boiling**, Bromley's [*Chem. Eng. Prog.*, **46**, 221 (1950)] correlation may be used:

$$h = b \left[\frac{k_v^3 (\rho_l - \rho_v) \rho_v g}{\mu_v D_o \Delta t_b} \right]^{1/4} \quad (5-110)$$

where $b = 4.306$ (SI) or 0.620 (U.S. customary). Katz, Myers, and Balekjian [*Pet. Refiner*, **34**(2), 113 (1955)] report boiling heat-transfer coefficients on finned tubes.

HEAT TRANSFER BY RADIATION

GENERAL REFERENCES: Much of the pertinent literature on radiative heat transfer has been surveyed in the following texts: Goody, *Atmospheric Radiation*, Clarendon Press, Oxford, 1964. Sparrow and Cess, *Radiation Heat Transfer*, Brooks/Cole Publishing Company, Belmont, Calif., 1966. Hottel and Sarofim, *Radiative Transfer*, McGraw-Hill, New York, 1967. Love, *Radiative Heat Transfer*, Merrill, Columbus, 1968. Siegel and Howell, *Thermal Radiation Heat Transfer*, NASA SP-164, GPO, Washington, 1968. Edwards, *Radiation Heat Transfer Notes*, Hemisphere Publishing Corp., 1981; Howell and Siegel, *Thermal Radiative Heat Transfer*, McGraw-Hill, 3d ed., 1992; Brewster, *Thermal Radiative Transfer and Properties*, Wiley, 1992; Modest, *Radiative Heat Transfer*, McGraw-Hill, 1993.

Additional sources are the *Journal of Applied Optics* and the *Journal of the Optical Society of America*, particularly for surface properties; the *Journal of Quantitative Spectroscopy and Radiative Transfer* for gas properties; the *Journal of Heat Transfer* and the *International Journal of Heat and Mass Transfer* for broad coverage; and the *Journal of the Institute of Energy* for applications to industrial furnaces.

Thermal radiation—electromagnetic energy in transport—is emitted within matter excited by temperature; it is absorbed in other matter at distances from the source which depend on the mean free path of the photons emitted. The ratio of the mean free path involved in an energy-transport process to a characteristic dimension of the system of interest determines the mathematical structure of the formulation. In molecular conduction this ratio is minute (unless the system or the density of matter is minute, which is the case of free molecular flow), and a differential equation of energy diffusion is involved. In gas radiation the ratio is generally large enough to give rise to an integral equation, with an unknown function inside the integral. Solids gener-

ally have small enough photon mean free paths (high enough absorption coefficients) for the radiation escaping through the surface to have originated close to the surface; radiative loss is then identifiable with its surface temperature, but an integral equation is still involved if all the surfaces of an enclosure filled with a diathermanous medium like air are not specified as to temperature or are not black.

Radiation differs from conduction and convection not only in mathematical structure but in its much higher sensitivity to temperature. It is of dominating importance in furnaces because of their temperature, and in cryogenic insulation because of the vacuum existing between particles. The temperature at which it accounts for roughly half of the total heat loss from a surface in air depends on such factors as surface emissivity and the convection coefficient. For pipes in free convection, this is room temperature; for fine wires of low emissivity it is above red heat. Gases at combustion-chamber temperatures lose more than 90 percent of their energy by radiation from the carbon dioxide, water vapor, and particulate matter.

NOMENCLATURE FOR RADIATIVE TRANSFER

Terms that are defined at specific places in the text are excluded.

a = effective energy fraction of blackbody spectrum in which a nongray gas absorbs.

A = area.

c = number concentration of particles in a cloud.

c_1, c_2 = first and second Planck-law constants.

^{*} Reported by Westwater in Drew and Hoopes, *Advances in Chemical Engineering*, vol. I, Academic, New York, 1956, p. 15.

[†] Forster, *J. Appl. Phys.*, **25**, 1067 (1954); Forster and Zuber, *J. Appl. Phys.*, **25**, 474 (1954); Forster and Zuber, Conference on Nuclear Engineering, University of California, Los Angeles, 1955; excellent treatise on boiling of liquids by Westwater in Drew and Hoopes, *Advances in Chemical Engineering*, vol. I, Academic, New York, 1956.

- C = axis-to-axis distance of separation of tubes.
 C_b = mean specific heat of combustion products from base temperature T_b to leaving-gas temperature T_E .
 C = cold-surface fraction of a furnace enclosure.
 C_W = correction factor for pressure broadening of radiation from water vapor.
 d = particle diameter.
 D = tube diameter; characteristic dimension; dimensionless firing density.
 D' = reduced firing density.
 E = hemispherical emissive power of a blackbody.
 f = fraction of blackbody radiation lying below λ .
 f_v = volume fraction of space occupied by particles.
 F = direct view factor; F_{ij} , fraction of isotropic radiation from A_i intercepted directly by A_j .
 \bar{F} = total view factor from black source to black sink, with allowance for refractory surfaces (subscripts identify source and sink).
 \mathcal{F}_{ij} = total view factor, radiation from i to j both directly and indirectly, expressed as fraction of blackbody radiation from A_i .
 \overline{gs} = direct-exchange area between gas volume and surface.
 GS = total-exchange area between gas and surface; subscript R indicates allowance for radiatively adiabatic surfaces.
 h = coefficient of convective heat transfer.
 \bar{H} = enthalpy of fuel plus air entering combustion chamber.
 I = intensity, radiant-energy-flux density per unit solid angle of divergence.
 \bar{ij} = shorthand for $\overline{s_i s_j}$.
 k = absorption or emission coefficient; or thermal conductivity.
 K = constant defined in connection with Eq. (5-147).
 L = mean beam length; L_0 , at vanishingly small optical thickness; L_m , average value.
 L = wall-loss group.
 L_c = dimensionless convective loss.
 L_o = dimensionless wall-opening loss.
 L_r = dimensionless refractory-wall loss.
 \dot{m} = mass flow rate.
 n = refractive index.
 p = partial pressure, atm.; subscript c , CO₂; subscript w , water vapor.
 P = total pressure atm.
 q = heat-flux density, energy per time-area.
 Q = heat flux, energy per time.
 r = separating distance; or electrical resistivity; or refractory (radiatively adiabatic) surface.
 $\overline{ss} \equiv AF$, direct-exchange area (subscripts identify surface zones).
 $SS \equiv A\mathcal{F}$, total-exchange area.
 T = absolute temperature. Subscript 1 (or G), radiating surface (or gas) temperature; subscript E , exit-gas; subscript o , base temperature; subscript F , pseudoadiabatic flame temperature based on C_p , averaged from T_o to T_E .
 U = overall coefficient of heat transfer, gas convection to refractory wall to ambient air.
 W = total leaving-flux density (also radiosity).
 α = absorptivity or absorbance; α_{12} , absorbance of surface 1 for radiation from surface 2.
 Δ = difference between radiating temperature and leaving-gas temperature divided by the pseudoadiabatic flame temperature T_F .
 ϵ = emissivity or emittance.
 η = thermal efficiency. Subscript G , gas-side; subscript 1, sink-side.
 θ = polar angle.
 λ = wavelength.
 μm = micrometer (m^{-6}).
 ρ = reflectance; ρ_s , specular reflectance.
 σ = Stefan-Boltzmann constant.
 τ = ratio of temperature to T_F . Subscript G , gas; subscript 1 sink; subscript o , base.
 τ = transmittance.
 ω = solid angle.
 ω = albedo of a surface.

NATURE OF THERMAL RADIATION

Consider a pencil of radiation, defined as all the rays passing through each of two small widely separated areas dA_1 and dA_2 . The rays at dA_1 will have a solid angle of divergence $d\Omega_1$ equal to the apparent area of dA_2 viewed from dA_1 , divided by the square of the separating distance. Let the normal to dA_1 make the angle θ_1 with the pencil. The flux density q (energy per time-area) normal to the beam and per unit solid angle of its divergence is called the intensity I , and the flux $d\dot{Q}_1$ (energy per time) through the area dA_1 (of apparent area $dA_1 \cos \theta_1$ normal to the beam) is therefore given by

$$d\dot{Q}_1 = dA_1(\cos \theta_1)q = I dA_1(\cos \theta_1) d\Omega_1 \quad (5-111)$$

The intensity I along a pencil, in the absence of absorption or scatter, is constant (unless the beam passes into a medium of different refractive index n ; then $I_1/n_1^2 = I_2/n_2^2$).

The emissive power* of a surface is the flux density (energy per time-surface area) due to emission from it throughout a hemisphere. If the intensity I of emission from a surface is independent of the angle of emission, Eq. (5-111) may be integrated to show that the surface emissive power is πI , though the emission is throughout 2π sr.

Blackbody Radiation Engineering calculations of thermal radiation from surfaces are best keyed to the radiation characteristics of the blackbody, or ideal radiator. The characteristic properties of a blackbody are that it absorbs all the radiation incident on its surface and that the quality and intensity of the radiation it emits are completely determined by its temperature. The total radiative flux throughout a hemisphere from a black surface of area A and absolute temperature T is given by the Stefan-Boltzmann law:

$$\dot{Q} = A\sigma T^4 \quad \text{or} \quad q = \sigma T^4 \quad (5-112)$$

The Stefan-Boltzmann constant σ has the value $(0.1713)(10^{-8})$ Btu/(ft² · h · °R⁴); $(1.00)(10^{-8})$ CHU/(ft² · h · K⁴); $(4.88)(10^{-8})$ kcal/(m² · h · K⁴); $(1.356)(10^{-12})$ cal (cm² · s · K⁴); $(5.67)(10^{-12})$ W/(cm² · K⁴); $(5.67)(10^{-8})$ W/(m² · K⁴); or in terms of Planck constants, $c_1(\pi/c_2)^{4/15}$. From the definition of emissive power, σT^4 is the total emissive power of a blackbody, called E ; the intensity I_B of blackbody emission is E/π or $\sigma T^4/\pi$.

The spectral distribution of energy flux from a black body is expressed by Planck's law:

$$E_\lambda d\lambda = (2\pi hc^2 n^2 \lambda^{-5}) / (e^{hc/\lambda kT} - 1) d\lambda \quad (5-113)$$

$$\equiv (n^2 c_1 \lambda^{-5}) / (e^{c_2/\lambda T} - 1) d\lambda \quad (5-114)$$

where $E_\lambda d\lambda$ is the hemispherical flux density lying in the wavelength range λ to $\lambda + d\lambda$; h is Planck's constant, $(6.6256)(10^{-27})$ erg · s; c is the velocity of light in vacuo, $(2.9979)(10^{10})$ cm/s; k is the Boltzmann constant, $(1.3805)(10^{-16})$ erg/K; λ is the wavelength measured in vacuo; and n is the refractive index of the emitter ($\lambda = n\lambda_m$, where λ_m is the wavelength measured in the medium; $E_\lambda d\lambda = E_{\lambda m} d\lambda_m$, where E_λ and $E_{\lambda m}$ are both measured in the medium; engineers commonly use E_λ). Equation (10-191) may be written

$$\frac{E_\lambda}{n^2 T^5} = \frac{c_1(\lambda T)^{-5}}{e^{c_2/\lambda T} - 1} \quad (5-115)$$

The first and second Planck-law constants c_1 and c_2 are respectively $(3.740)(10^{-16})$ (J · m²)/s and $(1.4388)(10^{-2})$ m · K. The term $E_\lambda/n^2 T^5$, clearly a function only of the product λT , is given in Fig. 5-11 which may be visualized as the monochromatic emissive power versus wavelength measured in vacuo of a black surface at 1 K discharging in vacuo.

The wavelength of maximum intensity is seen to be inversely proportional to the absolute temperature. The relation is known as **Wien's displacement law**: $\lambda_{\text{max}} T = (2.898)(10^{-3})$ m · K. This can be misleading, however, since the wavelength of maximum intensity depends on whether intensity is defined in terms of wavelength interval or frequency interval. More useful displacement laws refer to the value of λT corresponding to maximum energy per unit fractional change in wavelength or frequency $[(3.67)(10^{-3})$ m · K] or to the value of λT corresponding to half of the energy $[(4.11)(10^{-3})$ m · K]. Figure

* Various called, in the literature, emittance, total hemispherical intensity, or radiant flux density.

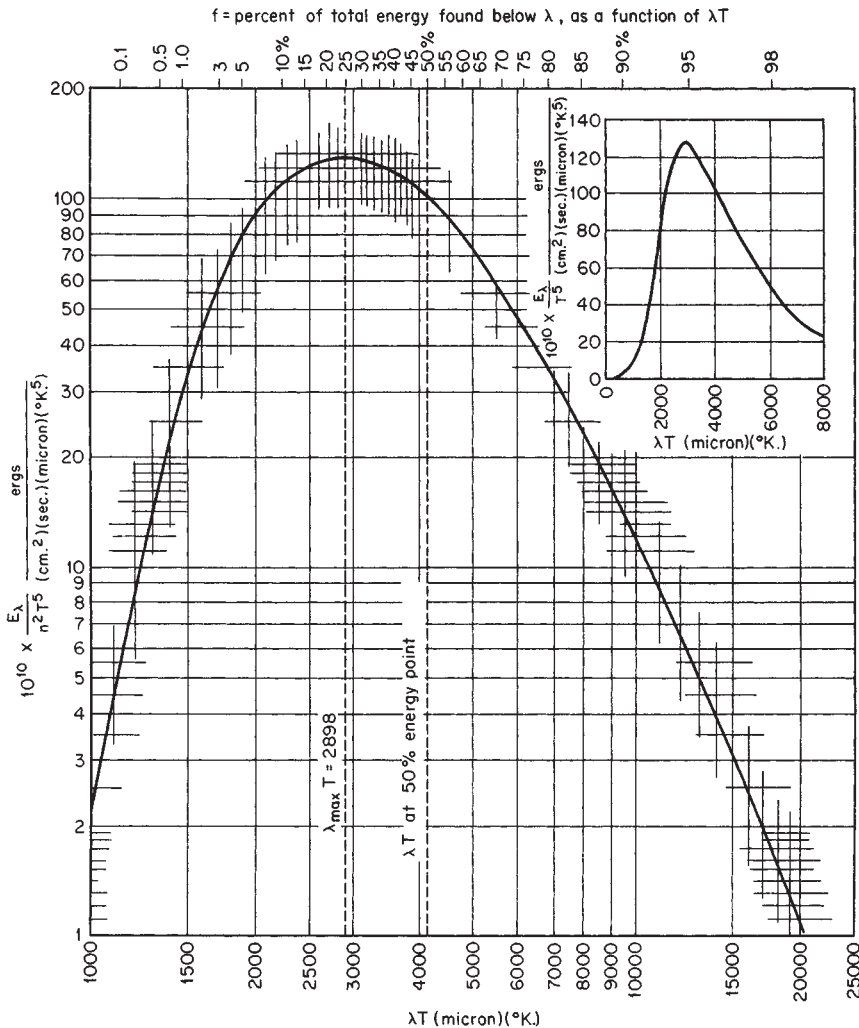


FIG. 5-11 Distribution of energy in the spectrum of a blackbody. To convert microns to micrometers, multiply by unity. To convert ergs per square centimeter-second-micron- K^5 to watts per square meter, per meter, per K^5 , multiply by 10^{-3} .

5-11 carries, at the top, a scale giving the fraction f of the total energy in the spectrum that lies below λT . A generalization useful for identifying the spectral range of greatest interest in evaluations of radiative transfer is that roughly half of the energy from a black surface lies within the twofold range of λT geometrically centered on 3.67×10^{-3} , i.e., from $\lambda T = (3.67/\sqrt{2})(10^{-3})$ to $(3.67 \times \sqrt{2})(10^{-3})$ m·K.

One limiting form of the Planck equation, approached as $\lambda T \rightarrow 0$, is the **Wien equation** [Eqs. (5-113) and (5-114)] with the 1 missing in the denominator. The error is less than 1 percent when $\lambda T < (3)(10^{-3})$ m·K or when $T < 4800$ K if an optical pyrometer with red screen ($\lambda = 0.65 \mu\text{m}$) is used.

RADIATIVE EXCHANGE BETWEEN SURFACES OF SOLIDS

Emittance and Absorptance The ratio of the total radiating power of a real surface to that of a black surface at the same temperature is called the **emittance** of the surface (for a perfectly plane surface, the **emissivity**), designated by ϵ . Subscripts λ , θ , and n may be assigned to differentiate monochromatic, directional, and surface-normal values respectively from the total hemispherical value. If radi-

ation is incident on a surface, the fraction absorbed is called the **absorptance (absorptivity)**, a term to which two subscripts may be appended, the first to identify the temperature of the surface and the second to identify the spectral energy distribution of the surface.

According to **Kirchhoff's law**, the emissivity and absorptivity of a surface in surroundings at its own temperature are the same for both monochromatic and total radiation. When the temperatures of the surface and its surroundings differ, the total emissivity and absorptivity of the surface often are found to be different, but, because absorptivity is substantially independent of irradiation density, the monochromatic emissivity and absorptivity of surfaces are for all practical purposes the same. The difference between total emissivity and absorptivity depends on the variation, with wavelength, of ϵ_λ and on the difference between the emitter temperature and the effective source temperature.

Consider radiative exchange between a body of area A_1 and temperature T_1 and black surroundings at T_2 . The net interchange is given by

$$\begin{aligned} \dot{Q}_{1=2} &= A_1 \int_0^\infty [\epsilon_\lambda E_\lambda(T_1) - \alpha_\lambda E_\lambda(T_2)] d\lambda \\ &= A_1(\epsilon_1 \sigma T_1^4 - \alpha_{12} \sigma T_2^4) \end{aligned} \quad (5-116)$$

where $\epsilon_1 = \int_0^1 \epsilon_\lambda df_{\lambda T_1}$ (5-117)

and $\alpha_{12} = \int_0^1 \epsilon_\lambda df_{\lambda T_2}$ (5-118)

The value of ϵ_1 (or α_{12} , the absorptivity of surface A_1 for blackbody radiation at T_2) is the area under a curve of ϵ_λ versus f , the latter read as a function of λT_1 (or λT_2) from the top ordinate of Fig. 5-11. For a gray surface, $\epsilon_1 = \alpha_{12} = \epsilon_\lambda$. A selective surface is one whose ϵ_λ changes dramatically with wavelength. If this change is unidirectional, ϵ_1 and α_{12} are, according to Eqs. (5-116) to (5-118), markedly different when the absolute-temperature ratio is far from 1; e.g., when $T_1 = 294$ K (530°R; ambient temperature), and $T_2 = 6000$ K (10,800°R; effective solar temperature), $\epsilon_1 = 0.9$ and $\alpha_{12} = 0.1$ to 0.2 for a white paint, but ϵ_1 can be as low as 0.12 and α_{12} above 0.9 for a thin layer of copper oxide on bright aluminum.

The effect of radiation-source temperature on the low-temperature absorptivity of a number of additional materials is presented in Fig. 5-12. It will be noted that polished aluminum (curve 15) and anodized (surface-oxidized) aluminum (curve 13), representative of metals and nonmetals respectively, respond oppositely to a change in the temperature of the radiation source. The absorptance of surfaces for solar

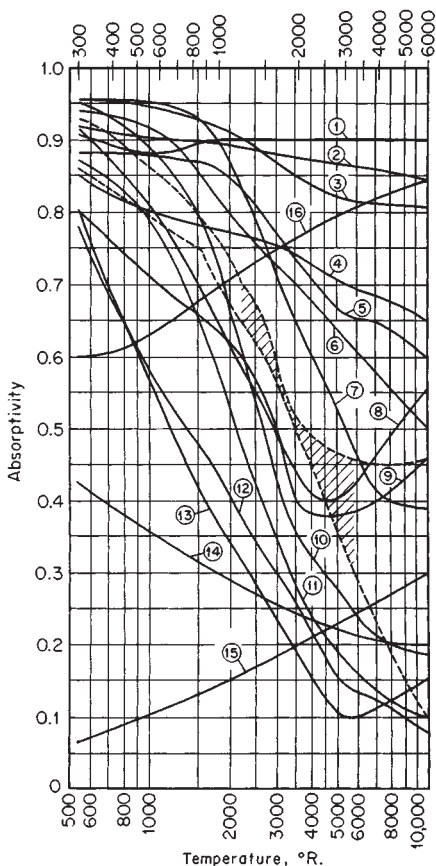


FIG. 5-12 Variation of absorptivity with temperature of radiation source. (1) Slate composition roofing. (2) Linoleum, red brown. (3) Asbestos slate. (4) Soft rubber, gray. (5) Concrete. (6) Porcelain. (7) Vitreous enamel, white. (8) Red brick. (9) Cork. (10) White dutch tile. (11) White chamotte. (12) MgO, evaporated. (13) Anodized aluminum. (14) Aluminum paint. (15) Polished aluminum. (16) Graphite. The two dashed lines bound the limits of data on gray paving brick, asbestos paper, wood, various cloths, plaster of paris, lithopone, and paper. To convert degrees Rankine to kelvins, multiply by (5.556/10)⁻¹.

radiation may be read from the right of Fig. 10-45, if solar radiation is assumed to consist of blackbody radiation from a source at 5800 K (10,440°R).

Although values of emittance and absorptance depend in very complex ways on the real and imaginary components of the refractive index and on the geometrical structure of the surface layer, the generalizations that follow are possible.

Polished Metals

1. ϵ_λ in the infrared is governed by free-electron contributions, is quite low, and is a function of the resistivity-wavelength quotient r/λ (Fig. 5-13). For $\lambda > 8\mu\text{m}$, $\epsilon_{\lambda,n}$ is approximately $0.0365 \sqrt{r/\lambda}$, where r is in ohm-meters and λ in micrometers (the Drude or Hagen-Rubens relation). At shorter wavelengths, bound-electron contributions become significant and ϵ_λ increases, sometimes exhibiting maxima; values of 0.4 to 0.8 are common in the visible spectrum (0.4 to 0.7 μm). ϵ_λ is approximately proportional to the square root of the absolute temperature ($\epsilon_\lambda \propto \sqrt{r}$, and $r \propto T$) in the far infrared ($\lambda > 8\mu\text{m}$), is temperature-insensitive in the near infrared (0.7 to 1.5 μm), and decreases slightly as temperature increases in the visible.

2. Total emittance is substantially proportional to absolute temperature; at moderate temperature, $\epsilon_n = 0.058T\sqrt{rT}$, where T is in kelvin.

3. The total absorptance of a metal at T_1 for radiation from a black or gray source at T_2 is equal to the emissivity evaluated at the geometric mean of T_1 and T_2 . Figure 5-13 gives values of ϵ_λ , $\epsilon_{\lambda,n}$, and their ratio as a function of r/λ (dashed lines); and total emissivities ϵ , ϵ_n , and their ratio as a function of rT (solid lines). Although the figure is based on free-electron contributions to emissivity in the far infrared, the relations for total emissivity are remarkably good even at high temperatures. Unless extraordinary pains are taken to prevent oxidation, however, a metallic surface may exhibit several times the emittance or absorptance of a polished specimen. The emittance of iron and steel, for example, varies widely with degree of oxidation and roughness; clean metallic surfaces have an emittance of from 0.05 to 0.45 at ambient temperatures to 0.4 to 0.7 at high temperatures; oxidized and/or rough surfaces range from 0.6 to 0.95 at low temperatures to 0.9 to 0.95 at high temperatures.

Refractory Materials Grain size and concentration of trace impurities are important.

1. Most refractory materials have an ϵ_λ of 0.8 to 1.0 at wavelengths beyond 2 to 4 μm ; ϵ_λ decreases rapidly toward shorter wavelengths for materials that are white in the visible but retains its high value for black materials such as FeO and Cr₂O₃. Small concentrations of FeO

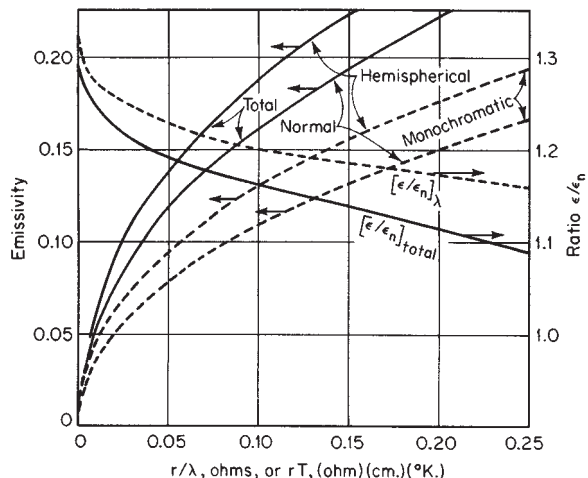


FIG. 5-13 Hemispherical and normal emissivities of metals and their ratio. Dashed lines: monochromatic (spectral) values versus r/λ . Solid lines: total values versus rT . To convert ohm-centimeter-kelvins to ohm-meter-kelvins, multiply by 10^{-2} .

and Cr_2O_3 or other colored oxides can cause marked increases in the emittance of materials that normally are white. The sensitivity of the emittance of refractory oxides to small additions of absorbing materials is demonstrated by the results of calculations, shown in Fig. 5-14, of the emittance of a semi-infinite absorbing-scattering medium as a function of its albedo: the ratio of the scatter coefficient to the sum of scatter and absorption coefficients. The results, pertinent to the radiative properties of fibrous materials, paints, oxide coatings, and refractories, show that when absorption accounts for only 0.5 percent (10 percent) of the total attenuation within the medium, the emittance is greater than 0.15 (0.5). ϵ_h for refractory materials varies little with temperature, with the exception of some white oxides which at high temperatures become good emitters in the visible spectrum as a consequence of the induced electronic transitions.

2. Refractory materials generally have a total emittance which is high (0.7 to 1.0) at ambient temperatures and decreases with increase in temperature; a change from 1000 to 1570°C (1850 to 2850°F) may cause a decrease in ϵ of one-fourth to one-third.

3. The emittance and absorptance increase with increase in grain size over a grain-size range of 1 to 200 μm .

4. The ratio ϵ/ϵ_n of hemispherical to normal emissivity of polished surfaces varies with refractive index n from 1 at $n = 1.0$ to 0.93 at $n = 1.5$ (common glass) and back to 0.96 at $n = 3$.

5. The ratio ϵ/ϵ_n for a surface composed of particulate matter which scatters isotropically varies with ϵ from 1 when $\epsilon = 1$ to 0.8 when $\epsilon = 0.07$ (see Fig. 5-14).

6. The total absorptance shows a decrease with increase in temperature of the radiation source similar to the decrease in emittance with increase in the specimen temperature.

Figure 5-12 shows a regular variation of α_{12} with T_2 . When T_2 is not very different from T_1 , α_{12} may be expressed as $\epsilon_1(T_2/T_1)^m$. It may be shown that Eq. (5-116) is then approximated by

$$\dot{Q}_{1,\text{net}} = \sigma A_1 \epsilon_{\text{av}} \left(1 + \frac{m}{4} \right) (T_1^4 - T_2^4) \quad (5-119)$$

where ϵ_{av} is evaluated at the arithmetic mean of T_1 and T_2 . For metals m is about 0.5; for nonmetals it is small and negative.

Table 5-6, based on a critical evaluation of early data, is illustrative of the emittance of materials encountered in engineering practice; it shows the wide variation possible in the emissivity of a particular material due to variations in surface roughness and thermal pretreatment. (With few exceptions the values refer to emission normal to the surface; see above for conversion to hemispherical values.) More recent data support the range of emittance values given in Table 5-6 and their dependence on surface conditions. Extensive compilations of data are provided by Schmidt and Furthmann (*Mitt. Kaiser-Wilhelm-Inst. Eisenforsch.*, 109, 225), covering data to 1928; by Gubareff, Jansen, and Torborg [*Thermal Radiation Properties Sur-*

vey, Honeywell Research Center, Minneapolis, 1960), covering data to 1940; and by Goldsmith, Waterman, and Hirschhorn [*Thermophysical Properties of Matter*, Purdue University (Touloukian, Ed.), Plenum, 1970].

For opaque materials, the reflectance ρ is the complement of the absorptance. The directional distribution of the reflected radiation depends on the material, its degree of roughness or grain size, and, if a metal, its state of oxidation. Polished surfaces of homogeneous materials reflect specularly. In contrast, the intensity of the radiation reflected from a perfectly diffuse, or Lambert, surface is independent of direction. The directional distribution of reflectance of many oxidized metals, refractory materials, and natural products approximates that of a perfectly diffuse reflector. A better model, adequate for many calculational purposes, is achieved by assuming that the total reflectance ρ is the sum of diffuse and specular components ρ_D and ρ_S .

Black-Surface Enclosures

View Factor and Direct-Exchange Area When several surfaces are present, the need arises for evaluating a geometrical factor F_i , called the direct view factor. In the following discussion, restriction is to black surfaces, the intensity from which is independent of angle of emission. Define F_{12} as the fraction of the radiation leaving surface A_1 in all directions which is intercepted by surface A_2 . Since the net interchange between A_1 and A_2 must be zero when their temperatures are alike, it follows that $A_1 F_{12} = A_2 F_{21}$. This product, having the dimensions of area, is called the direct-exchange area and is designated for brevity by $\overline{12}$ ($\equiv 21$). It is sometimes designated $s_1 s_2$. Clearly, $11 + 12 + 13 + \dots = A_1$; and when A_1 cannot "see" itself, $11 = 0$.

From Eq. (5-111) and the definition of F :

$$\begin{aligned} A_1 F_{12} &\equiv s_1 s_2 \equiv \frac{Q_{1-2}}{E_1} = \int_{A_1} \int_{A_2} \frac{dA_1 (\cos \theta_1) d\Omega_1}{\pi} \\ &= \int_{A_1} \int_{A_2} \frac{dA_1 (\cos \theta_1) dA_2 (\cos \theta_2)}{\pi r^2} \end{aligned} \quad (5-120)$$

where $A(\cos \theta)$ is the projection of A normal to r , the line connecting dA_1 and dA_2 . Values of $s_1 s_2$ (or of F_{12}) may be obtained by integrating either Eq. (5-120) or an equivalent contour integral (see Hottel and Sarofim, *Radiative Transfer*, McGraw-Hill, New York, 1967, chap. 2). Such values are given for opposed parallel disks or rectangles in Fig. 5-15. For rectangles of dimensions L_1 and L_2 , $F \cong \sqrt{F_1 F_2}$, where F_1 and F_2 are for squares of sides L_1 and L_2 . The view factor for rectangles in perpendicular planes and having a common edge length x and ratios Y and Z of widths to common length is given by

$$F_{YZ} = \frac{1}{\pi Y} \left[\frac{1}{4} \ln \left[(1+Y^2) \left(\frac{Y^2}{1+Y^2} \right)^{Y^2} \left(\frac{Z^2}{Y^2+Z^2} \right)^{Z^2} \left(\frac{1+Z^2}{1+Y^2+Z^2} \right)^{1-Y^2-Z^2} \right] \right. \\ \left. + Y \tan^{-1} \frac{1}{Y} + Z \tan^{-1} \frac{1}{Z} - \sqrt{Y^2+Z^2} \tan^{-1} \frac{1}{\sqrt{Y^2+Z^2}} \right] \quad (5-121)$$

The direct-exchange area is given by

$$\overline{s_1 s_2} = \frac{x^2}{\pi} \quad (5-122)$$

When the maximum dimensions of each of two plane surfaces is small relative to their center-to-center separating distance r , Eq. (5-120) gives

$$\overline{12} = \frac{A_1 (\cos \theta_1) A_2 (\cos \theta_2)}{\pi r^2} \quad (5-123)$$

and when, in addition, the normals to A_1 and A_2 are in a common plane,

$$\overline{12} = A_1 A_2 n_1 n_2 / \pi r^2 \quad (5-124)$$

where n_1 is the normal-to- A_1 component of the distance to A_2 . Equation (5-124) is, for example, in error only by +7 percent for the case of opposed squares separated by 3 times their side dimension. The view factors are given for finite coaxial coextensive cylinders in Fig. 5-16,

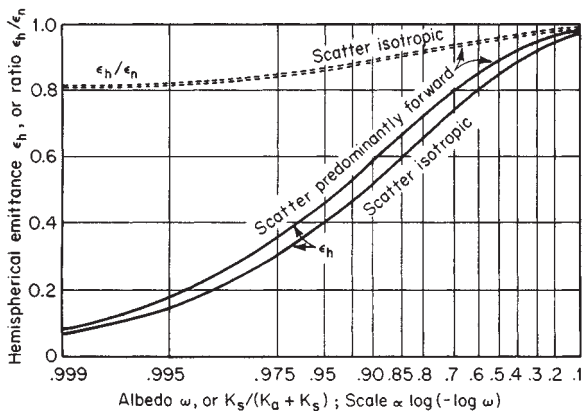


FIG. 5-14 Hemispherical emittance ϵ_h and the ratio of hemispherical to normal emittance ϵ_h/ϵ_n for a semi-infinite absorbing-scattering medium.

TABLE 5-6 Normal Total Emissivity of Various Surfaces

A. Metals and Their Oxides					
Surface	$t, ^\circ\text{F}^\circ$	Emissivity ^a	Surface	$t, ^\circ\text{F}^\circ$	Emissivity ^a
Aluminum			Sheet steel, strong rough oxide layer	75	0.80
Highly polished plate, 98.3% pure	440–1070	0.039–0.057	Dense shiny oxide layer	75	0.82
Polished plate	73	0.040	Cast plate:		
Rough plate	78	0.055	Smooth	73	0.80
Oxidized at 1110°F	390–1110	0.11–0.19	Rough	73	0.82
Aluminum-surfaced roofing	100	0.216	Cast iron, rough, strongly oxidized	100–480	0.95
Calorized surfaces, heated at 1110°F.			Wrought iron, dull oxidized	70–680	0.94
Copper	390–1110	0.18–0.19	Steel plate, rough	100–700	0.94–0.97
Steel	390–1110	0.52–0.57	High temperature alloy steels (see Nickel Alloys).		
Brass			Molten metal		
Highly polished:			Cast iron	2370–2550	0.29
73.2% Cu, 26.7% Zn	476–674	0.028–0.031	Mild steel	2910–3270	0.28
62.4% Cu, 36.8% Zn, 0.4% Pb, 0.3% Al	494–710	0.033–0.037	Lead		
82.9% Cu, 17.0% Zn	530	0.030	Pure (99.96%), unoxidized	260–440	0.057–0.075
Hard rolled, polished:			Gray oxidized	75	0.281
But direction of polishing visible	70	0.038	Oxidized at 390°F.	390	0.63
But somewhat attacked	73	0.043	Mercury	32–212	0.09–0.12
But traces of stearin from polish left on	75	0.053	Molybdenum filament	1340–4700	0.096–0.292
Polished	100–600	0.096	Monel metal, oxidized at 1110°F	390–1110	0.41–0.46
Rolled plate, natural surface	72	0.06	Nickel		
Rubbed with coarse emery	72	0.20	Electroplated on polished iron, then polished	74	0.045
Dull plate	120–660	0.22	Technically pure (98.9% Ni, + Mn), polished	440–710	0.07–0.087
Oxidized by heating at 1110°F	390–1110	0.61–0.59	Electroplated on pickled iron, not polished	68	0.11
Chromium; see Nickel Alloys for Ni-Cr steels	100–1000	0.08–0.26	Wire	368–1844	0.096–0.186
Copper			Plate, oxidized by heating at 1110°F	390–1110	0.37–0.48
Carefully polished electrolytic copper	176	0.018	Nickel oxide	1200–2290	0.59–0.86
Commercial, emiered, polished, but pits remaining	66	0.030	Nickel alloys		
Commercial, scraped shiny but not mirror-like	72	0.072	Chromnickel	125–1894	0.64–0.76
Polished	242	0.023	Nickelin (18–32 Ni; 55–68 Cu; 20 Zn), gray oxidized	70	0.262
Plate, heated long time, covered with thick oxide layer	77	0.78	KA-2S alloy steel (8% Ni; 18% Cr), light silvery, rough, brown, after heating	420–914	0.44–0.36
Plate heated at 1110°F	390–1110	0.57	After 42 hr. heating at 980°F.	420–980	0.62–0.73
Cuprous oxide	1470–2010	0.66–0.54	NCT-3 alloy (20% Ni; 25% Cr.), brown, splotched, oxidized from service	420–980	0.90–0.97
Molten copper	1970–2330	0.16–0.13	NCT-6 alloy (60% Ni; 12% Cr), smooth, black, firm adhesive oxide coat from service	520–1045	0.89–0.82
Gold			Platinum		
Pure, highly polished	440–1160	0.018–0.035	Pure, polished plate	440–1160	0.054–0.104
Iron and steel			Strip	1700–2960	0.12–0.17
Metallic surfaces (or very thin oxide layer):			Filament	80–2240	0.036–0.192
Electrolytic iron, highly polished	350–440	0.052–0.064	Wire	440–2510	0.073–0.182
Polished iron	800–1880	0.144–0.377	Silver		
Iron freshly emiered	68	0.242	Polished, pure	440–1160	0.0198–0.0324
Cast iron, polished	392	0.21	Polished	100–700	0.0221–0.0312
Wrought iron, highly polished	100–480	0.28	Steel, see Iron.		
Cast iron, newly turned	72	0.435	Tantalum filament	2420–5430	0.194–0.31
Polished steel casting	1420–1900	0.52–0.56	Tin—bright tinned iron sheet	76	0.043 and 0.064
Ground sheet steel	1720–2010	0.55–0.61	Tungsten		
Smooth sheet iron	1650–1900	0.55–0.60	Filament, aged	80–6000	0.032–0.35
Cast iron, turned on lathe	1620–1810	0.60–0.70	Filament	6000	0.39
Oxidized surfaces:			Zinc		
Iron plate, pickled, then rusted red	68	0.612	Commercial, 99.1% pure, polished	440–620	0.045–0.053
Completely rusted	67	0.685	Oxidized by heating at 750°F.	750	0.11
Rolled sheet steel	70	0.657	Galvanized sheet iron, fairly bright	82	0.228
Oxidized iron	212	0.736	Galvanized sheet iron, gray oxidized	75	0.276
Cast iron, oxidized at 1100°F	390–1110	0.64–0.78			
Steel, oxidized at 1100°F	390–1110	0.79			
Smooth oxidized electrolytic iron	260–980	0.78–0.82			
Iron oxide	930–2190	0.85–0.89			
Rough ingot iron	1700–2040	0.87–0.95			
B. Refractories, Building Materials, Paints, and Miscellaneous					
Asbestos			Carbon		
Board	74	0.96	T-carbon (Gebr. Siemens) 0.9% ash (this started with emissivity at 260°F. of 0.72, but on heating changed to values given)	260–1160	0.81–0.79
Paper	100–700	0.93–0.945	Carbon filament	1900–2560	0.526
Brick			Candle soot	206–520	0.952
Red, rough, but no gross irregularities	70	0.93	Lampblack-waterglass coating	209–362	0.959–0.947
Silica, unglazed, rough	1832	0.80			
Silica, glazed, rough	2012	0.85			
Grog brick, glazed	2012	0.75			
See Refractory Materials below.					

TABLE 5-6 Normal Total Emissivity of Various Surfaces (Concluded)

B. Refractories, Building Materials, Paints, and Miscellaneous					
Surface	$t, ^\circ\text{F}^\circ$	Emissivity ^o	Surface	$t, ^\circ\text{F}^\circ$	Emissivity ^o
Same	260–440	0.957–0.952	Oil paints, sixteen different, all colors	212	0.92–0.96
Thin layer on iron plate	69	0.927	Aluminum paints and lacquers		
Thick coat	68	0.967	10% Al, 22% lacquer body, on rough or smooth surface	212	0.52
Lampblack, 0.003 in. or thicker	100–700	0.945	26% Al, 27% lacquer body, on rough or smooth surface	212	0.3
Enamel, white fused, on iron	66	0.897	Other Al paints, varying age and Al content	212	0.27–0.67
Glass, smooth	72	0.937	Al lacquer, varnish binder, on rough plate	70	0.39
Gypsum, 0.02 in. thick on smooth or blackened plate	70	0.903	Al paint, after heating to 620°F.	300–600	0.35
Marble, light gray, polished	72	0.931	Paper, thin		
Oak, planed	70	0.895	Pasted on tinned iron plate	66	0.924
Oil layers on polished nickel (lube oil)	68		On rough iron plate	66	0.929
Polished surface, alone		0.045	On black lacquered plate	66	0.944
+0.001-in. oil		0.27	Plaster, rough lime	50–190	0.91
+0.002-in. oil		0.46	Porcelain, glazed	72	0.924
+0.005-in. oil		0.72	Quartz, rough, fused	70	0.932
Infinitely thick oil layer		0.82	Refractory materials, 40 different	1110–1830	
Oil layers on aluminum foil (linseed oil)			poor radiators		$\left[\begin{array}{l} 0.65 \\ 0.70 \\ 0.80 \\ 0.85 \end{array} \right] - \left[\begin{array}{l} 0.75 \\ 0.85 \\ 1.00 \end{array} \right]$
Al foil	212	0.087†	good radiators		
+1 coat oil	212	0.561	Roofing paper	69	0.91
+2 coats oil	212	0.574	Rubber		
Paints, lacquers, varnishes			Hard, glossy plate	74	0.945
Snowwhite enamel varnish or rough iron plate	73	0.906	Soft, gray, rough (reclaimed)	76	0.859
Black shiny lacquer, sprayed on iron	76	0.875	Serpentine, polished	74	0.900
Black shiny shellac on tinned iron sheet	70	0.821	Water	32–212	0.95–0.963
Black matte shellac	170–295	0.91			
Black lacquer	100–200	0.80–0.95			
Flat black lacquer	100–200	0.96–0.98			
White lacquer	100–200	0.80–0.95			

^oWhen two temperatures and two emissivities are given, they correspond, first to first and second to second, and linear interpolation is permissible. °C = (°F – 32)/1.8.

†Although this value is probably high, it is given for comparison with the data by the same investigator to show the effect of oil layers. See Aluminum, Part A of this table.

and for an infinite plane parallel to a system of rows of parallel tubes as curves 1 and 3 of Fig. 5-17.

The exchange area between any two area elements of a sphere is independent of their relative shape and position and is simply the product of the areas divided by the area of the whole sphere; i.e., any spot on a sphere has equal views of all other spots.

For surfaces in two-dimensional systems (with third dimension infinite), A_1F_{12} per unit length in the third dimension may be obtained simply by evaluating, in a cross-sectional view, the sum of lengths of crossed strings from the ends of A_1 to the ends of A_2 less the sum of uncrossed strings from and to the same points, all divided by 2. The strings must be so drawn that all the flux from one surface to the other must cross each of a pair of crossed strings and neither of a pair of uncrossed ones. If one surface can see the other around both sides of an obstruction, two more pairs of strings are involved.

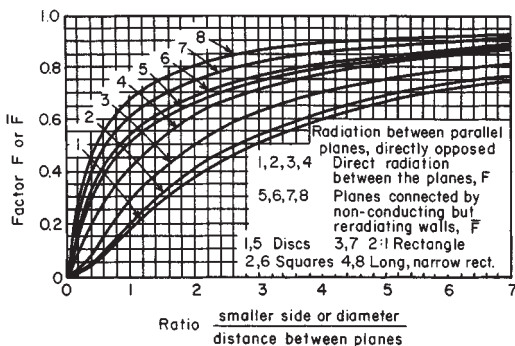


FIG. 5-15 Radiation between parallel planes, directly opposed.

Example 3: Calculation of View Factor Evaluate the view factor between two parallel circular tubes long enough compared with their diameter D or their axis-to-axis separating distance C to make the problem two-dimensional. With reference to Fig. 5-18, the crossed-strings method yields, per unit of axial length,

$$A_1F_{12} = \frac{2(EFGH - HJ)}{2} = D \left[\sin^{-1} \frac{D}{C} + \left[\left(\frac{C}{D} \right)^2 - 1 \right]^{1/2} - \frac{C}{D} \right]$$

Results for a large number of other cases are given by Hottel and Sarofim (op. cit., chap. 2) and Hamilton and Morgan (NACA-TN2836, December 1952). A comprehensive bibliography is provided by Siegel and Howell (*Thermal Radiation Heat Transfer*, McGraw-Hill, 1992).

The view factor F may often be evaluated from that for simpler configurations by the application of three principles: that of reciprocity, $A_iF_{ij} = A_jF_{ji}$; that of conservation, $\sum F_{ij} = 1$; and that due to Yamauti [*Res. Electrotech. Lab. (Tokyo)*, 148, 1924; 194, 1927; 250, 1929], showing that the exchange areas AF between two pairs of surfaces are equal when there is a one-to-one correspondence for all sets of symmetrically placed pairs of elements in the two surface combinations.

Example 4: Calculation of Exchange Area The exchange area between the two squares 1 and 4 of Fig. 5-19 is to be evaluated. The following exchange areas may be obtained from Eq. 5-121. F for common-side rectangles: $\bar{13} = 0.24$, $24 = 2 \times 0.29 = 0.58$, $(1+2)(3+4) = 3 \times 0.32 = 0.96$. Expression of $(1+2)(3+4)$ in terms of its components yields $(1+2)(3+4) = 13 + 14 + 23 + 24$. And by the Yamauti principle $14 = 23$, since for every pair of elements in 1 and 4 there is a corresponding pair in 2 and 3. Therefore,

$$\bar{14} = \frac{(1+2)(3+4) - \bar{13} - 24}{2} = 0.07$$

Figure 5-16 may be used in the same way.

Non-Black-Surface Enclosures In the following discussion we are concerned with enclosures containing gray sources and sinks, radiatively adiabatic surfaces, and no absorbing gas. The calculation of interchange between a source and a sink under conditions involving successive multiple reflections from other source-sink surfaces in the

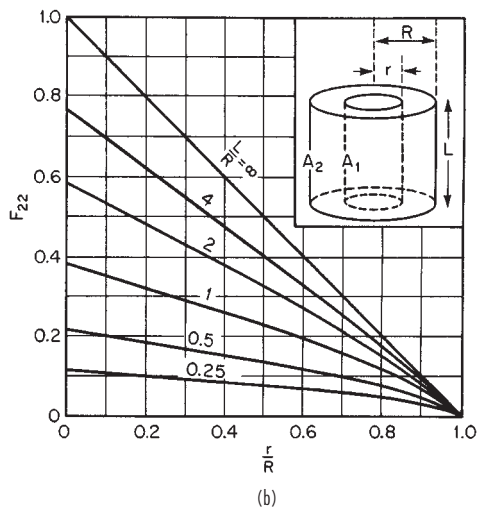
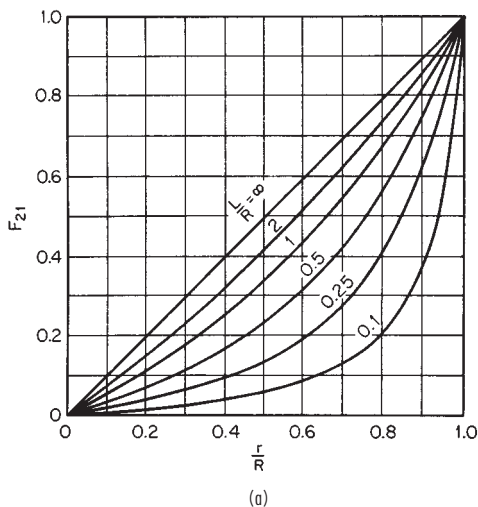


FIG. 5-16 View factors for a system of two concentric coaxial cylinders. (a) Outer cylinder to inner cylinder. (b) Inner surface of outer cylinder to itself.

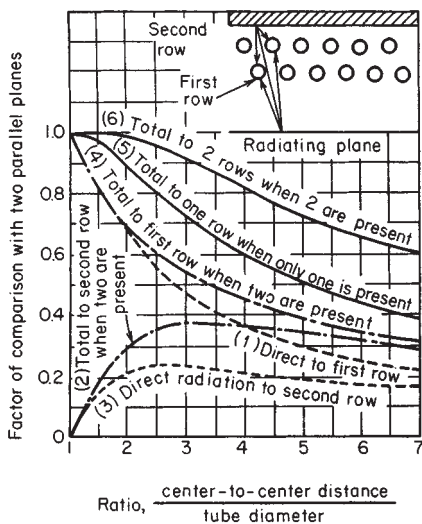


FIG. 5-17 Distribution of radiation to rows of tubes irradiated from one side. Dashed lines: direct view factor F from plane to tubes. Solid lines: total view factor F for black tubes backed by a refractory surface.

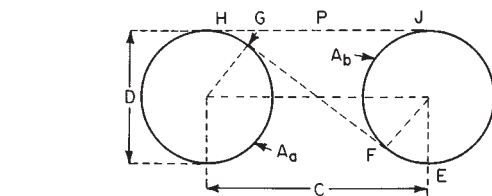


FIG. 5-18 Direct exchange between parallel circular tubes.

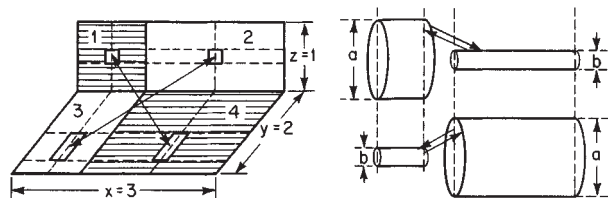


FIG. 5-19 Illustration of the Yamauti principle.

enclosure, as well as reradiation from refractory surfaces which are in radiative equilibrium, can become complicated.

Zone Method Let a zone of a furnace enclosure be an area small enough to make all elements of itself have substantially equivalent "views" of the rest of the enclosure. (In a furnace containing a symmetry plane, parts of a single zone would lie on either side of the plane.) Zones are of two classes: source-sink surfaces, designated by numerical subscripts and having areas A_1, A_2, \dots , and emissivities $\epsilon_1, \epsilon_2, \dots$; and surfaces at which the net radiant-heat flux is zero (filled by the average refractory wall in which difference between internal convection and external loss is minute compared with incident radiation), designated by letter subscripts starting with r , and having areas A_r, A_s, \dots . It may be shown (see, for example, Hottel and Sarofim, op. cit., chap. 3) that the net radiation interchange between source-sink zones i and j is given by

$$\dot{Q}_{i=j} = A_i \mathcal{F}_{ij} \sigma T_i^4 - A_j \mathcal{F}_{ji} \sigma T_j^4 \quad (5-125)$$

\mathcal{F}_{ij} is called the **total view factor** from i to j , and the term $A_i \mathcal{F}_{ij}$, sometimes designated $S_i S_j$, is called the **total interchange area** shared by areas A_i and A_j and depends on the shape of the enclosure and the emissivity and absorptivity of the source and sink zones. Restriction here is to gray source-sink zones, for which $A_i \mathcal{F}_{ij} = A_j \mathcal{F}_{ji}$; the more general case is treated elsewhere (Hottel and Sarofim, op. cit., chap. 5).

Evaluation of the $A \mathcal{F}$'s that characterize an enclosure involves solution of a system of radiation balances on the surfaces. If the assumption is made that all the zones of the enclosure are gray and emit and reflect diffusely,^o then the direct-exchange area ij , as evaluated for the black-surface pair A_i and A_j , applies to emission and reflections between them. If at a surface the total leaving-flux density, emitted plus reflected, is denoted by W (and called by some the **radiosity** and by others the **exitance**), radiation balances take the form:

^o So-called Lambert surfaces, which emit or reflect with an intensity independent of angle; approximately satisfied by most nonmetallic, tarnished, oxidized, or rough surfaces.

For source-sink j ,

$$A_j \varepsilon_j E_j + \rho_j \sum_i (\bar{i}j) W_i = A_j W_j \quad (5-126)$$

For adiabatic surface r ,

$$\sum_i (\bar{i}r) W_i = A_r W_r \quad (5-127)$$

where ρ is reflectance and the summation is over all surfaces in the enclosure. In matrix notation, Eq. (10-196) becomes, with source or sink zones represented by 1, 2, 3 . . . and adiabatic zones by r, s, t, \dots ,

$$\begin{bmatrix} \bar{11} - \frac{A_1}{\rho_1} & \bar{12} & \bar{1r} & \bar{1s} \\ \bar{12} & \bar{22} - \frac{A_2}{\rho_2} & \bar{2r} & \bar{2s} \\ \bar{1r} & \bar{2r} & \bar{rr} - A_r & \bar{rs} \\ \bar{1s} & \bar{2s} & \bar{rs} & \bar{ss} - A_s \end{bmatrix} \begin{bmatrix} W_1 \\ W_2 \\ W_r \\ W_s \end{bmatrix} = \begin{bmatrix} -\frac{A_1 \varepsilon_1}{\rho_1} E_1 \\ -\frac{A_2 \varepsilon_2}{\rho_2} E_2 \\ 0 \\ 0 \end{bmatrix} \quad (5-128)$$

This represents a system of simultaneous equations equal in number to the number of rows of the square matrix. Each equation consists, on the left, of the sum of the products of the members of a row of the square matrix and the corresponding members of the W -column matrix and, on the right, of the member of that row in the third matrix. With this set of equations solved for W_i , the net flux at any surface A_i is given by

$$\dot{Q}_{i,\text{net}} = (A_i \varepsilon_i / \rho_i) (E_i - W_i) \quad (5-129)$$

Refractory temperature is obtained from $W_r = E_r = \sigma T_r^4$.

The more general use of Eq. (5-128) is to obtain the set of total interchange areas $A_i \bar{\mathcal{F}}$ which constitute a complete description of the effect of shape, size, and emissivity on radiative flux, independent of the presence or absence of other transfer mechanisms. It may be shown that

$$A_i \bar{\mathcal{F}}_{ij} \equiv A_i \bar{\mathcal{F}}_{ji} \equiv \bar{S}_i \bar{S}_j = \frac{A_i \varepsilon_i}{\rho_i} \left[\frac{A_j \varepsilon_j}{\rho_j} \left(-\frac{D'_{ij}}{D} \right) - \delta_{ij} \varepsilon_j \right] \quad (5-130)$$

where D is the determinant of the square coefficient matrix in Eq. (5-128) and D'_{ij} is the cofactor of its i th row and j th column, or $(-1)^{i+j}$ times the minor of D formed by crossing out the i th row and i th column, and δ_{ij} is the Kronecker delta, 1 when $i = j$, otherwise 0.

As an example, consider radiation between two surfaces A_1 and A_2 , which together form a complete enclosure. Equation (5-130) takes the form

$$A_1 \bar{\mathcal{F}}_{12} = \left(\frac{A_1 \varepsilon_1}{\rho_1} \right) \left(\frac{A_2 \varepsilon_2}{\rho_2} \right) \left(\frac{\bar{12}}{\begin{vmatrix} \bar{11} - \frac{A_1}{\rho_1} & \bar{12} \\ \bar{12} & \bar{22} - \frac{A_2}{\rho_2} \end{vmatrix}} \right) \quad (5-131)$$

Only one direct-view factor F_{12} or direct-exchange area $\bar{12}$ is needed because F_{11} equals $1 - F_{12}$ and F_{22} equals $1 - F_{21}$ equals $1 - F_{12} A_1 / A_2$. Then $\bar{11}$ equals $A_1 - \bar{12}$ and $\bar{22}$ equals $A_2 - \bar{21}$. With these substitutions, Eq. (5-131) becomes

$$A_1 \bar{\mathcal{F}}_{12} = \frac{A_1}{\frac{1}{F_{12}} + \frac{1}{\varepsilon_1} - 1 + \frac{A_1}{A_2} \left(\frac{1}{\varepsilon_2} - 1 \right)} \quad (5-132)$$

Special cases include

1. Parallel plates, large compared to clearance. Substitution of $F_{12} = 1$ and $A_1 = A_2$ gives

$$A_1 \bar{\mathcal{F}}_{12} = \frac{A_1}{\frac{1}{\varepsilon_1} + \frac{1}{\varepsilon_2} - 1} \quad (5-133)$$

2. Sphere of area A_1 concentric with surrounding sphere of area A_2 . $F_{12} = 1$. Then

$$A_1 \bar{\mathcal{F}}_{12} = \frac{A_1}{\frac{1}{\varepsilon_1} + \left(\frac{A_1}{A_2} \right) \left(\frac{1}{\varepsilon_2} - 1 \right)} \quad (5-134)$$

3. Body of surface A_1 having no negative curvature, surrounded by very much larger surface A_2 . $F_{12} = 1$ and $A_1/A_2 \rightarrow 0$. Then

$$\bar{\mathcal{F}}_{12} = \varepsilon_1 \quad (5-135)$$

Many furnace problems are adequately handled by dividing the enclosure into but two source-sink zones A_1 and A_2 and any number of no-flux zones A_r, A_s, \dots . For this case Eq. (5-130) yields

$$\frac{1}{A_1 \bar{\mathcal{F}}_{12}} \left(\equiv \frac{1}{A_2 \bar{\mathcal{F}}_{21}} \right) = \frac{1}{A_1} \left(\frac{1}{\varepsilon_1} - 1 \right) + \frac{1}{A_2} \left(\frac{1}{\varepsilon_2} - 1 \right) + \frac{1}{A_1 \bar{F}_{12}} \quad (5-136)$$

where the expression $A_1 \bar{F}_{12}$ ($\equiv A_2 \bar{F}_{21}$) represents the total interchange area for the limiting case of a black source and black sink (the refractory emissivity is of no moment). The factor \bar{F} is known exactly for a few geometrically simple cases and may be approximated for others. If A_1 and A_2 are equal parallel disks, squares, or rectangles, connected by nonconducting but reradiating refractory walls, then \bar{F} is given by Fig. 5-15, curves 5 to 8. If A_1 represents an infinite plane and A_2 is one or two rows of infinite parallel tubes in a parallel plane and if the only other surface is a refractory surface behind the tubes, \bar{F}_{12} is given by curve 5 or 6 of Fig. 5-17.

If an enclosure may be divided into several radiant-heat sources or sinks A_1, A_2 , etc., and the rest of the enclosure (reradiating refractory surface) may be lumped together as A_r at a uniform temperature T_r , then the total interchange area for zone pairs in the black system is given by

$$A_1 \bar{F}_{12} (\equiv A_2 \bar{F}_{21}) = \bar{12} + \frac{(\bar{1r})(\bar{r2})}{A_r - rr} \quad (5-137)$$

For the two-source-sink-zone system to which Eq. (5-136) applies, Eq. (5-137) simplifies to

$$A_1 \bar{F}_{12} = \bar{12} + 1/(1/\bar{1r} + 1/2\bar{r}) \quad (5-138)$$

and if A_1 and A_2 each can see none of itself, there is further simplification to

$$\begin{aligned} A_1 \bar{F}_{12} &= \bar{12} + \frac{1}{1/(A_1 - \bar{12}) + 1/(A_2 - \bar{12})} \\ &= \frac{A_1 A_2 - (\bar{12})^2}{A_1 + A_2 - 2(\bar{12})} \end{aligned} \quad (5-139)$$

which necessitates the evaluation of but one geometrical factor F .

Equation (5-136) covers many of the problems of radiant-heat interchange between source and sink in a furnace enclosure. The error due to single zoning of source and sink is small even if the views of the enclosure from different parts of each zone are quite different, provided the emissivity is fairly high; the error in \bar{F} is zero if it is obtainable from Fig. 5-15 or 5-17, small if Eq. (5-137) is used and the variation in temperature over the refractory is small. An approach to any desired accuracy can be made by use of Eqs. (5-126) and (5-130) with division of the surfaces into more zones.

From the definitions of F , \bar{F} , and $\bar{\mathcal{F}}$ it is to be noted that

$$\begin{aligned} F_{11} + F_{12} + F_{13} + \dots + F_{1r} + F_{1s} + \dots &= 1 \\ \bar{F}_{11} + \bar{F}_{12} + \bar{F}_{13} + \dots &= 1 \\ \bar{\mathcal{F}}_{11} + \bar{\mathcal{F}}_{12} + \bar{\mathcal{F}}_{13} + \dots &= \varepsilon_1 \end{aligned}$$

Example 5: Radiation in a Furnace Chamber A furnace chamber of rectangular parallelepipedal form is heated by the combustion of gas inside vertical radiant tubes lining the sidewalls. The tubes are of 0.127-m (5-in) outside diameter on 0.305-m (12-in) centers. The stock forms a continuous plane on the hearth. Roof and end walls are refractory. Dimensions are shown in Fig. 5-20. The radiant tubes and stock are gray bodies having emissivities of 0.8 and 0.9 respectively. What is the net rate of heat transmission to the stock by radiation when the mean temperature of the tube surface is 816°C (1500°F) and that of the stock is 649°C (1200°F)?

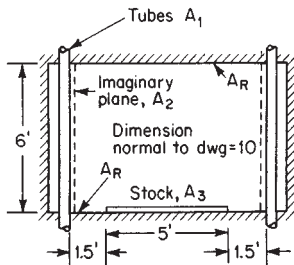


FIG. 5-20 Furnace-chamber cross section. To convert feet to meters, multiply by 0.3048.

This problem must be broken up into two parts, first considering the walls with their refractory-backed tubes. To imaginary planes A_2 of area 1.83 by 3.05 m (6 by 10 ft) and located parallel to and inside the rows of radiant tubes, the tubes emit radiation $\sigma T_1^4 A_1 \mathcal{F}_{21}$, which equals $\sigma T_1^4 A_2 \mathcal{F}_{21}$. To find \mathcal{F}_{21} , use Fig. 5-17, curve 5, from which $\bar{F}_{21} = 0.81$. Then from Eq. (10-200)

$$\mathcal{F}_{21} = \frac{1}{\left(\frac{1}{1-1}\right) + \left(\frac{12}{5\pi}\right)\left(\frac{1}{0.8}-1\right) + \frac{1}{0.81}} = 0.702$$

This amounts to saying that the system of refractory-backed tubes is equal in radiating power to a continuous plane A_2 replacing the tubes and refractory back of them, having a temperature equal to that of the tubes and an equivalent or effective emissivity of 0.702.

The new simplified furnace now consists of an enclosure formed by two 1.83-by-3.05-m (6-by-10-ft) radiating sidewalls (area A_2 , emissivity 0.702), a 1.52-by-3.05-m (5-by-10-ft) receiving plane on the floor A_3 , and refractory surfaces A_1 to complete the enclosure (ends, roof, and floor side strips). The desired heat transfer is

$$\dot{Q}_{2 \rightarrow 3} = \sigma(T_1^4 - T_3^4)A_2 \mathcal{F}_{23}$$

To evaluate \mathcal{F}_{23} , start with the direct interchange factor F_{23} . $F_{23} = F$ from A_2 to $(A_3 + a$ strip of A_3 , alongside A_3 , which has a common edge with A_2) minus F from A_2 to the strip only. These two F 's may be evaluated from Fig. 5-20 and Eq. (5-121). For the first F , $Y = 1.83/3.05$, $Z = 1.98/3.05$, and $F = 0.239$; for the second F , $Y = 1.83/3.05$, $Z = 0.46/3.05$, and $F = 0.100$. Then $F_{23} = 0.239 - 0.10 = 0.139$. Now \bar{F} may be evaluated. From Eq. 5-137 et seq.,

$$A_2 \bar{F}_{23} = \bar{23} + \frac{1}{1/2r + 1/3r} \bar{F}_{23} = F_{23} + \frac{1}{(1/F_{23}) + (A_2/A_3)(1/F_{3r})}$$

Since A_2 "sees" A_r , A_3 , and some of itself (the plane opposite), $F_{23} = 1 - F_{22} - F_{23}$. F_{22} , the direct interchange factor between parallel 1.83-by-3.05-m (6-by-10-ft) rectangles separated by 2.44 m (8 ft), may be taken as the geometric mean of the factors for 1.83-m (6-ft) squares separated by 2.44 m (8 ft) and for 3.05-m (10-ft) squares separated by 2.44 m (8 ft). These come from Fig. 5-15, curve 2, according to which $F_{22} = \sqrt{0.13 \times 0.255} = 0.182$. Then $F_{2r} = 1 - 0.182 - 0.139 = 0.679$. The other required direct factor is $F_{3r} = 1 - F_{32} = 1 - F_{23} A_2/A_3 = 1 - (0.139)(11.14)/4.65 = 0.666$. Then

$$\bar{F}_{23} = 0.139 + \frac{1}{(1/0.679) + (11.14/4.65)(1/0.666)} = 0.336$$

Having \bar{F}_{23} , we may now evaluate the factor \mathcal{F}_{23} :

$$\mathcal{F}_{23} = \frac{1}{(1/0.336) + [(1/0.702) - 1] + (11.14/4.65)[(1/0.9) - 1]} = 0.273$$

$$\dot{Q}_{\text{net}} = \sigma(T_1^4 - T_3^4)A_2 \mathcal{F}_{23} = 5.67(10.89^4 - 9.22^4)(11.15)(0.273) = 118,000 \text{ J/s (402,000 Btu/h)}$$

A result of interest is obtained by dividing the term $A_2 \mathcal{F}_{23}(11.15 \times 0.273)$, or 3.04 by the actual area A_1 of the radiating tubes $(0.127\pi)(18.3)(2) = 14.6 \text{ m}^2$ (157 ft²). Thus $3.04/14.6 = 0.208$, which means that the net radiation from a tube to the stock is 20.8 percent as much as if the tube were black and completely surrounded by black stock.

Integral Formulation The zone method has the purpose of dodging the solution of an integral equation. If in Eq. (5-126) the zone on which the radiation balance is formulated is decreased to a differential element, that equation becomes

$$dA_i \epsilon_i E_j + \rho_j \int \frac{dA_j dA_i (\cos \theta_i)(\cos \theta_j) W_i}{r^2} = dA_j W_j \quad (5-140)$$

which is an integral equation with the unknown function W inside the integral. Integration is over the entire surface area. Exact solutions have been carried out for only a few simple cases. One of these is the evaluation of emittance of an isothermal spherical cavity, for which $dA_i dA_j (\cos \theta_i)(\cos \theta_j)/r^2$ in the integral of Eq. (5-140) becomes $dA_i dA_j/4\pi R^2$, where R is the sphere radius. For this special case W is, from Eq. (10-202), constant over the inner surface of the cavity and given by

$$W = \frac{\epsilon E}{1 - \rho(1 - A_i/4\pi R^2)} \quad (5-141)$$

where A_i is the curved area of a hole in the sphere's surface. The ratio W/E is the effective emittance of the hole as sensed by a narrow-angle receiver viewing the cavity interior. If the material of construction of the cavity is a diffuse emitter and reflector and has an emissivity of 0.5 and the cavity is to appear at least 98 percent black, the curved area A_i of the hole must be smaller than 2 percent of the total surface area of the sphere.

Enclosures of Surfaces That Are Not Diffuse Reflectors If no restriction that the surfaces be diffuse emitters and reflectors is imposed, Eq. (5-140) becomes much more complex. The W 's are replaced by πI 's and ϵ_j , I_j , and I_j all become functions of the angle of the leaving beam, and ρ_j goes inside the integral and becomes a function of angles of incidence and reflection. Seldom are such details of reflectance known. When they are and a solution is needed, the Monte Carlo method of tracing the history of a large number of beams emitted from random positions and in random initial directions is probably the best method of obtaining a solution. Another approach is possible, however, because of the tendency of most surfaces to fit a simpler reflection model. The total reflectance $\rho(\equiv 1 - \epsilon)$ can be represented by the sum of a diffuse component ρ_D and a specular component ρ_S . For applications see Hottel and Sarofim (op. cit., chap. 5). The method yields the following relation for exchange between concentric spheres or infinite cylinders:

$$A_1 \mathcal{F}_{12} \equiv S_1 S_2 = \frac{1}{1/A_1 \epsilon_1 + (1/A_2)(1/\epsilon_2 - 1) + [\rho_{S2}/(1 - \rho_{S2})](1/A_1 - 1/A_2)} \quad (5-142)$$

When there is no specular reflectance, the third term in the denominator drops out, in agreement with Eqs. (5-134) and (5-135). When the reflectance is exclusively specular, the denominator becomes $1/A_1 \epsilon_1 + \rho_{S2}/A_1(1 - \rho_{S2})$, easily derivable from first principles.

EMISSIONS OF COMBUSTION PRODUCTS

The radiation from a flame is due to radiation from burning soot particles of microscopic and submicroscopic dimensions, from suspended larger particles of coal, coke, or ash, and from the water vapor and carbon dioxide in the hot gaseous combustion products. The contribution of radiation emitted by the combustion process itself, so-called chemiluminescence, is relatively negligible. Common to these problems is the effect of the shape of the emitting volume on the radiative flux; this is considered first.

Mean Beam Lengths Evaluation of radiation from a nonisothermal volume is beyond the scope of this section (see Hottel and Sarofim, *Radiative Transfer*, McGraw-Hill, New York, 1967, chap. 11). Consider an isothermal gas confined within the volume bounded by the solid angle $d\Omega$ with vertex at dA and making the angle θ with the normal to dA . The ratio of the emission to dA from the gas to that from a blackbody at the gas temperature and filling the field of view $d\Omega$ is called the gas emissivity ϵ . Clearly, ϵ depends on the path length L through the volume to dA . A hemispherical volume radiating to a spot on the center of its base represents the only case in which L is independent of direction. Flux at that spot relative to hemispherical blackbody flux is thus an alternative way to visualize emissivity.

The flux density to a small area of interest on the envelope of an emitter volume of any shape can be matched by that at the base of a hemispherical volume of some radius L , which is called the mean beam length. It is found that although the ratio of L to a characteristic dimension D of the shape varies with opacity, the variation is small enough for most engineering purposes to permit use of a constant ratio L_M/D ,

where L_M is the average mean beam length. L_M can be defined to apply either to a spot on the envelope or to any finite portion of its area. An important limiting case is that of opacity approaching zero ($pD \rightarrow 0$, where p = partial pressure of the emitter constituent). For this case, L (called L_0) equals $4V/A$ (V = gas volume; A = bounding area) when interest is in radiation to the entire envelope. For the range of pD encountered in practice, the optimum value of L (now L_M) lies between 0.8 to 0.95 times L_0 . For shapes not reported in Table 5-7, a factor of 0.88 (or $L_M = 0.88L_0 = 3.5V/A$) is recommended.

Instead of using the average-mean-beam-length concept to approximate $A_1[\epsilon(L_m)]$ (the flux per unit black emissive power from a gas volume partially bounded by a surface of area A_1), one may calculate the flux rigorously by integration, over the gas volume and over A_1 , of the expression $4k \, dv \, \tau(r) \, dA \cos \theta / \pi r^2$. Here k is the emission coefficient of the gas, and $\tau(r)$ is the transmittance through the distance r between dv and dA . The result has the dimensions of area and, by analogy to gs , is called gs_1 , the direct-exchange area between the gas zone and the surface zone (Hottel and Sarofim, op. cit., chap. 7). The use of $A_1[\epsilon(L_m)]$ instead of gs_1 is adequate when the problem is such that all the gas can be treated as a single zone in contact with A_1 , and having a mean radiating temperature, but the gs concept is clearly useful if allowance is to be made for temperature variations within the gas.

Gaseous Combustion Products Radiation from water vapor and carbon dioxide occurs in spectral bands in the infrared. In magnitude it overshadows convection at furnace temperatures.

Carbon Dioxide The contribution ϵ_c to the emissivity of a gas containing CO_2 depends on gas temperature T_C , on the CO_2 partial pressure-beam length product $p_c L$ and, to a much lesser extent, on the total pressure P . Constants for use in evaluating ϵ_c at a total pressure of 101.3 kPa (1 atm) are given in Table 5-8 (more on this later). The gas absorptivity α_c equals the emissivity when the absorbing gas and the emitter are at the same temperature. When the emitter surface temperature is T_1 , α_c is $(T_C/T_1)^{0.65}$ times ϵ_c , evaluated using Table 5-8 at T_1 instead of T_C and at $p_c L T_1 / T_C$ instead of $p_c L$. Line broadening, due to

increases either in total pressure or in partial pressure of CO_2 , makes a correction necessary. However, at a total pressure of 101.3 kPa (1 atm) the correction factor may be ignored, since it decreases with increase in temperature and is never more than 4 percent at temperatures above 1111 K (2000°R). Estimations of the correction in systems up to 1013.3 kPa (10 atm) are given by Hottel and Sarofim (op. cit., p. 228), and by Edwards [*J. Opt. Soc. Am.*, **50**, 617 (1960)] who in addition presents data on CO_2 -band emission for use in calculations involving spectrally selective surfaces. The principal emission bands of CO_2 are at about 2.64 to 2.84, 4.13 to 4.5, and 13 to 17 μm .

Water Vapor The contribution ϵ_w to the emissivity of a gas containing H_2O depends on T_C and $p_w L$ and on total pressure P and partial pressure p_w . Table 5-8 gives constants for use in evaluating ϵ_w . Allowance for departure from the special pressure conditions is made by multiplying ϵ_w by a correction factor C_w read from Fig. 5-21 as a function of $(p_w + P)$ and $p_w L$. The absorptivity α_w of water vapor for blackbody radiation is ϵ_w , evaluated from Table 5-8 but at T_1 instead of T_C and at $p_w L T_1 / T_C$ instead of $p_w L$. Multiply by $(T_C/T_1)^{0.45}$.

The correction factor C_w still applies. Spectral data for water vapor, tabulated for 371 wavelength intervals from 1 to 40 μm , are also available [Ferriso, Ludwig, and Thompson, *J. Quant. Spectros. Radiat. Transfer*, **6**, 241–273 (1966)]. The principal emission is in bands at about 2.55 to 2.84, 5.6 to 7.6, and 12 to 25 μm .

Carbon Dioxide–Water–Vapor Mixtures When these gases are present together, the total radiation due to both is somewhat less than the sum of the separately calculated effects, because each gas is somewhat opaque to radiation from the other in the wavelength regions 2.7 and 15 μm .

Allowance for spectral overlap, the effect of pressure, and the effect of soot luminosity would make computation tedious. Table 5-8 gives constants for use in direct calculation, for $\text{H}_2\text{O}/\text{CO}_2$ mixtures, of the product term $\epsilon_c T$. The product term is used because it varies much less with T than does ϵ_c alone. Constants are given for mixtures, in nonradiating gases, of water vapor alone, CO_2 alone, and four p_w/p_c mixtures.

TABLE 5-7 Mean Beam Lengths for Volume Radiation

Shape	Characteristic dimension, D	L_0/D	L_M/D
Sphere	Diameter	0.67	0.63
Infinite cylinder	Diameter	1.0	0.94
Semi-infinite cylinder, radiating to:			
Center of base	Diameter	1.0	0.90
Entire base	Diameter	0.81	0.65
Right-circle cylinder, ht. = diam. radiating to:			
Center of base	Diameter	0.76	0.71
Whole surface	Diameter	0.67	0.60
Right-circle cylinder, ht. = 0.5 diam. radiating to:			
End	Diameter	0.47	0.43
Side	Diameter	0.52	0.46
Total surface	Diameter	0.50	0.45
Right-circle cylinder, ht. = 2 × diam. radiating to:			
End	Diameter	0.73	0.60
Side	Diameter	0.82	0.76
Total surface	Diameter	0.80	0.73
Infinite cylinder, half-circle cross section radiating to middle of flats	Radius		1.26
Rectangular parallelepipeds:			
1:1:1 (cube)	Edge	0.67	0.60
1:1:4, radiating to:			
1 × 4 face	Shortest edge	0.90	0.82
1 × 1 face	Shortest edge	0.86	0.71
Whole surface	Shortest edge	0.89	0.81
1:2:6, radiating to:			
2 × 6 face	Shortest edge	1.18	
1 × 6 face	Shortest edge	1.24	
1 × 2 face	Shortest edge	1.18	
Whole surface	Shortest edge	1.2	
Clearance	Clearance	2.00	1.76
Infinite parallel planes			
Space outside bank of parallel tubes on equilateral triangular centers			
Tube diam. = clearance	Clearance 3.4	2.8	0.82
Tube diam. = ½ clearance	Clearance 4.45	3.8	0.85
Tube centers on squares, diam. = clearance	Clearance 4.1	3.5	0.85

TABLE 5-8 Emissivity ϵ_g of $H_2O:CO_2$ Mixtures

Limited range for furnaces, valid over 25-fold range of $p_{w+c}L$, 0.046–1.15 m atm (0.15–3.75 ft. atm)

p_w/p_c	0	$\frac{1}{2}$	1	2	3	∞
$\frac{p_w}{p_w + p_c}$	0	$\frac{1}{2}(0.3-0.42)$	$\frac{1}{2}(0.42-0.5)$	$\frac{2}{3}(0.6-0.7)$	$\frac{3}{4}(0.7-0.8)$	1
	CO ₂ only	corresponding to (CH ₂) _n , covering coal, heavy oils, pitch	corresponding to (CH ₂) _n , covering distillate oils, paraffins, olefines	corresponding to CH ₄ , covering natural gas and refinery gas	corresponding to (CH ₆) _n , covering future high H ₂ fuels	H ₂ O only

Constants b and n of Eq., $\epsilon_c T = b(pL - 0.015)^n$, $pL = \text{m atm}$, $T = \text{K}$

T, K	b	n	b	n	b	n	b	n	b	n	b	n
1000	188	0.209	384	0.33	416	0.34	444	0.34	455	0.35	416	0.400
1500	252	0.256	448	0.38	495	0.40	540	0.42	548	0.42	548	0.523
2000	267	0.316	451	0.45	509	0.48	572	0.51	594	0.52	632	0.640

Constants b and n of Eq., $\epsilon_c T = b(pL - 0.05)^n$, $pL = \text{ft. atm}$, $T = \text{°R}$

$T, \text{°R}$	b	n	b	n	b	n	b	n	b	n	b	n
1800	264	0.209	467	0.33	501	0.34	534	0.34	541	0.35	466	0.400
2700	335	0.256	514	0.38	555	0.40	591	0.42	600	0.42	530	0.523
3600	330	0.316	476	0.45	519	0.48	563	0.51	577	0.52	532	0.640

Full range, valid over 2000-fold range of $p_{w+c}L$, 0.005–10.0 m atm (0.016–32.0 ft. atm)
 Constants of Eq., $\log_{10} \epsilon_c T_C = a_0 + a_1 \log pL + a_2 \log^2 pL + a_3 \log^3 pL$

$\frac{p_w}{p_c}$	$\frac{p_w}{p_w + p_c}$	$pL = \text{m atm}, T = \text{K}$					$pL = \text{ft. atm}, T = \text{°R}$				
		T, K	a_0	a_1	a_2	a_3	$T, \text{°R}$	a_0	a_1	a_2	a_3
0	0	1000	2.2661	0.1742	-0.0390	0.0040	1800	2.4206	0.2176	-0.0452	0.0040
		1500	2.3954	0.2203	-0.0433	0.00562	2700	2.5248	0.2695	-0.0521	0.00562
		2000	2.4104	0.2602	-0.0651	-0.00155	3600	2.5143	0.3621	-0.0627	-0.00155
$\frac{1}{2}$	$\frac{1}{2}$	1000	2.5754	0.2792	-0.0648	0.0017	1800	2.6691	0.3474	-0.0674	0.0017
		1500	2.6451	0.3418	-0.0685	-0.0043	2700	2.7074	0.4091	-0.0618	-0.0043
		2000	2.6504	0.4279	-0.0674	-0.0120	3600	2.6686	0.4879	-0.0489	-0.0120
1	$\frac{1}{2}$	1000	2.6090	0.2799	-0.0745	-0.0006	1800	2.7001	0.3563	-0.0736	-0.0006
		1500	2.6862	0.3450	-0.0816	-0.0039	2700	2.7423	0.4561	-0.0756	-0.0039
		2000	2.7029	0.4440	-0.0859	-0.0135	3600	2.7081	0.5210	-0.0650	-0.0135
2	$\frac{2}{3}$	1000	2.6367	0.2723	-0.0804	0.0030	1800	2.7296	0.3577	-0.0850	0.0030
		1500	2.7178	0.3386	-0.0990	-0.0030	2700	2.7724	0.4384	-0.0944	-0.0030
		2000	2.7482	0.4464	-0.1086	-0.0139	3600	2.7461	0.5474	-0.0871	-0.0139
3	$\frac{3}{4}$	1000	2.6432	0.2715	-0.0816	0.0052	1800	2.7359	0.3599	-0.0896	0.0052
		1500	2.7257	0.3355	-0.0981	0.0045	2700	2.7811	0.4403	-0.1051	0.0045
		2000	2.7592	0.4372	-0.1122	-0.0065	3600	2.7599	0.5478	-0.1021	-0.0065
∞	1	1000	2.5995	0.3015	-0.0961	0.0119	1800	2.6720	0.4102	-0.1145	0.0119
		1500	2.7083	0.3969	-0.1309	0.00123	2700	2.7238	0.5330	-0.1328	0.00123
		2000	2.7709	0.5099	-0.1646	-0.0165	3600	2.7215	0.6666	-0.1391	-0.0165

NOTE: $p_w/(p_w + p_c)$ of $\frac{1}{2}$, $\frac{1}{3}$, $\frac{2}{3}$, and $\frac{3}{4}$ may be used to cover the ranges 0.2–0.4, 0.4–0.6, 0.6–0.7, and 0.7–0.8, respectively, with a maximum error in ϵ_c of 5 percent at $pL = 6.5$ m atm, less at lower pL s. Linear interpolation reduces the error generally to less than 1 percent. Linear interpolation or extrapolation on T introduces an error generally below 2 percent, less than the accuracy of the original data.

Four suffice, since a change halfway from one mixture ratio to the adjacent one changes the emissivity by a maximum of but 5 percent; linear interpolation may be used if considered necessary. The constants are given for three temperatures, adequate for linear interpolation since $\epsilon_c T$ changes a maximum of one-sixth due to a change from one temperature base halfway to the adjacent one. The interpolation relation, with T_H and T_L representing the higher and lower base temperatures bracketing T , and with the brackets in the term $[A(x)]$ indicating that the parentheses refer not to a multiplier but to an argument, is

$$\frac{\overline{\epsilon_c T_C}}{\epsilon_c T_C} = \frac{[\overline{\epsilon_c T_H}(pL)](T_C - T_L) + [\overline{\epsilon_c T_L}(pL)](T_H - T_C)}{500} \quad (5-143)$$

Extrapolation to a temperature that is above the highest or below the lowest of the three base temperatures in Table 5-8 uses the same formulation, but one of its terms becomes negative.

The gas absorptivity may also be obtained from the constants for emissivities. The product $\overline{\alpha}_{c,T_1}$ (gas absorptivity for black surface radiation), x (surface temperature), is $\epsilon_c T_1$ evaluated at T_1 instead of T_C and at pLT_1/T_C instead of pL , then multiplied by $(T_C/T_1)^{0.5}$, or

$$\overline{\alpha}_{c,T_1} = \left[\overline{\epsilon_c T_1} \left(\frac{pLT_1}{T_C} \right) \right] \left(\frac{T_C}{T_1} \right)^{0.5} \quad (5-144)$$

The exponent 0.5 is an adequate average of the exponents for the pure components. The interpolation relation for absorptivity is

$$\overline{\alpha}_{c,T_1} = \left[\overline{\epsilon_c T_H} \left(\frac{pLT_H}{T_C} \right) \right] \left(\frac{T_C}{T_H} \right)^{0.5} \left(\frac{T_1 - T_L}{500} \right) + \left[\overline{\epsilon_c T_L} \left(\frac{pLT_L}{T_C} \right) \right] \left(\frac{T_C}{T_L} \right)^{0.5} \left(\frac{T_H - T_1}{500} \right) \quad (5-145)$$

The base temperature pair T_H and T_L can be different for evaluating ϵ_c and $\overline{\alpha}_{c,T_1}$ if T_C and T_1 are far enough apart.

Example 6: Calculation of Gas Emissivity and Absorptivity

This example will use only SI units, except that pressure will be in atm, not kPa. Flue gas containing 6 percent CO₂ and 11 percent H₂O vapor, wet basis, flows through a bank of tubes of 0.1016 in (4-in) outside diameter on equilateral 0.2032 m (8-in) triangular centers. In a section in which the gas and tube surface temperatures are 691°C (964 K) and 413°C (686 K), what are the emissivity and absorptivity of the gas? From Table 5-8, $L_m = (2.8)(0.01016) = 0.2845$ m (only SI units will be used in this example). $p = p_w + p_c = 0.17$ atm; $pL = 0.0484$ m atm, barely large enough to justify the short method, the top part of Table 5-8. $p_w/p_c = 11/6$, near enough to 2 to use col. 5. Since both T_C and T_1 are below the lowest T in the top part of the table, use the nearest pair, $T_H = 1500$ K and $T_L = 1000$ K. At T_H , $b = 540$, $n = 0.42$. $\epsilon_c T_H = 540(0.0484 - 0.015)^{0.42} = 129.5$. At T_L ,

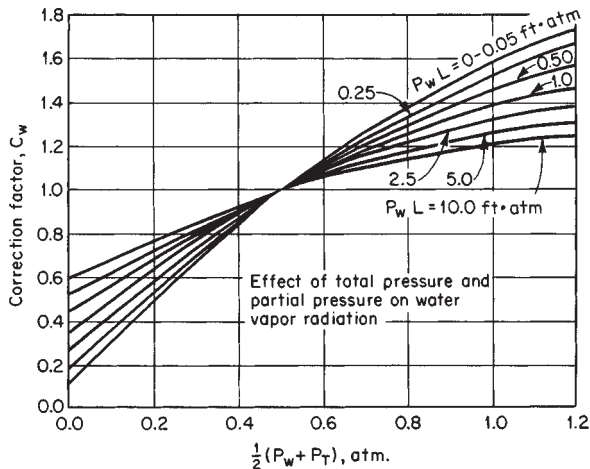


FIG. 5-21 Correction factor for converting emissivity of water vapor to values of P_w and P_r other than 0 to 1 atm respectively. To convert atmosphere-feet to kilopascal-meters, multiply by 30.89; to convert atmospheres to kilopascals, multiply by $(1.0133)(10^2)$.

$b = 444$, $n = 0.34$, $\overline{\alpha_{c_i} T_i} = 444(0.0484 - 0.015)^{0.34} = 139.8$. From interpolation Eq. (5-143) (here extrapolation), $\epsilon_c T_c = [129.5(964 - 1000) + 139.5(1500 - 964)]/500 = 140.2$. For $\overline{\alpha_{c_i} T_i}$ with $T_i = T_H = 1500$, $pL T_H / T_c = 0.0753$. From Eq. (5-144), $\overline{\alpha_{c_i} T_H} = 540(0.0753 - 0.015)^{0.42}(964/1500)^{0.5} = 133.1$. Similarly, $\overline{\alpha_{c_i} T_i} = 444(0.0502 - 0.015)^{0.34}(964/1000)^{0.5} = 139.7$. From Eq. (5-145)

$$\overline{\alpha_{c_i} T_i} = \frac{133.1(686 - 1000) + 139.7(1500 - 686)}{500} = 143.8$$

Then $\epsilon_c = 140.2/964 = 0.145$ and $\alpha_{c_i} = 143.8/686 = 0.210$. If the longer method (the bottom part of Table 5-8) were used, $\epsilon_c = 0.141$ and $\alpha_{c_i} = 0.206$.

Other Gases Because of their practical importance, the emissivities of CO_2 and H_2O have been studied much more extensively than those of other gases, and the values summarized in the preceding paragraphs are based on extensive measurement of both total and integrated spectral values. Correction for pressure has reduced the disagreement among experimenters. A summary of the less adequate information on other gases appears in Table 5-9.

Flames and Particle Clouds

Luminous Flames Luminosity conventionally refers to soot radiation; it is important when combustion occurs under such conditions that the hydrocarbons in the flame are subject to heat in the absence of sufficient air well mixed on a molecular scale. Because soot parti-

cles are small relative to the wavelength of the radiation of interest [diameters $(2)(10^{-8})$ to $(1.4)(10^{-7})$ m (200 to 1400 Å)], the monochromatic emissivity ϵ_λ depends on the total particle volume per unit volume of space f_c regardless of particle size. It is given by

$$\epsilon_\lambda = 1 - e^{-Kf_c L/\lambda} \quad (5-146)$$

where L is the path length. Use of the perfect gas law and a material balance allows the restatement of the above to

$$\epsilon_\lambda = 1 - e^{-KPSL/\lambda T} \quad (5-147)$$

where P is the total pressure (atm) and S is the mole fraction of soot in the gas. S depends on the fractional conversion f_c of the fuel carbon to soot and is the mole fraction, wet basis, of carbon in gaseous form (CO_2 , CO , CH_4 , etc.) times $f_c/(1 - f_c)$ or, with negligible error, times f_c , which is a very small number. Evaluation of K is complex, and its numerical value depends somewhat on the age of the soot, the temperature at which it is formed, and its hydrogen content. It is recommended that $K = 0.526$ [K/atm].

The total emissivity of soot ϵ_s is obtained by integration over the wavelength spectrum, giving

$$\epsilon_s = 1 - \frac{15}{4} \left[\Psi^{(3)} \left(1 + \frac{KPSL}{c_2} \right) \right], \quad (5-148)$$

where $\Psi^{(3)}(x)$ is the pentagamma function of x . It may be shown that an excellent approximation to Eq. (5-148) is

$$\epsilon_s = 1 - [1 + 34.9SPL]^{-4} \quad (5-149)$$

where PL is in atm m. The error is less the lower ϵ_s , and is only 0.5 percent at $\epsilon_s = 0.5$ and 0.8 percent at 0.67.

There is at present no method of predicting soot concentration of a luminous flame analytically; reliance must be placed on experimental measurement on flames similar to that of interest. Visual observation is misleading; a flame so bright as to hide the wall behind it may be far from a "black" radiator. The chemical kinetics and fluid mechanics of soot burnout have not progressed far enough to evaluate the soot fraction f_c for relatively complex systems. Additionally, the soot in a combustion chamber is highly localized, and a mean value is needed for calculation of the radiative heat transfer performance of the chamber. On the basis of limited experience with fitting data to a model, the following procedure is being estimated: (1) When pitch, or a highly aromatic fuel, is burned, one percent of the fuel carbon appears as soot. This produces values of ϵ_s of 0.4–0.5 and ϵ_{c_i} of 0.6–0.7. These values are lower than some measurements on pitch flames, but the measurements are usually taken through the flame at points of high luminosity. (2) When No. 2 fuel oil is burned, 33 percent of the fuel carbon appears as soot (but that number varies greatly with burner design). (3) When natural gas is burned, any soot contribution to emissivity may be ignored. Admittedly, the numbers given should be functions of burner design and excess air, and they should be considered tentative, subject to change when good data show they are off target. The Inter-

TABLE 5-9 Total Emissivities of Some Gases

Temperature $P_w L$, (atm)(ft)	1000°R			1600°R			2200°R			2800°R		
	0.01	0.1	1.0	0.01	0.1	1.0	0.01	0.1	1.0	0.01	0.1	1.0
NH_3^a	0.047	0.20	0.61	0.020	0.120	0.44	0.0057	0.051	0.25	(0.001)	(0.015)	(0.14)
SO_2^b	0.020	0.13	0.28	0.013	0.090	0.32	0.0085	0.051	0.27	0.0058	0.043	0.20
CH_4^c	0.020	0.060	0.15	0.023	0.072	0.194	0.022	0.070	0.185	0.019	0.059	0.17
CO^d	0.011	0.031	0.061	0.022	0.057	0.10	0.022	0.050	0.080	(0.012)	(0.035)	(0.050)
NO^e	0.0046	0.018	0.060	0.0046	0.021	0.070	0.0019	0.010	0.040	0.00078	0.004	0.025
HCl^f	0.00022	0.00079	0.0020	0.00036	0.0013	0.0033	0.00037	0.0014	0.0036	0.00029	0.0010	0.0027

NOTE: Figures in this table are taken from plots in Hottel and Sarofim, *Radiative Transfer*, McGraw-Hill, New York, 1967, chap. 6. Values in parentheses are extrapolated. To convert degrees Rankine to kelvins, multiply by $(5.556)(10^{-1})$. To convert atmosphere-feet to kilopascal-meters, multiply by 30.89.

^aTotal-radiation measurements of Port (Sc.D. thesis in chemical engineering, MIT, 1940) at 1-atm total pressure, $L = 1.68$ ft, T to 2000°R.

^bCalculations of Guerrieri (S.M. thesis in chemical engineering, MIT, 1932) from room-temperature absorption measurements of Coblentz (*Investigations of Infrared Spectra*, Carnegie Institution, Washington, 1905) with poor allowance for temperature.

^cBand measurements of Lee and Happel [*Ind. Eng. Chem. Fundam.*, **3**, 167 (1964)] at T up to 2050°R plus calculations to extrapolate temperature to 3800°R.

^dTotal-radiation measurements of Ullrich (Sc.D. thesis in chemical engineering, MIT, 1953) at 1-atm total pressure, $L = 1.68$ ft, T to 2200°R.

^eCalculations of Malkmus and Thompson [*J. Quant. Spectros. Radiat. Transfer*, **2**, 16 (1962)], to $T = 5400$ °R and $PL = 30$ atm · ft.

^fCalculations of Malkmus and Thompson [*J. Quant. Spectros. Radiat. Transfer*, **2**, 16 (1962)], to $T = 5400$ °R and $PL = 300$ atm · ft.

national Flame Foundation has recorded data on many luminous flames from gas, oil, and coal (see *J. Inst. Energy*, formerly *J. Inst. Fuel*, 1956 to present).

Combined Soot, H₂O, and CO₂ Radiation The spectral overlap of H₂O and CO₂ radiation has been taken into account by the constants for obtaining ϵ_C . Additional overlap occurs when soot emissivity ϵ_s is added. If the emission bands of water vapor and CO₂ were randomly placed in the spectrum and soot radiation were gray, the combined emissivity would be ϵ_C plus ϵ_s minus an overlap correction $\epsilon_C\epsilon_s$. But monochromatic soot emissivity is higher the shorter the wavelength, and in a highly sooted flame at 1500 K half the soot emission lies below 2.5 μm where H₂O and CO₂ emission is negligible. Then the correction $\epsilon_C\epsilon_s$ must be reduced, and the following is recommended:

$$\epsilon_{C+s} = \epsilon_C + \epsilon_s - M\epsilon_C\epsilon_s \quad (5-150)$$

where M depends mostly on T_C and to a much less extent on optical density SPL . Values that have been calculated from this simple model can be represented with acceptable error by

$$M = 1.07 + 18 SPL - 0.27 \left(\frac{T}{1000} \right) \quad (5-151)$$

Clouds of Large Black Particles The emissivity ϵ_M of a cloud of particles with a perimeter large compared with wavelength λ is

$$\epsilon_M = 1 - e^{-(a/v)L} \quad (5-152)$$

where a/v is the projected area of the particles per unit volume of space. If the particles have no negative curvature (a particle can see none of itself) and are randomly oriented, a is $a'/4$, where a' is the actual surface area; and if the particles are uniform, $a/v = cA = cA'/4$ where A and A' are the projected and total areas of each particle and c is the number concentration of particles. For spherical particles, this gives

$$\epsilon_M = 1 - e^{-(\pi/4)cd^2L} = 1 - e^{-1.5f_v L/d} \quad (5-153)$$

As an example, consider heavy fuel oil (CH_{1.5}, specific gravity, 0.95) atomized to a surface mean particle diameter of d , burned with 20 percent excess air to produce coke-residue particles having the original drop diameter and suspended in combustion products at 1204°C (2200°F). The flame emissivity due to the particles along a path of L m will be, with d in micrometers,

$$\epsilon_M = 1 - e^{-24.3L/d} \quad (5-154)$$

With 200- μm particles and an L of 3.05 m (10 ft), the particle contribution to emissivity will be 0.31. Soot luminosity will increase this; particle burnout will decrease it.

Clouds of Nonblack Particles The correction for nonblackness of the particles is complicated by multiple scatter of the radiation reflected by each particle. The emissivity ϵ_M of a cloud of gray particles of individual surface emissivity ϵ_1 can be estimated by the use of Eq. (5-151), with its exponent multiplied by ϵ_1 , if the optical thickness $(a/v)L$ does not exceed about 2. Modified Eq. (5-151) would predict an approach of ϵ_M to 1 as $L \rightarrow \infty$, an impossibility in a scattering system; the asymptotic value of ϵ_M can be read from Fig. 5-14 as ϵ_h , with albedo ω given by particle-surface reflectance $1 - \epsilon_1$. Particles with a perimeter lying between 0.5 and 5 times the wavelength of interest can be handled with difficulty by use of the Mie equations (see Hottel and Sarofim, *op. cit.*, chaps. 12 and 13).

Summation of Separate Contributions to Gas or Flame Emissivity Flame emissivity ϵ_{C+s} due to joint emission from gas and soot has already been treated. If massive-particle emissivity ϵ_M , such as from fly ash, coal char, or carbonaceous cenospheres from heavy fuel oil, are present, it is recommended that the total emissivity be approximated by

$$\epsilon_{C+s} + \epsilon_M - (\epsilon_{C+s})(\epsilon_M)$$

RADIATIVE EXCHANGE BETWEEN GASES OR SUSPENDED MATTER AND A BOUNDARY

Local Radiative Exchange The interchange rate \dot{Q} between an isothermal gas mass at T_C and its isothermal black bounding surface of area A_1 is given by

$$\dot{Q} = A_1 \sigma (T_C^4 \epsilon_C - T_1^4 \alpha_{C1}) \quad (5-155)$$

Evaluation of α_{C1} is unnecessary when T_1 is less than one-half T_C ; α_{C1} may then be assumed equal to ϵ_C .

If the bounding surface is gray rather than black, multiplication of Eq. (5-154) by surface emissivity ϵ_1 allows properly for reduction of the primary beams, gas-to-surface or surface-to-gas, but secondary reflections are ignored. The correction then lies between ϵ_1 and 1, and for most industrially important surfaces with $\epsilon_1 > 0.8$ a value of $(1 + \epsilon_1)/2$ is adequate. Rigorous allowance for this and other factors is presented later, e.g., Eq. (5-163).

If the bounding walls are mostly sink-type surfaces of area A_1 and temperature T_1 , but in small part refractory surfaces of area A_r in radiative equilibrium at unknown temperature T_r , an energy balance on A_r is in principle necessary to determine T_r and the effect on energy flux. However, the total heat transfer to the sink may be visualized as corresponding to its having an effective area equal to its own plus a fraction x of that of the refractory, with the only temperatures involved being those of the gas and the heat sink. The fraction x varies from zero when the ratio of refractory to heat-sink surface is very high to unity when the ratio is very low and the value of ϵ_C is low. If A_r is small compared with A_1 , a value for x of 0.7 may be used in the approximate method.

Long Exchanger This case, in which axial radiative flux is ignored, includes most radiatively modified heat exchangers of interest to chemical engineers. When the gas temperature transverse to the flow direction is reasonably uniform and the chamber is long compared with its mean hydraulic radius, the opposed upstream and downstream fluxes through the flow cross section will substantially cancel (hot combustion products through tubes or across tube banks, tunnel kilns, billet-reheating furnaces, Example 7). Under these conditions, the radiative contribution to local flux density q may be formulated in terms of local temperatures and beam lengths or exchange areas evaluated for a two-dimensional system infinite in the flow direction. The local flux density at the sink A_1 is then

$$q(T_C, T_1) = q_r(T_C, T_1) + h(T_C - T_1) \quad (5-156)$$

where h is the local convective heat-transfer coefficient and $q_r(T_C, T_1)$ the radiation contribution calculated from T_C , T_1 , ϵ_C , and ϵ_1 by using the approximate treatment in the preceding subsection or the more rigorous treatment in the following subsection. If $\dot{m}C_p$ is the hourly heat capacity of the gas stream, the temperature of which changes by dT_C over the sink-area increment dA_1 , then

$$[q(T_C, T_1)]dA_1 = -\dot{m}C_p dT_C \quad (5-157)$$

from which

$$A_1 = \dot{m} \int_{T_{C,\text{outlet}}}^{T_{C,\text{inlet}}} \frac{C_p dT_C}{q(T_C, T_1)} \quad (5-158)$$

The area under a curve of C_p/q versus T_C or $1/q$ versus the specific enthalpy i may be used to solve for the area A_1 required to obtain a given outlet temperature or to obtain the outlet temperature given A_1 . Three points generally suffice to determine the area under the curve within 10 percent.

Instead of using graphical integration, which can handle any complexity of variation of flux density q with T_C and T_1 along an interchanger flow path, one may evaluate a mean flux density based on mean gas and sink temperatures, based in turn on terminal temperatures. It has been found empirically that fair results are obtained by the use of a mean surface temperature equal to the arithmetic mean of the terminal surface temperatures and by the use of a mean gas temperature equal to the mean surface temperature plus the logarithmic mean of the temperature difference, gas to surface, at the two ends of the exchanger. When radiation dominates the transfer process, however, graphical integration is safer.

Example 7: Radiation in Gases Flue gas containing 6 percent carbon dioxide and 11 percent water vapor by volume (wet basis) flows through the convection bank of an oil tube still consisting of rows of 0.102-m (4-in) tubes on 0.203-m (8-in) centers, nine 7.62-m (25-ft) tubes in a row, the rows staggered to put the tubes on equilateral triangular centers. The flue gas enters at 871°C (1144 K, 1600°F) and leaves at 538°C (811 K, 1000°F). The oil flows in a countercurrent direction to the gas and rises from 316 to 427°C (600 to 800°F). Tube surface emissivity is 0.8. What is the average heat-input rate, due to gas radiation alone, per square meter of external tube area?

With each row of tubes there is associated $(0.203)(\sqrt{3}/2) = 0.176 \text{ m}$ (0.577 ft) of wall height, of area $[(0.203)(9)(2) + (7.62)(2)]0.176 - (9)(2)(\pi)(0.0508)^2 = 3.18 \text{ m}^2$ (34.2 ft²). One row of tubes has an area of $(\pi)(0.102)(7.62)(9) = 22.0 \text{ m}^2$ (236 ft²). If the recommended factor of 0.7 on the refractory area is used, the effective area of the tubes is $[22.0 + (0.7)(3.18)]/22.0 = 1.10 \text{ m}^2/\text{m}^2$ of actual area. The exact evaluation of the outside tube temperature from the known oil temperature would involve a knowledge of the oil-film coefficient, tube-wall resistance, and rate of heat flow into the tube, the evaluation usually involving trial and error. However, for the present purpose the temperature drop through the tube wall and oil film will be assumed to be 41.7°C (75°F), making the tube surface temperatures 357°C (675°F) and 468°C (875°F); the average is 412°C (775°F). The radiating gas temperature is

$$t_g = 412 + \frac{(871 - 468) - (538 - 357)}{2.3 \log [(871 - 468)/(538 - 357)]}$$

$$= 412 + 278 = 690^\circ\text{C} \text{ (1274}^\circ\text{F)}$$

These temperatures, partial pressures, and dimensions were used in Example 6 to determine gas emissivity and absorptivity, $\epsilon_c = 0.145$; $\alpha_{c1} = 0.210$. The approximate effective emissivity of the boundary is $(0.8 + 1)/2 = 0.9$. Then from Eq. (5-155), modified to allow for sink emissivity and for the presence of a small amount of refractory boundary,

$$\dot{Q}/A_1 = q = (0.9)(1.10)\sigma(T_c^4 \epsilon_c - T_1^4 \alpha_c)$$

$$= (0.9)(1.10)(5.67)[(9.63)^4(0.145) - (6.85)^4(0.210)]$$

$$= 4405 \text{ J/(m}^2 \text{ tube area}\cdot\text{s)} [1396, \text{ Btu/(ft}^2 \text{ tube area}\cdot\text{h)}]$$

This is equivalent to a convection coefficient of 4405/278, or 15.85 W/(m²)(K) which is of the order of magnitude expected of the convection coefficient itself. Radiation rapidly becomes dominant as the system temperature rises.

Total-Exchange Areas $\overline{S_1 S_2}$ and $\overline{GS_1}$ The arguments leading to the development of the interchange factor $A_i \mathcal{F}_{ij}$ ($= S_i S_j$) between surfaces apply to the case of absorption within the gas volume if in the evaluation of the direct-exchange areas allowance is made for attenuation of the radiant beam through the gas. This necessitates nothing more than redefinition, in Eqs. (5-126) to (5-130), of every term \bar{ij} ($= S_i S_j = A_i F_{ij}$) to represent, per unit black emissive power, flux from A_i through an absorbing gas to A_j . This may be visualized as multiplication of $A_i F_{ij}$ by the mean gas transmittance T_{ij} ($= 1 - \epsilon_c$ for a gray gas). In a system containing an isothermal gas and source-sink boundaries of areas $A_1 \dots A_n$, the total emission from A_1 per unit of its black emissive power is $\epsilon_1 A_1$, of which $S_1 S_1 + S_1 S_2 + \dots + S_1 S_n$ is absorbed in the various source-sink surfaces by multiple reflections. The difference has been absorbed in the gas and is called the gas-surface total-exchange area $\overline{GS_1}$

$$\overline{GS_1} = A_1 \epsilon_1 - \sum_i \overline{S_1 S_i} \quad (5-159)$$

Note that though $\overline{S_1 S_i}$ is never used in calculating radiative exchange, its value is necessary for use of Eq. (5-159) to calculate $\overline{GS_1}$.

If the gas volume is not isothermal and is zoned, an additional magnitude, the gas-to-gas total-exchange area $G_i G_j$, arises (see Hottel and Sarofim, *Radiative Transfer*, McGraw-Hill, New York, 1967, chap. 11). Space does not permit derivations of special cases; only the single-gas-zone system is treated here.

Single-Gas-Zone/Two-Surface-Zone Systems An enclosure consisting of but one isothermal gas zone and two gray surface zones can, properly specified, model so many industrially important radiation problems as to merit detailed presentation. One can evaluate the total radiation flux between any two of the three zones, including multiple reflection at all surfaces.

$$\dot{Q}_{G \leftrightarrow 1} = \overline{GS_1} \sigma (T_c^4 - T_1^4)$$

$$\dot{Q}_{1 \leftrightarrow 2} = \overline{S_1 S_2} \sigma (T_1^4 - T_2^4)$$

The total-exchange area takes a relatively simple closed form, even when important allowance is made for gas radiation not being gray and when a reduction of the number of system parameters is introduced by assuming that one of the surface zones, if refractory, is radiatively adiabatic. Before allowance is made for these factors, the case of a gray gas enclosed by two source-sink surface zones will be presented. Modification of Eq. 5-130, as discussed in the first paragraph of this subsection, combined with the assumption that a single mean beam length applies to all transfers; that is, that there is but one gas transmittance $\tau (= 1 - \epsilon_c)$, gives

$$\overline{S_1 S_2} = \frac{A_1 \epsilon_1 \epsilon_2 F_{12}}{1/\tau + \tau \rho_1 \rho_2 (1 - F_{12}/C_2) - \rho_1 (1 - F_{12}) - \rho_2 (1 - F_{21})} \quad (5-160)$$

$$\overline{S_1 S_1} = \frac{A_1 \epsilon_1^2 (F_{11} + \rho_2 (F_{12}/C_2 - 1))}{1/\tau + \tau \rho_1 \rho_2 (1 - F_{12}/C_2) - \rho_1 (1 - F_{12}) - \rho_2 (1 - F_{21})} \quad (5-161)$$

$$\overline{GS_1} = \frac{A_1 \epsilon_1 \epsilon_c (1/\tau + \rho_2 (F_{12}/C_2 - 1))}{1/\tau + \tau \rho_1 \rho_2 (1 - F_{12}/C_2) - \rho_1 (1 - F_{12}) - \rho_2 (1 - F_{21})} \quad (5-162)$$

These three expressions suffice to formulate total-exchange areas for gas-enclosing arrangements which include, for example, the four cases illustrated in Table 5-10.

An additional surface arrangement of importance is a single-zone surface enclosing gas. With the gas assumed gray, the simplest derivation of $\overline{GS_1}$ is to note that the emission from surface A_1 per unit of its blackbody emissive power is $A_1 \epsilon_1$, of which the fractions ϵ_c and $(1 - \epsilon_c) \epsilon_1$ are absorbed by the gas and the surface, respectively, and the surface-reflected residue always repeats this distribution. Therefore,

$$\overline{GS_1}^{\text{single surface zone surrounding gray gas}} \equiv \overline{GS_1} = A_1 \epsilon_1 \frac{\epsilon_c}{\epsilon_c + (1 - \epsilon_c) \epsilon_1} = \frac{A_1}{\frac{1}{\epsilon_c} + \frac{1}{\epsilon_1} - 1} \quad (5-163)$$

Alternatively, $\overline{GS_1}$ could be obtained from Case 1 of Table 5-10 by letting plane area A_1 approach 0, leaving A_2 as the sole surface zone.

Departure of gas from grayness has so marked an effect on radiative transfer that the subject will be presented prior to discussion of the systems covered by Table 5-10.

The Effect of Nongrayness of Gas on Total-Exchange Area A radiating gas departs from grayness in two ways: (1) Its transmittance τ through successive path lengths L_m due to surface reflection, instead of being constant, keeps increasing because at the wavelengths of high absorption the incremental absorption decreases with increasing pathlength; (2) Gas emissivity ϵ_c and absorptivity α_{c1} are not the same unless T_1 equals T_c . The total emissivity of a real gas, the spectral emissivity, and absorptivity ϵ_λ that varies in any way with λ can be expressed as the a -weighted mean of a suitable number of gray-gas emissivity or absorptivity terms $\epsilon_{c,i}$ or $\alpha_{c,i}$, representing the gray-gas emissivity or absorptivity in the energy fractions a_i of the blackbody spectrum. Then

$$\epsilon_c = \sum_0^n a_i \epsilon_{c,i} = \sum_0^n a_i (1 - e^{-k_i p L}) \quad (5-164)$$

For simplicity, n should be as low as is consistent with small error. The retention of but two terms is feasible when one considers that if α_{c1} is so fitted that the first absorption and the second following surface reflection are correct, then further attenuation of the beam by successive surface reflections makes the errors in those absorptions decrease in importance. Let the gas be modeled as the sum of one gray gas plus a clear gas, with the gray gas occupying the energy fraction a of the blackbody spectrum and the clear gas the fraction $(1 - a)$. Then

$$[\epsilon_c(pL)] = a(1 - e^{-kpL}) + (1 - a)0$$

$$[\epsilon_c(2pL)] = a(1 - e^{-2kpL}) + (1 - a)0 \quad (5-165)$$

Solution of these gives

$$a = \frac{\epsilon_c(pL)}{2 - \frac{\epsilon_c(2pL)}{\epsilon_c(pL)}}$$



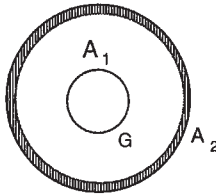
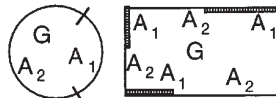
$$kpL = -\ln \left[1 - \frac{\epsilon_c(pL)}{a} \right] \quad (5-166)$$

Note that these values are specific to the subject problem in which the mean beam length is L_m , with $\epsilon_{c,i}$ evaluated from basic data, such as Table 5-8. $(1 - e^{-kpL})$ in Eq. (5-165) represents the emissivity of a gray gas, which will be called $\epsilon_{c,i}$. For later use, note that,

$$\epsilon_{c,i} = \frac{\epsilon_c(pL)}{a} \quad (5-167)$$

To allow for the difference between emissivity and absorptivity and combine them into a single emissivity-absorptivity term called effec-

TABLE 5-10 Total-Exchange Areas for Four Arrangements of Two-Zone-Surface Enclosures of a Gray Gas

			
<p>A plane surface A_1 and a surface A_2 completing the enclosure</p> <p>$F_{12} = 1$</p> $\frac{\overline{S_1 S_2}}{A_1} = \frac{\epsilon_1 \epsilon_2}{D_1}$ $\frac{\overline{GS_1}}{A_1} = \frac{\epsilon_1 \epsilon_C (1/\tau + \rho_2 A_1/A_2)}{D_1}$ $\frac{\overline{GS_2}}{A_2} = \frac{\epsilon_2 \epsilon_C (1/\tau + \rho_1 A_1/A_2)}{D_1}$ $\frac{\overline{S_1 S_1}}{A_1} = \frac{\epsilon_1^2 \tau \rho_2 A_1/A_2}{D_1}$ $D_1 \equiv \frac{1}{\tau} - \rho_2 \left[1 - \frac{A_1}{A_2} (1 - \tau \rho_1) \right]$	<p>Infinite parallel planes</p> <p>$F_{12} = F_{21} = 1$</p> $\frac{\overline{S_1 S_2}}{A_1} = \frac{\epsilon_1 \epsilon_2}{D_2}$ $\frac{\overline{GS_1}}{A_1} = \frac{\epsilon_1 \epsilon_C (1/\tau + \rho_2)}{D_2}$ $\frac{\overline{S_1 S_1}}{A_1} = \frac{\epsilon_1^2 \rho_2 \tau}{D_2}$ <p>$D_2 \equiv 1/\tau - \tau \rho_1 \rho_2$</p>	<p>Concentric spherical or infinite cylindrical surface zones, A_1 inside</p> <p>$F_{12} = 1; F_{21} = A_1/A_2$</p> $\frac{\overline{S_1 S_2}}{A_1} = \frac{\epsilon_1 \epsilon_2}{D_3}$ $\frac{\overline{GS_1}}{A_1} = \frac{\epsilon_1 \epsilon_C (1/\tau + \rho_2 A_1/A_2)}{D_3}$ $\frac{\overline{GS_2}}{A_2} = \frac{\epsilon_2 \epsilon_C (1/\tau + \rho_1 A_1/A_2)}{D_3}$ $\frac{\overline{S_1 S_1}}{A_1} = \frac{\epsilon_1^2 \rho_2 \tau A_1/A_2}{D_3}$ <p>$D_3 \equiv \frac{1}{\tau} - \rho_2 \left[1 - \frac{A_1}{A_2} (1 - \tau \rho_1) \right]$</p>	<p>Two-surface-zone spherical surface, each zone one or more parts; or speckled enclosure, any shape</p> <p>$F_{12} = F_{22} = C_2; F_{21} = F_{11} = C_1$</p> $\frac{\overline{S_1 S_2}}{A_1} = \frac{\epsilon_1 \epsilon_2 C_2}{D_4}$ $\frac{\overline{GS_1}}{A_1} = \frac{\epsilon_1 \epsilon_C / \tau}{D_4}$ $\frac{\overline{S_1 S_1}}{A_1} = \frac{\epsilon_1^2 C_1}{D_4}$ <p>$D_4 \equiv 1/\tau - \rho_1 C_1 - \rho_2 C_2$</p>

tive emissivity $\epsilon_{C,e}$, one must first evaluate absorptivity α_{C1} using Eq. (5-161). Formulation of the net direct exchange can then be used to define $\epsilon_{C,e}$:

$$\sigma(\epsilon_C T_C^4 - \alpha_{C1} T_1^4) \equiv \sigma \epsilon_{C,e} (T_C^4 - T_1^4)$$

$$\text{or} \quad \epsilon_{C,e} = \frac{\epsilon_{C,e} - \alpha_{C1} (T_1^4/T_C^4)}{1 - (T_1/T_C)^4} \quad (5-168)$$

The emissivity and absorptivity of use in converting gray-gas total-exchange areas to real-gas values are $\epsilon_{C,e}$ and a_e , the latter obtained by using Eq. (5-166), except that $\epsilon_{C,e} (pL)$ replaces $\epsilon_C (pL)$; the same for $\epsilon_{C,e} (2pL)$. This means that, for the conversion, four terms will have to be formulated: $\epsilon_C (pL)$, $\epsilon_C (2pL)$, $\alpha_{C1} (pL)$, and $\alpha_{C1} (2pL)$. The gray emissivity term $\epsilon_{C,e}$ of Eq. (5-167) now becomes $\epsilon_{C,e}/a_e$.

Conversion of gray-gas total exchange areas \overline{GS} and \overline{SS} to their nongray form depends on the fact that the relation between radiative transfer and blackbody emissive power σT^4 is linear and proportional. The gray-gas-equivalent emissivity $\epsilon_{C,e}/a_e$ is applicable only to the energy fraction a_e of σT^4 . In consequence, to convert \overline{GS} or \overline{SS} to its nongray form, wherever ϵ_C or τ appears in \overline{GS} it must be replaced by $\epsilon_{C,e}/a_e$ or $(1 - \epsilon_{C,e}/a_e)$, respectively; the overall result is then multiplied by a_e . The converted \overline{SS} is in two parts: The gray-gas contribution involves, as above, replacement of ϵ_C by $\epsilon_{C,e}/a_e$ and τ by $(1 - \epsilon_{C,e}/a_e)$, and the result multiplied by a_e ; for the clear-gas contribution, ϵ_C is replaced by 0 and τ by 1, and the result is multiplied by $(1 - a_e)$ and added to the gray-gas contribution.

The simplest application of this simple gray-plus-clear model of gas radiation is the case of a single gas zone surrounded by a single surface zone, Eq. (5-163) for a gray gas. The gray-plus-clear model gives

$$\frac{\overline{GS_1}}{A_1} = \frac{a_e}{\frac{\epsilon_{C,e}}{\epsilon_1} + \frac{1}{\epsilon_1} - 1} \quad (5-169)$$

Example 8: Effective Gas Emissivity Methane is burned to completion with 20 percent excess air (air half-saturated with water vapor at 298 K (60°F), 0.0088 mols H₂O/mol dry air) in a furnace chamber of floor dimensions 3 × 10 m and height 5 m. The whole surface is a gray-energy sink of emissivity 0.8

at 1000 K. The surrounding gas is at 1500 K and is well stirred. Find the effective gas emissivity $\epsilon_{C,e}$, the weighting factor a_e , and the surface radiative flux density.

Solution: Combustion is $1\text{CH}_4 + 2 \times 1.2\text{O}_2 + 2 \times 1.2 \times 79/21\text{N}_2 + 2 \times 1.2 \times 100/21 \times 0.0088\text{H}_2\text{O}$, going to $1\text{CO}_2 + [2 + 2 \times 1.2 \times (100/21) \times 0.0088]\text{H}_2\text{O} + 0.4\text{O}_2 + 9.03\text{N}_2 = 12.53$ moles per mole of CH₄; $p_e + p_w = (1 + 2.1)/12.53 = 0.2474$ atm. The mean beam length, $L_m = 0.88 \times 4V/A_f = 0.88 \times 4(10 \times 3 \times 5)/[2 \times (10 \times 3 + 10 \times 5 + 3 \times 5)] = 2.779$ m. $pL_m = 0.2474 \times 2.779 = 0.6875$ m atm. From emissivity Table 5-8, $b(1500) = 540$; $n(1500) = 0.42$; $b(1000) = 444$; $n(1000) = 0.34$. $\epsilon_C(pL) = 540(0.6875 - 0.015)^{0.42}/1500 = 0.3047$; $\alpha_{C1}(pL) = 444(0.6875 \times 1000/1500 - 0.015)^{0.34} (1500/1000)^{0.5}/1000 = 0.4124$. Then $\epsilon_{C,e}(pL) = [0.3047 - 0.4124(1000/1500)^4]/[1 - (1000/1500)^4] = 0.2782$. Repeat all 3 computations for $pL = 2 \times 0.6875$ to give $\epsilon_C(2pL) = 0.4096$, $\alpha_{C1}(2pL) = 0.5250$, $\epsilon_{C,e}(2pL) = 0.3812$. Then $a_e = 0.2782/(2 - 0.3812/0.2782) = 0.4418$ and the emissivity substitute $= 0.2782/0.4418 = 0.6297$. For a single enveloping surface zone, the total-exchange area comes from Eq. (5-169); $\overline{GS_1}/A_1 = a_e/(a_e/\epsilon_{C,e} + 1/\epsilon_1 - 1) = 0.4418/(0.4418/0.2782 + 1/0.8 - 1) = 0.2404$. The flux density is $\dot{Q}/A = q = (\overline{GS_1}/A)\sigma(T_C^4 - T_1^4) = 0.2404 \times 56.7 \times [(1500/1000)^4 - (1000/1000)^4] = 55.37$ kW/m² (17,550 Btu/sq ft hr). (Note that allowing for average humidity in air adds 5 percent to H₂O and approximately 2 percent to gas emissivity.)

Total-exchange areas for the basic one-gas two-surface model [Eqs. (5-160) to (5-162)], used to evaluate the cases in Table 5-10, take the following form when converted by the above described procedure to their nongray form:

$$\frac{\overline{S_1 S_2}}{A_1} = \frac{a_e A_1 F_{12} \epsilon_1 \epsilon_2}{1/(1 - \epsilon_{C,e}/a_e) + (1 - \epsilon_{C,e}/a_e) \rho_1 \rho_2 (1 - F_{12} C_2) - \rho_1 (1 - F_{12}) - \rho_2 (1 - F_{21})} + \frac{(1 - a_e) A_1 F_{12} \epsilon_1 \epsilon_2}{1 + \rho_1 \rho_2 (1 - F_{12} C_2) - \rho_1 (1 - F_{12}) - \rho_2 (1 - F_{21})} \quad (5-170)$$

$$\frac{\overline{GS_1}}{A_1} = \frac{A_1 \epsilon_1 \epsilon_{C,e} (1/(1 - \epsilon_{C,e}/a_e) + \rho_2 (F_{12}/C_2 - 1))}{1/(1 - \epsilon_{C,e}/a_e) + (1 - \epsilon_{C,e}/a_e) \rho_1 \rho_2 (1 - F_{12} C_2) - \rho_1 (1 - F_{12}) - \rho_2 (1 - F_{21})} \quad (5-171)$$

Modification of Table 5-10 to make the total-exchange areas conform to the gray-plus-clear gas model is straightforward, following the instructions presented above. The results are given in Table 5-11.

TABLE 5-11 Conversion of Some Total-Exchange Areas to Their Gray-Plus-Clear Values1. Plane slab A_1 and surface A_2 , completing an enclosure of gas ($F_{12} = 1$)

$$\frac{\overline{S_1 S_2}}{A_1} = \frac{a\epsilon_1\epsilon_2}{D_1} + \frac{(1-a)\epsilon_1\epsilon_2}{1-\rho_2(1-\epsilon_1A_1/A_2)}$$

$$\left[D_1 = \frac{1}{1-\epsilon_C/a} - \rho_2 \left(1 - \left(\frac{A_1}{A_2} \right) \left(\epsilon_1 + \frac{\rho_1\epsilon_C}{a} \right) \right) \right]$$

$$\frac{\overline{GS_1}}{A_1} = \frac{\epsilon_1\epsilon_C(1/(1-\epsilon_C/a) + \rho_2A_1/A_2)}{D_1}$$

$$\frac{\overline{GS_2}}{A_2} = \frac{\epsilon_2\epsilon_C(1/(1-\epsilon_C/a) + \rho_1A_1/A_2)}{D_1}$$

2. Infinite parallel planes, gas between ($F_{12} = F_{21} = 1$)

$$\frac{\overline{S_1 S_2}}{A_1} = \frac{a\epsilon_1\epsilon_2}{D_2} + \frac{(1-a)\epsilon_1\epsilon_2}{1-\rho_1\rho_2}$$

$$\left[D_2 = \frac{1}{1-\epsilon_C/a} - \left(1 - \frac{\epsilon_C}{a} \right) \rho_1\rho_2 \right]$$

$$\frac{\overline{GS_1}}{A_1} = \frac{\epsilon_1\epsilon_C(1/(1-\epsilon_C/a) + \rho_2)}{D_2}$$

3. Concentric spherical or infinite cylindrical surface zones, A_1 inside ($F_{12} = 1$; $F_{21} = A_1/A_2$)

$$\frac{\overline{S_1 S_2}}{A_1} = \frac{a\epsilon_1\epsilon_2}{D_3} + \frac{(1-a)\epsilon_1\epsilon_2}{1-\rho_2(1-\epsilon_1A_1/A_2)}$$

$$D_3 = \frac{1}{(1-\epsilon_C/a)} - \rho_2 \left[1 - \left(\frac{A_1}{A_2} \right) \left(\epsilon_1 + \frac{\rho_1\epsilon_C}{a} \right) \right]$$

$$\frac{\overline{GS_1}}{A_1} = \frac{\epsilon_1\epsilon_C(1/(1-\epsilon_C/a) + \rho_2A_1/A_2)}{D_3}$$

$$\frac{\overline{GS_2}}{A_2} = \frac{\epsilon_2\epsilon_C(1/(1-\epsilon_C/a) + \rho_1A_1/A_2)}{D_3}$$

4. Spherical enclosure of two surface zones or "speckled" $A_1:A_2$ enclosure ($F_{12} = F_{22} = C_2$; $F_{21} = F_{11} = C_1$)

$$\frac{\overline{S_1 S_2}}{A_1} = \frac{a\epsilon_1\epsilon_2C_2}{D_4} + \frac{(1-a)\epsilon_1\epsilon_2C_2}{1-\rho_1C_1-\rho_2C_2}$$

$$\left[D_4 = \frac{1}{(1-\epsilon_C/a)} - \rho_1C_1 - \rho_2C_2 \right]$$

$$\left[C_1 = \frac{A_1}{A_1 + A_2} \right]$$

$$\frac{\overline{GS_1}}{A_1} = \frac{\epsilon_1\epsilon_C(1-\epsilon_C/a)}{D_4}$$

Treatment of Refractory Walls Partially Enclosing a Radiating Gas Another modification of the results in Table 5-10 becomes important when one of the surface zones is radiatively adiabatic; the need to find its temperature can be eliminated. If surface A_2 , now called A_r , is radiatively adiabatic, its net radiative exchange with A_1 must equal its net exchange with the gas.

$$\overline{GS_r}(T_C^4 - T_r^4) = \overline{S_r S_1}(T_r^4 - T_1^4)$$

or

$$\frac{T_C^4 - T_r^4}{1/\overline{GS_r}} = \frac{T_r^4 - T_1^4}{1/S_r S_1} = \frac{T_C^4 - T_1^4}{1/\overline{GS_r} + 1/S_r S_1} \quad (5-172)$$

The net flux from gas G is $\overline{GS_1}\sigma(T_C^4 - T_1^4) + \overline{GS_r}\sigma(T_C^4 - T_r^4)$ which, with replacement of the last term using Eq. (5-172), gives the single term

$$\sigma(T_C^4 - T_1^4) \left[\overline{GS_1} + \frac{1}{\frac{1}{\overline{GS_r}} + \frac{1}{S_r S_1}} \right]$$

The bracketed term is called $(\overline{GS_1})_R$, the total exchange area from G to A_1 with assistance from a refractory surface. In summary,

$$\dot{Q}_{G \leftrightarrow 1} = (\overline{GS_1})_R \sigma(T_C^4 - T_1^4) = \left[\overline{GS_1} + \frac{1}{\frac{1}{\overline{GS_r}} + \frac{1}{S_r S_1}} \right] \sigma(T_C^4 - T_1^4) \quad (5-173)$$

Table 5-10 supplies the forms for the three terms needed to formulate $(\overline{GS_1})_R$, with A_r substituted for A_2 . If, in addition, allowance is to be made for the gas not being gray, $\epsilon_{C,r}$ and a_r are evaluated using values of the emissivity and absorptivity calculated using Table 5-8, and the procedure described in the previous subsection is followed with $\epsilon_{C,r}/a_r$ replacing ϵ_C together with the addition of a clear-gas contribution, when SS is at issue. It is tempting to say that a surface A_2 (or A_r) could be made radiatively adiabatic simply by assigning its reflectance ρ a value of 1, making the terms in the brackets of Eq. (5-173) much easier to evaluate and the result much simpler. This is valid only if the gas is gray. If it is not, A_r is a net absorber of radiation

in the spectral energy fraction a (or a_c) and a net emitter in the clear-gas fraction $(1 - a)$.

Conversion of \overline{GS} to $(\overline{GS})_R$ will be carried out for two of the four cases of Table 5-10. Case 1 is an idealization of a metal-heating slab furnace or glass furnace, with its plane sink A_1 combining with refractory surface A_r to complete the enclosure. With insertion into Eq. (5-173) of \overline{GS}_1 , \overline{GS}_r , and $S_r S_1$ after converting each to its gray plus clear form, one obtains

$$\frac{(\overline{GS})_R}{A_1} = \frac{\epsilon_C}{D_1} \left[\epsilon_1 \left(\rho_2 \frac{C_1}{C_r} + \frac{1}{1 - \epsilon_C} \right) + \frac{1}{\rho_1 + (C_r/C_1)[1 - (\epsilon_C/a)]} + \frac{\epsilon_r}{\epsilon_C \left[a \left(\epsilon_r + \rho_1 \epsilon_1 \frac{C_1}{C_r} \right) \right]} \right] + (1 - a) D_1 \quad (5-174)$$

where $D_1 = 1/(1 - \epsilon_C/a) - \rho_1[1 - (C_r/C_1)[1 - \rho_1(1 - \epsilon_C/a)]]$.

Conversion of $(\overline{GS})_R$ to applicability to a gray gas comes by making a equal 1, producing the enormous simplification to

$$\left[\frac{(\overline{GS})_R}{A_1} \right]_{\text{gray}} = \frac{1}{\frac{1 + C_1(1/\epsilon_C - 2)}{1 - C_1\epsilon_C} + \frac{\rho_1}{\epsilon_1}} \quad (5-175)$$

Note that the emissivity and reflectance of the refractory are without effect on $(\overline{GS})_R$ if the gas is gray.

The second conversion of \overline{GS} to $(\overline{GS})_R$ will be Case 4 of Table 5-10, the two-surface-zone enclosure with computation simplified by assuming that the direct-view factor from any spot to a surface equals the fraction of the whole enclosure that the surface occupies (the speckled-furnace model). This case can be considered an idealization of many processing furnaces such as distilling and cracking coil furnaces, with parts of the enclosure tube-covered and part left refractory. (But the refractory under the tubes is not to be classified as part of the refractory zone.) Again, one starts with substitution into Eq. (5-173) of the terms \overline{GS}_1 , \overline{GS}_r , and $S_r S_1$ from Table 5-10, Case 4, with all terms first converted to their gray-plus-clear form. To indicate the procedure, one of the components, $S_r S_1$, will be formulated.

$$\frac{S_r S_1}{A_1} = a \frac{C_r \epsilon_1 \epsilon_r}{D_4} + (1 - a) \frac{C_r \epsilon_1 \epsilon_r}{1 - \rho_1 C_1 - \rho_r C_r} = \frac{C_r \epsilon_1 \epsilon_r}{D_4} \left(1 + \frac{\epsilon_C(1 - a)(a - \epsilon_C)}{1 - \rho_1 C_1 - \rho_r C_r} \right)$$

With $D_4 = 1/(1 - \epsilon_C/a) - \rho_1 C_1 - \rho_r C_r$, the result of the full substitution simplifies to

$$\frac{(\overline{GS})_R}{A_1} = \frac{1}{C_1 \left(\frac{1}{\epsilon_C} - \frac{1}{a} \right) + \frac{1}{\epsilon_1} + \frac{1/a - 1}{\epsilon_1 + \epsilon_r(C_r/C_1)}} \quad (5-176)$$

For a gray gas ($a = 1$), the above becomes

$$\frac{(\overline{GS})_R}{A_1} = \frac{1}{C_1 \left(\frac{1}{\epsilon_C} - 1 \right) + \frac{1}{\epsilon_1}} \quad (5-177)$$

Eq. (5-176) has wide applicability.

COMBUSTION CHAMBER HEAT TRANSFER

Treatment of radiative transfer in combustion chambers is available at varying levels of complexity, including allowance for temperature variation in both gas and refractory walls (Hottel and Sarofim,

Radiative Transfer, McGraw-Hill, New York, 1967, chap. 14). A less rigorous treatment suffices, however, for handling many problems. There are two limiting cases: the long chamber with gas temperature varying only in the direction of gas flow (already treated) and the compact chamber containing a gas or a flame to which can be assigned an effective or average radiating temperature. The latter will be considered.

Stirred-Chamber Model; Refractory Wall Loss Negligible

What furnace engineers most need is a closed-form solution of the problem, theoretically sound in structure and therefore containing a minimum number of parameters and no empirical constants and, preferably, physically visualizable. They can then (1) correlate data on existing furnaces, (2) develop a performance equation for standard design, or (3) estimate performance of a new furnace type on which no data are available.

An equation representing an energy balance on a combustion chamber of two surface zones, a heat sink A_1 at temperature T_1 , and a refractory surface A_r assumed radiatively adiabatic at T_r , is most simply solved if the total enthalpy input H is expressed as $\dot{m} \bar{C}_p (T_F - T_o)$; \dot{m} is the mass rate of fuel plus air; and T_F is a pseudoadiabatic flame temperature based on a mean specific heat from base temperature T_o up to the gas exit temperature T_E rather than up to T_F . The heat transfer rate \dot{Q} out of the gas is then $\dot{H} - \dot{m} \bar{C}_p (T_E - T_o)$ or $\dot{m} \bar{C}_p (T_F - T_E)$. The energy balance, with ambient temperature taken as conventional base T_o , is

$$(\dot{Q} =) \dot{H} - \dot{m} \bar{C}_p (T_E - T_o) = (\overline{GS})_R \sigma (T_C^4 - T_1^4) + h_1 A_1 (T_C - T_1) + A_o F_o \sigma (T_C^4 - T_o^4) + U A_r (T_C - T_o) \quad (5-178)$$

To make the relation dimensionless, divide through by $(\overline{GS})_R \sigma T_F^4$ and let all temperatures, expressed as ratios to T_F , be called τ . For clarity, the terms are tabulated:

$$\dot{m} \bar{C}_p / (\overline{GS})_R \sigma T_F^4 = D, \text{ dimensionless firing density}$$

$$\text{l.h.s. term} = D(1 - \tau_E)$$

$$\text{1st r.h.s. term} = \tau_C^4 - \tau_1^4$$

$$(h_1 A_1) / (\overline{GS})_R \sigma T_F^4 = L_c, \text{ convection number (dimensionless)}$$

$$A_o F_o / (\overline{GS})_R \sigma T_F^4 = L_o, \text{ wall-openings loss number, (dimensionless)}$$

$$U A_r / (\overline{GS})_R \sigma T_F^4 = L_r, \text{ refractory-wall loss number (dimensionless)}$$

The equation then becomes

$$D(1 - \tau_E) = \tau_C^4 - \tau_1^4 + L_c(\tau_C - \tau_1) + L_o(\tau_C^4 - \tau_o^4) + L_r(\tau_C - \tau_o) \quad (5-179)$$

This equation has two unknowns (τ_C and τ_E), and an empirical relation between them is needed. Many have been tried, and one of the best is to assume that the excess of T_C over T_E expressed as a ratio to T_F (zero for a perfectly stirred chamber) is a constant Δ [$\equiv (T_C - T_E)/T_F$]. Although Δ should vary with burner type, the effects of firing rate and percent excess air are small. In the absence of performance data on the kind of furnace under study, assume $\Delta = 300/T_F$, °R or $170/T_F$, K. The left side of Eq. (5-178) then becomes $D(1 - \tau_C + \Delta)$, and with coefficients of τ_C and τ_C^4 collected, the equation becomes

$$\tau_C^4 + \left(\frac{D + L_c + L_r}{1 + L_o} \right) \tau_C - \left(\frac{\tau_1^4 + L_c \tau_1 + L_o \tau_o^4 + L_r \tau_o + D(1 + \Delta)}{1 + L_o} \right) = 0 \quad (5-180)$$

Though this is a quartic equation, it is capable of explicit solution because of the absence of second and third degree terms. Trial-and-error enters, however, because $(\overline{GS})_R$ and \bar{C}_p are mild functions of T_C and related T_E , respectively, and a preliminary guess of T_C is necessary. An ambiguity can exist in interpretation of terms. If part of the enclosure surface consists of screen tubes over the chamber-gas exit to a convection section, radiative transfer to those tubes is included in the chamber energy balance, but convection is not, because it has no effect on chamber gas temperature.

With Eq. (5-180) solved, the gas-side efficiency η_G is $(1 - \tau_C + \Delta)/(1 - \tau_o)$. The sink-side efficiency η_1 is less by the amount $(L_o(\tau_C^4 - \tau_o^4) + L_r(\tau_C - \tau_o))/D(1 - \tau_o)$ and is also given by $[(\overline{GS})_R \sigma (T_C^4 - T_1^4) + h_1 A_1 (T_C - T_1)]/H$. It must be remembered that the efficiency η_1

includes the losses through the wall from the backside of any wall-mounted heat sinks. Though the results must be considered approximations, depending as they do on the empirical Δ , the equation may be used to find the effect of firing rate, excess air, and air pre-heat on efficiency. With some performance data available, the small effect of various factors on Δ may be found.

The first term on the right side of Eq. (5-179) is so nearly dominant for most furnaces that consideration of the main features of chamber performance is clarified by ignoring the loss terms L_o and L_r or by assuming that they and L_c have a constant mean value. The relation of a modified chamber efficiency $\eta_{C1}(1 - \tau_o)$ to a modified firing density $D/(1 - \tau_o)$ and to the normalized sink temperature $\tau = T_1/T_F$ is shown in Fig. 5-23, which is based on Eq. (5-178), with the radiative and convective transfer terms $(GS_1)_R \sigma (T_C^3 - T_1^3) + h_1 A_1 (T_C - T_1)$ replaced by a combined radiation/conduction term $(GS_1)_{R,c} \sigma (T_C^3 - T_1^3)$, where $(GS_1)_{R,c} = (GS_1)_R + h_1 A_1 / 4\sigma T_{C1}^3$; T_{C1} is adequately approximated by the arithmetic mean of T_C and T_1 .

Example 9: Radiation in a Furnace Consider a furnace 3 m \times 10 m \times 5 m fired with methane and 20 percent excess air, at a methane firing rate of 2500 kg/hr. Two rows of 5-inch (0.127 m) tubes (outer diameter) are mounted on equilateral triangular centers, with center-to-center distance twice the tube diameter, on 60 percent of the interior surface of the chamber. The radiative properties of the gases for an enclosure of these dimensions, containing the same combustion products, have been estimated in Example 8 for a gas temperature of 1500 K and a sink temperature of 1000 K: 12.53 moles of combustion products are generated per mole of fuel, with a mean molar heat capacity between a base temperature of 298 K and the exit gas exit temperature T_E , adequately represented for this example by $\overline{MC}_p = 7.01 + 0.875 (T/1000)$ over a T_E range of 800 to 1600 K. The lower heating value of CH_4 is 191,760 cal/g mole. The air is preheated to 600°C, and has a mean \overline{MC}_p of 7.31 cal/g mole. The alloy tube emissivity ϵ_1 is 0.7 and may be assumed gray; the mean tube surface temperature is 700°C. The convection coefficient, gas-to-tube plane and to refractory surface is 0.0170 kW/m²°C; $h_{o,s}$ on the outside surface is 0.0114 kW/m²°C. The 0.343-m-thick refractory walls and roof have a k of 0.00050 kW/m²°C and an assumed ϵ_r of 0.6; the walls are pierced by four 0.10-m \times 0.23-m peepholes. The gas exit area, 1 m \times 10 m, is tube-screen-covered.

What is the sink-side efficiency η_1 , the gas exit temperature T_E , and the mean flux density through the tube surface?

Solution: Temporary basis—1 mole entering CH_4 . Since no molar change occurs when CH_4 burns completely with half-saturated entering air 20 percent in excess of stoichiometric, the total number of moles produced equal 11.53 moles. Entering enthalpy = 191,760 + 11.53 \times 7.31(600 - 25) = 240,220 Kcal/kg mol CH_4 . H [of Eq. (5-178)] = 240,220 \times (2500/16.04) = 37.44E6 Kcal/hr \times 4.186/3600 = 43.54E3 Kw. \dot{m} = [16.04 + 2 \times 1.2(100/21)](29 + 0.0088 \times 18.016)](2500/16.04) = 54,440 kg/hr. Trial and error solution necessitates several sets of computations of T_C to check assumed T_E ; only the last of these will be given. The first, to save time by using results attained elsewhere, assumes $T_C = 1500$ K; the resulting T_C is 369 K higher. The second set assumes $T_C = 2017$ K; the resulting T_C is 80 K lower. Linear interpolation indicates the third set should assume $T_C = 1934$ K. That set is presented: $T_E = 1934 - 170 = 1764$. $\overline{MC}_p = 7.01 + 0.875 \times (1764/1000) = 8.554$ cal/(gmol)(K). $T_F = 240,220/(12.53 \times 8.554) +$

298 = 2539 K. $\overline{C}_p = (8.554/16.04)(4.186/3600) = 0.6201E-3$ kw-hr/(kg)(K). For ϵ_C , $pL_m = 0.247 \times 2.779 = 0.6875$ m atm. Use of Table 5-8, with $T_H = 2000$ K ($b = 572$, $n = 0.51$) and $T_L = 1500$ ($b = 540$, $n = 0.42$) gives $\epsilon_C(pL) = [572(0.6875 - 0.015)^{0.51}(1934 - 1500) + 540(0.6725)^{0.42}(2000 - 1934)]/(500 \times 1934) = 0.2409$. For α_{C1} , with $T_1 = 1000$, Table 5-8 gives $b = 444$, $n = 0.34$. $\alpha_{C1}(pL) = 444(0.6875 \times 1000/1934 - 0.015)^{0.34}(1934/1000)^{0.5}/1000 = 0.4281$. $\epsilon_{C,c}(pL) = [0.2409 - 0.4281(1000/1934)^4]/(1 - 1/1.934^4) = 0.2265$. $2pL_m = 2 \times 0.6875 = 1.375$ m atm. $\epsilon_C(2pL) = [572(1.375 - 0.015)^{0.51} \times 434 + 540(1.36)^{0.42} \times 66]/(500 \times 1934) = 0.3422$. $\alpha_{C1}(2pL) = 444 \times (1.375 \times 1000/1934 - 0.015)^{0.34}(1934)^{0.5}/1000 = 0.5459$. $\epsilon_{C,c}(2pL) = [0.3422 - 0.5459(1/1.934)^4]/(1 - 1/1.934^4) = 0.3265$. $a_r = 0.2265/(2 - 0.3265/0.2265) = 0.4056$. Of all these, only $\epsilon_{C,c}(pL)$ and a_r will be used from here on. From Eq. (5-176), $(GS_1)_R / A_1 = 1/[0.6(1/0.2265 - 1/0.4056) + 1/0.87 + (1/0.4056 - 1)/(0.87 + 0.6(0.4/0.6))] = 0.2879$. $A_1 = (3 \times 10 + 3 \times 5 + 10 \times 5) \times 2 = 190 \times 0.6 = 114$ m². A_r (with floor area omitted for loss) = $190 \times 0.4 - 10 \times 3 = 46$ m². $(GS_1)_R = 0.2879 \times 114 = 32.82$ m². $(GS_1)_R \sigma T_F^3 = 32.82 \times (56.7E - 12) \times 2539^3 = 30.46$ kw/K. $D = 54,440 \times (0.6201E - 3)/30.46 = 1.1083$. $\Delta = 170/2539 = 0.06696$. $L_c = 0.017 \times 114/30.46 = 0.0636$. $L_o = 4 \times 0.1 \times 0.23 \times 0.335/32.82 = 9.4E - 4$. $L_r = 0.0012 \times 46/30.46 = 0.001812$. In Eq. (5-180), the coefficient of τ_C equals $(1.1083 + 0.0636 + 0.0018)/1.00094 = 1.1726$. The constant in the equation equals $[(100/2539)^4 + 0.0636(1/2.539) + 0.00094 \times 0.1174^4 + 0.00181(298/2539) + 1.1083(1 + 170/2539)]/1.00094 = 1.2307$. The equation to solve is: $\tau_C^4 + 1.1726\tau_C - 1.2307 = 0$. Solution gives $\tau_C = 0.7620$; $T_C = 0.762 \times 2539 = 1935$ K. $T_r = 1765$ K, only 1 K above value assumed for obtaining \overline{C}_p and ϵ_C . $\eta_C = (1 - \tau_C)/(1 - \tau_o) = (1 - 1765/2539)/(1 - 298/2539) = 0.3454$. Sink-side efficiency $\eta_1 = 0.3454 - [0.00094(0.762^4 - 0.1174^4)] + 0.001812(0.762 - 0.1174)/1.1083(1 - 0.1174) = 0.344$, not including convection to screen tubes covering gas exit. $q_{\text{plane of sink}} = (H\eta_1)/A_1 = 43,540 \times 0.3439/114 = 131.3$ kw/m². $q_{\text{tube surf}} = 131.3(2D/2\pi D) = 41.8$ kw/m² \times 3412 \times 0.3048² = 13,300 Btu/(ft²)(hr). $T_E = 1765$ K = 1492°C = 2717°F.

In Fig. 5-22, the shaded areas indicate the operating regimes of a wide range of furnace types. Note the significant properties of the function presented. (1) As firing rate D' goes down, the efficiency rises and approaches $1 - \tau_1$ in the limit. (This conclusion is modified if wall losses are significant.) (2) Changes in sink temperature have little effect if $\tau_1 < 0.3$. (3) As the furnace walls approach complete coverage by a black sink [$CE_1 \rightarrow 1$ in Eqs. (5-176) and (5-177)] and as convection becomes unimportant, the effect of flame emissivity on D becomes one of inverse proportionality; thus at very high firing rates at which efficiency approaches inverse proportionality to D , the efficiency of heat transfer varies directly as ϵ_C (gas-turbine chambers), but at low firing rates ϵ_C has relatively little effect. (4) When $CE_1 \ll 1$ because of a nonblack sink or much refractory surface, the effect of changing flame emissivity is to produce a much less than proportional effect on heat flux.

The factor Δ , the allowance for imperfect stirring, must be estimated. Values in the range of 93 to 149°C (200 to 300°F) have been found to produce data correlation for a series of tests on marine boilers.

Equation (5-179) and Fig. 5-22 serve as a framework for correlating the performance of furnaces with flow patterns—plug flow, parabolic

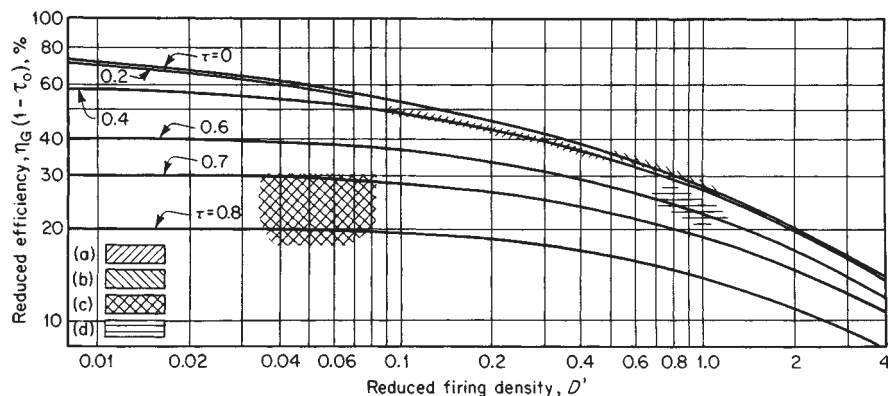


FIG. 5-22 Thermal performance of well-stirred furnace chambers; reduced efficiency as a function of reduced firing density D and reduced sink temperature τ_1 . (a) Radiant section, oil tube stills, cracking coils. (b) Domestic boiler combustion chambers. (c) Open-hearth furnaces. (d) Soaking pits.

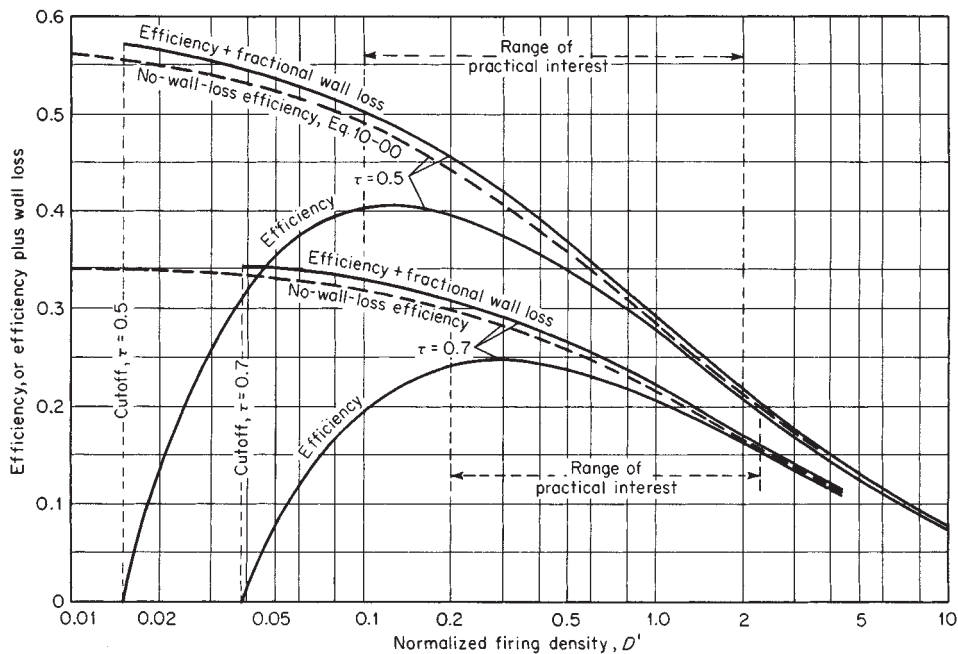


FIG. 5-23 Effect of wall-loss factor L on combustion-chamber performance; $L' = 0.02$, and $\tau = 0.5$ and 0.7 .

profile, and recirculatory flow—which differ from the well-stirred model [Hottel and Sarofim, *Int. J. Mass Heat Transfer*, **8**, 1153 (1965)]. As expected, plug-flow furnaces show somewhat higher efficiency, mild-recirculation types somewhat lower efficiency, and strong-recirculation furnaces a performance closely similar to that of the well-stirred model.

If data on several furnaces of a single class are available, a similar treatment can lead to a partially empirical equation based on simplified rules for obtaining $(GS)_{R,c}$ or an effective Δ . Because Eq. (5-178) has a structure which covers a wide range of furnace types and has a sound theoretical basis, it provides safer structures of empirical design equations than many such equations available in the engineering literature.

MASS TRANSFER

GENERAL REFERENCES: Bird, Stewart, and Lightfoot, *Transport Phenomena*, Wiley, New York, 1960. Cussler, *Diffusion: Mass Transfer in Fluid Systems*, Cambridge University Press, Cambridge, 1984. Danner and Daubert, *Manual for Predicting Chemical Process Design Data*, AIChE, New York, 1983. Daubert and Danner, *Physical and Thermodynamic Properties of Pure Chemicals*, Taylor and Francis, Bristol, PA, 1989–1995. Fahien, *Fundamentals of Transport Phenomena*, McGraw-Hill, New York, 1983. Foust, Wenzel, Clump, Maus, and Andersen, *Principles of Unit Operations*, 2d ed., Wiley, New York, 1980. Gammon, Marsh, and Dewan, *Transport Properties and Related Thermodynamic Data of Binary Mixtures*, AIChE, New York, Part 1, 1993; Part 2, 1994. Geankoplis, *Transport Processes and Unit Operations*, 3d ed., Prentice Hall, Englewood Cliffs, NJ, 1993. Hines and Maddox, *Mass Transfer: Fundamentals and Applications*, Prentice Hall, Englewood Cliffs, NJ, 1985. Kirwan, “Mass Transfer Principles,” Chap. 2 in Rousseau, R. W. (ed.), *Handbook of Separation Process Technology*, Wiley, New York, 1987. McCabe, Smith, and Harriott, *Unit Operations of Chemical Engineering*, 5th ed., McGraw-Hill, New York, 1993. Reid, Prausnitz, and Poling, *The Properties of Gases and Liquids*, 4th ed., McGraw-Hill, New York, 1987. Schwartzberg and Chao, *Food Technol.*, **36**(2), 73 (1982). Sherwood, Pigford, and Wilke, *Mass Transfer*, McGraw-Hill, New York, 1975. Skelland, *Diffusional Mass Transfer*, Wiley, New York, 1974. Taylor and Krishna, *Multicomponent Mass Transfer*, Wiley, New York, 1993. Treybal, *Mass-Transfer Operations*, 3d ed., McGraw-Hill, New York, 1980.

INTRODUCTION

This part of Sec. 5 provides a concise guide to solving problems in situations commonly encountered by chemical engineers. It deals with

diffusivity and mass-transfer coefficient estimation and common flux equations, although material balances are also presented in typical coordinate systems to permit a wide range of problems to be formulated and solved.

Mass-transfer calculations involve transport properties, such as diffusivities, and other empirical factors that have been found to relate mass-transfer rates to measured “driving forces” in myriad geometries and conditions. The context of the problem dictates whether the fundamental or more applied coefficient should be used. One key distinction is that, whenever there is flow parallel to an interface through which mass transfer occurs, the relevant coefficient is an empirical combination of properties and conditions. Conversely, when diffusion occurs in stagnant media or in creeping flow without transverse velocity gradients, ordinary diffusivities may be suitable for solving the problem. In either case, it is strongly suggested to employ data, whenever available, instead of relying on correlations.

Units employed in diffusivity correlations commonly followed the cgs system. Similarly, correlations for mass transfer correlations used the cgs or English system. In both cases, only the most recent correlations employ SI units. Since most correlations involve other properties and physical parameters, often with mixed units, they are repeated here as originally stated. Common conversion factors are listed in Table 1-4.

Fick's First Law This law relates flux of a component to its composition gradient, employing a constant of proportionality called a

Nomenclature and Units—Mass Transfer

Symbols	Definition	SI units	U.S. customary units
a	Effective interfacial mass transfer area per unit volume	m^2/m^3	ft^2/ft^3
A_{cs}	Cross-sectional area of vessel	m^2 or cm^2	ft^2
A'	Constant (see Table 5-28-1)		
a_p	See a		
c	Concentration = P/RT for an ideal gas	mol/m^3 or mol/l or $gequiv/l$	$lbmol/ft^3$
c_i	Concentration of component $i = x_i c$ at gas-liquid interface	mol/m^3 or mol/l or $gequiv/l$	$lbmol/ft^3$
c_p	Specific heat	$kJ/(kg \cdot K)$	$Btu/(lb \cdot ^\circ F)$
d	Characteristic length	m or cm	ft
d_b	Bubble diameter	m	ft
d_c	Column diameter	m or cm	ft
d_{drop}	Sauter mean diameter	m	ft
d_{imp}	Impeller diameter	m	ft
d_{pore}	Pore diameter	m or cm	ft
$D_{A'A}$	Self-diffusivity (= D_A at $x_A = 1$)	m^2/s or cm^2/s	ft^2/h
D_{AB}	Mutual diffusivity	m^2/s or cm^2/s	ft^2/h
D_{AB}^∞	Mutual diffusivity at infinite dilution of A in B	m^2/s or cm^2/s	ft^2/h
D_{eff}	Effective diffusivity within a porous solid = $\epsilon_p D/\tau$	m^2/s	ft^2/h
D_K	Knudsen diffusivity for gases in small pores	m^2/s or cm^2/s	ft^2/h
D_L	Liquid phase diffusion coefficient	m^2/s	ft^2/h
D_S	Surface diffusivity	m^2/s or cm^2/s	ft^2/h
E	Energy dissipation rate/mass		
E_s	Activation energy for surface diffusion	J/mol or cal/mol	
f	Friction factor for fluid flow	Dimensionless	Dimensionless
F	Faraday's constant	96,487 Coulomb/gequiv	
g	Acceleration due to gravity	m/s^2	ft/h^2
g_c	Conversion factor	1.0	4.17×10^8 lb ft/[lbf h ²]
G	Gas-phase mass flux	$kg/(s \cdot m^2)$	$lb/(h \cdot ft^2)$
G_a	Dry air flux	$kg/(s \cdot m^2)$	$lb/(h \cdot ft^2)$
G_M	Molar gas-phase mass flux	$kmol/(s \cdot m^2)$	$(lbmol)/(h \cdot ft^2)$
h'	Heat transfer coefficient	$W/(m^2 \cdot K) = J/(s \cdot m^2 \cdot K)$	$Btu/(h \cdot ft^2 \cdot ^\circ F)$
h_T	Total height of tower packing	m	ft
H	Compartment height	m	ft
H	Henry's law constant	$kPa/(mole\text{-fraction solute in liquid phase})$	$(lbf/in^2)/(mole\text{-fraction solute in liquid phase})$
H'	Henry's law constant	$kPa/[kmol/(m^3 \text{ solute in liquid phase})]$	$(lbf/in^2)/[(lbmol)/(ft^3 \text{ solute in liquid phase})]$ or $atm/[(lbmole)/(ft^3 \text{ solute in liquid phase})]$
H_C	Height of one transfer unit based on gas-phase resistance	m	ft
H_{OC}	Height of one overall gas-phase mass-transfer unit	m	ft
H_L	Height of one transfer unit based on liquid-phase resistance	m	ft
H_{OL}	Height of one overall liquid-phase mass-transfer unit	m	ft
HTU	Height of one transfer unit (general)	m	ft
j_D	Chilton-Colburn factor for mass transfer, Eq. (5-291)	Dimensionless	Dimensionless
j_H	Chilton-Colburn factor for heat transfer	Dimensionless	Dimensionless
j_M	See j_D		
m_A	Mass flux of A by diffusion with respect to the mean mass velocity	$kmol/(m^2 \cdot s)$ or $mol/(cm^2 \cdot s)$	$lbmol/(ft^2 \cdot h)$
M_A	Molar flux of A by diffusion with respect to mean molar velocity	$kmol/(m^2 \cdot s)$ or $mol/(cm^2 \cdot s)$	$lbmol/(ft^2 \cdot h)$
v_A	Molar flux of A with respect to mean volume velocity	$kmol/(m^2 \cdot s)$	$lbmol/(ft^2 \cdot h)$
J_{si}	Molar flux by surface diffusion	$kmol/(m^2 \cdot s)$ or $gmol/(cm^2 \cdot s)$	$lbmol/(ft^2 \cdot h)$
k	Boltzmann's constant	8.9308×10^{-10} gequiv ohm/s	
k	Film mass transfer coefficient	m/s or cm/s	ft/hr
k	Thermal conductivity	$(J \cdot m)/(s \cdot m^2 \cdot K)$	$Btu/(h \cdot ft \cdot ^\circ F)$
k'	Mass-transfer coefficient for dilute systems	$kmol/[(s \cdot m^2)(kmol/m^3)]$ or m/s	$lbmol/[(h \cdot ft^2)(lbmol/ft^3)]$ or ft/hr
k_G	Gas-phase mass-transfer coefficient for dilute systems	$kmol/[(s \cdot m^2)(kPa \text{ solute partial pressure})]$	$lbmol/[(h \cdot ft^2)lbf/in^2 \text{ solute partial pressure}]$
k'_G	Gas-phase mass-transfer coefficient for dilute systems	$kmol/[(s \cdot m^2)(mole fraction in gas)]$	$lbmol/[(h \cdot ft^2)(mole fraction in gas)]$
k_{Ga}	Volumetric gas-phase mass-transfer	$kmol/[(s \cdot m^3)(mole fraction)]$	$(lbmol)/[(h \cdot ft^3)(mole fraction)]$
k_{Ca}	Overall volumetric gas-phase mass-transfer coefficient for concentrated systems	$kmol/(s \cdot m^3)$	$lbmol/(h \cdot ft^3)$
k_L^o	Liquid phase mass transfer coefficient for pure absorption (no reaction)	$kmol/(s \cdot m^2)$	$lbmol/(h \cdot ft^2)$
k_L	Liquid-phase mass-transfer coefficient for dilute systems	$kmol/[(s \cdot m^2)(mole\text{-fraction solute in liquid})]$	$(lbmol)/[(h \cdot ft^2)(mole\text{-fraction solute in liquid})]$
k'_L	Liquid-phase mass-transfer coefficient for dilute systems	$kmol/[(s \cdot m^2)(kmol/m^3)]$ or m/s	$(lbmol)/[(h \cdot ft^2)(lbmol/ft^3)]$ or ft/h
k_L	Liquid-phase mass-transfer coefficient for concentrated systems	$kmol/(s \cdot m^2)$	$lbmol/(h \cdot ft^2)$
k_{La}	Volumetric liquid-phase mass-transfer coefficient for dilute systems	$kmol/[(s \cdot m^3)(mole fraction)]$	$(lbmol)/[(h \cdot ft^3)(mole fraction)]$
K	Overall mass transfer coefficient	m/s or cm/s	ft/h
K	$\alpha/R =$ specific conductance	ohm/cm	
K_C	Overall gas-phase mass-transfer coefficient for dilute systems	$kmol/[(s \cdot m^2)(mole fraction)]$	$(lbmol)/[(h \cdot ft^2)(mole fraction)]$

Nomenclature and Units—Mass Transfer (Continued)

Symbols	Definition	SI units	U.S. customary units
\bar{K}_G	Overall gas-phase mass-transfer coefficient for concentrated systems	kmol/(s·m ²)	lbmol/(h·ft ²)
$K_G a$	Overall volumetric gas-phase mass-transfer dilute systems	kmol/[(s·m ³)(mole-fraction solute in gas)]	(lbmol)/[(h·ft ³)(mole-fraction solute in gas)]
$K_G' a$	Overall volumetric gas-phase mass-transfer dilute systems	kmol/[(s·m ³)(kPa solute partial pressure)]	(lbmol)/[(h·ft ³)(lbf/in ² solute partial pressure)]
$(Ka)_{II}$	Overall enthalpy mass-transfer coefficient	kmol/[(s·m ²)(mole fraction)]	lb/[(h·ft ²)(lb water/lb dry air)]
K_L	Overall liquid-phase mass-transfer coefficient	kmol/[(s·m ²)(mole fraction)]	(lbmol)/[(h·ft ²)(mole fraction)]
\bar{K}_L	Liquid-phase mass-transfer coefficient for concentrated systems	kmol/(s·m ²)	(lbmol)/(h·ft ²)
$K_L a$	Overall volumetric liquid-phase mass-transfer coefficient for dilute systems	kmol/[(s·m ³)(mole-fraction solute in liquid)]	(lbmol)/[(h·ft ³)(mole-fraction solute in liquid)]
$\bar{K}_L' a$	Overall volumetric liquid-phase mass-transfer coefficient for concentrated systems	kmol/(s·m ³)	(lbmol)/(h·ft ³)
L	Liquid-phase mass flux	kg/(s·m ²)	lb/(h·ft ²)
L_M	Molar liquid-phase mass flux	kmol/(s·m ²)	(lbmol)/(h·ft ²)
m	Slope of equilibrium curve = dy/dx (mole-fraction solute in gas)/(mole-fraction solute in liquid)	Dimensionless	Dimensionless
m	Molality of solute	mol/1000 g solvent	
M_i	Molecular weight of species i	kg/kmol or g/mol	lb/lbmol
M	Mass in a control volume V	kg or g	lb
$ n_+ , n_- $	Valences of cationic and anionic species	Dimensionless	Dimensionless
n'	See Table 5-28-1	Dimensionless	Dimensionless
n_A	Mass flux of A with respect to fixed coordinates	kg/(s·m ²)	lb/(h·ft ²)
N	Impeller speed	Revolution/s	Revolution/min
N'	Number deck levels	Dimensionless	Dimensionless
N_A	Interphase mass-transfer rate of solute A per interfacial area with respect to fixed coordinates	kmol/(s·m ²)	(lbmol)/(h·ft ²)
N_c	Number of components	Dimensionless	Dimensionless
N_{Fr}	Froude Number ($d_{imp} N^2/g$)	Dimensionless	Dimensionless
N_{Gr}	Grashof number $\left(\frac{g x^3}{(\mu \rho)^2} \left(\frac{\rho_\infty}{\rho_s} - 1 \right) \right)$	Dimensionless	Dimensionless
N_{OG}	Number of overall gas-phase mass-transfer units	Dimensionless	Dimensionless
N_{OL}	Number of overall liquid-phase mass-transfer units	Dimensionless	Dimensionless
NTU	Number of transfer units (general)	Dimensionless	Dimensionless
N_{Kn}	Knudson number = $l/d_{p, \text{nom}}$	Dimensionless	Dimensionless
N_{Pr}	Prandtl number ($c_p \mu / k$)	Dimensionless	Dimensionless
N_{Re}	Reynolds number (Gd/μ_G)	Dimensionless	Dimensionless
N_{Sc}	Schmidt number ($\mu_G/\rho_G D_{AB}$) or ($\mu_L/\rho_L D_L$)	Dimensionless	Dimensionless
N_{Sh}	Sherwood number ($k_c R T / D_{AB} \rho r$)	Dimensionless	Dimensionless
N_{St}	Stanton number (k_c/C_M) or (k_L/L_M)	Dimensionless	Dimensionless
N_{We}	Weber number ($\rho_s N^2 d_{imp}^3 / \sigma$)	Dimensionless	Dimensionless
p	Solute partial pressure in bulk gas	kPa	lbf/in ²
$p_{B,M}$	Log mean partial pressure difference of stagnant gas B	Dimensionless	Dimensionless
p_i	Solute partial pressure at gas-liquid interface	kPa	lbf/in ²
p_T	Total system pressure	kPa	lbf/in ²
P	Pressure	Pa	lbf/in ² or atm
P	Power	Watts	
P_c	Critical pressure	Pa	lbf/in ² or atm
Per	Perimeter/area	m ⁻¹	ft ⁻¹
Q	Volumetric flow rate	m ³ /s	ft ³ /h
r_A	Radius of dilute spherical solute	Å	
R	Gas constant	8.314 J/mol K = 8.314 Pa m ³ /(mol K) = 82.057 atm cm ³ /mol K	10.73 ft ³ psia/lbmol-h
R	Solution electrical resistance	ohm	
R_i	Radius of gyration of the component i molecule	Å	
s	Fractional surface-renewal rate	s ⁻¹	h ⁻¹
S	Tower cross-sectional area = $\pi d^2/4$	m ²	ft ²
t	Contact time	s	h
t_f	Formation time of drop	s	h
T	Temperature	K	°R
T_b	Normal boiling point	K	°R
T_c	Critical temperature	K	°R
T_r	Reduced temperature = T/T_c	Dimensionless	Dimensionless
u, v	Fluid velocity	m/s or cm/s	ft/h
u_o	Blowing or suction velocity	m/s	ft/h
u_∞	Velocity away from object	m/s	ft/h
u_L	Superficial liquid velocity in vertical direction	m/s	ft/h
v_s	Slip velocity	m/s	ft/h
v_T	Terminal velocity	m/s	ft/h
v_{TS}	Stokes law terminal velocity	m/s	ft/h
V	Packed volume in tower	m ³	ft ³
V	Control volume	m ³ or cm ³	ft ³
V_b	Volume at normal boiling point	m ³ /kmol or cm ³ /mol	ft ³ /lbmol
V_i	Molar volume of i at its normal boiling point	m ³ /kmol or cm ³ /mol	ft ³ /lbmol
\bar{v}_i	Partial molar volume of i	m ³ /kmol or cm ³ /mol	ft ³ /lbmol

Nomenclature and Units—Mass Transfer (Concluded)

Symbols	Definition	SI units	U.S. customary units
V_{ml}	Molar volume of the liquid-phase component i at the melting point	$m^3/kmol$ or cm^3/mol	$ft^3/lbmol$
V_{tower}	Tower volume per area	m^3/m^2	ft^3/ft^2
w	Width of film	m	ft
x	Length along plate	m	ft
x	Mole-fraction solute in bulk-liquid phase	(kmol solute)/(kmol liquid)	(lbmol solute)/(lb mol liquid)
x_A	Mole fraction of component A	kmole A/kmole fluid	lbmole A/lb mole fluid
x^o	Mole-fraction solute in bulk liquid in equilibrium with bulk-gas solute concentration y	(kmol solute)/(kmol liquid)	(lbmol solute)/(lbmol liquid)
x_{BM}	Logarithmic-mean solvent concentration between bulk liquid and interface values	(kmol solvent)/(kmol liquid)	(lbmol solvent)/(lbmol liquid)
x_{BM}^o	Logarithmic-mean inert-solvent concentration between bulk-liquid value and value in equilibrium with bulk gas	(kmol solvent)/(kmol liquid)	(lbmol solvent)/(lbmol liquid)
x_i	Mole-fraction solute in liquid at gas-liquid interface	(kmol solute)/(kmol liquid)	(lbmol solute)/(lbmol liquid)
y	Mole-fraction solute in bulk-gas phase	(kmol solute)/(kmol gas)	(lbmol solute)/(lbmol gas)
y_{BM}	Logarithmic-mean inert-gas concentration (5-262)	(kmol inert gas)/(kmol gas)	(lbmol inert gas)/(lbmol gas)
y_{BM}^o	Logarithmic-mean inert-gas concentration	(kmol inert gas)/(kmol gas)	(lbmol inert gas)/(lbmol gas)
y_i	Mole fraction solute in gas at interface	(kmole solute)/(kmol gas)	(lbmol solute)/(lbmol gas)
y_i^o	Mole-fraction solute in gas at interface in equilibrium with the liquid-phase interfacial solute concentration x_i	(kmol solute)/(kmol gas)	(lbmol solute)/(lbmol gas)
z	Direction of unidimensional diffusion	m	ft

Greek symbols

α	$1 + N_B/N_A$	Dimensionless	Dimensionless
α_c	Conductance cell constant (measured)	cm^{-1}	
β	$M_A^{1/2} P_c^{1/3} / T_c^{5/6}$	Dimensionless	Dimensionless
δ	Effective thickness of stagnant-film layer	m	ft
ϵ	Fraction of discontinuous phase in continuous phase for two-phase flow	Dimensionless	Dimensionless
ϵ	Void fraction available for gas flow or fractional gas holdup	m^3/m^3	ft^3/ft^3
ϵ_A	Characteristic Lennard-Jones energy	Dimensionless	Dimensionless
ϵ_{AB}	$(\epsilon_A \epsilon_B)^{1/2}$	Dimensionless	Dimensionless
γ_i	Activity coefficient of solute i	Dimensionless	Dimensionless
γ_{\pm}	Mean ionic activity coefficient of solute	Dimensionless	Dimensionless
λ_c, λ_a	Infinite dilution conductance of cation and anion	$cm^2/(equiv\text{-ohm})$	
Λ	$1000 K/C = \lambda_c + \lambda_a = \Lambda_o + f(C)$	$cm^2/ohm\ gequiv$	
Λ_o	Infinite dilution conductance	$cm^2/gequiv\ ohm$	
μ_i	Dipole moment of i	Debeyes	
μ_i	Viscosity of pure i	cP or Pa s	lb/(h-ft)
μ_G	Gas-phase viscosity	$kg/(s\cdot m)$	lb/(h-ft)
μ_L	Liquid-phase viscosity	$kg/(s\cdot m)$	lb/(h-ft)
ν	Kinematic viscosity = ρ/μ	m^2/s	ft^2/h
ρ	Density of A	kg/m^3 or g/cm^3	lb/ft^3
ρ_c	Critical density of A	kg/m^3 or g/cm^3	lb/ft^3
ρ_c	Density continuous phase	kg/m^3	lb/ft^3
ρ_G	Gas-phase density	kg/m^3	lb/ft^3
$\bar{\rho}_L$	Average molar density of liquid phase	$kmol/m^3$	(lbmol)/ft ³
ρ_p	Particle density	kg/m^3 or g/cm^3	lb/ft^3
ρ_r	Reduced density = ρ/ρ_c	Dimensionless	Dimensionless
Ψ_i	Parachor of component $i = V_i \sigma^{1/4}$		
Ψ	Parameter, Table 5-28-G	Dimensionless	Dimensionless
Ψ	Shape factor, Table 5-27-A	Dimensionless	Dimensionless
σ	Interfacial tension	dyn/cm	lbf/ft
σ_i	Characteristic length	Å	
σ_i	Surface tension of component i	dyn/cm	
σ_{AB}	Binary pair characteristic length = $(\sigma_A + \sigma_B)/2$	Å	
τ	Intraparticle tortuosity	Dimensionless	Dimensionless
ω	Pitzer's acentric factor = $-[1.0 + \log_{10}(P^o/P_c)]$	Dimensionless	
ω	Rotational velocity	Radians/s	
Ω	Diffusion collision integral = $f(kT/\epsilon_{AB})$	Dimensionless	Dimensionless

Subscript

A	Solute component in liquid or gas phase
B	Inert-gas or inert-solvent component
G	Gas phase
m	Mean value
L	Liquid phase
super	Superficial velocity

Superscript

°	At equilibrium
---	----------------

diffusivity. It can be written in several forms, depending on the units and frame of reference. Three that are related but not identical are

$$vJ_A = -D_{AB} \frac{dc_A}{dz} \approx mJ_A = -cD_{AB} \frac{dx_A}{dz} \approx mJ_A = -\rho D_{AB} \frac{dw_A}{dz} \quad (5-181)$$

The first equality (on the left-hand side) corresponds to the molar flux with respect to the volume average velocity, while the equality in the center represents the molar flux with respect to the molar average velocity and the one on the right is the mass flux with respect to the mass average velocity. These must be used with consistent flux expressions for fixed coordinates and for N_C components, such as:

$$N_A = vJ_A + c_A \sum_{i=1}^{N_C} N_i \bar{V}_i = mJ_A + x_A \sum_{i=1}^{N_C} N_i = \frac{mJ_A + w_A \sum_{i=1}^{N_C} n_i}{M_A} \quad (5-182)$$

In each case, the term containing the summation accounts for *conveyance*, which is the amount of component A carried by the net flow in the direction of diffusion. Its impact on the total flux can be as much as 10 percent. In most cases it is much less, and it is frequently ignored. Some people refer to this as the “convective” term, but that conflicts with the other sense of convection which is promoted by flow perpendicular to the direction of flux.

Mutual Diffusivity, Mass Diffusivity, Interdiffusion Coefficient Diffusivity is denoted by D_{AB} and is defined by Fick's first law as the ratio of the flux to the concentration gradient, as in Eq. (5-181). It is analogous to the thermal diffusivity in Fourier's law and to the kinematic viscosity in Newton's law. These analogies are flawed because both heat and momentum are conveniently defined with respect to fixed coordinates, irrespective of the direction of transfer or its magnitude, while mass diffusivity most commonly requires information about bulk motion of the medium in which diffusion occurs. For liquids, it is common to refer to the limit of infinite dilution of A in B using the symbol, D_{AB}^0 .

When the flux expressions are consistent, as in Eq. (5-182), the diffusivities in Eq. (5-181) are identical. As a result, experimental diffusivities are often measured under constant volume conditions but may be used for applications involving open systems. It turns out that the two versions are very nearly equivalent for gas-phase systems because there is negligible volume change on mixing. That is not usually true for liquids, however.

Self Diffusivity Self-diffusivity is denoted by $D_{A'A}$ and is the measure of mobility of a species in itself; for instance, using a small concentration of molecules tagged with a radioactive isotope so they can be detected. Tagged and untagged molecules presumably do not have significantly different properties. Hence, the solution is ideal, and there are no gradients to “force” or “drive” diffusion. This kind of diffusion is presumed to be purely statistical in nature.

In the special case that A and B are similar in molecular weight, polarity, and so on, the self-diffusion coefficients of pure A and B will be approximately equal to the mutual diffusivity, D_{AB} . Second, when A and B are the less mobile and more mobile components, respectively, their self-diffusion coefficients can be used as rough lower and upper bounds of the mutual diffusion coefficient. That is, $D_{A'A} \leq D_{AB} \leq D_{B'B}$. Third, it is a common means for evaluating diffusion for gases at high pressure. Self-diffusion in liquids has been studied by many [Easteal *AIChE J.* **30**, 641 (1984), Ertl and Dullien, *AIChE J.* **19**, 1215 (1973), and Vadovic and Colver, *AIChE J.* **18**, 1264 (1972)].

Tracer Diffusivity Tracer diffusivity, denoted by $D_{A'B}$ is related to both mutual and self-diffusivity. It is evaluated in the presence of a second component B , again using a tagged isotope of the first component. In the dilute range, tagging A merely provides a convenient method for indirect composition analysis. As concentration varies, tracer diffusivities approach mutual diffusivities at the dilute limit, and they approach self-diffusivities at the pure component limit. That is, at the limit of dilute A in B , $D_{A'B} \rightarrow D_{AB}^0$ and $D_{B'A} \rightarrow D_{B'B}^0$; likewise at the limit of dilute B in A , $D_{B'A} \rightarrow D_{BA}^0$ and $D_{A'B} \rightarrow D_{A'A}^0$.

Neither the tracer diffusivity nor the self-diffusivity has much practical value except as a means to understand ordinary diffusion and as

order-of-magnitude estimates of mutual diffusivities. Darken's equation [Eq. (5-220)] was derived for tracer diffusivities but is often used to relate mutual diffusivities at moderate concentrations as opposed to infinite dilution.

Mass-Transfer Coefficient Denoted by k_c , k_x , K_x , and so on, the mass-transfer coefficient is the ratio of the flux to a concentration (or composition) difference. These coefficients generally represent rates of transfer that are much greater than those that occur by diffusion alone, as a result of convection or turbulence at the interface where mass transfer occurs. There exist several principles that relate that coefficient to the diffusivity and other fluid properties and to the intensity of motion and geometry. Examples that are outlined later are the film theory, the surface renewal theory, and the penetration theory, all of which pertain to idealized cases. For many situations of practical interest like investigating the flow inside tubes and over flat surfaces as well as measuring external flow through banks of tubes, in fixed beds of particles, and the like, correlations have been developed that follow the same forms as the above theories. Examples of these are provided in the subsequent section on mass-transfer coefficient correlations.

Problem Solving Methods Most, if not all, problems or applications that involve mass transfer can be approached by a systematic course of action. In the simplest cases, the unknown quantities are obvious. In more complex (e.g., multicomponent, multiphase, multidimensional, nonisothermal, and/or transient) systems, it is more subtle to resolve the known and unknown quantities. For example, in multicomponent systems, one must know the fluxes of the components before predicting their effective diffusivities and vice versa. More will be said about that dilemma later. Once the known and unknown quantities are resolved, however, a combination of conservation equations, definitions, empirical relations, and properties are applied to arrive at an answer. Figure 5-24 is a flowchart that illustrates the primary types of information and their relationships, and it applies to many mass-transfer problems.

CONTINUITY AND FLUX EXPRESSIONS

Material Balances Whenever mass-transfer applications involve equipment of specific dimensions, flux equations alone are inadequate to assess results. A material balance or continuity equation must also be used. When the geometry is simple, macroscopic balances suffice. The following equation is an overall mass balance for such a unit having N_m bulk-flow ports and N_n ports or interfaces through which diffusive flux can occur:

$$\frac{dM}{dt} = \sum_{i=1}^{N_m} m_i + \sum_{i=1}^{N_n} n_i A_{cs_i} \quad (5-183)$$

where M represents the mass in the unit volume V at any time t ; m_i is the mass flow rate through the i th port; and n_i is the mass flux through the i th port, which has a cross-sectional area of A_{cs_i} . The corresponding balance equation for individual components includes a reaction term:

$$\frac{dM_j}{dt} = \sum_{i=1}^{N_m} m_{ij} + \sum_{i=1}^{N_n} n_{ij} A_{cs_i} + r_j V \quad (5-184)$$

For the j th component, $m_{ij} = m_i w_{ij}$ is the component mass flow rate in stream i ; w_{ij} is the mass fraction of component j in stream i ; and r_j is the net reaction rate (mass generation minus consumption) per unit volume V that contains mass M . If it is inconvenient to measure mass flow rates, the product of density and volumetric flow rate is used instead.

In addition, most situations that involve mass transfer require material balances, but the pertinent area is ambiguous. Examples are packed columns for absorption, distillation, or extraction. In such cases, flow rates through the discrete ports (nozzles) must be related to the mass-transfer rate in the packing. As a result, the mass-transfer rate is determined via flux equations, and the overall material balance incorporates the stream flow rates m_i and integrated fluxes. In such instances, it is common to begin with the most general, differential material balance equations. Then, by eliminating terms that are negligible, the simplest applicable set of equations remains to be solved.

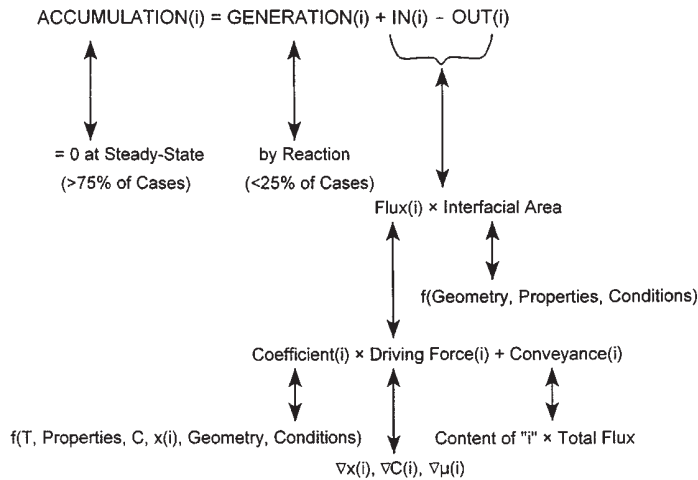


FIG. 5-24 Flowchart illustrating problem solving approach using mass-transfer rate expressions in the context of mass conservation.

Table 5-12 provides material balances for Cartesian, cylindrical, and spherical coordinates. The generic form applies over a unit cross-sectional area and constant volume:

$$\frac{\partial \rho_j}{\partial t} = -\nabla \cdot n_j + r_j \quad (5-185a)$$

where $n_j = \rho v_j$. Applying Fick's law and expressing composition as concentration gives

$$\frac{\partial c_j}{\partial t} = -v \cdot \nabla c_j + D_j \nabla^2 c_j + r_j \quad (5-185b)$$

Flux Expressions: Simple Integrated Forms of Fick's First Law Simplified flux equations that arise from Eqs. (5-181) and (5-182) can be used for unidimensional, steady-state problems with binary mixtures. The boundary conditions represent the compositions x_{A_L} and x_{A_R} at the left-hand and right-hand sides of a hypothetical layer having thickness Δz . The principal restriction of the following equations is that the concentration and diffusivity are assumed to be constant. As written, the flux is positive from left to right, as depicted in Fig. 5-25.

1. Equimolar counterdiffusion ($N_A = -N_B$)

$$N_A = M J_A = -D_{AB} c \frac{dx_A}{dz} = \frac{D_{AB}}{\Delta z} c (x_{A_L} - x_{A_R}) \quad (5-189)$$

2. Unimolar diffusion ($N_A \neq 0, N_B = 0$)

$$N_A = M J_A + x_A N_A = \frac{D_{AB}}{\Delta z} c \ln \frac{1 - x_{A_R}}{1 - x_{A_L}} \quad (5-190)$$

3. Steady state diffusion ($N_A \neq -N_B \neq 0$)

$$N_A = M J_A + x_A (N_A + N_B) = \frac{N_A}{N_A + N_B} \frac{D_{AB}}{\Delta z} c \ln \frac{\frac{N_A}{N_A + N_B} - x_{A_R}}{\frac{N_A}{N_A + N_B} - x_{A_L}} \quad (5-191)$$

The unfortunate aspect of the last relationship is that one must know a priori the ratio of the fluxes to determine the magnitudes. It is not possible to solve simultaneously the pair of equations that apply for components A and B because the equations are not independent.

Stefan-Maxwell Equations Following Eq. (5-182), a simple and intuitively appealing flux equation for applications involving N_c components is

$$N_i = -c D_{im} \nabla x_i + x_i \sum_{j=1}^{N_c} N_j \quad (5-192)$$

In the late 1800s, the development of the kinetic theory of gases led to a method for calculating multicomponent gas diffusion (e.g., the flux of each species in a mixture). The methods were developed simultaneously by Stefan and Maxwell. The problem is to determine the diffusion coefficient D_{im} . The Stefan-Maxwell equations are simpler in principle since they employ binary diffusivities:

$$\nabla x_i = \sum_{j=1}^{N_c} \frac{1}{c D_{ij}} (x_i N_j - x_j N_i) \quad (5-193)$$

If Eqs. (5-192) and (5-193) are combined, the multicomponent diffusion coefficient may be assessed in terms of binary diffusion coefficients [see Eq. (5-204)]. For gases, the values D_{ij} of this equation are approximately equal to the binary diffusivities for the ij pairs. The Stefan-Maxwell diffusion coefficients may be negative, and the method may be applied to liquids, even for electrolyte diffusion [Kraaijeveld, Wesselingh, and Kuiken, *Ind. Eng. Chem. Res.*, **33**, 750 (1994)]. Approximate solutions have been developed by linearization [Toor, H.L., *AIChE J.*, **10**, 448 and 460 (1964); Stewart and Prober, *Ind. Eng. Chem. Fundam.*, **3**, 224 (1964)]. Those differ in details but yield about the same accuracy. More recently, efficient algorithms for solving the equations exactly have been developed (see Taylor and Krishna, Krishnamurthy and Taylor, and Taylor and Webb).

TABLE 5-12 Continuity Equation in Various Coordinate Systems

Coordinate System	Equation
Cartesian	$\frac{\partial \rho_j}{\partial t} = -\left(\frac{\partial n_{x_j}}{\partial x} + \frac{\partial n_{y_j}}{\partial y} + \frac{\partial n_{z_j}}{\partial z}\right) + r_j \quad (5-186)$
Cylindrical	$\frac{\partial \rho_j}{\partial t} = -\left(\frac{1}{r} \frac{\partial m_{r_j}}{\partial r} + \frac{1}{r} \frac{\partial n_{\theta_j}}{\partial \theta} + \frac{\partial n_{z_j}}{\partial z}\right) + r_j \quad (5-187)$
Spherical	$\frac{\partial \rho_j}{\partial t} = -\left(\frac{1}{r^2} \frac{\partial r^2 n_{r_j}}{\partial r} + \frac{1}{r \sin \theta} \frac{\partial n_{\theta_j} \sin \theta}{\partial \theta} + \frac{1}{r \sin \theta} \frac{\partial n_{\phi_j}}{\partial \phi}\right) + r_j \quad (5-188)$

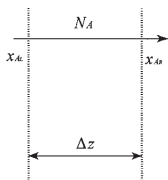


FIG. 5-25 Hypothetical film and boundary conditions.

DIFFUSIVITY ESTIMATION—GASES

Whenever measured values of diffusivities are available, they should be used. Typically, measurement errors are less than those associated with predictions by empirical or even semitheoretical equations. A few general sources of data are Sec. 2 of this handbook, Schwartzberg and Chao; Reid et al.; Gammon et al.; and Daubert and Danner. Many other more restricted sources are listed under specific topics later in this subsection.

Before using diffusivities from either data or correlations, it is a good idea to check their reasonableness with respect to values that have been commonly observed in similar situations. Table 5-13 is a compilation of several rules of thumb. These values are not authoritative; they simply represent guidelines based on experience.

Diffusivity correlations for gases are outlined in Table 5-14. Specific parameters for individual equations are defined in the specific text regarding each equation. References are given after Table 5-19. The errors reported for Eq. (5-194) through (5-197) were compiled by Reid et al., who compared the predictions with 68 experimental values of D_{AB} . Errors cited for Eqs. (5-198) to (5-202) were reported by the authors.

Binary Mixtures—Low Pressure—Nonpolar Components
 Many evaluations of correlations are available (Elliott and Watts; Lugg; Marrero and Mason). The differences in accuracy of the correlations are minor, and thus the major concern is ease of calculation. The Fuller-Schettler-Giddings equation is usually the simplest correlation to use and is recommended by Reid et al.

Chapman-Enskog (Bird et al.) and Wilke-Lee The inherent assumptions of these equations are quite restrictive (i.e., low density,

TABLE 5-13 Rules of Thumb for Diffusivities (See Cussler, Reid et al., Schwartzberg and Chao)

Continuous phase	D_i magnitude		D_i range		Comments
	m ² /s	cm ² /s	m ² /s	cm ² /s	
Gas at atmospheric pressure	10 ⁻⁵	0.1	10 ⁻⁴ –10 ⁻⁶	1–10 ⁻²	Accurate theories exist, generally within ±10%; $D_i P \cong \text{constant}; D_i \propto T^{1.66 \text{ to } 2.0}$
Liquid	10 ⁻⁹	10 ⁻⁵	10 ⁻⁸ –10 ⁻¹⁰	10 ⁻⁴ –10 ⁻⁶	Approximate correlations exist, generally within ±25%
Liquid occluded in solid matrix	10 ⁻¹⁰	10 ⁻⁶	10 ⁻⁸ –10 ⁻¹²	10 ⁻⁴ –10 ⁻⁸	Hard cell walls: $D_{\text{eff}}/D_i = 0.1$ to 0.2. Soft cell walls: $D_{\text{eff}}/D_i = 0.3$ to 0.9
Polymers and glasses	10 ⁻¹²	10 ⁻⁸	10 ⁻¹⁰ –10 ⁻¹⁴	10 ⁻⁶ –10 ⁻¹⁰	Approximate theories exist for dilute and concentrated limits; strong composition dependence
Solid	10 ⁻¹⁴	10 ⁻¹⁰	10 ⁻¹⁰ –10 ⁻³⁴	10 ⁻⁶ –10 ⁻³⁰	Approximate theories exist; strong temperature dependence

TABLE 5-14 Correlations of Diffusivities for Gases

Authors ^a	Equation	Error
1. Binary Mixtures—Low Pressure—Nonpolar		
Chapman-Enskog	$D_{AB} = \frac{0.001858T^{3/2} M_{AB}^{1/2}}{P\sigma_{AB}^2 \Omega_D}$ (5-194)	7.3%
Wilke-Lee [65]	$D_{AB} = \frac{(0.0027 - 0.0005 M_{AB}^{1/2}) T^{3/2} M_{AB}^{1/2}}{P\sigma_{AB}^2 \Omega_D}$ (5-195)	7.0%
Fuller-Schettler-Giddings [19]	$D_{AB} = \frac{0.001T^{1.75} M_{AB}^{1/2}}{P[(\sum v)^{1/3} + (\sum v)_B^{1/3}]^2}$ (5-196)	5.4%
2. Binary Mixtures—Low Pressure—Polar		
Brokaw [4]	$D_{AB} = \frac{0.001858T^{3/2} M_{AB}^{1/2}}{P\sigma_{AB}^2 \Omega_D}$ (5-197)	9.0%
3. Self-Diffusivity—High Pressure		
Mathur-Thodos [37]	$D_{AA} = \frac{10.7 \times 10^{-5} T_r}{\beta \rho_r}$, $\{\rho_r \leq 1.5\}$ (5-198)	5%
Lee-Thodos [31]	$D_{AA} = \frac{0.77 \times 10^{-5} T_r}{\rho_r \delta}$, $\{\rho_r \leq 1\}$ (5-199)	0.5%
Lee-Thodos [32]	$D_{AA} = \frac{(0.007094G + 0.001916)^{2.5} T_r}{\delta}$, $[\rho_r > 1, G < 1]$ (5-200)	17%
4. Supercritical Mixtures		
Sun and Chen [56]	$D_{AB} = \frac{1.23 \times 10^{-10} T}{\mu^{0.799} V_{cA}^{0.49}}$ (5-201)	5%
Catchpole and King [6]	$D_{AB} = 5.152 D_e T_r \frac{(\rho_r^{-0.667} - 0.4510)(1 + M_A/M_B) R}{(1 + (V_{cB}/V_{cA})^{0.333})^2}$ (5-202)	10%

^aReferences are listed on pages 5-7 and 5-8.

TABLE 5-15 Estimates for ε_i and σ_i (K, Å, atm, cm³, mol)

Critical point	$\varepsilon/k = 0.75 T_c$	$\sigma = 0.841 V_c^{1/3}$ or $2.44 (T/P_c)^{1/3}$
Critical point	$\varepsilon/k = 65.3 T_c z_c^{3.6}$	$\sigma = \frac{1.866 V_c^{1/3}}{z_c^{1.3}}$
Normal boiling point	$\varepsilon/k = 1.15 T_b$	$\sigma = 1.18 V_b^{1/3}$
Melting point	$\varepsilon/k = 1.92 T_m$	$\sigma = 1.222 V_m^{1/3}$
Acentric factor	$\varepsilon/k = (0.7915 + 0.1693 \omega) T_c$	$\sigma = (2.3551 - 0.087 \omega) \left(\frac{T_c}{P_c}\right)^{1/3}$

NOTE: These values may not agree closely, so usage of a consistent basis is suggested (e.g., data at the normal boiling point).

spherical atoms), and the intrinsic potential function is empirical. Despite that, they provide good estimates of D_{AB} for many polyatomic gases and gas mixtures, up to about 1000 K and a maximum of 70 atm. The latter constraint is because observations for many gases indicate that $D_{AB}P$ is constant up to 70 atm.

The characteristic length is $\sigma_{AB} = (\sigma_A + \sigma_B)/2$ in Å. In order to estimate Ω_D for Eqs. (5-194) or (5-195), two empirical equations are available. The first is:

$$\Omega_D = (44.54T^{0-4.909} + 1.911T^{0-1.575})^{0.10} \quad (5-203a)$$

where $T^\circ = kT/\varepsilon_{AB}$ and $\varepsilon_{AB} = (\varepsilon_A \varepsilon_B)^{1/2}$. Estimates for σ_i and ε_i are given in Table 5-15. This expression shows that Ω_D is proportional to temperature roughly to the -0.49 power at low temperatures and to the -0.16 power at high temperature. Thus, gas diffusivities are proportional to temperatures to the 2.0 power and 1.66 power, respectively, at low and high temperatures. The second is:

$$\Omega_D = \frac{A}{T^{0.8}} + \frac{C}{\exp(DT^\circ)} + \frac{E}{\exp(FT^\circ)} + \frac{G}{\exp(HT^\circ)} \quad (5-203b)$$

where $A = 1.06036$, $B = 0.15610$, $C = 0.1930$, $D = 0.47635$, $E = 1.03587$, $F = 1.52996$, $G = 1.76474$, and $H = 3.89411$.

Fuller-Schettler-Giddings The parameters and constants for this correlation were determined by regression analysis of 340 experimental diffusion coefficient values of 153 binary systems. Values of $\sum v_i$ used in this equation are in Table 5-16.

Binary Mixtures—Low Pressure—Polar Components The Brokaw correlation was based on the Chapman-Enskog equation, but σ_{AB}^* and Ω_D^* were evaluated with a modified Stockmayer potential for polar molecules. Hence, slightly different symbols are used. That potential model reduces to the Lennard-Jones 6-12 potential for interactions between nonpolar molecules. As a result, the method should yield accurate predictions for polar as well as nonpolar gas mixtures. Brokaw presented data for 9 relatively polar pairs along with the prediction. The agreement was good: an average absolute error of 6.4 percent, considering the complexity of some of

the gas pairs [e.g., (CH₃)₂O & CH₃Cl]. Despite that, Reid, *op. cit.*, found the average error was 9.0 percent for combinations of mixtures (including several polar-nonpolar gas pairs), temperatures and pressures. In this equation, Ω_D is calculated as described previously, and other terms are:

$$\begin{aligned} \Omega_{D^*} &= \Omega_D + 0.19 \delta_{AB}^2/T^\circ & T^\circ &= kT/\varepsilon_{AB}^* \\ \sigma_{AB}^* &= (\sigma_A^* \sigma_B^*)^{1/2} & \sigma_i &= [1.585 V_{hi}/(1 + 1.3 \delta_i^2)]^{1/3} \\ \delta_{AB} &= (\delta_A \delta_B)^{1/2} & \delta_i &= 1.94 \times 10^3 \mu_i^2/V_{hi} T_{hi} \\ \varepsilon_{AB}^* &= (\varepsilon_A \varepsilon_B)^{1/2} & \varepsilon_i/k &= 1.18 (1 + 1.3 \delta_i^2) T_{hi} \end{aligned}$$

Self-Diffusivity—High Pressure The criterion of high pressure is vague at best. For most “permanent” gases, such as the major constituents of air, it would mean $P > 70$ atm. For less volatile components, the criterion would be lower. At present, accurate prediction of mutual diffusion coefficients for dense gas mixtures is not possible. One major reason for this is the scarcity of data. Most high-pressure diffusion experiments have measured the self-diffusion coefficient. The general observation is that the product DP is near constant at low pressure, is not constant at high pressure, but rather decreases as pressure increases. In addition, although there are usually negligible composition effects on diffusivity of gases at low pressures, the effects are not negligible at high pressures.

Mathur-Thodos showed that for reduced densities less than unity, the product $D_{AA}P$ is approximately constant at a given temperature. Thus, by knowing the value of the product at low pressure, it is possible to estimate its value at a higher pressure. They found at higher pressures the density increases, but the product $D_{AA}P$ decreases rapidly. In their correlation, $\beta = M_A^{1/2} P_C^{1/3} / T_r^{5/6}$.

Lee-Thodos presented a generalized treatment of self-diffusivity for gases (and liquids). These correlations have been tested for more than 500 data points each. The average deviation of the first is 0.51 percent, and that of the second is 17.2 percent. $\delta = M_A^{1/2} / P_c^{1/2} V_c^{5/6}$, s/cm², and where $G = (X^\circ - X)/(X^\circ - 1)$, $X = \rho_r / T_r^{0.1}$, and $X^\circ = \rho_r / T_r^{0.1}$ evaluated at the solid melting point.

Lee and Thodos expanded their earlier treatment of self-diffusivity to cover 58 substances and 975 data points, with an average absolute deviation of 5.26 percent. Their correlation is too involved to repeat here, but those interested should refer to the original paper.

Supercritical Mixtures *DeBenedetti-Reid* showed that conventional correlations based on the Stokes-Einstein relation (for liquid phase) tend to overpredict diffusivities in the supercritical state. Nevertheless, they observed that the Stokes-Einstein group $D_{AB}\mu T$ was constant. Thus, although no general correlation applies, only one data point is necessary to examine variations of fluid viscosity and/or temperature effects. They explored certain combinations of aromatic solids in SF₆ and CO₂.

Sun-Chen examined tracer diffusion data of aromatic solutes in alcohols up to the supercritical range and found their data correlated with average deviations of 5 percent and a maximum deviation of 17 percent for their rather limited set of data.

Catchpole-King examined binary diffusion data of near-critical fluids in the reduced density range of 1 to 2.5 and found that their data correlated with average deviations of 10 percent and a maximum deviation of 60 percent. They observed two classes of behavior. For the first, no correction factor was required ($R = 1$). That class was comprised of alcohols as solvents with aromatic or aliphatic solutes, or carbon dioxide as a solvent with aliphatics except ketones as solutes, or

TABLE 5-16 Atomic Diffusion Volumes for Use in Estimating D_{AB} by the Method of Fuller, Schettler, and Giddings

Atomic and Structural Diffusion-Volume Increments, v_i (cm ³ /mol)			
C	16.5	(Cl)	19.5
H	1.98	(S)	17.0
O	5.48	Aromatic ring	-20.2
(N)	5.69	Heterocyclic ring	-20.2
Diffusion Volumes for Simple Molecules, Σv_i (cm ³ /mol)			
H ₂	7.07	CO	18.9
D ₂	6.70	CO ₂	26.9
He	2.88	N ₂ O	35.9
N ₂	17.9	NH ₃	14.9
O ₂	16.6	H ₂ O	12.7
Air	20.1	(CCl ₂ F ₂)	114.8
Ar	16.1	(SF ₂)	69.7
Kr	22.8	(Cl ₂)	37.7
(Xe)	37.9	(Br ₂)	67.2
Ne	5.59	(SO ₂)	41.1

Parentheses indicate that the value listed is based on only a few data points.

ethylene as a solvent with aliphatics except ketones and naphthalene as solutes. For the second class, the correction factor was $R = X^{0.17}$. The class was comprised of carbon dioxide with aromatics; ketones and carbon tetrachloride as solutes; and aliphatics (propane, hexane, dimethyl butane), sulfur hexafluoride, and chlorotrifluoromethane as solvents with aromatics as solutes. In addition, sulfur hexafluoride combined with carbon tetrachloride, and chlorotrifluoromethane combined with 2-propanone were included in that class. In all cases, $X = (1 + (V_{C^*}/V_{C^*})^{1/3})^2 / (1 + M_A/M_B)$ was in the range of 1 to 10.

Low-Pressure/Multicomponent Mixtures These methods are outlined in Table 5-17. Stefan-Maxwell equations were discussed earlier. *Smith-Taylor* compared various methods for predicting multicomponent diffusion rates and found that Eq. (5-204) was superior among the effective diffusivity approaches, though none is very good. They also found that linearized and exact solutions are roughly equivalent and accurate.

Blanc provided a simple limiting case for dilute component i diffusing in a stagnant medium (i.e., $N \approx 0$), and the result, Eq. (5-205), is known as Blanc's law. The restriction basically means that the compositions of all the components, besides component i , are relatively large and uniform.

Wilke obtained solutions to the Stefan-Maxwell equations. The first, Eq. (5-206), is simple and reliable under the same conditions as Blanc's law. This equation applies when component i diffuses through a stagnant mixture. It has been tested and verified for diffusion of toluene in hydrogen + air + argon mixtures and for diffusion of ethyl propionate in hydrogen + air mixtures (Fairbanks and Wilke). When the compositions vary from one boundary to the other, Wilke recommends that the arithmetic average mole fractions be used. Wilke also suggested using the Stefan-Maxwell equation, which applies when the fluxes of two or more components are significant. In this situation, the mole fractions are arithmetic averages of the boundary conditions, and the solution requires iteration because the ratio of fluxes is not known a priori.

DIFFUSIVITY ESTIMATION—LIQUIDS

Many more correlations are available for diffusion coefficients in the liquid phase than for the gas phase. Most, however, are restricted to binary diffusion at infinite dilution D_{AB}^0 or to self-diffusivity D_{AA} . This reflects the much greater complexity of liquids on a molecular level. For example, gas-phase diffusion exhibits negligible composition effects and deviations from thermodynamic ideality. Conversely, liquid-phase diffusion almost always involves volumetric and thermodynamic effects due to composition variations. For concentrations greater than a few mole percent of A and B , corrections are needed to obtain the true diffusivity. Furthermore, there are many conditions that do not fit any of the correlations presented here. Thus, careful consideration is needed to produce a reasonable estimate. Again, if diffusivity data are available at the conditions of interest, then they are strongly preferred over the predictions of any correlations.

Stokes-Einstein and Free-Volume Theories The starting point for many correlations is the Stokes-Einstein equation. This equation is derived from continuum fluid mechanics and classical thermodynamics for the motion of large spherical particles in a liquid.

For this case, the need for a molecular theory is cleverly avoided. The Stokes-Einstein equation is (Bird et al.)

$$D_{AB} = \frac{kT}{6\pi r_A \mu_B} \quad (5-207)$$

where A refers to the solute and B refers to the solvent. This equation is applicable to very large unhydrated molecules ($M > 1000$) in low-molecular-weight solvents or where the molar volume of the solute is greater than $500 \text{ cm}^3/\text{mol}$ (Reddy and Doraiswamy; Wilke and Chang). Despite its intellectual appeal, this equation is seldom used "as is." Rather, the following principles have been identified: (1) The diffusion coefficient is inversely proportional to the size $r_A \approx V_A^{1/3}$ of the solute molecules. Experimental observations, however, generally indicate that the exponent of the solute molar volume is larger than one-third. (2) The term $D_{AB}\mu_B/T$ is approximately constant only over a 10-to-15 K interval. Thus, the dependence of liquid diffusivity on properties and conditions does not generally obey the interactions implied by that grouping. For example, Robinson et al. found that: $\ln D_{AB} \propto -1/T$. (3) Finally, pressure does not affect liquid-phase diffusivity much, since μ_B and V_A are only weakly pressure-dependent. Pressure does have an impact at very high levels.

Another advance in the concepts of liquid-phase diffusion was provided by Hildebrand, who adapted a theory of viscosity to self-diffusivity. He postulated that $D_{AA} = B(V - V_{ms})/V_{ms}$, where D_{AA} is the self-diffusion coefficient, V is the molar volume, and V_{ms} is the molar volume at which fluidity is zero (i.e., the molar volume of the solid phase at the melting temperature). The difference $(V - V_{ms})$ can be thought of as the free volume, which increases with temperature; and B is a proportionality constant.

Ertl and Duillen [ibid.] found that Hildebrand's equation could not fit their data with B as a constant. They modified it by applying an empirical exponent n (a constant greater than unity) to the volumetric ratio. The new equation is not generally useful, however, since there is no means for predicting n . The theory does identify the free volume as an important physical variable, since $n > 1$ for most liquids implies that diffusion is more strongly dependent on free volume than is viscosity.

Dilute Binary Nonelectrolytes: General Mixtures These correlations are outlined in Table 5-18.

Wilke-Chang This correlation for D_{AB}^0 is one of the most widely used, and it is an empirical modification of the Stokes-Einstein equation. It is not very accurate, however, for water as the solute. Otherwise, it applies to diffusion of very dilute A in B . The average absolute error for 251 different systems is about 10 percent. ϕ_B is an association factor of solvent B that accounts for hydrogen bonding.

Component B	ϕ_B
Water	2.26
Methanol	1.9
Ethanol	1.5
Propanol	1.2
Others	1.0

The value of ϕ_B for water was originally stated as 2.6, although when the original data were reanalyzed, the empirical best fit was 2.26.

TABLE 5-17 Relationships for Diffusivities of Multicomponent Gas Mixtures at Low Pressure

Authors*	Equation
Stefan-Maxwell, Smith and Taylor [53]	$D_{im} = \left[1 - x_i \left(\sum_{j=1}^{NC} N_j \right) / N_i \right] \left[\sum_{j=1}^{NC} \left[\left(x_j - \frac{x_i N_j}{N_i} \right) D_{ij} \right] \right]^{-1} \quad (5-204)$
Blanc [13]	$D_{im} = \left(\sum_{j=1}^{NC} \frac{x_j}{D_{ij}} \right)^{-1} \quad (5-205)$
Wilke [63]	$D_{im} = \left(\sum_{j \neq i}^{NC} \frac{x_j}{D_{ij}} \right)^{-1} \quad (5-206)$

*References are listed at the beginning of this subsection.

TABLE 5-18 Correlations for Diffusivities of Dilute, Binary Mixtures of Nonelectrolytes in Liquids

Authors ^o	Equation	Error
1. General Mixtures		
Wilke-Chang [64]	$D_{AB}^{\circ} = \frac{7.4 \times 10^{-8} (\Phi_B M_B)^{1/2} T}{\mu_B V_A^{0.6}} \quad (5-208)$	20%
Tyn-Calus [59]	$D_{AB}^{\circ} = \frac{8.93 \times 10^{-8} (V_A V_B^2)^{1/6} (\Psi_B / \Psi_A)^{0.6} T}{\mu_B} \quad (5-209)$	10%
Umesi-Danner [60]	$D_{AB}^{\circ} = \frac{2.75 \times 10^{-8} (R_B / R_A^{2/3}) T}{\mu_B} \quad (5-210)$	16%
Siddiqi-Lucas [52]	$D_{AB}^{\circ} = \frac{9.89 \times 10^{-8} V_B^{0.265} T}{V_A^{0.45} \mu_B^{0.907}} \quad (5-211)$	13%
2. Gases in Low Viscosity Liquids		
Sridhar-Potter [54]	$D_{AB}^{\circ} = D_{BB} \left(\frac{V_{c_B}}{V_{c_A}} \right)^{2/3} \left(\frac{V_B}{V_{mB}} \right) \quad (5-212)$	18%
Chen-Chen [7]	$D_{AB}^{\circ} = 2.018 \times 10^{-9} \frac{(\beta V_{c_B})^{2/3} (RT_{c_B})^{1/2}}{M_A^{1/6} (M_B V_{c_A})^{1/3}} (V_r - 1) \left(\frac{T}{T_{c_B}} \right)^{1/2} \quad (5-213)$	6%
3. Aqueous Solutions		
Hayduk-Laudie [25]	$D_{AW}^{\circ} = \frac{13.16 \times 10^{-5}}{\mu_w^{1.14} V_A^{0.589}} \quad (5-214)$	18%
Siddiqi-Lucas [52]	$D_{AW}^{\circ} = 2.98 \times 10^{-7} V_A^{-0.5473} \mu_w^{-1.026} T \quad (5-215)$	13%
4. Hydrocarbon Mixtures		
Hayduk-Minhas [26]	$D_{AB}^{\circ} = 13.3 \times 10^{-8} T^{1.47} \mu_B^{(10.2V_A - 0.791)} V_A^{-0.71} \quad (5-216)$	5%
Matthews-Akgerman [38]	$D_{AB}^{\circ} = 32.88 M_A^{-0.61} V_D^{-1.04} T^{0.5} (V_B - V_D) \quad (5-217)$	5%
Riazi-Whitson [48]	$D_{AB} = 1.07 \frac{(\rho D_{AB})^{\circ}}{\rho} \left(\frac{\mu}{\mu^{\circ}} \right)^{-0.27 - 0.38 \omega + (-0.05 + 0.1 \omega) P_r} \quad (5-218)$	15%

^oReferences are listed on pages 5-7 and 5-8.

Random comparisons of predictions with 2.26 versus 2.6 show no consistent advantage for either value, however. It has been suggested to replace the exponent of 0.6 with 0.7 and to use an association factor of 0.7 for systems containing aromatic hydrocarbons. These modifications, however, are not recommended by Umesi and Danner. Lees and Sarram present a comparison of the association parameters. The average absolute error for 87 different solutes in water is 5.9 percent.

Tyn-Calus This correlation requires data in the form of molar volumes and parachors $\psi_i = V_i \sigma_i^{1/4}$ (a property which, over moderate temperature ranges, is nearly constant), measured at the same temperature (not necessarily the temperature of interest). The parachors for the components may also be evaluated at different temperatures from each other. Quale has compiled values of ψ_i for many chemicals. Group contribution methods are available for estimation purposes (Reid et al.). The following suggestions were made by Reid et al.: The correlation is constrained to cases in which $\mu_B < 30$ cP. If the solute is water or if the solute is an organic acid and the solvent is not water or a short-chain alcohol, dimerization of the solute A should be assumed for purposes of estimating its volume and parachor. For example, the appropriate values for water as solute at 25°C are $V_W = 37.4$ cm³/mol and $\psi_W = 105.2$ cm³g^{1/4}/s^{1/2}mol. Finally, if the solute is nonpolar, the solvent volume and parachor should be multiplied by $8\mu_B$.

Umesi-Danner They developed an equation for nonaqueous solvents with nonpolar and polar solutes. In all, 258 points were involved in the regression. R_i is the radius of gyration in Å of the component molecule, which has been tabulated by Passut and Danner for 250 compounds. The average absolute deviation was 16 percent, compared with 26 percent for the Wilke-Chang equation.

Siddiqi-Lucas In an impressive empirical study, these authors examined 1275 organic liquid mixtures. Their equation yielded an average absolute deviation of 13.1 percent, which was less than that for the Wilke-Chang equation (17.8 percent). Note that this correlation does not encompass aqueous solutions; those were examined and a separate correlation was proposed, which is discussed later.

Binary Mixtures of Gases in Low-Viscosity, Nonelectrolyte Liquids *Sridhar-Potter* derived an equation for predicting gas diffusion through liquid by combining existing correlations. Hildebrand had postulated the following dependence of the diffusivity for a gas in a liquid: $D_{AB}^{\circ} = D_{B'B} (V_{cB}/V_{cA})^{2/3}$, where $D_{B'B}$ is the solvent self-diffusion coefficient and V_{c_i} is the critical volume of component i , respectively. To correct for minor changes in volumetric expansion, Sridhar and Potter multiplied the resulting equation by V_B/\bar{V}_{mB} , where \bar{V}_{mB} is the molar volume of the liquid B at its melting point and $D_{B'B}$ can be estimated by the equation of Ertl and Dullien (see p. 5-50). Sridhar and Potter compared experimentally measured diffusion coefficients for twenty-seven data points of eleven binary mixtures. Their average absolute error was 13.5 percent, but Chen and Chen analyzed about 50 combinations of conditions and 3 to 4 replicates each and found an average error of 18 percent. This correlation does not apply to hydrogen and helium as solutes. However, it demonstrates the usefulness of self-diffusion as a means to assess mutual diffusivities and the value of observable physical property changes, such as molar expansion, to account for changes in conditions.

Chen-Chen Their correlation was based on diffusion measurements of 50 combinations of conditions with 3 to 4 replicates each and exhibited an average error of 6 percent. In this correlation, $V_r = V_B/[0.9724 (V_{mB} + 0.04765)]$ and V_{mB} = the liquid molar volume at the

melting point, as discussed previously. Their association parameter β [which is different from the definition of that symbol in Eq. (5-219)] accounts for hydrogen bonding of the solvent. Values for acetonitrile and methanol are: $\beta = 1.58$ and 2.31 , respectively.

Dilute Binary Mixtures of a Nonelectrolyte in Water The correlations that were suggested previously for general mixtures, unless specified otherwise, may also be applied to diffusion of miscellaneous solutes in water. The following correlations are restricted to the present case, however.

Hayduk-Laudie They presented a simple correlation for the infinite dilution diffusion coefficients of nonelectrolytes in water. It has about the same accuracy as the Wilke-Chang equation (about 5.9 percent). There is no explicit temperature dependence, but the 1.14 exponent on μ_w compensates for the absence of T in the numerator. That exponent was misprinted (as 1.4) in the original article and has been reproduced elsewhere erroneously.

Siddiqi-Lucas These authors examined 658 aqueous liquid mixtures in an empirical study. They found an average absolute deviation of 19.7 percent. In contrast, the Wilke-Chang equation gave 35.0 percent and the Hayduk-Laudie correlation gave 30.4 percent.

Dilute Binary Hydrocarbon Mixtures Hayduk-Minhas presented an accurate correlation for normal paraffin mixtures that was developed from 58 data points consisting of solutes from C_5 to C_{36} and solvents from C_5 to C_{16} . The average error was 3.4 percent for the 58 mixtures.

Matthews-Akgerman The free-volume approach of Hildebrand was shown to be valid for binary, dilute liquid paraffin mixtures (as well as self-diffusion), consisting of solutes from C_8 to C_{16} and solvents of C_6 and C_{12} . The term they referred to as the "diffusion volume" was simply correlated with the critical volume, as $V_D = 0.308 V_c$. We can infer from Table 5-15 that this is approximately related to the volume at the melting point as $V_D = 0.945 V_m$. Their correlation was valid for diffusion of linear alkanes at temperatures up to 300°C and pressures up to 3.45 MPa. Matthews et al. and Erkey and Akgerman completed similar studies of diffusion of alkanes, restricted to n -hexadecane and n -octane, respectively, as the solvents.

Riazi-Whitson They presented a generalized correlation in terms of viscosity and molar density that was applicable to both gases and liquids. The average absolute deviation for gases was only about 8 percent, while for liquids it was 15 percent. Their expression relies on the Chapman-Enskog correlation [Eq. (5-194)] for the low-pressure diffusivity and the Stiel-Thodos correlation for low-pressure viscosity:

$$\mu^\circ = \frac{x_A \mu_A^\circ M_A^{1/2} + x_B \mu_B^\circ M_B^{1/2}}{x_A M_A^{1/2} + x_B M_B^{1/2}}$$

where $\mu_i^\circ \xi_i = 3.4 \times 10^{-4} T_{r,i}^{0.94}$ for $T_{r,i} < 1.5$ or $\mu_i^\circ \xi_i = 1.778 \times 10^{-4} (4.58 T_{r,i} - 1.67)^{5/8}$ for $T_{r,i} > 1.5$. In these equations, $\xi_i = T_i^{1/6} P_i^{2/3} M_i^{1/2}$, and units are in cP, atm, K, and mol. For dense gases or liquids, the Chung et al. or Jossi-Stiel-Thodos correlation may be used to estimate viscosity. The latter is:

$$(\mu - \mu^\circ) \xi + 10^{-4} = (0.1023 + 0.023364 \rho_r + 0.058533 \rho_r^2 - 0.040758 \rho_r^3 + 0.093324 \rho_r^4)$$

$$\text{where } \xi = \frac{(x_A T_{c,A} + x_B T_{c,B})^{1/6}}{(x_A M_A + x_B M_B)^{1/2} (x_A P_{c,A} + x_B P_{c,B})}$$

$$\text{and } \rho_r = (x_A V_{c,A} + x_B V_{c,B}) \rho.$$

Dilute Binary Mixtures of Nonelectrolytes with Water as the Solute Olander modified the Wilke-Chang equation to adapt it to the infinite dilution diffusivity of water as the solute. The modification he recommended is simply the division of the right-hand side of the Wilke-Chang equation by 2.3. Unfortunately, neither the Wilke-Chang equation nor that equation divided by 2.3 fit the data very well. A reasonably valid generalization is that the Wilke-Chang equation is accurate if water is very insoluble in the solvent, such as pure hydrocarbons, halogenated hydrocarbons, and nitro-hydrocarbons. On the other hand, the Wilke-Chang equation divided by 2.3 is accurate for solvents in which water is very soluble, as well as those that have low viscosities. Such solvents include alcohols, ketones, carboxylic acids,

and aldehydes. Neither equation is accurate for higher-viscosity liquids, especially diols.

Dilute Dispersions of Macromolecules in Nonelectrolytes The Stokes-Einstein equation has already been presented. It was noted that its validity was restricted to large solutes, such as spherical macromolecules and particles in a continuum solvent. The equation has also been found to predict accurately the diffusion coefficient of spherical latex particles and globular proteins. Corrections to Stokes-Einstein for molecules approximating spheroids is given by Tanford. Since solute-solute interactions are ignored in this theory, it applies in the dilute range only.

Hiss-Cussler Their basis is the diffusion of a small solute in a fairly viscous solvent of relatively large molecules, which is the opposite of the Stokes-Einstein assumptions. The large solvent molecules investigated were not polymers or gels but were of moderate molecular weight so that the macroscopic and microscopic viscosities were the same. The major conclusion is that $D_{AB}^\circ \mu^{2/3} = \text{constant}$ at a given temperature and for a solvent viscosity from 5×10^{-3} to 5 Pa s or greater (5 to $5 \times 10^3 \text{ cP}$). This observation is useful if D_{AB}° is known in a given high-viscosity liquid (oils, tars, etc.). Use of the usual relation of $D_{AB}^\circ \propto 1/\mu$ for such an estimate could lead to large errors.

Concentrated, Binary Mixtures of Nonelectrolytes Several correlations that predict the composition dependence of D_{AB} are summarized in Table 5-19. Most are based on known values of D_{AB}° and D_{BA}° . In fact, a rule of thumb states that, for many binary systems, D_{AB}° and D_{BA}° bound the D_{AB} vs. x_A curve. Cullinan's equation predicts diffusivities even in lieu of values at infinite dilution, but requires accurate density, viscosity, and activity coefficient data.

Since the infinite dilution values D_{AB}° and D_{BA}° are generally unequal, even a thermodynamically ideal solution like $\gamma_A = \gamma_B = 1$ will exhibit concentration dependence of the diffusivity. In addition, non-ideal solutions require a thermodynamic correction factor to retain the true "driving force" for molecular diffusion, or the gradient of the chemical potential rather than the composition gradient. That correction factor is:

$$\beta_A = 1 + \frac{\partial \ln \gamma_A}{\partial \ln x_A} \quad (5-219)$$

Caldwell-Babb Darken observed that solid-state diffusion in metallurgical applications followed a simple relation. His equation related the tracer diffusivities and mole fractions to the mutual diffusivity:

$$D_{AB} = (x_A D_B + x_B D_A) \beta_A \quad (5-220)$$

Caldwell and Babb used virtually the same equation to evaluate the mutual diffusivity for concentrated mixtures of common liquids.

Van Geet and Adamson tested that equation for the n -dodecane (A) and n -octane (B) system and found the average deviation of D_{AB} from experimental values to be -0.68 percent. In addition, that equation was tested for benzene + bromobenzene, n -hexane + n -dodecane, benzene + CCl_4 , octane + decane, heptane + cetane, benzene + diphenyl, and benzene + nitromethane with success. For systems that depart significantly from thermodynamic ideality, it breaks down, sometimes by a factor of eight. For example, in the binary systems acetone + CCl_4 , acetone + chloroform, and ethanol + CCl_4 , it is not accurate. Thus, it can be expected to be fairly accurate for nonpolar hydrocarbons of similar molecular weight but not for polar-polar mixtures. Siddiqi et al. found that this relation was superior to those of Vignes and Leffler and Cullinan for a variety of mixtures. Umesi and Danner found an average absolute deviation of 13.9 percent for 198 data points.

Rathbun-Babb suggested that Darken's equation could be improved by raising the thermodynamic correction factor β_A to a power, n , less than unity. They looked at systems exhibiting negative deviations from Raoult's law and found $n = 0.3$. Furthermore, for polar-nonpolar mixtures, they found $n = 0.6$. In a separate study, Siddiqi and Lucas followed those suggestions and found an average absolute error of 3.3 percent for nonpolar-nonpolar mixtures, 11.0 percent for polar-nonpolar mixtures, and 14.6 percent for polar-polar mixtures. Siddiqi et al. examined a few other mixtures and found that $n = 1$ was probably best. Thus, this approach is, at best, highly dependent on the type of components being considered.

TABLE 5-19 Correlations of Diffusivities for Concentrated, Binary Mixtures of Nonelectrolyte Liquids

Authors ^o	Equation	
Caldwell-Babb [5]	$D_{AB} = (x_A D_{BA}^o + x_B D_{AB}^o) \beta_A$	(5-221)
Rathbun-Babb [46]	$D_{AB} = (x_A D_{BA}^o + x_B D_{AB}^o) \beta_A^*$	(5-222)
Vignes [62]	$D_{AB} = D_{AB}^{o, \beta} D_{BA}^{o, \beta} \beta_A$	(5-223)
Leffler-Cullinan [34]	$D_{AB} \mu_{mix} = (D_{AB}^o \mu_B)^{x_B} (D_{BA}^o \mu_A)^{x_A} \beta_A$	(5-224)
Cussler [12]	$D_{AB} = D_0 \left[1 + \frac{K}{x_A x_B} \left(\frac{\partial \ln x_A}{\partial \ln a_A} - 1 \right) \right]^{-1/2}$	(5-225)
Cullinan [10]	$D_{AB} = \frac{kT}{2\pi \mu_{mix} (V/A)^{1/3}} \left[\frac{2\pi x_A x_B \beta_A}{1 + \beta_A (2\pi x_A x_B - 1)} \right]^{1/2}$	(5-226)
Asfour-Dullien [2]	$D_{AB} = \left(\frac{D_{AB}^o}{\mu_B} \right)^{x_B} \left(\frac{D_{BA}^o}{\mu_A} \right)^{x_A} \zeta \mu \beta_A$	(5-227)
Siddiqi-Lucas [52]	$D_{AB} = (C_B \bar{V}_B D_{AB}^o + C_A \bar{V}_A D_{BA}^o) \beta_A$	(5-228)

Relative errors for the correlations in this table are very dependent on the components of interest and are cited in the text.

^oSee pages 5-7 and 5-8 for references.

Vignes empirically correlated mixture diffusivity data for 12 binary mixtures. Later Ertl et al. evaluated 122 binary systems, which showed an average absolute deviation of only 7 percent. None of the latter systems, however, was very nonideal.

Leffler-Cullinan modified Vignes' equation using some theoretical arguments to arrive at Eq. (5-224), which the authors compared to Eq. (5-223) for the 12 systems mentioned above. The average absolute maximum deviation was only 6 percent. Umesi and Danner, however, found an average absolute deviation of 11.4 percent for 198 data points. For normal paraffins, it is not very accurate. In general, the accuracies of Eqs. (5-223) and (5-224) are not much different, and, since Vignes' is simpler to use, it is suggested. The application of either should be limited to nonassociating systems that do not deviate much from ideality ($0.95 < \beta_A < 1.05$).

Cussler studied diffusion in concentrated associating systems and has shown that, in associating systems, it is the size of diffusing clusters rather than diffusing solutes that controls diffusion. D_o is a reference diffusion coefficient discussed hereafter; a_A is the activity of component A; and K is a constant. By assuming that D_o could be predicted by Eq. (5-223) with $\beta = 1$, K was found to be equal to 0.5 based on five binary systems and validated with a sixth binary mixture. The limitations of Eq. (5-225) using D_o and K defined previously have not been explored, so caution is warranted. Gurkan showed that K should actually be closer to 0.3 (rather than 0.5) and discussed the overall results.

Cullinan presented an extension of Cussler's cluster diffusion theory. His method accurately accounts for composition and temperature dependence of diffusivity. It is novel in that it contains no adjustable constants, and it relates transport properties and solution thermodynamics. This equation has been tested for six very different mixtures by Rollins and Knaebel, and it was found to agree remarkably well with data for most conditions, considering the absence of adjustable parameters. In the dilute region (of either A or B), there are systematic errors probably caused by the breakdown of certain implicit assumptions (that nevertheless appear to be generally valid at higher concentrations).

Asfour-Dullien developed a relation for predicting alkane diffusivities at moderate concentrations that employs:

$$\zeta = \left(\frac{V_{fm}}{V_{fx_A} V_{fx_B}} \right)^{2/3} \frac{M_{x_A} M_{x_B}}{M_m} \quad (5-229)$$

where $V_{fx_i} = V_{fi}^{x_i}$; the fluid free volume is $V_{fi} = V_i - V_{mi}$ for $i = A, B$, and m , in which V_{mi} is the molar volume of the liquid at the melting point and

$$V_{ml_m} = \left(\frac{x_A^2}{V_{m_A}} + \frac{2x_A x_B}{V_{m_{AB}}} + \frac{x_B^2}{V_{m_B}} \right)^{-1/3}$$

and

$$V_{ml_{AB}} = \left[\frac{V_{m_A}^{1/3} + V_{m_B}^{1/3}}{2} \right]^3$$

and μ is the mixture viscosity; M_m is the mixture mean molecular weight; and β_A is defined by Eq. (5-219). The average absolute error of this equation is 1.4 percent, while the Vignes equation and the Leffler-Cullinan equation give 3.3 percent and 6.2 percent, respectively.

Siddiqi-Lucas suggested that component volume fractions might be used to correlate the effects of concentration dependence. They found an average absolute deviation of 4.5 percent for nonpolar-nonpolar mixtures, 16.5 percent for polar-nonpolar mixtures, and 10.8 percent for polar-polar mixtures.

Binary Electrolyte Mixtures When electrolytes are added to a solvent, they dissociate to a certain degree. It would appear that the solution contains at least three components: solvent, anions, and cations. If the solution is to remain neutral in charge at each point (assuming the absence of any applied electric potential field), the anions and cations diffuse effectively as a single component, as for molecular diffusion. The diffusion of the anionic and cationic species in the solvent can thus be treated as a binary mixture.

Nernst-Haskell The theory of dilute diffusion of salts is well developed and has been experimentally verified. For dilute solutions of a single salt, the well-known Nernst-Haskell equation (Reid et al.) is applicable:

$$D_{AB}^o = \frac{RT}{F^2} \frac{\left| \frac{1}{n_+} + \frac{1}{n_-} \right|}{\frac{1}{\lambda_+^o} + \frac{1}{\lambda_-^o}} = 8.9304 \times 10^{-10} T \frac{\left| \frac{1}{n_+} + \frac{1}{n_-} \right|}{\frac{1}{\lambda_+^o} + \frac{1}{\lambda_-^o}} \quad (5-230)$$

where D_{AB}^o = diffusivity based on molarity rather than normality of dilute salt A in solvent B, cm^2/s .

The previous definitions can be interpreted in terms of ionic-species diffusivities and conductivities. The latter are easily measured and depend on temperature and composition. For example, the equivalent conductance Λ is commonly tabulated in chemistry handbooks as the limiting (infinite dilution) conductance Λ_o and at standard concentrations, typically at 25°C. $\Lambda = 1000 K/C = \lambda_+ + \lambda_- = \Lambda_o + f(C)$, ($\text{cm}^2/\text{ohm gequiv}$); $K = \alpha/R$ = specific conductance, (ohm cm^{-1}); C = solution concentration, (gequiv/ℓ); α = conductance cell constant (measured), (cm^{-1}); R = solution electrical resistance, which is measured (ohm); and $f(C)$ = a complicated function of concentration. The resulting equation of the electrolyte diffusivity is

$$D_{AB} = \frac{|\lambda_+| + |\lambda_-|}{(|\lambda_+| / D_+) + (|\lambda_-| / D_-)} \quad (5-231)$$

where $|\lambda_{\pm}|$ represents the magnitude of the ionic charge and where the cationic or anionic diffusivities are $D_{\pm} = 8.9304 \times 10^{-10} T \lambda_{\pm} / |\lambda_{\pm}| \text{ cm}^2/\text{s}$. The coefficient is $kN_o/F^2 = R/F^2$. In practice, the equivalent conductance of the ion pair of interest would be obtained and supplemented with conductances of permutations of those ions and one independent cation and anion. This would allow determination of all the ionic conductances and hence the diffusivity of the electrolyte solution.

Gordon Typically, as the concentration of a salt increases from infinite dilution, the diffusion coefficient decreases rapidly from D_{AB}° . As concentration is increased further, however, D_{AB} rises steadily, often becoming greater than D_{AB}° . Gordon proposed the following empirical equation, which is applicable up to concentrations of 2N:

$$D_{AB} = D_{AB}^{\circ} \frac{1}{C_B \bar{V}_B} \frac{\mu_B}{\mu} \left(1 + \frac{\ln \gamma_{\pm}}{\ln m} \right) \quad (5-232)$$

where D_{AB}° is given by the Nernst-Haskell equation. References that tabulate γ_{\pm} as a function of m , as well as other equations for D_{AB} , are given by Reid et al.

Multicomponent Mixtures No simple, practical estimation methods have been developed for predicting multicomponent liquid-diffusion coefficients. Several theories have been developed, but the necessity for extensive activity data, pure component and mixture volumes, mixture viscosity data, and tracer and binary diffusion coefficients have significantly limited the utility of the theories (see Reid et al.).

The generalized Stefan-Maxwell equations using binary diffusion coefficients are not easily applicable to liquids since the coefficients are so dependent on conditions. That is, in liquids, each D_j can be strongly composition dependent in binary mixtures and, moreover, the binary D_{ij} is strongly affected in a multicomponent mixture. Thus, the convenience of writing multicomponent flux equations in terms of binary coefficients is lost. Conversely, they apply to gas mixtures because each D_{ij} is practically independent of composition by itself and in a multicomponent mixture (see Taylor and Krishna for details).

One particular case of multicomponent diffusion that has been examined is the dilute diffusion of a solute in a homogeneous mixture (e.g., of A in B + C). Umesu and Danner compared the three equations given below for 49 ternary systems. All three equations were equivalent, giving average absolute deviations of 25 percent.

Perkins-Geankoplis

$$D_{am} \mu_m^{0.8} = \sum_{\substack{j=1 \\ j \neq A}}^n x_j D_{Aj}^{\circ} \mu_j^{0.8} \quad (5-233)$$

Cullinan This is an extension of Vignes' equation to multicomponent systems:

$$D_{am} = \prod_{\substack{j=1 \\ j \neq A}}^n (D_{Aj}^{\circ})^{x_j} \quad (5-234)$$

Leffler-Cullinan They extended their binary relation to an arbitrary multicomponent mixture, as follows:

$$D_{am} \mu_m = \prod_{\substack{j=1 \\ j \neq A}}^n (D_{Aj}^{\circ} \mu_j)^{x_j} \quad (5-235)$$

where D_{Aj} is the dilute binary diffusion coefficient of A in j; D_{Am} is the dilute diffusion of A through m; x_j is the mole fraction; μ_j is the viscosity of component j; and μ_m is the mixture viscosity.

Akita Another case of multicomponent dilute diffusion of significant practical interest is that of gases in aqueous electrolyte solutions. Many gas-absorption processes use electrolyte solutions. Akita presents experimentally tested equations for this case.

Graham-Dranoff They studied multicomponent diffusion of electrolytes in ion exchangers. They found that the Stefan-Maxwell interaction coefficients reduce to limiting ion tracer diffusivities of each ion.

Pinto-Graham Pinto and Graham studied multicomponent diffusion in electrolyte solutions. They focused on the Stefan-Maxwell equations and corrected for solvation effects. They achieved excellent results for 1-1 electrolytes in water at 25°C up to concentrations of 4M.

DIFFUSION OF FLUIDS IN POROUS SOLIDS

Diffusion in porous solids is usually the most important factor controlling mass transfer in adsorption, ion exchange, drying, heterogeneous catalysis, leaching, and many other applications. Some of the

applications of interest are outlined in Table 5-20. Applications of these equations are found in Secs. 16, 22, and 23.

Diffusion within the largest cavities of a porous medium is assumed to be similar to ordinary or bulk diffusion except that it is hindered by the pore walls (see Eq. 5-236). The tortuosity τ that expresses this hindrance has been estimated from geometric arguments. Unfortunately, measured values are often an order of magnitude greater than those estimates. Thus, the effective diffusivity D_{eff} (and hence τ) is normally determined by comparing a diffusion model to experimental measurements. The normal range of tortuosities for silica gel, alumina, and other porous solids is $2 \leq \tau \leq 6$, but for activated carbon, $5 \leq \tau \leq 65$.

In small pores and at low pressures, the mean free path ℓ of the gas molecule (or atom) is significantly greater than the pore diameter d_{pore} . Its magnitude may be estimated from

$$\ell = \frac{3.2 \mu}{P} \left[\frac{RT}{2\pi M} \right]^{1/2}, \text{ in m}$$

As a result, collisions with the wall occur more frequently than with other molecules. This is referred to as the Knudsen mode of diffusion and is contrasted with ordinary or bulk diffusion, which occurs by intermolecular collisions. At intermediate pressures, both ordinary diffusion and Knudsen diffusion may be important [see Eqs. (5-239) and (5-240)].

For gases and vapors that adsorb on the porous solid, surface diffusion may be important, particularly at high surface coverage [see Eqs. (5-241) and (5-244)]. The mechanism of surface diffusion may be viewed as molecules hopping from one surface site to another. Thus, if adsorption is too strong, surface diffusion is impeded, while if adsorption is too weak, surface diffusion contributes insignificantly to the overall rate. Surface diffusion and bulk diffusion usually occur in parallel [see Eqs. (5-245) and (5-246)]. Although D_s is expected to be less than D_{eff} , the solute flux due to surface diffusion may be larger than that due to bulk diffusion if $\partial q_1 / \partial z \gg \partial C_1 / \partial z$. This can occur when a component is strongly adsorbed and the surface coverage is high. For all that, surface diffusion is not well understood. The references in Table 5-20 should be consulted for further details.

INTERPHASE MASS TRANSFER

Transfer of material between phases is important in most separation processes in which two phases are involved. When one phase is pure, mass transfer in the pure phase is not involved. For example, when a pure liquid is being evaporated into a gas, only the gas-phase mass transfer need be calculated. Occasionally, mass transfer in one of the two phases may be neglected even though pure components are not involved. This will be the case when the resistance to mass transfer is much larger in one phase than in the other. Understanding the nature and magnitudes of these resistances is one of the keys to performing reliable mass transfer. In this section, mass transfer between gas and liquid phases will be discussed. The principles are easily applied to the other phases.

Mass-Transfer Principles: Dilute Systems When material is transferred from one phase to another across an interface that separates the two, the resistance to mass transfer in each phase causes a concentration gradient in each, as shown in Fig. 5-26 for a gas-liquid interface. The concentrations of the diffusing material in the two phases immediately adjacent to the interface generally are unequal, even if expressed in the same units, but usually are assumed to be related to each other by the laws of thermodynamic equilibrium. Thus, it is assumed that the thermodynamic equilibrium is reached at the gas-liquid interface almost immediately when a gas and a liquid are brought into contact.

For systems in which the solute concentrations in the gas and liquid phases are dilute, the rate of transfer may be expressed by equations which predict that the rate of mass transfer is proportional to the difference between the bulk concentration and the concentration at the gas-liquid interface. Thus

$$N_A = k'_c(p - p_i) = k'_l(c_i - c) \quad (5-248)$$

where N_A = mass-transfer rate, k'_c = gas-phase mass-transfer coefficient, k'_l = liquid-phase mass-transfer coefficient, p = solute partial pressure in

TABLE 5-20 Relations for Diffusion in Porous Solids

Mechanism	Equation	Applies to	References*
Bulk diffusion in pores	$D_{\text{eff}} = \frac{\epsilon_p D}{\tau}$ (5-236)	Gases or liquids in large pores. $N_{K_n} = \ell/d_{\text{pore}} < 0.01$	[67]
Knudsen diffusion	$D_K = 48.5 d_{\text{pore}} \left(\frac{T}{M}\right)^{1/2}$ in m^2/s (5-237)	Dilute (low pressure) gases in small pores. $N_{K_n} = \ell/d_{\text{pore}} > 10$	Geankoplis, [68, 69]
	$D_{K_{\text{eff}}} = \frac{\epsilon_p D_K}{\tau}$		
	$N_i = -D_K \frac{dC_i}{dz}$ (5-238)	" " " "	
Combined bulk and Knudsen diffusion	$D_{\text{eff}} = \left(\frac{1 - \alpha x_A}{D_{\text{eff}}} + \frac{1}{D_{K_{\text{eff}}}}\right)^{-1}$ (5-239)	" " " "	Geankoplis, [66, 69]
	$\alpha = 1 + \frac{N_B}{N_A}$	$N_A \neq N_B$	
	$D_{\text{eff}} = \left(\frac{1}{D_{\text{eff}}} + \frac{1}{D_{K_{\text{eff}}}}\right)^{-1}$ (5-240)	$N_A = N_B$	
Surface diffusion	$J_{s_i} = -D_{\text{seff}} \rho_p \left(\frac{dq_i}{dz}\right)$ (5-241)	Adsorbed gases or vapors	[66, 68, 69]
	$D_{\text{seff}} = \frac{\epsilon_p D_s}{\tau}$ (5-242)	" " " "	
	$D_{s0} = \frac{D_{s0=0}}{(1 - \theta)}$ (5-243)	θ = fractional surface coverage ≤ 0.6	
	$D_s = D'_s(q) \exp\left(\frac{-E_s}{RT}\right)$ (5-244)	" " " "	
Parallel bulk and surface diffusion	$J = -\left[D_{\text{eff}} \left(\frac{dp_i}{dz}\right) + D_{\text{seff}} \rho_p \left(\frac{dq_i}{dz}\right)\right]$ (5-245)	" " " "	[68]
	$J = -D_{\text{app}} \left(\frac{dp_i}{dz}\right)$ (5-246)	" " " "	
	$D_{\text{app}} = D_{\text{eff}} + D_{\text{seff}} \rho_p \left(\frac{dq_i}{dp_i}\right)$ (5-247)	" " " "	

*See pages 5-7 and 5-8 for references.

bulk gas, p_i = solute partial pressure at interface, c = solute concentration in bulk liquid, and c_i = solute concentration in liquid at interface.

The mass-transfer coefficients k'_C and k'_L by definition are equal to the ratios of the molal mass flux N_A to the concentration driving forces $(p - p_i)$ and $(c_i - c)$ respectively. An alternative expression for the rate of transfer in dilute systems is given by

$$N_A = k_C(y - y_i) = k_L(x_i - x) \quad (5-249)$$

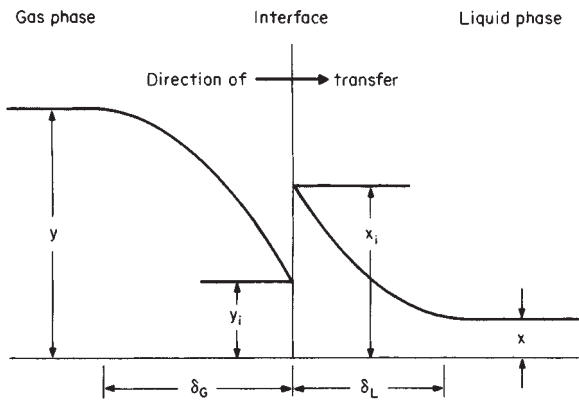


FIG. 5-26 Concentration gradients near a gas-liquid interface.

where N_A = mass-transfer rate, k_C = gas-phase mass-transfer coefficient, k_L = liquid-phase mass-transfer coefficient, y = mole-fraction solute in bulk-gas phase, y_i = mole-fraction solute in gas at interface, x = mole-fraction solute in bulk-liquid phase, and x_i = mole-fraction solute in liquid at interface.

The mass-transfer coefficients defined by Eqs. (5-248) and (5-249) are related to each other as follows:

$$k_C = k'_C p_T \quad (5-250)$$

$$k_L = k'_L \bar{\rho}_L \quad (5-251)$$

where p_T = total system pressure employed during the experimental determinations of k'_C values and $\bar{\rho}_L$ = average molar density of the liquid phase. The coefficient k_C is relatively independent of the total system pressure and therefore is more convenient to use than k'_C , which is inversely proportional to the total system pressure.

The above equations may be used for finding the interfacial concentrations corresponding to any set of values of x and y provided the ratio of the individual coefficients is known. Thus

$$(y - y_i)/(x_i - x) = k_L/k_C = k'_L \bar{\rho}_L / k'_C p_T = L_M H_C / G_M H_L \quad (5-252)$$

where L_M = molar liquid mass velocity, G_M = molar gas mass velocity, H_L = height of one transfer unit based on liquid-phase resistance, and H_C = height of one transfer unit based on gas-phase resistance. The last term in Eq. (5-252) is derived from Eqs. (5-271) and (5-273).

Equation (5-252) may be solved graphically if a plot is made of the equilibrium vapor and liquid compositions and a point representing

the bulk concentrations x and y is located on this diagram. A construction of this type is shown in Fig. 5-27, which represents a gas-absorption situation.

The interfacial mole fractions y_i and x_i can be determined by solving Eq. (5-252) simultaneously with the equilibrium relation $y_i^\circ = F(x_i)$ to obtain y_i and x_i . The rate of transfer may then be calculated from Eq. (5-249).

If the equilibrium relation $y_i^\circ = F(x_i)$ is sufficiently simple, e.g., if a plot of y_i° versus x_i is a straight line, not necessarily through the origin, the rate of transfer is proportional to the difference between the bulk concentration in one phase and the concentration (in that same phase) which would be in equilibrium with the bulk concentration in the second phase. One such difference is $y - y^\circ$, and another is $x^\circ - x$. In this case, there is no need to solve for the interfacial compositions, as may be seen from the following derivation.

The rate of mass transfer may be defined by the equation

$$N_A = K_C(y - y^\circ) = k_C(y - y_i) = k_L(x_i - x) = K_L(x^\circ - x) \quad (5-253)$$

where K_C = overall gas-phase mass-transfer coefficient, K_L = overall liquid-phase mass-transfer coefficient, y° = vapor composition in equilibrium with x , and x° = liquid composition in equilibrium with vapor of composition y . This equation can be rearranged to the formula

$$\frac{1}{K_C} = \frac{1}{k_C} \left(\frac{y - y^\circ}{y - y_i} \right) = \frac{1}{k_C} + \frac{1}{k_C} \left(\frac{y_i - y^\circ}{y - y_i} \right) = \frac{1}{k_C} + \frac{1}{k_L} \left(\frac{y_i - y^\circ}{x_i - x} \right) \quad (5-254)$$

in view of Eq. (5-252). Comparison of the last term in parentheses with the diagram of Fig. 5-27 shows that it is equal to the slope of the chord connecting the points (x, y°) and (x_i, y_i) . If the equilibrium curve is a straight line, then this term is the slope m . Thus

$$1/K_C = (1/k_C + m/k_L) \quad (5-255)$$

When Henry's law is valid ($p_A = Hx_A$ or $p_A = H'c_A$), the slope m can be computed according to the relationship

$$m = H/p_T = H'\bar{v}_L/p_T \quad (5-256)$$

where m is defined in terms of mole-fraction driving forces compatible with Eqs. (5-249) through (5-255), i.e., with the definitions of k_L , k_C , and K_C .

If it is desired to calculate the rate of transfer from the overall concentration difference based on bulk-liquid compositions ($x^\circ - x$), the appropriate overall coefficient K_L is related to the individual coefficients by the equation

$$1/K_L = (1/k_L + 1/mk_C) \quad (5-257)$$

Conversion of these equations to a k'_C , k'_L basis can be accomplished readily by direct substitution of Eqs. (5-250) and (5-251).

Occasionally one will find k'_L or K'_L values reported in units (SI) of meters per second. The correct units for these values are kmol/

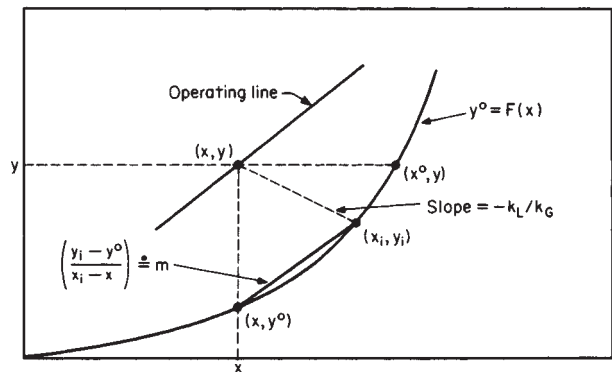


FIG. 5-27 Identification of concentrations at a point in a countercurrent absorption tower.

[(s-m²)(kmol/m³)], and Eq. (5-251) is the correct equation for converting them to a mole-fraction basis.

When k'_C and K'_C values are reported in units (SI) of kmol/[(s-m²)(kPa)], one must be careful in converting them to a mole-fraction basis to multiply by the total pressure actually employed in the original experiments and *not* by the total pressure of the system to be designed. This conversion is valid for systems in which Dalton's law of partial pressures ($p = y p_T$) is valid.

Comparison of Eqs. (5-255) and (5-257) shows that for systems in which the equilibrium line is straight, the overall mass transfer coefficients are related to each other by the equation

$$K_L = mK_C \quad (5-258)$$

When the equilibrium curve is not straight, there is no strictly logical basis for the use of an overall transfer coefficient, since the value of m will be a function of position in the apparatus, as can be seen from Fig. 5-27. In such cases the rate of transfer must be calculated by solving for the interfacial compositions as described above.

Experimentally observed rates of mass transfer often are expressed in terms of overall transfer coefficients even when the equilibrium lines are curved. This procedure is empirical, since the theory indicates that in such cases the rates of transfer may not vary in direct proportion to the overall bulk concentration differences ($y - y^\circ$) and ($x^\circ - x$) at all concentration levels even though the rates may be proportional to the concentration difference in each phase taken separately, i.e., ($x_i - x$) and ($y - y_i$).

In most types of separation equipment such as packed or spray towers, the interfacial area that is effective for mass transfer cannot be accurately determined. For this reason it is customary to report experimentally observed rates of transfer in terms of transfer coefficients based on a unit volume of the apparatus rather than on a unit of interfacial area. Such volumetric coefficients are designated as $K_{C,a}$, $k_{L,a}$, etc., where a represents the interfacial area per unit volume of the apparatus. Experimentally observed variations in the values of these volumetric coefficients with variations in flow rates, type of packing, etc., may be due as much to changes in the effective value of a as to changes in k . Calculation of the overall coefficients from the individual volumetric coefficients is made by means of the equations

$$1/K_{C,a} = (1/k_{C,a} + m/k_{L,a}) \quad (5-259)$$

$$1/K_{L,a} = (1/k_{L,a} + 1/mk_{C,a}) \quad (5-260)$$

Because of the wide variation in equilibrium, the variation in the values of m from one system to another can have an important effect on the overall coefficient and on the selection of the type of equipment to use. For example, if m is large, the liquid-phase part of the overall resistance might be extremely large where k_L might be relatively small. This kind of reasoning must be applied with caution, however, since species with different equilibrium characteristics are separated under different operating conditions. Thus, the effect of changes in m on the overall resistance to mass transfer may partly be counterbalanced by changes in the individual specific resistances as the flow rates are changed.

Mass-Transfer Principles: Concentrated Systems When solute concentrations in the gas and/or liquid phases are large, the equations derived above for dilute systems no longer are applicable. The correct equations to use for concentrated systems are as follows:

$$N_A = \hat{K}_C(y - y_i)/y_{BM} = \hat{K}_L(x_i - x)/x_{BM} = \hat{K}'_C(y - y^\circ)/y'_{BM} = \hat{K}'_L(x^\circ - x)/x'_{BM} \quad (5-261)$$

where ($N_B = 0$)

$$y_{BM} = \frac{(1 - y) - (1 - y_i)}{\ln [(1 - y)/(1 - y_i)]} \quad (5-262)$$

$$y'_{BM} = \frac{(1 - y) - (1 - y^\circ)}{\ln [(1 - y)/(1 - y^\circ)]} \quad (5-263)$$

$$x_{BM} = \frac{(1 - x) - (1 - x_i)}{\ln [(1 - x)/(1 - x_i)]} \quad (5-264)$$

$$x'_{BM} = \frac{(1 - x) - (1 - x^\circ)}{\ln [(1 - x)/(1 - x^\circ)]} \quad (5-265)$$

and where \hat{k}_G and \hat{k}_L are the gas-phase and liquid-phase mass-transfer coefficients for concentrated systems and \hat{K}_G and \hat{K}_L are the overall gas-phase and liquid-phase mass-transfer coefficients for concentrated systems. These coefficients are defined later in Eqs. (5-268) to (5-270).

The factors y_{BM} and x_{BM} arise from the fact that, in the diffusion of a solute through a second stationary layer of insoluble fluid, the resistance to diffusion varies in proportion to the concentration of the insoluble stationary fluid, approaching zero as the concentration of the insoluble fluid approaches zero. See Eq. (5-190).

The factors y_{BM}° and x_{BM}° cannot be justified on the basis of mass-transfer theory since they are based on overall resistances. These factors therefore are included in the equations by analogy with the corresponding film equations.

In dilute systems the logarithmic-mean insoluble-gas and nonvolatile-liquid concentrations approach unity, and Eq. (5-261) reduces to the dilute-system formula. For equimolar counter diffusion (e.g., binary distillation), these log-mean factors should be omitted. See Eq. (5-189).

Substitution of Eqs. (5-262) through (5-265) into Eq. (5-261) results in the following simplified formula:

$$\begin{aligned} N_A &= \hat{k}_G \ln [(1-y_i)/(1-y)] \\ &= \hat{K}_G \ln [(1-y^{\circ})/(1-y)] \\ &= \hat{k}_L \ln [(1-x)/(1-x_i)] \\ &= \hat{K}_L \ln [(1-x)/(1-x^{\circ})] \end{aligned} \quad (5-266)$$

Note that the units of \hat{k}_G , \hat{K}_G , \hat{k}_L , and \hat{K}_L are all identical to each other, i.e., $\text{kmol}/(\text{s}\cdot\text{m}^2)$ in SI units.

The equation for computing the interfacial gas and liquid compositions in concentrated systems is

$$\begin{aligned} (y-y_i)/(x_i-x) &= \hat{k}_L y_{BM}/\hat{k}_G x_{BM} \\ &= L_M H_G y_{BM}/G_M H_L x_{BM} = k_L/k_G \end{aligned} \quad (5-267)$$

This equation is identical to the one for dilute systems since $\hat{k}_G = k_G y_{BM}$ and $\hat{k}_L = k_L x_{BM}$. Note, however, that when \hat{k}_G and \hat{k}_L are given, the equation must be solved by trial and error, since x_{BM} contains x_i and y_{BM} contains y_i .

The overall gas-phase and liquid-phase mass-transfer coefficients for concentrated systems are computed according to the following equations:

$$\frac{1}{\hat{K}_G} = \frac{y_{BM}}{y_{BM}^{\circ}} \frac{1}{\hat{k}_G} + \frac{x_{BM}}{y_{BM}^{\circ}} \frac{1}{\hat{k}_L} \left(\frac{y_i - y^{\circ}}{x_i - x} \right) \quad (5-268)$$

$$\frac{1}{\hat{K}_L} = \frac{x_{BM}}{x_{BM}^{\circ}} \frac{1}{\hat{k}_L} + \frac{y_{BM}}{x_{BM}^{\circ}} \frac{1}{\hat{k}_G} \left(\frac{x^{\circ} - x_i}{y - y_i} \right) \quad (5-269)$$

When the equilibrium curve is a straight line, the terms in parentheses can be replaced by the slope m as before. In this case the overall mass-transfer coefficients for concentrated systems are related to each other by the equation

$$\hat{K}_L = m \hat{K}_G (x_{BM}^{\circ}/y_{BM}^{\circ}) \quad (5-270)$$

All these equations reduce to their dilute-system equivalents as the inert concentrations approach unity in terms of mole fractions of inert concentrations in the fluids.

HTU (Height Equivalent to One Transfer Unit) Frequently the values of the individual coefficients of mass transfer are so strongly dependent on flow rates that the quantity obtained by dividing each coefficient by the flow rate of the phase to which it applies is more nearly constant than the coefficient itself. The quantity obtained by this procedure is called the height equivalent to one transfer unit, since it expresses in terms of a single length dimension the height of apparatus required to accomplish a separation of standard difficulty.

The following relations between the transfer coefficients and the values of HTU apply:

$$H_G = G_M/k_G a y_{BM} = G_M/\hat{K}_G a \quad (5-271)$$

$$H_{OG} = G_M/K_G a y_{BM}^{\circ} = G_M/\hat{K}_G a \quad (5-272)$$

$$H_L = L_M/k_L a x_{BM} = L_M/\hat{k}_L a \quad (5-273)$$

$$H_{OL} = L_M/K_L a x_{BM}^{\circ} = L_M/\hat{K}_L a \quad (5-274)$$

The equations that express the addition of individual resistances in terms of HTUs, applicable to either dilute or concentrated systems, are

$$H_{OC} = \frac{y_{BM}}{y_{BM}^{\circ}} H_G + \frac{m G_M}{L_M} \frac{x_{BM}}{y_{BM}^{\circ}} H_L \quad (5-275)$$

$$H_{OL} = \frac{x_{BM}}{x_{BM}^{\circ}} H_L + \frac{L_M}{m G_M} \frac{y_{BM}}{x_{BM}^{\circ}} H_G \quad (5-276)$$

These equations are strictly valid only when m , the slope of the equilibrium curve, is constant, as noted previously.

NTU (Number of Transfer Units) The NTU required for a given separation is closely related to the number of theoretical stages or plates required to carry out the same separation in a stagewise or plate-type apparatus. For equimolar counterdiffusion, such as in a binary distillation, the number of overall gas-phase transfer units N_{OG} required for changing the composition of the vapor stream from y_1 to y_2 is

$$N_{OG} = \int_{y_2}^{y_1} \frac{dy}{y - y^{\circ}} \quad (5-277)$$

When diffusion is in one direction only, as in the absorption of a soluble component from an insoluble gas,

$$N_{OG} = \int_{y_2}^{y_1} \frac{y_{BM}^{\circ} dy}{(1-y)(y-y^{\circ})} \quad (5-278)$$

The total height of packing required is then

$$h_T = H_{OG} N_{OG} \quad (5-279)$$

When it is known that H_{OG} varies appreciably within the tower, this term must be placed inside the integral in Eqs. (5-277) and (5-278) for accurate calculations of h_T . For example, the packed-tower design equation in terms of the overall gas-phase mass-transfer coefficient for absorption would be expressed as follows:

$$h_T = \int_{y_2}^{y_1} \left[\frac{G_M}{K_G a y_{BM}^{\circ}} \right] \frac{y_{BM}^{\circ} dy}{(1-y)(y-y^{\circ})} \quad (5-280)$$

where the first term under the integral can be recognized as the HTU term. Convenient solutions of these equations for special cases are discussed later.

Definitions of Mass-Transfer Coefficients \hat{k}_G and \hat{k}_L The mass-transfer coefficient is defined as the ratio of the molar mass flux N_A to the concentration driving force. This leads to many different ways of defining these coefficients. For example, gas-phase mass-transfer rates may be defined as

$$N_A = k_G(y-y_i) = k'_G(p-p_i) = \hat{k}_G(y-y_i)/y_{BM} \quad (5-281)$$

where the units (SI) of k_G are $\text{kmol}/[(\text{s}\cdot\text{m}^2)(\text{mole fraction})]$, the units of k'_G are $\text{kmol}/[(\text{s}\cdot\text{m}^2)(\text{kPa})]$, and the units of \hat{k}_G are $\text{kmol}/(\text{s}\cdot\text{m}^2)$. These coefficients are related to each other as follows:

$$k_G = k_G y_{BM} = k'_G p_T y_{BM} \quad (5-282)$$

where p_T is the total system pressure (it is assumed here that Dalton's law of partial pressures is valid).

In a similar way, liquid-phase mass-transfer rates may be defined by the relations

$$N_A = k_L(x_i-x) = k'_L(c_i-c) = \hat{k}_L(x_i-x)/x_{BM} \quad (5-283)$$

where the units (SI) of k_L are $\text{kmol}/[(\text{s}\cdot\text{m}^2)(\text{mole fraction})]$, the units of k'_L are $\text{kmol}/[(\text{s}\cdot\text{m}^2)(\text{kmol}/\text{m}^3)]$ or meters per second, and the units of \hat{k}_L are $\text{kmol}/(\text{s}\cdot\text{m}^2)$. These coefficients are related as follows:

$$\hat{k}_L = k_L x_{BM} = k'_L \bar{\rho}_L x_{BM} \quad (5-284)$$

where $\bar{\rho}_L$ is the molar density of the liquid phase in units (SI) of kilomoles per cubic meter. Note that, for dilute solutions where $x_{BM} \approx 1$, k_L and \hat{k}_L will have identical numerical values. Similarly, for dilute gases $\hat{k}_G \approx k_G$.

Simplified Mass-Transfer Theories In certain simple situations, the mass-transfer coefficients can be calculated from first principles. The film, penetration, and surface-renewal theories are attempts to extend these theoretical calculations to more complex sit-

uations. Although these theories are often not accurate, they are useful to provide a physical picture for variations in the mass-transfer coefficient.

For the special case of steady-state unidirectional diffusion of a component through an inert-gas film in an ideal-gas system, the rate of mass transfer is derived as

$$N_A = \frac{D_{AB} p_T}{RT \delta_C} \frac{(y - y_i)}{y_{BM}} = \frac{D_{AB} p_T}{RT \delta_C} \ln \frac{1 - y_i}{1 - y} \quad (5-285)$$

where D_{AB} is the diffusion coefficient or "diffusivity," δ_C is the "effective" thickness of a stagnant-gas layer which would offer a resistance to molecular diffusion equal to the experimentally observed resistance, and R is the gas constant. [Nernst, *Z. Phys. Chem.*, **47**, 52 (1904); Whitman, *Chem. Mat. Eng.*, **29**, 149 (1923), and Lewis and Whitman, *Ind. Eng. Chem.*, **16**, 1215 (1924)].

The film thickness δ_C depends primarily on the hydrodynamics of the system and hence on the Reynolds number and the Schmidt number. Thus, various correlations have been developed for different geometries in terms of the following dimensionless variables:

$$N_{Sh} = \hat{k}_C RT d / D_{AB} p_T = f(N_{Re}, N_{Sc}) \quad (5-286)$$

where N_{Sh} is the Sherwood number, $N_{Re} (= Gd/\mu_C)$ is the Reynolds number based on the characteristic length d appropriate to the geometry of the particular system; and $N_{Sc} (= \mu_C/\rho_C D_{AB})$ is the Schmidt number.

According to this analysis one can see that for gas-absorption problems, which often exhibit unidirectional diffusion, the most appropriate driving-force expression is of the form $(y - y_i)/y_{BM}$, and the most appropriate mass-transfer coefficient is therefore \hat{k}_C . This concept is to be found in all the key equations for the design of mass-transfer equipment.

The Sherwood-number relation for gas-phase mass-transfer coefficients as represented by the film diffusion model in Eq. (5-286) can be rearranged as follows:

$$N_{Sh} = (\hat{k}_C/G_M) N_{Re} N_{Sc} = N_{St} N_{Re} N_{Sc} = f(N_{Re}, N_{Sc}) \quad (5-287)$$

where $N_{St} = \hat{k}_C/G_M = \hat{k}_C \rho_{BM}/G_M$ is known as the Stanton number. This equation can now be stated in the alternative functional forms

$$N_{St} = \hat{k}_C/G_M = g(N_{Re}, N_{Sc}) \quad (5-288)$$

$$j_D = N_{St} \cdot N_{Sc}^{2/3} \quad (5-289)$$

where j is the Chilton-Colburn "j factor" for mass transfer (discussed later).

The important point to note here is that the gas-phase mass-transfer coefficient \hat{k}_C depends principally upon the transport properties of the fluid (N_{Sc}) and the hydrodynamics of the particular system involved (N_{Re}). It also is important to recognize that specific mass-transfer correlations can be derived only in conjunction with the investigator's particular assumptions concerning the numerical values of the effective interfacial area a of the packing.

The stagnant-film model discussed previously assumes a steady state in which the local flux across each element of area is constant; i.e., there is no accumulation of the diffusing species within the film. Higbie [*Trans. Am. Inst. Chem. Eng.*, **31**, 365 (1935)] pointed out that industrial contactors often operate with repeated brief contacts between phases in which the contact times are too short for the steady state to be achieved. For example, Higbie advanced the theory that in a packed tower the liquid flows across each packing piece in laminar flow and is remixed at the points of discontinuity between the packing elements. Thus, a fresh liquid surface is formed at the top of each piece, and as it moves downward, it absorbs gas at a decreasing rate until it is mixed at the next discontinuity. This is the basis of penetration theory.

If the velocity of the flowing stream is uniform over a very deep region of liquid (total thickness, $\delta_T \gg \sqrt{Dt}$), the time-averaged mass-transfer coefficient according to penetration theory is given by

$$k'_L = 2\sqrt{D_L/\pi t} \quad (5-290)$$

where k'_L is liquid-phase mass-transfer coefficient, D_L is liquid-phase diffusion coefficient, and t is contact time.

In practice, the contact time t is not known except in special cases in which the hydrodynamics are clearly defined. This is somewhat

similar to the case of the stagnant-film theory in which the unknown quantity is the thickness of the stagnant layer δ (in film theory, the liquid-phase mass-transfer coefficient is given by $k'_L = D_L/\delta$).

The penetration theory predicts that k'_L should vary by the square root of the molecular diffusivity, as compared with film theory, which predicts a first-power dependency on D . Various investigators have reported experimental powers of D ranging from 0.5 to 0.75, and the Chilton-Colburn analogy suggests a $2/3$ power.

Penetration theory often is used in analyzing absorption with chemical reaction because it makes no assumption about the depths of penetration of the various reacting species, and it gives a more accurate result when the diffusion coefficients of the reacting species are not equal. When the reaction process is very complex, however, penetration theory is more difficult to use than film theory, and the latter method normally is preferred.

Danckwerts [*Ind. Eng. Chem.*, **42**, 1460 (1951)] proposed an extension of the penetration theory, called the surface renewal theory, which allows for the eddy motion in the liquid to bring masses of fresh liquid continually from the interior to the surface, where they are exposed to the gas for finite lengths of time before being replaced. In his development, Danckwerts assumed that every element of fluid has an equal chance of being replaced regardless of its age. The Danckwerts model gives

$$k'_L = \sqrt{Ds} \quad (5-291)$$

where s = fractional rate of surface renewal.

Note that both the penetration and the surface-renewal theories predict a square-root dependency on D . Also, it should be recognized that values of the surface-renewal rate s generally are not available, which presents the same problems as δ and t in the film and penetration models.

The predictions of correlations based on the film model often are nearly identical to predictions based on the penetration and surface-renewal models. Thus, in view of its relative simplicity, the film model normally is preferred for purposes of discussion or calculation. It should be noted that none of these theoretical models has proved adequate for making a priori predictions of mass-transfer rates in packed towers, and therefore empirical correlations such as those outlined later in Table 5-28, must be employed.

Mass-Transfer Correlations Because of the tremendous importance of mass transfer in chemical engineering, a very large number of studies have determined mass-transfer coefficients both empirically and theoretically. Some of these studies are summarized in Tables 5-21 to 5-28. Each table is for a specific geometry or type of contactor, starting with flat plates, which have the simplest geometry (Table 5-21); then wetted wall columns (Table 5-22); flow in pipes and ducts (Table 5-23); submerged objects (Table 5-24); drops and bubbles (Table 5-25); agitated systems (Table 5-26); packed beds of particles for adsorption, ion exchange, and chemical reaction (Table 5-27); and finishing with packed bed two-phase contactors for distillation, absorption and other unit operations (Table 5-28). Graphical correlations for the Bolles and Fair correlation (Table 5-28-G) are in Figs. 5-28 to 5-30. Although extensive, these tables are not meant to be encyclopedic. For simple geometries, one may be able to determine a theoretical (T) form of the mass-transfer correlation. For very complex geometries, only an empirical (E) form can be found. In systems of intermediate complexity, semiempirical (S) correlations where the form is determined from theory and the coefficients from experiment are often useful. Although the major limitations and constraints in use are usually included in the tables, obviously many details cannot be included in this summary form. Readers are strongly encouraged to check the references before using the correlations in important situations. Note that even authoritative sources occasionally have typographical errors in the fairly complex correlation equations. Thus, it is a good idea to check several sources, including the original paper. The references will often include figures comparing the correlations with data. These figures are very useful since they provide a visual picture of the scatter in the data.

Since there are often several correlations that are applicable, how does one choose the correlation to use? First, the engineer must determine which correlations are closest to the current situation. This

TABLE 5-21 Mass Transfer Correlations for a Single Flat Plate or Disk—Transfer to or from Plate to Fluid

Situation	Correlation	Comments E = Empirical, S = Semiempirical, T = Theoretical	References*
A. Laminar, local, flat plate, forced flow Laminar, average, flat plate, forced flow j -factors	$N_{Sh,x} = \frac{k'x}{D} = 0.323(N_{Re,x})^{1/2}(N_{Sc})^{1/3}$ Coefficient 0.332 is a better fit. $N_{Sh,avg} = \frac{k'_m L}{D} = 0.646(N_{Re,L})^{1/2}(N_{Sc})^{1/3}$ k'_m is mean mass-transfer coefficient for dilute systems. $j_D = j_H = \frac{f}{2} = 0.664(N_{Re,L})^{-1/2}$	[T] Low M.T. rates. Low mass-flux, constant property systems. $N_{Sh,x}$ is local k . Use with arithmetic difference in concentration. Coefficient 0.323 is Blasius' approximate solution. $N_{Re,x} = \frac{xu_\infty \rho}{\mu}$, x = length along plate $N_{Re,L} = \frac{Lu_\infty \rho}{\mu}$, 0.664 (Polhausen) is a better fit for $N_{Sc} > 0.6$, $N_{Re,x} < 3 \times 10^5$. [S] Analogy: $N_{Sc} = 1.0$, f = drag coefficient. j_D is defined in terms of k'_m .	[100] p. 183 [108] p. 526 [146] p. 79 [150] p. 518 [151] p. 110 [151] p. 271
B. Laminar, local, flat plate, blowing or suction and forced flow	$N_{Sh,x} = \frac{k'x}{D} = (\text{Slope})_{y=0} (N_{Re,x})^{1/2}(N_{Sc})^{1/3}$	[T] Blowing is positive. Other conditions as above. $\frac{u_o}{u_\infty} \sqrt{N_{Re,x}}$ $\frac{u_\infty}{(\text{Slope})_{y=0}} \quad 0.6 \quad 0.5 \quad 0.25 \quad 0.0 \quad -2.5$ $(\text{Slope})_{y=0} \quad 0.01 \quad 0.06 \quad 0.17 \quad 0.332 \quad 1.64$	[100] p. 185 [150] p. 271
C. Laminar, local, flat plate, natural convection vertical plate	$N_{Sh,x} = \frac{k'x}{D} = 0.508N_{Sc}^{1/2}(0.952 + N_{Sc})^{-1/4}N_{Gr}^{1/4}$	[T] Low MT rates. Dilute systems, $\Delta\rho/\rho \ll 1$. $N_{Gr}N_{Sc} < 10^8$. Use with arithmetic concentration difference. x = length from plate bottom. $N_{Gr} = \frac{gx^3}{(\mu/\rho)^2} \left(\frac{\rho_\infty}{\rho_0} - 1 \right)$	[151] p. 120
D. Laminar, stationary disk Laminar, spinning disk	$N_{Sh} = \frac{k'd_{disk}}{D} = \frac{8}{\pi}$ $N_{Sh} = \frac{k'd_{disk}}{D} = 0.879N_{Re}^{1/2}N_{Sc}^{1/3}$	[T] Stagnant fluid. Use arithmetic concentration difference. [T] Asymptotic solution for large N_{Sc} . $N_{Re} < \sim 10^4$ $u = \omega d_{disk}/2$, ω = rotational speed, rad/s. Rotating disks are often used in electrochemical research.	[146] p. 240 [117] p. 60 [146] p. 240
E. Laminar, inclined, plate	$N_{Sh,avg} = 0.783N_{Re,fil}^{1/9}N_{Sc}^{1/3} \left(\frac{x^3 \rho^3 g \sin \alpha}{\mu^2} \right)^{2/9}$ $N_{Sh,avg} = \frac{k'_m x}{D}$ $\delta_{film} = \left(\frac{3\mu Q}{w\rho g \sin \alpha} \right)^{1/3} = \text{film thickness}$	[T] Constant-property liquid film with low mass-transfer rates. Use arithmetic concentration difference. $N_{Re,fil} = \frac{4Q\rho}{\mu^2} < 2000$ w = width of plate, δ_f = film thickness, α = angle of inclination, x = distance from start soluble surface. Newtonian fluid. Solute does not penetrate past region of linear velocity profile. Differences between theory and experiment.	[151] p. 130 [146] p. 209
F. Turbulent, local flat plate, forced flow Turbulent, average, flat plate, forced flow	$N_{Sh,x} = \frac{k'x}{D} = 0.0292N_{Re,x}^{0.8}$ $N_{Sh,avg} = \frac{k'L}{D} = 0.0365N_{Re,L}^{0.8}$, average coefficient	[S] Low mass-flux with constant property system. Use with arithmetic concentration difference. $N_{Sc} = 1.0$, $N_{Re,x} > 10^5$ Based on Prandtl's 1/7-power velocity law, $\frac{u}{u_\infty} = \left(\frac{y}{\delta} \right)^{1/7}$	[100] p. 191 [146] p. 201 [151] p. 221
G. Laminar and turbulent, flat plate, forced flow	$j_D = j_H = \frac{f}{2} = 0.037N_{Re,L}^{-0.2}$	Chilton-Colburn analogies, $N_{Sc} = 1.0$, (gases), f = drag coefficient. Corresponds to item 5-21-F and refers to same conditions. $8000 < N_{Re} < 300,000$. Can apply analogy, $j_D = f/2$, to entire plate (including laminar portion) if average values are used.	[100] p. 193 [109] p. 112 [146] p. 201 [151] p. 271

TABLE 5-21 Mass Transfer Correlations for a Single Flat Plate or Disk—Transfer to or from Plate to Fluid (Concluded)

Situation	Correlation	Comments E = Empirical, S = Semiempirical, T = Theoretical	References ^o
H. Laminar and turbulent, flat plate, forced flow	$N_{Sh,avg} = 0.037N_{Re,L}^{1/3}N_{Sc}^{0.8}(N_{Re,L}^{0.8} - 15,500)$ to $N_{Re,L} = 320,000$ $N_{Sh,avg} = 0.037N_{Sc}^{1/3}$ $\times \left(N_{Re,L}^{0.8} - N_{Re,Cr}^{0.8} + \frac{0.664}{0.037} N_{Re,Cr}^{1/2} \right)$ in range 3×10^5 to 3×10^6 .	[E] Use arithmetic concentration difference. $N_{Sh,avg} = \frac{k'_m L}{D}, N_{Sc} > 0.5$ Entrance effects are ignored. $N_{Re,Cr}$ is transition laminar to turbulent.	[109] p. 112 [146] p. 201
I. Turbulent, local flat plate, natural convection, vertical plate Turbulent, average, flat plate, natural convection, vertical plate	$N_{Sh,x} = \frac{k'x}{D} = 0.0299N_{Gr}^{2/5}N_{Sc}^{7/15}$ $\times (1 + 0.494N_{Sc}^{2/3})^{-2/5}$ $N_{Sh,avg} = 0.0249N_{Gr}^{2/5}N_{Sc}^{7/15} \times (1 + 0.494N_{Sc}^{2/3})^{-2/5}$	[S] Low solute concentration and low transfer rates. Use arithmetic concentration difference. $N_{Gr} = \frac{gx^3}{(\mu\rho)^2} \left(\frac{\rho_\infty}{\rho_0} - 1 \right)$ $N_{Gr} > 10^{10}$ Assumes laminar boundary layer is small fraction of total. $N_{Sh,avg} = \frac{k'_m L}{D}$	[151] p. 225
J. Turbulent, vertical plate	$N_{Sh,avg} = \frac{k'_m x}{D} = 0.327N_{Re,fil}^{2/9}N_{Sc}^{1/3} \left(\frac{x^3 \rho^2 g}{\mu^2} \right)^{2/9}$ $\delta_{fil} = 0.172 \left(\frac{Q^2}{w^2 g} \right)^{1/3}$	[E] See 5-21-E for terms. $N_{Re,fil} = \frac{4Q\rho}{w\mu^2} > 2360$ Solute remains in laminar sublayer.	[151] p. 229
K. Turbulent, spinning disk	$N_{Sh} = \frac{k'd_{disk}}{D} = 5.6N_{Re}^{1.1}N_{Sc}^{1/3}$	[E] Use arithmetic concentration difference. $6 \times 10^5 < N_{Re} < 2 \times 10^6$ $120 < N_{Sc} < 1200$ $u = \omega d_{disk}/2$ where ω = rotational speed, radians/s. $N_{Re} = \rho \omega d^2/2\mu$.	[82] [146] p. 241
L. Mass transfer to a flat plate membrane in a stirred vessel	$N_{Sh} = \frac{k'd_{tank}}{D} = aN_{Re}^b N_{Sc}^c$ a depends on system. $a = 0.0443$ [73, 165]; b is often 0.65 – 0.70 [110]. If $N_{Re} = \frac{\omega d_{tank}^2 \rho}{\mu}$ $b = 0.785$ [73]. c is often 0.33 but other values have been reported [110].	[E] Use arithmetic concentration difference. ω = stirrer speed, radians/s. Useful for laboratory dialysis, R.O., U.F., and microfiltration systems.	[73] [110] p. 965 [165] p. 738

^oSee pages 5-7 and 5-8 for references.

involves recognizing the similarity of geometries, which is often challenging, and checking that the range of parameters in the correlation is appropriate. For example, the Bravo, Rocha, and Fair correlation for distillation with structured packings with triangular cross-sectional channels (Table 5-28-H) uses the Johnstone and Pigford correlation for rectification in vertical wetted wall columns (Table 5-22-D). Recognizing that this latter correlation pertains to a rather different application and geometry was a nontrivial step in the process of developing a correlation. If several correlations appear to be applicable, check to see if the correlations have been compared to each other and to the data. When a detailed comparison of correlations is not available, the following heuristics may be useful:

1. Mass-transfer coefficients are derived from models. They must be employed in a similar model. For example, if an arithmetic concentration difference was used to determine k , that k should only be used in a mass-transfer expression with an arithmetic concentration difference.

2. Semiempirical correlations are often preferred to purely empirical or purely theoretical correlations. Purely empirical correlations are dangerous to use for extrapolation. Purely theoretical correlations may predict trends accurately, but they can be several orders of magnitude off in the value of k .

3. Correlations with broader data bases are often preferred.

4. The analogy between heat and mass transfer holds over wider ranges than the analogy between mass and momentum transfer. Good heat transfer data (without radiation) can often be used to predict mass-transfer coefficients.

5. More recent data is often preferred to older data, since end effects are better understood, the new correlation often builds on earlier data and analysis, and better measurement techniques are often available.

6. With complicated geometries, the product of the interfacial area per volume and the mass-transfer coefficient is required. Correlations of ka_p or of HTU are more accurate than individual correlations of k and a_p since the measurements are simpler to determine the product ka_p or HTU.

7. Finally, if a mass-transfer coefficient looks too good to be true, it probably is incorrect.

To determine the mass-transfer rate, one needs the interfacial area in addition to the mass-transfer coefficient. For the simpler geometries, determining the interfacial area is straightforward. For packed beds of particles a , the interfacial area per volume can be estimated as shown in Table 5-27-A. For packed beds in distillation, absorption, and so on in Table 5-28, the interfacial area per volume is included with the mass-transfer coefficient in the correlations for HTU. For agitated liquid-liquid systems, the interfacial area can be estimated

TABLE 5-22 Mass Transfer Correlations for Falling Films with a Free Surface in Wetted Wall Columns—Transfer between Gas and Liquid

Situation	Correlation	Comments E = Empirical, S = Semiempirical, T = Theoretical	References*
A. Laminar, vertical wetted wall column	$N_{Sh,avg} = \frac{k'_m x}{D} \approx 3.41 \frac{x}{\delta_{film}}$ (first term of infinite series) $\delta_{film} = \left(\frac{3\mu Q}{w\rho g} \right)^{1/3} = \text{film thickness}$ $w = \text{film width (circumference in column)}$	[T] Low rates M.T. Use with log mean concentration difference. Parabolic velocity distribution in films. $N_{Re, film} = \frac{4QP}{w\mu} < 20$ Derived for flat plates, used for tubes if $r_{tube} \left(\frac{\rho g}{2\sigma} \right)^{1/2} > 3.0.$ σ = surface tension If $N_{Re, film} > 20$, surface waves and rates increase. An approximate solution $D_{apparent}$ can be used. Ripples are suppressed with a wetting agent good to $N_{Re} = 1200$.	[146] p. 78 [151] p. 137 [161] p. 50
B. Turbulent, vertical wetted wall column	$N_{Sh,avg} = \frac{k'_m d_t}{D} = 0.023 N_{Re}^{0.83} N_{Sc}^{0.44}$ A coefficient 0.0163 has also been reported using N_{Re}' , where $v = v$ of gas relative to liquid film.	[E] Use with log mean concentration difference for correlations in B and C. N_{Re} is for gas. N_{Sc} for vapor in gas. $2000 < N_{Re} \leq 35,000$, $0.6 \leq N_{Sc} \leq 2.5$. Use for gases, d_t = tube diameter.	[88] p. 266 [93] [100] p. 181 [146] p. 211 [151] p. 265 [159] p. 212 [161] p. 71
C. Turbulent, vertical wetted wall column with ripples	$N_{Sh,avg} = \frac{k'_m d_t}{D} = 0.00814 N_{Re}^{0.83} N_{Sc}^{0.44} \left(\frac{4QP}{w\mu} \right)^{0.15}$ $N_{Sh,avg} = \frac{k'_m d_t}{D} = 0.023 N_{Re}^{0.83} N_{Sc}^{0.44}$	[E] For gas systems with rippling. Fits B for $\left(\frac{4QP}{w\mu} \right) = 1000$ $30 \leq \left(\frac{4QP}{w\mu} \right) < 1200$	[88] p. 266 [106] [146] p. 213
D. Rectification in vertical wetted wall column with turbulent vapor flow, Johnstone and Pigford correlation	$N_{Sh,avg} = \frac{k'_C d_{col} p_{BM}}{D v p} = 0.0328 (N_{Re}')^{0.77} N_{Sc}^{0.33}$ $3000 < N_{Re}' < 40,000, 0.5 < N_{Sc} < 3$ $N_{Re}' = \frac{d_{col} v_{rel} \rho_g}{\mu_v}, v_{rel} = \text{gas velocity relative to liquid film} = \frac{3}{2} u_{avg} \text{ in film}$	[E] Use logarithmic mean driving force at two ends of column. Based on four systems with gas-side resistance only. p_{BM} = logarithmic mean partial pressure of nondiffusing species B in binary mixture. p = total pressure Modified form is used for structured packings (See Table 5-28-H).	[105] [146] p. 214

*See pages 5-7 and 5-8 for references.

from the dispersed phase holdup and mean drop size correlations. Godfrey, Obi, and Reeve [*Chem. Engr. Prog.* **85**, 61 (Dec. 1989)] summarize these correlations. For many systems, $d_{drop}/d_{imp} = (\text{const})N_{We}^{-0.6}$ where $N_{We} = \rho_c N^2 d_{imp}^3 / \sigma$.

Effects of Total Pressure on k'_C and k'_L . The influence of total system pressure on the rate of mass transfer from a gas to a liquid or to a solid has been shown to be the same as would be predicted from stagnant-film theory as defined in Eq. (5-285), where

$$\hat{k}_C = D_{AB} p_T / RT \delta_C \quad (5-292)$$

Since the quantity $D_{AB} p_T$ is known to be relatively independent of the pressure, it follows that the rate coefficients k'_C , $k'_C y_{BM}$, and $k'_C p_T y_{BM}$ ($= k'_C p_{BM}$) do not depend on the total pressure of the system, subject to the limitations discussed later.

Investigators of tower packings normally report $k'_C a$ values measured at very low inlet-gas concentrations, so that $y_{BM} = 1$, and at total pressures close to 100 kPa (1 atm). Thus, the correct rate coefficient for use in packed-tower designs involving the use of the driving force $(y - y_i)/y_{BM}$ is obtained by multiplying the reported $k'_C a$ values by the value of p_T employed in the actual test unit (e.g., 100 kPa) and *not* the total pressure of the system to be designed.

From another point of view one can correct the reported values of $k'_C a$ in kmol/[(s·m³)(kPa)], valid for a pressure of 101.3 kPa (1 atm), to some other pressure by dividing the quoted values of $k'_C a$ by the design pressure and multiplying by 101.3 kPa, i.e., ($k'_C a$ at design pressure p_T) = ($k'_C a$ at 1 atm) \times 101.3/ p_T .

One way to avoid a lot of confusion on this point is to convert the experimentally measured $k'_C a$ values to values of $\hat{k}_C a$ straightaway, before beginning the design calculations. A design based on the rate coefficient $\hat{k}_C a$ and the driving force $(y - y_i)/y_{BM}$ will be independent of the total system pressure with the following limitations: caution should be employed in assuming that $\hat{k}_C a$ is independent of total pressure for systems having significant vapor-phase nonidealities, for systems that operate in the vicinity of the critical point, or for total pressures higher than about 3040 to 4050 kPa (30 to 40 atm).

Experimental confirmations of the relative independence of \hat{k}_C with respect to total pressure have been widely reported. Deviations do occur at extreme conditions. For example, Bretznajder (*Prediction of Transport and Other Physical Properties of Fluids*, Pergamon Press, Oxford, 1971, p. 343) discusses the effects of pressure on the $D_{AB} p_T$ product and presents experimental data on the self-diffusion of CO₂ which show that the D - p product begins to decrease at a pressure of

TABLE 5-23 Mass-Transfer Correlations for Flow in Pipes and Ducts—Transfer is from Wall to Fluid

Situation	Correlation	Comments E = Empirical, S = Semiempirical, T = Theoretical	References ^o																		
A. Tubes, laminar, fully developed parabolic velocity profile, developing concentration profile, constant wall concentration	$N_{Sh} = \frac{k'd_t}{D} = 3.66 + \frac{0.0665(d_t/x)N_{Re}N_{Sc}}{1 + 0.04[(d_t/x)N_{Re}N_{Sc}]^{2/3}}$	[T] Use log mean concentration difference. For $\frac{x/d_t}{N_{Re}N_{Sc}} < 0.10$, $N_{Re} < 2100$. x = distance from tube entrance. Good agreement with experiment at values $10^4 > \frac{\pi}{4} \frac{d_t}{x} N_{Re}N_{Sc} > 10$	[98] [100] p. 176 [108] p. 525 [151] p. 159																		
B. Tubes, fully developed concentration profile	$N_{Sh} = \frac{k'd_t}{D} = 3.66$	[T] Subset of 5-23-A for fully developed concentration profile. $\frac{x/d_t}{N_{Re}N_{Sc}} > 0.1$	[98] [151] p. 165																		
C. Tubes, approximate solution	$N_{Sh,x} = \frac{k'd_t}{D} = 1.077 \left(\frac{d_t}{x}\right)^{1/3} (N_{Re}N_{Sc})^{1/3}$ $N_{Sh,avg} = \frac{k'd_t}{D} = 1.615 \left(\frac{d_t}{L}\right)^{1/3} (N_{Re}N_{Sc})^{1/3}$	[T] For arithmetic concentration difference. $\frac{W}{\rho D x} > 400$ Leveque's approximation: Concentration BL is thin. Assume velocity profile is linear. High mass velocity. Fits liquid data well.	[151] p. 166																		
D. Tubes, laminar, uniform plug velocity, developing concentration profile, constant wall concentration	$N_{Sh,avg} = \frac{1}{2} \frac{d_t}{L} N_{Re}N_{Sc} \left[\frac{1 - 4 \sum_{j=1}^{\infty} a_j^2 \exp\left(\frac{-2a_j^2(x/r_t)}{N_{Re}N_{Sc}}\right)}{1 + 4 \sum_{j=1}^{\infty} a_j^2 \exp\left(\frac{-2a_j^2(x/r_t)}{N_{Re}N_{Sc}}\right)} \right]$ <p>Graetz solution for heat transfer written for M.T.</p>	[T] Use arithmetic concentration difference. Fits gas data well, for $\frac{W}{D\rho x} < 50$ (fit is fortuitous). $N_{Sh,avg} = (k'_m d_t)/D$. $a_1 = 2.405$, $a_2 = 5.520$, $a_3 = 8.654$, $a_4 = 11.792$, $a_5 = 14.931$. Graphical solutions are in references.	[91] p. 443 [120] [151] p. 150																		
E. Laminar, fully developed parabolic velocity profile, constant mass flux at wall	$N_{Sh,x} = \left[\frac{11}{48} - \frac{1}{2} \sum_{j=1}^{\infty} \frac{\exp[-\lambda_j^2(x/r_t)/(N_{Re}N_{Sc})]}{C_j \lambda_j^4} \right]^{-1}$ <table border="1" data-bbox="319 911 760 1041"> <thead> <tr> <th>j</th> <th>λ_j^2</th> <th>C_j</th> </tr> </thead> <tbody> <tr> <td>1</td> <td>25.68</td> <td>7.630×10^{-3}</td> </tr> <tr> <td>2</td> <td>83.86</td> <td>2.058×10^{-3}</td> </tr> <tr> <td>3</td> <td>174.2</td> <td>0.901×10^{-3}</td> </tr> <tr> <td>4</td> <td>296.5</td> <td>0.487×10^{-3}</td> </tr> <tr> <td>5</td> <td>450.9</td> <td>0.297×10^{-3}</td> </tr> </tbody> </table>	j	λ_j^2	C_j	1	25.68	7.630×10^{-3}	2	83.86	2.058×10^{-3}	3	174.2	0.901×10^{-3}	4	296.5	0.487×10^{-3}	5	450.9	0.297×10^{-3}	[T] Use log mean concentration difference. $N_{Re} < 2100$ $N_{Sh,x} = \frac{k'd_t}{D}$ $N_{Re} = \frac{v d_t \rho}{\mu}$	[149] [151] p. 167
j	λ_j^2	C_j																			
1	25.68	7.630×10^{-3}																			
2	83.86	2.058×10^{-3}																			
3	174.2	0.901×10^{-3}																			
4	296.5	0.487×10^{-3}																			
5	450.9	0.297×10^{-3}																			
F. Laminar, alternate	$N_{Sh} = 4.36 + \frac{0.023(d_t/L)N_{Re}N_{Sc}}{1 + 0.0012(d_t/L)N_{Re}N_{Sc}}$	[T] $N_{Sh} = \frac{k'd_t}{D}$ Use log mean concentration difference. $N_{Re} < 2100$	[98] [100] p. 176																		
G. Laminar, fully developed concentration and velocity profile	$N_{Sh} = \frac{k'd_t}{D} = \frac{48}{11} = 4.3636$	[T] Use log mean concentration difference. $N_{Re} < 2100$	[98] [151] p. 167																		
H. Vertical tubes, laminar flow, forced and natural convection	$N_{Sh,avg} = 1.62 N_{Gz}^{1/3} \left[1 \pm 0.0742 \frac{(N_{Gr} N_{Sc} d/L)^{3/4}}{N_{Gz}} \right]^{1/3}$	[T] Approximate solution. Use minus sign if forced and natural convection oppose each other. $N_{Gz} = \frac{N_{Re} N_{Sc} d}{L}$ $N_{Gr} = \frac{g \Delta \rho d^3}{\rho \nu^2}$ Good agreement with experiment.	[140]																		
I. Tubes, laminar, RO systems	$N_{Sh,avg} = \frac{k'_m d_t}{D} = 1.632 \left(\frac{u d_t^2}{DL}\right)^{1/3}$	Use arithmetic concentration difference. Thin concentration polarization layer, not fully developed. $N_{Re} < 2000$, L = length tube.	[73] [165] p. 738																		
J. Tubes and parallel plates, laminar RO	Graphical solutions for concentration polarization. Uniform velocity through walls.	[T]	[145] [165] p. 762																		

TABLE 5-23 Mass-Transfer Correlations for Flow in Pipes and Ducts—Transfer is from Wall to Fluid (Continued)

Situation	Correlation	Comments E = Empirical, S = Semiempirical, T = Theoretical	References*
K. Parallel plates, laminar, parabolic velocity, developing concentration profile, constant wall concentration	Graphical solution	[T] Low transfer rates.	[151] p. 176
L. 5-23-K, fully developed	$N_{Sh} = \frac{k'(2h)}{D} = 7.6$	[T] h = distance between plates. Use log mean concentration difference. $\frac{N_{Re} N_{Sc}}{x/(2h)} < 20$	[151] p. 177
M. Parallel plates, laminar, parabolic velocity, developing concentration profile, constant mass flux at wall	Graphical solution	[T] Low transfer rates.	[151] p. 176
N. 5-23-M, fully developed	$N_{Sh} = \frac{k'(2h)}{D} = 8.23$	[T] Use log mean concentration difference. $\frac{N_{Re} N_{Sc}}{x/(2h)} < 20$	[151] p. 177
O. Laminar flow, vertical parallel plates, forced and natural convection	$N_{Sh,avg} = 1.47 N_{Gr}^{1/3} \left[1 \pm 0.0989 \frac{(N_{Gr} N_{Sc} h/L)^{3/4}}{N_{Gr}} \right]^{1/3}$	[T] Approximate solution. Use minus sign if forced and natural convection oppose each other. $N_{Gr} = \frac{N_{Re} N_{Sc} h}{L}$ $N_{Gr} = \frac{g \Delta \rho h^3}{\rho \nu^2}$ Good agreement with experiment.	[140]
P. Parallel plates, laminar, RO systems	$N_{Sh,avg} = \frac{k'(2H_p)}{D} = 2.354 \left(\frac{u H_p^2}{DL} \right)^{1/3}$	Thin concentration polarization layer. Short tubes, concentration profile not fully developed. Use arithmetic concentration difference.	[73] [165] p. 738
Q. Tubes, turbulent	$N_{Sh,avg} = \frac{k'_m d_t}{D} = 0.023 N_{Re}^{0.83} N_{Sc}^{1/3}$	[E] Use with log mean concentration difference at two ends of tube. $2100 < N_{Re} < 35,000$ $0.6 < N_{Sc} < 3000$ From wetted wall column and dissolution data—see Table 5-22-B. Good fit for liquids.	[88] p. 266 [100] p. 181 [120] [161] p. 72
R. Tubes, turbulent	$N_{Sh,avg} = \frac{k'_m d_t}{D} = 0.023 N_{Re}^{0.83} N_{Sc}^{0.44}$	[E] Evaporation of liquids. Use with log mean concentration difference. See item above. Better fit for gases. $2000 < N_{Re} < 35,000$ $0.6 < N_{Sc} < 2.5$.	[93][100] p. 181 [109] p. 112 [146] p. 211
S. Tubes, turbulent	$N_{Sh} = \frac{k' d_t}{D} = 0.0096 N_{Re}^{0.913} N_{Sc}^{0.346}$	[E] $430 < N_{Sc} < 100,000$. Dissolution data. Use for high N_{Sc} .	[122] p. 668
T. Tubes, turbulent, smooth tubes, Reynolds analogy	$N_{Sh} = \frac{k' d_t}{D} = \left(\frac{f}{2} \right) N_{Re} N_{Sc}$ f = Fanning friction factor	[T] Use arithmetic concentration difference. N_{Sc} near 1.0 Turbulent core extends to wall. Of limited utility.	[91] p. 438 [100] p. 171 [151] p. 239 [159] p. 250
U. Tubes, turbulent, smooth tubes, Chilton-Colburn analogy	$j_D = j_H = \frac{f}{2}$ If $\frac{f}{2} = 0.023 N_{Re}^{-0.2}$, $j_D = \frac{N_{Sh}}{N_{Re} N_{Sc}^{1/3}} = 0.023 N_{Re}^{-0.2}$ $N_{Sh} = \frac{k' d_t}{D}$ $j_D = j_H = f(N_{Re}, \text{ geometry and B.C.})$	[T] Use log-mean concentration difference. Relating j_D to $f/2$ approximate. N_{Pr} and N_{Sc} near 1.0. Low concentration. Results about 20% lower than experiment. $3 \times 10^4 < N_{Re} < 10^6$	[72] p. 400, 647 [80][88] p. 269 [151] p. 264 [159] p. 251
V. Tubes, turbulent, smooth tubes, constant surface concentration, Prandtl analogy	$N_{Sh} = \frac{k' d_t}{D} = \frac{(f/2) N_{Re} N_{Sc}}{1 + 5\sqrt{f/2}(N_{Sc} - 1)}$ $\frac{f}{2} = 0.04 N_{Re}^{-0.25}$	[T] Use arithmetic concentration difference. Improvement over Reynolds analogy. Best for N_{Sc} near 1.0.	[72] p. 647 [80] [100] p. 173 [132] [151] p. 241

*See pages 5-7 and 5-8 for references.

TABLE 5-23 Mass-Transfer Correlations for Flow in Pipes and Ducts—Transfer is from Wall to Fluid (Concluded)

Situation	Correlation	Comments E = Empirical, S = Semiempirical, T = Theoretical	References ^o
W. Tubes, turbulent, smooth tubes, constant surface concentration, Von Karman analogy	$N_{Sh} = \frac{(f/2)N_{Re}N_{Sc}}{1 + 5\sqrt{f/2} \left\{ (N_{Sc} - 1) + \ln \left[1 + \frac{5}{6}(N_{Sc} - 1) \right] \right\}}$ $\frac{f}{2} = 0.04 N_{Re}^{-0.25}$	[T] Use arithmetic concentration difference. $N_{Sh} = k' d_t / D$. Improvement over Prandtl, $N_{Sc} < 25$.	[100] p. 173 [151] p. 243 [159] p. 250 [162]
X. Tubes, turbulent, smooth tubes, constant surface concentration	For $0.5 < N_{Sc} < 10$: $N_{Sh,avg} = 0.0097 N_{Re}^{9/10} N_{Sc}^{1/2} \times (1.10 + 0.44 N_{Sc}^{-1/3} - 0.70 N_{Sc}^{-1/6})$ For $10 < N_{Sc} < 1000$: $N_{Sh,avg} = \frac{0.0097 N_{Re}^{9/10} N_{Sc}^{1/2} (1.10 + 0.44 N_{Sc}^{-1/3} - 0.70 N_{Sc}^{-1/6})}{1 + 0.064 N_{Sc}^{1/2} (1.10 + 0.44 N_{Sc}^{-1/3} - 0.70 N_{Sc}^{-1/6})}$ For $N_{Sc} > 1000$: $N_{Sh,avg} = 0.0102 N_{Re}^{9/10} N_{Sc}^{1/3}$	[S] Use arithmetic concentration difference. Based on partial fluid renewal and an infrequently replenished thin fluid layer for high N_{Sc} . Good fit to available data. $N_{Re} = \frac{u_{bulk} d_t}{\nu}$ $N_{Sh,avg} = \frac{k'_{avg} d_t}{D}$	[100] p. 179 [131]
Y. Turbulent flow, tubes	$N_{St} = \frac{N_{Sh}}{N_{Pe}} = \frac{N_{Sh}}{N_{Re} N_{Sc}} = 0.0149 N_{Re}^{-0.12} N_{Sc}^{-2/3}$	[E] Smooth pipe data. Data fits within 4% except at $N_{Sc} > 20,000$, where experimental data is underpredicted. $N_{Sc} > 100, 10^5 > N_{Re} > 2100$	[124]
Z. Turbulent flow, noncircular ducts	Use correlations with $d_{eq} = \frac{4 \text{ cross-sectional area}}{\text{wetted perimeter}}$ Parallel plates: $d_{eq} = 4 \frac{2hw}{2w + 2h}$	Can be suspect for systems with sharp corners.	[151] p. 289 [165] p. 738

^oSee pages 5-7 and 5-8 for references.

approximately 8100 kPa (80 atm). For reduced temperatures higher than about 1.5, the deviations are relatively modest for pressures up to the critical pressure. However, deviations are large near the critical point (see also p. 5-49). The effect of pressure on the gas-phase viscosity also is negligible for pressures below about 5060 kPa (50 atm).

For the liquid-phase mass-transfer coefficient \hat{k}_L , the effects of total system pressure can be ignored for all practical purposes. Thus, when using \hat{k}_C and \hat{k}_L for the design of gas absorbers or strippers, the primary pressure effects to consider will be those which affect the equilibrium curves and the values of m . If the pressure changes affect the hydrodynamics, then \hat{k}_C , \hat{k}_L , and a can all change significantly.

Effects of Temperature on \hat{k}_C and \hat{k}_L The Stanton-number relationship for gas-phase mass transfer in packed beds,

$$N_{St} = \hat{k}_C / G_M = g(N_{Re}, N_{Sc}) \quad (5-293)$$

indicates that for a given system geometry the rate coefficient \hat{k}_C depends only on the Reynolds number and the Schmidt number. Since the Schmidt number for a gas is independent of temperature, the principal effect of temperature upon \hat{k}_C arises from changes in the gas viscosity with changes in temperature. For normally encountered temperature ranges, these effects will be small owing to the fractional powers involved in Reynolds-number terms (see Tables 5-21 to 5-28). It thus can be concluded that for all practical purposes \hat{k}_C is independent of temperature and pressure in the normal ranges of these variables.

For modest changes in temperature the influence of temperature upon the interfacial area a may be neglected. For example, in experiments on the absorption of SO_2 in water, Whitney and Vivian [Chem. Eng. Prog., 45, 323 (1949)] found no appreciable effect of temperature upon $k'_c a$ over the range from 10 to 50°C.

With regard to the liquid-phase mass-transfer coefficient, Whitney and Vivian found that the effect of temperature upon $k_L a$ could be explained entirely by variations in the liquid-phase viscosity and diffusion coefficient with temperature. Similarly, the oxygen-desorption data of Sherwood and Holloway [Trans. Am. Inst. Chem. Eng., 36, 39 (1940)] show that the influence of temperature upon H_L can be explained by the effects of temperature upon the liquid-phase viscosity and diffusion coefficients.

It is important to recognize that the effects of temperature on the liquid-phase diffusion coefficients and viscosities can be very large and therefore must be carefully accounted for when using \hat{k}_L or H_L data. For liquids the mass-transfer coefficient \hat{k}_L is correlated in terms of design variables by relations of the form

$$N_{St} = \hat{k}_L / L_M = f(N_{Re}, N_{Sc}) \quad (5-294)$$

A general relation for H_L which may be used as the basis for applying temperature corrections is as follows:

$$H_L = b N_{Re}^a N_{Sc}^{1/2} \quad (5-295)$$

where b is a proportionality constant and the exponent a may range from about 0.2 to 0.5 for different packings and systems. The liquid-phase diffusion coefficients may be corrected from a base temperature T_1 to another temperature T_2 by using the Einstein relation as recommended by Wilke [Chem. Eng. Prog., 45, 218 (1949)]:

$$D_2 = D_1 (T_2 / T_1) (\mu_1 / \mu_2) \quad (5-296)$$

The Einstein relation can be rearranged to the following equation for relating Schmidt numbers at two temperatures:

$$N_{Sc,2} = N_{Sc,1} (T_1 / T_2) (\rho_1 / \rho_2) (\mu_2 / \mu_1)^2 \quad (5-297)$$

TABLE 5-24 Mass Transfer Correlations for Flow Past Submerged Objects

Situation	Correlation	Comments E = Empirical, S = Semiempirical, T = Theoretical	References ^o												
A. Single sphere	$N_{Sh} = \frac{k'_C p_{BLM} R T d_s}{PD} = \frac{2r}{r - r_s}$ <table border="1" data-bbox="317 222 694 267"> <tr> <td>r/r_s</td> <td>2</td> <td>5</td> <td>10</td> <td>50</td> <td>∞ (asymptotic limit)</td> </tr> <tr> <td>N_{Sh}</td> <td>4.0</td> <td>2.5</td> <td>2.22</td> <td>2.04</td> <td>2.0</td> </tr> </table>	r/r_s	2	5	10	50	∞ (asymptotic limit)	N_{Sh}	4.0	2.5	2.22	2.04	2.0	<p>[T] Use with log mean concentration difference. r = distance from sphere, r_s, d_s = radius and diameter of sphere. No convection.</p>	[151] p. 18
r/r_s	2	5	10	50	∞ (asymptotic limit)										
N_{Sh}	4.0	2.5	2.22	2.04	2.0										
B. Single sphere, creeping flow with forced convection	$N_{Sh} = \frac{k'd}{D} = [4.0 + 1.21(N_{Re} N_{Sc})^{2/3}]^{1/2}$ $N_{Sh} = \frac{k'd}{D} = a(N_{Re} N_{Sc})^{1/3}$ <p>$a = 1.01, 1.0, \text{ or } 0.991$</p>	<p>[T] Use with log mean concentration difference. Average over sphere. Numerical calculations. (N_{Re}, N_{Sc}) < 10,000 N_{Re} < 1.0. Constant sphere diameter. Low mass-transfer rates.</p> <p>[T] Fit to above ignoring molecular diffusion.</p>	<p>[78][109] p. 114 [122] p. 671 [146] p. 214</p> <p>[117] p. 80</p> <p>146 p. 215</p>												
C. Single spheres, molecular diffusion, and forced convection, low flow rates	$N_{Sh} = 2.0 + AN_{Re}^{1/2} N_{Sc}^{1/3}$ <p>$A = 0.5 \text{ to } 0.62$</p> <p>$A = 0.60.$</p> <p>$A = 0.95.$</p> <p>$A = 0.95.$</p> <p>$A = 0.544.$</p>	<p>[E] Use with log mean concentration difference. Average over sphere. Frössling Eq. ($A = 0.552$), $2 \leq N_{Re} \leq 800$, $0.6 \leq N_{Sc} \leq 2.7$. N_{Sh} lower than experimental at high N_{Re}.</p> <p>[E] Ranz and Marshall $2 \leq N_{Re} \leq 200$, $0.6 \leq N_{Sc} \leq 2.5$. See also Table 5-27-L.</p> <p>[E] Liquids $2 \leq N_{Re} \leq 2,000$. Graph in Ref. 146, p. 217–218.</p> <p>[E] $100 \leq N_{Re} \leq 700$; $1,200 \leq N_{Sc} \leq 1525$.</p> <p>[E] Use with arithmetic concentration difference. $N_{Sc} = 1$; $50 \leq N_{Re} \leq 350$.</p>	<p>[72] [89] p. 409, 647 [100], p. 194 109 p. 114 151 p. 276</p> <p>[72] p. 409, 647 [135] [146] p. 217 [151] p. 276</p> <p>[90][91] p. 446 [146] p. 217</p> <p>[139][151] p. 276</p> <p>[102][151] p. 276</p>												
D. 5-24-C	$N_{Sh} = \frac{k'd_s}{D} = 2.0 + 0.575 N_{Re}^{1/2} N_{Sc}^{0.35}$	<p>[E] Use with log mean concentration difference. $N_{Sc} \leq 1$, $N_{Re} < 1$.</p>	[94][151] p. 276												
E. 5-24-C	$N_{Sh} = \frac{k'd_s}{D} = 2.0 + 0.552 N_{Re}^{0.53} N_{Sc}^{1/3}$	<p>[E] Use with log mean concentration difference. $1.0 < N_{Re} \leq 48,000$ Gases: $0.6 \leq N_{Sc} \leq 2.7$.</p>	[91] p. 446												
F. Single spheres, forced concentration, any flow rate	$N_{Sh} = \frac{k'_f d_s}{D} = 2.0 + 0.59 \left[\frac{E^{1/3} J_p^{4/3} \rho}{\mu} \right]^{0.57} N_{Sc}^{1/3}$ <p>Energy dissipation rate per unit mass of fluid (ranges $570 < N_{Sc} < 1420$):</p> $E = \left(\frac{C_{Dr}}{2} \right) \left(\frac{v_r^3}{d_p} \right) \frac{m^2}{s^3}$ $2 < \left(\frac{E^{1/3} J_p^{4/3} \rho}{\mu} \right) < 63,000$	<p>[S] Correlates large amount of data and compares to published data. v_r = relative velocity between fluid and sphere, m/s. C_{Dr} = drag coefficient for single particle fixed in fluid at velocity v_r. See 5-27-G for calculation details and other applications.</p>	[125]												
G. Single spheres, forced convection, high flow rates, ignoring molecular diffusion	$N_{Sh} = \frac{k'd_s}{D} = 0.347 N_{Re}^{0.62} N_{Sc}^{1/3}$ $N_{Sh} = \frac{k'd_s}{D} = 0.33 N_{Re}^{0.6} N_{Sc}^{1/3}$ $N_{Sh} = \frac{k'd_s}{D} = 0.43 N_{Re}^{0.56} N_{Sc}^{1/3}$ $N_{Sh} = \frac{k'd_s}{D} = 0.692 N_{Re}^{0.514} N_{Sc}^{1/3}$	<p>[E] Use with arithmetic concentration difference. Liquids, $2000 < N_{Re} < 17,000$. High N_{Sc}, graph in Ref. 146, p. 217–218.</p> <p>[E] $1500 \leq N_{Re} \leq 12,000$.</p> <p>[E] $200 \leq N_{Re} \leq 4 \times 10^4$, “air” $\leq N_{Sc} \leq$ “water.”</p> <p>[E] $500 \leq N_{Re} \leq 5000$.</p>	<p>[91] p. 446 [157] [146] p. 217</p> <p>[151] p. 276</p> <p>[151] p. 276</p> <p>[128] [151] p. 276</p>												
H. Single cylinders, perpendicular flow	$N_{Sh} = \frac{k'd_s}{D} = AN_{Re}^{1/2} N_{Sc}^{1/3}, A = 0.82$ <p>$A = 0.74$</p> <p>$A = 0.582$</p> $j_D = 0.600(N_{Re})^{-0.457}$ $N_{Sh} = \frac{k'd_{col}}{D}$	<p>[E] $100 < N_{Re} \leq 3500$, $N_{Sc} = 1560$.</p> <p>[E] $120 \leq N_{Re} \leq 6000$, $N_{Sc} = 2.44$.</p> <p>[E] $300 \leq N_{Re} \leq 7600$, $N_{Sc} = 1200$.</p> <p>[E] Use with arithmetic concentration difference.</p>	<p>[151] p. 276</p> <p>[151] p. 276 [152]</p> <p>[151] p. 276</p>												
		<p>$50 \leq N_{Re} \leq 50,000$; gases, $0.6 \leq N_{Sc} \leq 2.6$; liquids; $1000 \leq N_{Sc} \leq 3000$. Data scatter $\pm 30\%$.</p>	[91] p. 450												

TABLE 5-24 Mass Transfer Correlations for Flow Past Submerged Objects (Concluded)

Situation	Correlation	Comments E = Empirical, S = Semiempirical, T = Theoretical	References*
I. 5-24-H	Can use $j_D = j_H$. Graphical correlation.	[E] Used with linear concentration difference.	[72] p. 408, 647
J. Rotating cylinder in an infinite liquid, no forced flow	$j'_D = \frac{k'}{v} N_{Sc}^{0.644} = 0.0791 N_{Re}^{-0.30}$ Results presented graphically to $N_{Re} = 241,000$. $N_{Re} = \frac{v d_{cyl} \mu}{\rho}$ where $v = \frac{\omega d_{cyl}}{2}$ = peripheral velocity $j_D = \frac{N_{Sh}}{N_{Re} N_{Sc}^{1/3}} = 0.74 N_{Re}^{-0.5}$ $N_{Re} = \frac{d_{ch} v \rho}{\mu}$, $d_{ch} = \frac{\text{total surface area}}{\text{perimeter normal to flow}}$ e.g., for cube with side length a , $d_{ch} = 1.27a$. $N_{Sh} = \frac{k' d_{ch}}{D}$	[E] Used with arithmetic concentration difference. $N_{Sh} = \frac{k' d_c}{D}$ 112 < N_{Re} ≤ 100,000, 835 < N_{Sc} < 11490 k' = mass-transfer coefficient, cm/s; ω = rotational speed, radian/s. Useful geometry in electrochemical studies.	[146] p. 236 [151] p. 273 [85] [146] p. 238
K. Oblate spheroid, forced convection	$j_D = \frac{N_{Sh}}{N_{Re} N_{Sc}^{1/3}} = 0.74 N_{Re}^{-0.5}$ $N_{Re} = \frac{d_{ch} v \rho}{\mu}$, $d_{ch} = \frac{\text{total surface area}}{\text{perimeter normal to flow}}$ e.g., for cube with side length a , $d_{ch} = 1.27a$. $N_{Sh} = \frac{k' d_{ch}}{D}$	[E] Used with arithmetic concentration difference. 120 ≤ N_{Re} ≤ 6000; standard deviation 2.1%. Eccentricities between 1:1 (spheres) and 3:1. Shape is often approximated by drops.	[151] p. 284 [152]
L. Other objects, including prisms, cubes, hemispheres, spheres, and cylinders; forced convection	$j_D = 0.692 N_{Re,p}^{-0.486}$, $N_{Re,p} = \frac{v d_{ch} \rho}{\mu}$ Terms same as in 5-24-J.	[E] Used with arithmetic concentration difference. 500 ≤ $N_{Re,p}$ ≤ 5000. Turbulent. Agrees with cylinder and oblate spheroid results, ± 15%. Assumes molecular diffusion and natural convection are negligible.	[109] p. 115 [127, 128] [151] p. 285
M. Other objects, molecular diffusion limits	$N_{Sh} = \frac{k' d_{ch}}{D} = A$ Spheres and cubes $A = 2$, tetrahedrons $A = 2\sqrt{6}$ octahedrons $2\sqrt{2}$.	[T] Use with arithmetic concentration difference. Hard to reach limits in experiments.	[109] p. 114
N. Shell side of microporous hollow fiber module for solvent extraction	$N_{Sh} = \beta [d_h (1 - \phi) / L] N_{Re}^{0.6} N_{Sc}^{0.33}$ $N_{Sh} = \frac{\bar{K} d_h}{D}$ $\beta = 5.8$ for hydrophobic membrane. $\beta = 6.1$ for hydrophilic membrane.	[E] Use with logarithmic mean concentration difference. $N_{Re} = \frac{d_h v \rho}{\mu}$, \bar{K} = overall mass-transfer coefficient d_h = hydraulic diameter $= \frac{4 \times \text{cross-sectional area of flow}}{\text{wetted perimeter}}$ ϕ = packing fraction of shell side. L = module length. Based on area of contact according to inside or outside diameter of tubes depending on location of interface between aqueous and organic phases. Can also be applied to gas-liquid systems with liquid on shell side.	[133]

See Table 5-27 for flow in packed beds.

*See pp. 5-7 and 5-8 for references.

Substitution of this relation into Eq. (5-295) shows that for a given geometry the effect of temperature on H_L can be estimated as

$$H_{L,2} = H_{L,1} (T_1/T_2)^{1/2} (\rho_1/\rho_2)^{1/2} (\mu_2/\mu_1)^{1-a} \quad (5-298)$$

In using these relations it should be noted that for equal liquid flow rates

$$H_{L,2}/H_{L,1} = (\hat{k}_L a)_1 / (\hat{k}_L a)_2 \quad (5-299)$$

Effects of System Physical Properties on \hat{k}_C and \hat{k}_L . When designing packed towers for nonreacting gas-absorption systems for

which no experimental data are available, it is necessary to make corrections for differences in composition between the existing test data and the system in question. For example, the test data of Fellinger for ammonia-water absorption on various packings are frequently used as a base (see Table 5-28-B). In these tests it is estimated that $H_C = 0.9H_{OC}$, so that one may wish to use these data as the basis for estimating H_C or $\hat{k}_C a$ values for other systems. This may be done by taking H_C proportional to $N_{Sc}^{0.5}$ and $\hat{k}_C a$ proportional to $N_{Sc}^{-0.5}$, based on a value of N_{Sc} for NH_3 -air of 0.66 at 25°C. The coefficient k_C varies as the diffusivity D_{AB} to the 0.5 power. It should be noted, however, that

TABLE 5-25 Mass-Transfer Correlations for Drops and Bubbles

Conditions	Correlations	Comments E = Empirical, S = Semiempirical, T = Theoretical	References ^o																																																								
A. Single liquid drop in immiscible liquid, drop formation, discontinuous (drop) phase coefficient	$\hat{k}_{d,f} = A \left(\frac{\rho_d}{M_d} \right)_{av} \left(\frac{D_d}{\pi t_f} \right)^{1/2}$ $A = \frac{24}{7} \text{ (penetration theory)}$ $A = 1.31 \text{ (semiempirical value)}$ $A = \left[\frac{24}{7} (0.8624) \right] \text{ (extension by fresh surface elements)}$	<p>[T,S] Use arithmetic mole fraction difference.</p> <p>Fits some, but not all, data. Low mass transfer rate. M_d = mean molecular weight of dispersed phase; t_f = formation time of drop. $k_{L,d}$ = mean dispersed liquid phase M.T. coefficient $\text{kmole}/[\text{s} \cdot \text{m}^2 \text{ (mole fraction)}]$.</p>	<p>[151] p. 399</p>																																																								
B. 5-25-A	$\hat{k}_{d,f} = 0.0432$ $\times \frac{d_p}{t_f} \left(\frac{\rho_d}{M_d} \right)_{av} \left(\frac{u_o}{d_p g} \right)^{0.089} \left(\frac{d_p^2}{t_f D_d} \right)^{-0.334} \left(\frac{\mu_d}{\sqrt{\rho_d d_p} \sigma_{gc}} \right)^{-0.601}$	<p>[E] Use arithmetic mole fraction difference.</p> <p>Based on 23 data points for 3 systems. Average absolute deviation 26%. Use with surface area of drop after detachment occurs. u_o = velocity through nozzle; σ = interfacial tension.</p>	<p>[151] p. 401 [154] p. 434</p>																																																								
C. Single liquid drop in immiscible liquid, drop formation, continuous phase coefficient	$\hat{k}_{c,f} = 4.6 \left(\frac{\rho_c}{M_c} \right)_{av} \sqrt{\frac{D_c}{\pi t_f}}$	<p>[T] Use arithmetic mole fraction difference.</p> <p>Based on rate of bubble growth away from fixed orifice. Approximately three times too high compared to experiments.</p>	<p>[151] p. 402</p>																																																								
D. 5-25-C	$k_{L,c} = 0.386$ $\times \left(\frac{\rho_c}{M_c} \right)_{av} \left(\frac{D_c}{t_f} \right)^{0.5} \left(\frac{\rho_c \sigma_{gc}}{\Delta \rho g t_f \mu_c} \right)^{0.407} \left(\frac{g t_f^2}{d_p} \right)^{0.148}$	<p>[E] Average absolute deviation 11% for 20 data points for 3 systems.</p>	<p>[151] p. 402 [154] p. 434</p>																																																								
E. Single liquid drop in immiscible liquid, free rise or fall, discontinuous phase coefficient, stagnant drops	$k_{L,d,m} = \frac{-d_p}{6t} \left(\frac{\rho_d}{M_d} \right)_{av} \ln \left\{ \frac{6}{\pi^2} \sum_{j=1}^{\infty} \frac{1}{j^2} \exp \left[\left(\frac{-D_d j^2 \pi^2 t}{(d_p/2)^2} \right) \right] \right\}$	<p>[T] Use with log mean mole fraction differences based on ends of column. t = rise time. No continuous phase resistance. Stagnant drops are likely if drop is very viscous, quite small, or is coated with surface active agent. $k_{L,d,m}$ = mean dispersed liquid M.T. coefficient.</p>	<p>[151] p. 404 [154] p. 435</p>																																																								
F. 5-25-E	$\hat{k}_{L,d,m} = \frac{-d_p}{6t} \left(\frac{\rho_d}{M_d} \right)_{av} \ln \left[1 - \frac{\pi D_d^{1/2} t^{1/2}}{d_p/2} \right]$	<p>[S] See 5-25-E. Approximation for fractional extractions less than 50%.</p>	<p>[151] p. 404 [154] p. 435</p>																																																								
C. 5-25-E, continuous phase coefficient, stagnant drops, spherical	$N_{Sh} = \frac{k_{L,c,m} d_c}{D_c} = 0.74 \left(\frac{\rho_c}{M_c} \right)_{av} N_{Re}^{1/2} (N_{Sc,c})^{1/3}$	<p>[E] $N_{Re} = \frac{v_s d_p \rho_c}{\mu_c}$, special case Eq. (5-254).</p>	<p>[151] p. 407</p>																																																								
H. 5-25-E, oblate spheroid	$N_{Sh} = \frac{k_{L,c,m} d_3}{D_c} = 0.74 \left(\frac{\rho_c}{M_c} \right)_{av} (N_{Re,3})^{1/2} (N_{Sc,c})^{1/3}$	<p>[E] Used with log mean mole fraction. Differences based on ends of extraction column; 100 measured values $\pm 2\%$ deviation. Based on area oblate spheroid.</p>	<p>[151] p. 285, 406, 407</p>																																																								
I. Single liquid drop in immiscible liquid, Free rise or fall, discontinuous phase coefficient, circulating drops	$k_{d,circ} = -\frac{d_p}{6\theta} \ln \left[\frac{3}{8} \sum_{j=1}^{\infty} B_j^2 \exp \left(-\frac{\lambda_j 64 D_d \theta}{d_p^2} \right) \right]$ <table border="1" data-bbox="335 1355 743 1529"> <thead> <tr> <th colspan="7">Eigenvalues for Circulating Drop</th> </tr> <tr> <th>$k_d d_p / D_d$</th> <th>λ_1</th> <th>λ_2</th> <th>λ_3</th> <th>B_1</th> <th>B_2</th> <th>B_3</th> </tr> </thead> <tbody> <tr> <td>3.20</td> <td>0.262</td> <td>0.424</td> <td></td> <td>1.49</td> <td>0.107</td> <td></td> </tr> <tr> <td>10.7</td> <td>0.680</td> <td>4.92</td> <td></td> <td>1.49</td> <td>0.300</td> <td></td> </tr> <tr> <td>26.7</td> <td>1.082</td> <td>5.90</td> <td>15.7</td> <td>1.49</td> <td>0.495</td> <td>0.205</td> </tr> <tr> <td>107</td> <td>1.484</td> <td>7.88</td> <td>19.5</td> <td>1.39</td> <td>0.603</td> <td>0.384</td> </tr> <tr> <td>320</td> <td>1.60</td> <td>8.62</td> <td>21.3</td> <td>1.31</td> <td>0.583</td> <td>0.391</td> </tr> <tr> <td>∞</td> <td>1.656</td> <td>9.08</td> <td>22.2</td> <td>1.29</td> <td>0.596</td> <td>0.386</td> </tr> </tbody> </table>	Eigenvalues for Circulating Drop							$k_d d_p / D_d$	λ_1	λ_2	λ_3	B_1	B_2	B_3	3.20	0.262	0.424		1.49	0.107		10.7	0.680	4.92		1.49	0.300		26.7	1.082	5.90	15.7	1.49	0.495	0.205	107	1.484	7.88	19.5	1.39	0.603	0.384	320	1.60	8.62	21.3	1.31	0.583	0.391	∞	1.656	9.08	22.2	1.29	0.596	0.386	<p>[T] Use with arithmetic concentration difference.</p> <p>θ = drop residence time. A more complete listing of eigenvalues is given by Refs. 86 and 99.</p> <p>$N_{Re,3} = \frac{v_s d_3 \rho_c}{\mu_c}$</p> <p>$v_s$ = slip velocity, $d_3 = \frac{\text{total drop surface area}}{\text{perimeter normal to flow}}$</p> <p>$k'_{L,d,circ}$ is m/s.</p>	<p>[86][99][151] p. 405 [161] p. 523</p>
Eigenvalues for Circulating Drop																																																											
$k_d d_p / D_d$	λ_1	λ_2	λ_3	B_1	B_2	B_3																																																					
3.20	0.262	0.424		1.49	0.107																																																						
10.7	0.680	4.92		1.49	0.300																																																						
26.7	1.082	5.90	15.7	1.49	0.495	0.205																																																					
107	1.484	7.88	19.5	1.39	0.603	0.384																																																					
320	1.60	8.62	21.3	1.31	0.583	0.391																																																					
∞	1.656	9.08	22.2	1.29	0.596	0.386																																																					
J. 5-25-I	$\hat{k}_{L,d,circ} = -\frac{d_p}{6\theta} \left(\frac{\rho_d}{M_d} \right)_{av} \ln \left[1 - \frac{R^{1/2} \pi D_d^{1/2} \theta^{1/2}}{d_p/2} \right]$	<p>[E] Used with mole fractions for extraction less than 50%, $R \approx 2.25$.</p>	<p>[151] p. 405</p>																																																								

TABLE 5-25 Mass-Transfer Correlations for Drops and Bubbles (Continued)

Conditions	Correlations	Comments E = Empirical, S = Semiempirical, T = Theoretical	References ^o
K. 5-25-I	$N_{Sh} = \frac{\hat{k}_{L,d,circ} d_p}{D_d}$ $= 31.4 \left(\frac{\rho_d}{M_{f,av}} \right) \left(\frac{4D_d t}{d_p^2} \right)^{-0.34} N_{Sc,d}^{-0.125} \left(\frac{d_p v_s \rho_c}{\sigma g_c} \right)^{-0.37}$	[E] Used with log mean mole fraction difference. d_p = diameter of sphere with same volume as drop. $856 \leq N_{Sc} \leq 79,800$, $2.34 \leq \sigma \leq 4.8$ dynes/cm.	[154] p. 435 [155]
L. Liquid drop in immiscible liquid, free rise or fall, continuous phase coefficient, circulating single drops	$N_{Sh,c} = \frac{k'_{L,c} d_p}{D_d}$ $= \left[2 + 0.463 N_{Re,drop}^{0.484} N_{Sc,c}^{0.339} \left(\frac{d_p g^{1/3}}{D^{2/3}} \right)^{0.072} \right] F$ $F = 0.281 + 1.615K + 3.73K^2 - 1.874K$ $K = N_{Re,drop}^{1/8} \left(\frac{\mu_c}{\mu_d} \right)^{1/4} \left(\frac{\mu_c v_s}{\sigma g_c} \right)^{1/6}$	[E] Used as an arithmetic concentration difference. $N_{Re,drop} = \frac{d_p v_s \rho_c}{\mu_c}$ Solid sphere form with correction factor F .	[103]
M. 5-25-L, circulating, single drop	$N_{Sh} = \frac{k_{L,c} d_p}{D_c} = 0.6 \left(\frac{\rho_c}{M_c} \right)_{av} N_{Re,drop}^{1/2} N_{Sc,c}^{1/2}$	[E] Used as an arithmetic concentration difference. Low σ . $N_{Re,drop} = \frac{d_p v_s \rho_c}{\mu_c}$	[151] p. 407
N. 5-25-L, circulating swarm of drops	$k_{L,c} = 0.725 \left(\frac{\rho_c}{M_c} \right)_{av} N_{Re,drop}^{-0.43} N_{Sc,c}^{-0.58} v_s (1 - \phi_d)$	[E] Used as an arithmetic concentration difference. Low σ , disperse-phase holdup of drop swarm. ϕ_d = volume fraction dispersed phase.	[151] p. 407 [154] p. 436
O. Liquid drops in immiscible liquid, free rise or fall, discontinuous phase coefficient, oscillating drops	$N_{Sh} = \frac{k_{L,d,osc} d_p}{D_d}$ $= 0.32 \left(\frac{\rho_d}{M_d} \right)_{av} \left(\frac{4D_d t}{d_p^2} \right)^{-0.14} N_{Re,drop}^{0.68} \left(\frac{\sigma^3 g^3 \rho_c^2}{g \mu_c^4 \Delta \rho} \right)^{0.10}$	[E] Used with a log mean mole fraction difference. Based on ends of extraction column. $N_{Re,drop} = \frac{d_p v_s \rho_c}{\mu_c}$ d_p = diameter of sphere with volume of drop. Average absolute deviation from data, 10.5%. $411 \leq N_{Re} \leq 3114$ Low interfacial tension (3.5–5.8 dynes), $\mu_c < 1.35$ centipoise.	[151] p. 406 [154] p. 435 [155]
P. 5-25-O	$k_{L,d,osc} = \frac{0.00375 v_s}{1 + \mu_d / \mu_c}$	[T] Use with log mean concentration difference. Based on end of extraction column. No continuous phase resistance. $k_{L,d,osc}$ in cm/s, v_s = drop velocity relative to continuous phase.	[146] p. 228 [151] p. 405
Q. Single liquid drop in immiscible liquid, range rigid to fully circulating	Rigid drops: $10^4 < N_{Pe,c} < 10^6$ $N_{Sh,c,rigid} = \frac{k_c d_p}{D_c} = 2.43 + 0.774 N_{Re}^{0.5} N_{Sc}^{0.33}$ $+ 0.0103 N_{Re} N_{Sc}^{0.33}$ Circulating drops: $10 < N_{Re} < 1200$, $190 < N_{Sc} < 241,000$, $10^3 < N_{Pe,c} < 10^6$ $N_{Sh,c,fully\ circular} = \left[\frac{2}{\pi^{0.5}} \right] N_{Pe,c}^{0.5}$ Drops in intermediate range: $\frac{N_{Sh,c} - N_{Sh,c,rigid}}{N_{Sh,c,fully\ circular} - N_{Sh,c,rigid}} = 1 - \exp [-(4.18 \times 10^{-3}) N_{Pe,c}^{0.42}]$	[E] Allows for slight effect of wake.	[156] p. 58 [158]
R. Coalescing drops in immiscible liquid, discontinuous phase coefficient	$\hat{k}_{d,coal} = 0.173 \frac{d_p}{t_f} \left(\frac{\rho_d}{M_d} \right)_{av} \left(\frac{\mu_d}{\rho_d D_d} \right)^{-1.115}$ $\times \left(\frac{\Delta \rho g d_p^2}{\sigma g_c} \right)^{1.302} \left(\frac{v_s^2 t_f}{D_d} \right)^{0.146}$	[E] Used with log mean mole fraction difference. 23 data points. Average absolute deviation 25%. t_f = formation time.	[151] p. 408
S. 5-25-R, continuous phase coefficient	$\hat{k}_{c,coal} = 5.959 \times 10^{-4} \left(\frac{\rho}{M} \right)_{av}$ $\times \left(\frac{D_c}{t_f} \right)^{0.5} \left(\frac{\rho_d v_s^3}{g \mu_c} \right)^{0.332} \left(\frac{d_p^2 \rho_c \rho_d v_s^3}{\mu_d \sigma g_c} \right)^{0.525}$	[E] Used with log mean mole fraction difference. 20 data points. Average absolute deviation 22%.	[151] p. 409

TABLE 5-25 Mass-Transfer Correlations for Drops and Bubbles (Concluded)

Conditions	Correlations	Comments E = Empirical, S = Semiempirical, T = Theoretical	References*
T. Single liquid drops in gas, gas side coefficient	$\frac{\hat{k}_g M_g d_p P}{D_{\text{gas}} \rho_g} = 2 + AN_{Re,g}^{1/2} N_{Sc,g}^{1/3}$ $A = 0.552 \text{ or } 0.60.$	[E] Used for spray drying (arithmetic partial pressure difference). $N_{Re,g} = \frac{d_p \rho_g v_s}{\mu_g}$, v_s = slip velocity between drop and gas stream. Sometimes written with: $\frac{M_g P}{\rho_g} = RT$	[88] p. 489 [111] p. 388 [135]
U. Single water drop in air, liquid side coefficient	$k_L = 2 \left(\frac{D_L}{\pi t} \right)^{1/2}$, short contact times $k_L = 10 \frac{D_L}{d_p}$, long contact times	[T] Use arithmetic concentration difference. Penetration theory. t = contact time of drop. Gives plot for $k_C a$ also. Air-water system.	[111] p. 389
V. Single bubbles of gas in liquid, continuous phase coefficient, very small bubbles	$N_{sh} = \frac{k'_c d_b}{D_c} = 1.0 (N_{Re} N_{Sc})^{1/3}$	[T] Solid-sphere Eq. (see Table 5-24-B). $d_b < 0.1$ cm, k'_c is average over entire surface of bubble.	[122] p. 673 [146] p. 214
W. 5-25-V, medium to large bubbles	$N_{sh} = \frac{k'_c d_b}{D_c} = 1.13 (N_{Re} N_{Sc})^{1/2}$	[T] Use arithmetic concentration difference. Droplet equation: $d_b > 0.5$ cm.	[146] p. 231
X. 5-25-W	$N_{sh} = \frac{k'_c d_b}{D_c} = 1.13 (N_{Re} N_{Sc})^{1/2} \left[\frac{d_b}{0.45 + 0.2d_b} \right]$	[S] Use arithmetic concentration difference. Modification of above (W), $d_b > 0.5$ cm. $500 \leq N_{Re} \leq 8000$. No effect SAA for $d_p > 0.6$ cm.	[104][146] p. 231
Y. Rising small bubbles of gas in liquid, continuous phase	$N_{sh} = \frac{k'_c d_b}{D_c} = 2 + 0.31 (N_{Gr})^{1/3} N_{Sc}^{1/3}$, $d_b < 0.25$ cm	[E] Use with arithmetic concentration difference. $N_{Re} = \frac{d_b^3 \rho_C - \rho_L g}{\mu_L D_L}$ = Raleigh number Note that $N_{Re} = N_{Gr} N_{Sc}$. Valid for single bubbles or swarms. Independent of agitation as long as bubble size is constant.	[79][91] p. 451 [109] p. 119 [161] p. 156
Z. 5-25-Y, large bubbles	$N_{sh} = \frac{k'_c d_b}{D_c} = 0.42 (N_{Gr})^{1/3} N_{Sc}^{1/2}$, $d_b > 0.25$ cm $\frac{\text{Interfacial area}}{\text{volume}} = a = \frac{6 H_g}{d_b}$	[E] Use with arithmetic concentration difference. H_g = fractional gas holdup, volume gas/total volume. For large bubbles, k'_c is independent of bubble size and independent of agitation or liquid velocity. Resistance is entirely in liquid phase for most gas-liquid mass transfer.	[79][91] p. 452 [109] p. 119 [114] p. 249

See Table 5-26 for agitated systems.

*See pages 5-7 and 5-8 for references.

there is conflicting evidence concerning this exponent ($3/4$ versus $1/2$) as discussed by Yadav and Sharma [*Chem. Eng. Sci.*, **34**, 1423 (1979)].

The existing data indicate that $k_L a$ is proportional to the square root of the solute-diffusion coefficient, and since the interfacial area a does not depend on D_L , it follows that k_L is proportional to $D_L^{0.5}$. An analysis of the design variables involved indicates that k_L should be proportional to $N_{Sc}^{-0.5}$ when the Reynolds number is held constant.

It should be noted that the influence of substituting solvents of widely differing viscosities upon the interfacial area a can be very large. One therefore should be cautious about extrapolating $k_L a$ data to account for viscosity effects between different solvent systems.

Effects of High Solute Concentrations on k_C and k_L . As discussed previously, the stagnant-film model indicates that k_C should be independent of y_{BM} and k_C should be inversely proportional to y_{BM} . The data of Vivian and Behrman [*Am. Inst. Chem. Eng. J.*, **11**, 656 (1965)] for the absorption of ammonia from an inert gas strongly suggest that the film model's predicted trend is correct. This is another indication that the most appropriate rate coefficient to use is k_C and the proper driving-force term is of the form $(y - y_i)/y_{BM}$.

The use of the rate coefficient k_L and the driving force $(x_i - x)/x_{BM}$ is believed to be appropriate. For many practical situations the liquid-phase solute concentrations are low, thus making this assumption unimportant.

Influence of Chemical Reactions on k_C and k_L . When a chemical reaction occurs, the transfer rate may be influenced by the chemical reaction as well as by the purely physical processes of diffusion and convection within the two phases. Since this situation is common in gas absorption, gas absorption will be the focus of this discussion. One must consider the impacts of chemical equilibrium and reaction kinetics on the absorption rate in addition to accounting for the effects of gas solubility, diffusivity, and system hydrodynamics.

There is no sharp dividing line between pure physical absorption and absorption controlled by the rate of a chemical reaction. Most cases fall in an intermediate range in which the rate of absorption is limited both by the resistance to diffusion and by the finite velocity of the reaction. Even in these intermediate cases the equilibria between the various diffusing species involved in the reaction may affect the rate of absorption.

TABLE 5-26 Mass-Transfer Correlations for Particles, Drops, and Bubbles in Agitated Systems

Situation	Correlation	Comments E = Empirical, S = Semiempirical, T = Theoretical	References*														
<p>A. Solid particles suspended in agitated vessel containing vertical baffles, continuous phase coefficient</p>	$\frac{k'_{LT} d_p}{D} = 2 + 0.6N_{Re,T}^{1/2} N_{Sc}^{1/3}$ <p>Replace v_{slip} with v_T = terminal velocity. Calculate Stokes' law terminal velocity</p> $v_{Ts} = \frac{d_p^2(\rho_p - \rho_c)g}{18\mu_c}$ <p>and correct:</p> <table border="1" data-bbox="322 373 730 425"> <tr> <td>$\frac{N_{Re,Ts}}{v_T/v_{Ts}}$</td> <td>1</td> <td>10</td> <td>100</td> <td>1,000</td> <td>10,000</td> <td>100,000</td> </tr> <tr> <td></td> <td>0.9</td> <td>0.65</td> <td>0.37</td> <td>0.17</td> <td>0.07</td> <td>0.023</td> </tr> </table> <p>Approximate: $k'_L = 2k'_{LT}$</p>	$\frac{N_{Re,Ts}}{v_T/v_{Ts}}$	1	10	100	1,000	10,000	100,000		0.9	0.65	0.37	0.17	0.07	0.023	<p>[S] Use log mean concentration difference. Modified Frossling equation:</p> $N_{Re,Ts} = \frac{v_{Ts} d_p \rho_c}{\mu_c}$ <p>(Reynolds number based on Stokes' law.)</p> $N_{Re,T} = \frac{v_T d_p \rho_c}{\mu_c}$ <p>(terminal velocity Reynolds number.) k'_L almost independent of d_p. Harriott suggests different correction procedures. Range k'_L/k'_{LT} is 1.5 to 8.0.</p>	<p>[97][146] p. 220</p> <p>[87]</p>
$\frac{N_{Re,Ts}}{v_T/v_{Ts}}$	1	10	100	1,000	10,000	100,000											
	0.9	0.65	0.37	0.17	0.07	0.023											
<p>B. 5-26-A</p>	<p>Graphical comparisons experiments and correlations.</p>	<p>[E,S] For spheres. Includes transpiration effects and changing diameters.</p>	<p>[78][146] p. 222</p>														
<p>C. Solid, neutrally buoyant particles, continuous phase coefficient</p>	$N_{Sh} = \frac{k'_L d_p}{D} = 2 + 0.47N_{Re,p}^{0.62} N_{Sc}^{0.36} \left(\frac{d_{imp}}{d_{tank}}\right)^{0.17}$ <p>Graphical comparisons are in Ref. 109, p. 116.</p>	<p>[E] Use log mean concentration difference. Density unimportant if particles are close to neutrally buoyant. [E] E = energy dissipation rate per unit mass fluid</p> $= \frac{P g_c}{V_{tank} \rho_c}, P = \text{power}$ $N_{Re,p} = \frac{E^{1/3} d_p^{4/3}}{\nu}$ <p>Also used for drops. Geometric effect (d_{imp}/d_{tank}) is usually unimportant. Ref. 118 gives a variety of references on correlations.</p>	<p>[109] p. 115 [118] p. 132 [161] p. 523</p>														
<p>D. 5-26-C, small particles</p>	$N_{Sh} = 2 + 0.52N_{Re,p}^{0.52} N_{Sc}^{1/3}, N_{Re,p} < 1.0$	<p>[E] Terms same as above.</p>	<p>[109] p. 116</p>														
<p>E. Solid particles with significant density difference</p>	$N_{Sh} = \frac{k'_L d_p}{D} = 2 + 0.44 \left(\frac{d_p v_{slip}}{\nu}\right)^{1/2} N_{Sc}^{0.38}$	<p>[E] Use log mean concentration difference. N_{Sh} standard deviation 11.1%. v_{slip} calculated by methods given in reference.</p>	<p>[118]</p>														
<p>F. Small solid particles, gas bubbles or liquid drops, $d_p < 2.5$ mm</p>	$N_{Sh} = \frac{k'_L d_p}{D} = 2 + 0.31 \left[\frac{d_p^3 \rho_p - \rho_c }{\mu_c D}\right]^{1/3}$	<p>[E] Use log mean concentration difference. $g = 9.80665$ m/s². Second term RHS is free-fall or rise term. For large bubbles, see Table 5-25-Z.</p>	<p>[79][91] p. 451 [114] p. 249</p>														
<p>G. Highly agitated systems; solid particles, drops, and bubbles; continuous phase coefficient</p>	$k'_L N_{Sc}^{2/3} = 0.13 \left[\frac{(P/V_{tank}) \mu_c g_c}{\rho_c^2}\right]^{1/4}$	<p>[E] Use arithmetic concentration difference. Use when gravitational forces overcome by agitation. Up to 60% deviation. Correlation prediction is low (Ref. 118). (P/V_{tank}) = power dissipated by agitator per unit volume liquid.</p>	<p>[79][83] p. 231 [91] p. 452</p>														
<p>H. Liquid drops in baffled tank with flat six-blade turbine</p>	$k'_c a = 2.621 \times 10^{-3} \frac{(ND)^{1/2}}{d_{imp}} \times \phi^{0.304} \left(\frac{d_{imp}}{d_{tank}}\right)^{1.582} N_{Re}^{1.929} N_{Oh}^{1.025}$	<p>[E] Use arithmetic concentration difference. Studied for five systems.</p> $N_{Re} = d_{imp}^2 N \rho_c / \mu_c, N_{Oh} = \mu_c / (\rho_c d_{imp} \sigma)^{1/2}$ <p>ϕ = volume fraction dispersed phase. N = impeller speed (revolutions/time). For $d_{tank} = h_{tanks}$, average absolute deviation 23.8%.</p>	<p>[154] p. 437</p>														
<p>I. Liquid drops in baffled tank, low volume fraction dispersed phase</p>	$N_{Sh} = \frac{k'_L d_p}{D} = 1.237 \times 10^{-5} N_{Sc}^{1/3} N^{2/3} \times N_{Fr}^{5/12} \left(\frac{d_{imp}}{d_p}\right) \left(\frac{d_p}{D_{tank}}\right)^{1/2} \left(\frac{\rho_c d_p^2}{\sigma}\right)^{5/4} \phi^{-1/2}$ <p>Stainless steel flat six-blade turbine. Tank had four baffles. Correlation recommended for $\phi \leq 0.06$ [Ref. 156] $a = 6\phi/d_{32}$, where d_{32} is Sauter mean diameter when 33% mass transfer has occurred.</p>	<p>[E] 180 runs, 9 systems, $\phi = 0.01$. k_c is time-averaged. Use arithmetic concentration difference.</p> $N_{Re} = \left(\frac{d_{imp}^2 N_{Sc}}{\mu_c}\right), N_{Fr} = \left(\frac{d_{imp} N^2}{g}\right)$ <p>d_p = particle or drop diameter; σ = interfacial tension, N/m; ϕ = volume fraction dispersed phase; a = interfacial volume, 1/m; and $k_c \alpha D_c^{2/3}$ implies rigid drops. Negligible drop coalescence. Average absolute deviation—19.71%. Graphical comparison given by Ref. 153.</p>	<p>[153, 156] p. 78</p>														

TABLE 5-26 Mass-Transfer Correlations for Particles, Drops, and Bubbles in Agitated Systems (Concluded)

Situation	Correlation	Comments E = Empirical, S = Semiempirical, T = Theoretical	References*
J. Gas bubble swarms in sparged tank reactors	$k'_L a \left(\frac{v}{g^2} \right)^{1/3} = C \left[\frac{P/V_L}{\rho(vg^4)^{1/3}} \right]^a \left[\frac{q_C}{V_L} \left(\frac{v}{g^2} \right)^{1/3} \right]^b$ Rushton turbines: $C = 7.94 \times 10^{-4}$, $a = 0.62$, $b = 0.23$. Intermig impellers: $C = 5.89 \times 10^{-4}$, $a = 0.62$, $b = 0.19$.	[E] Use arithmetic concentration difference. Done for biological system, O ₂ transfer. $h_{\text{tank}}/D_{\text{tank}} = 2.1$; P = power, kW. V_L = liquid volume, m ³ . q_C = gassing rate, m ³ /s. $k'_L a = s^{-1}$. Since $a = m^3/m^3$, v = kinematic viscosity, m ² /s. Low viscosity system. Better fit claimed with q_C/V_L than with u_C (see 5-26-K to O).	[143]
K. 5-26-J	$k'_L a = 2.6 \times 10^{-2} \left(\frac{P}{V_L} \right)^{0.4} u_C^{0.5}$	[E] Use arithmetic concentration difference. Ion free water $V_L < 2.6$, u_C = superficial gas velocity in m/s. $500 < P/V_L < 10,000$. P/V_L = watts/m ³ , V_L = liquid volume, m ³ .	[115, 137]
L. 5-26-J	$k'_L a = 2.0 \times 10^{-3} \left(\frac{P}{V_L} \right)^{0.7} u_C^{0.2}$	[E] Use arithmetic concentration difference. Water with ions. $0.002 < V_L < 4.4$, $500 < P/V_L < 10,000$. Same definitions as 5-26-J.	[115, 117]
M. 5-26-J, baffled tank with standard blade Rushton impeller	$k'_L a = 93.37 \left(\frac{P}{V_L} \right)^{0.76} u_C^{0.45}$	[E] Air-water. Same definitions as 5-26-J. $0.005 < u_C < 0.025$, $3.83 < N < 8.33$, $400 < P/V_L < 7000$. $h = D_{\text{tank}} = 0.305$ or 0.610 m. V_G = gas volume, m ³ , N = stirrer speed, rpm. Method assumes perfect liquid mixing.	[92, 115]
N. 5-26-M	$k'_L a \frac{d_{\text{imp}}^2}{D} = 7.57 \left[\frac{\mu_{\text{eff}}}{\rho D} \right]^{0.5} \left[\frac{\mu_C}{\mu_{\text{eff}}} \right]^{0.694}$ $\times \left[\frac{d_{\text{imp}}^2 N \rho_L}{\mu_{\text{eff}}} \right]^{1.11} \left(\frac{u_C d}{\sigma} \right)^{0.447}$ $d_{\text{imp}} = \text{impeller diameter, m; } D = \text{diffusivity, m}^2/\text{s}$	[E] Use arithmetic concentration difference. CO ₂ into aqueous carboxyl polymethylene. Same definitions as 5-26-M. μ_{eff} = effective viscosity from power law model, Pa·s. σ = surface tension liquid, N/m.	[115, 129]
O. 5-26-M, bubbles	$\frac{k'_L a d_{\text{imp}}^2}{D} = 0.060 \left(\frac{d_{\text{imp}}^2 N \rho}{\mu_{\text{eff}}} \right) \left(\frac{d_{\text{imp}}^2 N^2}{g} \right)^{0.19} \left(\frac{\mu_{\text{eff}} u_C}{\sigma} \right)^{0.6}$	[E] Use arithmetic concentration difference. O ₂ into aqueous glycerol solutions. O ₂ into aqueous millet jelly solutions. Same definitions as 5-26-M.	[115, 167]
P. Gas bubble swarm in sparged stirred tank reactor with solids present	$\frac{k'_L a}{(k'_L a)_0} = 1 - 3.54(\epsilon_s - 0.03)$ $300 \leq P/V_{\pi} < 10,000 \text{ W/m}^3, 0.03 \leq \epsilon_s \leq 0.12$ $0.34 \leq u_C \leq 4.2 \text{ cm/s}, 5 < \mu_L < 75 \text{ Pa}\cdot\text{s}$	[E] Use arithmetic concentration difference. Solids are glass beads, $d_p = 320 \mu\text{m}$. ϵ_s = solids holdup m ³ /m ³ liquid, $(k'_L a)_0$ = mass transfer in absence of solids. Ionic salt solution—noncoalescing.	[71, 144]
Q. 5-26-P	$\frac{k'_L a}{(k'_L a)_0} = 1 - \epsilon_s$	[E] Use arithmetic concentration difference. Variety of solids, $d_p > 150 \mu\text{m}$ (glass, amberlite, polypropylene). Tap water. Slope very different than item P. Coalescence may have occurred.	[71, 112]

See also Table 5-25.

*See pages 5-7 and 5-8 for references.

The gas-phase rate coefficient \hat{k}_C is not affected by the fact that a chemical reaction is taking place in the liquid phase. If the liquid-phase chemical reaction is extremely fast and irreversible, the rate of absorption may be governed completely by the resistance to diffusion in the gas phase. In this case the absorption rate may be estimated by knowing only the gas-phase rate coefficient \hat{k}_C or else the height of one gas-phase transfer unit $H_G = G_M/(\hat{k}_C A)$.

It should be noted that the highest possible absorption rates will occur under conditions in which the liquid-phase resistance is negligible and the equilibrium back pressure of the gas over the solvent is zero. Such situations would exist, for instance, for NH₃ absorption into an acid solution, for SO₂ absorption into an alkali solution, for vaporization of water into air, and for H₂S absorption from a dilute-gas stream into a strong alkali solution, provided there is a large excess of reagent in solution to consume all the dissolved gas. This is known as the gas-phase mass-transfer limited condition, when both the liquid-phase resistance and the back pressure of the gas equal zero. Even when the reaction is sufficiently reversible to allow a small back pres-

sure, the absorption may be gas-phase-controlled, and the values of \hat{k}_C and H_G that would apply to a physical-absorption process will govern the rate.

The liquid-phase rate coefficient \hat{k}_L is strongly affected by fast chemical reactions and generally increases with increasing reaction rate. Indeed, the condition for zero liquid-phase resistance ($m\hat{k}_L$) implies that either the equilibrium back pressure is negligible, or that \hat{k}_L is very large, or both. Frequently, even though reaction consumes the solute as it is dissolving, thereby enhancing both the mass-transfer coefficient and the driving force for absorption, the reaction rate is slow enough that the liquid-phase resistance must be taken into account. This may be due either to an insufficient supply of a second reagent or to an inherently slow chemical reaction.

In any event the value of \hat{k}_L in the presence of a chemical reaction normally is larger than the value found when only physical absorption occurs, \hat{k}_L^0 . This has led to the presentation of data on the effects of chemical reaction in terms of the "reaction factor" or "enhancement factor" defined as

TABLE 5-27 Mass Transfer Correlations for Fixed and Fluidized Beds

Transfer is to or from particles.

Situation	Correlation	Comments E = Empirical, S = Semiempirical, T = Theoretical	References°						
<p>A. Heat or mass transfer in packed bed for gases and liquids</p> <p>(shape factor, Ψ)</p>	$j_D = j_H = 0.91\Psi N_{Re}^{-0.51}, 0.01 < N_{Re} < 50$ <p>Equivalent $N_{Sh} = 0.91\Psi N_{Re}^{0.49} N_{Sc}^{1/3}$</p> $j_D = j_H = 0.61\Psi N_{Re}^{-0.41}, 50 < N_{Re} < 1000$ <p>Equivalent $N_{Sh} = 0.61\Psi N_{Re}^{0.59} N_{Sc}^{1/3}$</p> <table border="1" style="margin-left: auto; margin-right: auto;"> <tr> <td style="padding: 5px;">particle</td> <td style="padding: 5px;">sphere</td> <td style="padding: 5px;">cylinder</td> </tr> <tr> <td style="padding: 5px; text-align: center;">1.00</td> <td style="padding: 5px; text-align: center;">0.91</td> <td style="padding: 5px; text-align: center;">0.81</td> </tr> </table>	particle	sphere	cylinder	1.00	0.91	0.81	<p>[E] Different constants and shape factors reported in other references. Evaluate terms at film temperature or composition.</p> $N_{Sh} = \frac{k'd_s}{D}, j_D = \frac{N_{Sh}}{N_{Re} N_{Sc}^{1/3}}$ $N_{Re} = \frac{v_{super} \rho}{\mu \Psi a}, v_{super} = \text{superficial velocity}$ $a = \frac{\text{surface area}}{\text{volume}} = 6(1 - \epsilon)/d_p$ <p>For spheres, d_p = diameter. For nonspherical: $d_p = 0.567 \sqrt{\text{Part. Surf. Area}}$ Results are from too-short beds—use with caution.</p>	<p>[100] p. 194 [169]</p>
particle	sphere	cylinder							
1.00	0.91	0.81							
<p>B. For gases, fixed and fluidized beds, Gupta and Thodos correlation</p>	$j_H = j_D = \frac{2.06}{\epsilon N_{Re}^{0.575}}, 90 \leq N_{Re} \leq A$ <p>Equivalent:</p> $N_{Sh} = \frac{2.06}{\epsilon} N_{Re}^{0.425} N_{Sc}^{1/3}$ <p>For other shapes:</p> $\frac{\epsilon j_D}{(\epsilon j_D)_{sphere}} = 0.79 \text{ (cylinder) or } 0.71 \text{ (cube)}$ <p>Graphical results are available for N_{Re} from 1900 to 10,300.</p>	<p>[E] For spheres, $N_{Re} = \frac{v_{super} d_p \rho}{\mu}$</p> <p>$A = 2453$ [Ref. 151], $A = 4000$ [Ref. 100]. For $N_{Re} > 1900$, $j_H = 1.05j_D$. Heat transfer result is in absence of radiation.</p> $N_{Sh} = \frac{k'd_s}{D}$	<p>[95, 96]</p> <p>[100] p. 195 [151]</p>						
<p>C. For gases, for fixed beds, Petrovic and Thodos correlation</p>	$N_{Sh} = \frac{0.357}{\epsilon} N_{Re}^{0.641} N_{Sc}^{1/3}$	<p>[E] Packed spheres, deep beds, $3 < N_{Re} < 900$ can be extrapolated to $N_{Re} < 2000$. Corrected for axial dispersion with axial Peclet number = 2.0. Prediction is low at low N_{Re}. N_{Re} defined as in 5-27-A and B.</p>	<p>[130][141] p. 214 [163]</p>						
<p>D. For gases and liquids, fixed and fluidized beds</p>	$j_D = \frac{0.4548}{\epsilon N_{Re}^{0.4069}}, 10 \leq N_{Re} \leq 2000$ $j_D = \frac{N_{Sh}}{N_{Re} N_{Sc}^{1/3}}, N_{Sh} = \frac{k'd_s}{D}$	<p>[E] Packed spheres, deep bed. Average deviation $\pm 20\%$, $N_{Re} = d_p v_{super} \rho / \mu$. Can use for fluidized beds. $10 \leq N_{Re} \leq 4000$.</p>	<p>[85][91] p. 447</p>						
<p>E. For gases, fixed beds</p>	$j_D = \frac{0.499}{\epsilon N_{Re}^{0.382}}$	<p>[E] Data on sublimation of naphthalene spheres dispersed in inert beads. $0.1 < N_{Re} < 100$, $N_{Sc} = 2.57$. Correlation coefficient = 0.978.</p>	<p>[101]</p>						
<p>F. For liquids, fixed bed, Wilson and Geankoplis correlation</p>	$j_D = \frac{1.09}{\epsilon N_{Re}^{2/3}}, 0.0016 < N_{Re} < 55$ <p>$165 \leq N_{Sc} \leq 70,600$, $0.35 < \epsilon < 0.75$</p> <p>Equivalent:</p> $N_{Sh} = \frac{1.09}{\epsilon} N_{Re}^{1/3} N_{Sc}^{1/3}$ $j_D = \frac{0.25}{\epsilon N_{Re}^{0.31}}, 55 < N_{Re} < 1500, 165 \leq N_{Sc} \leq 10,690$ <p>Equivalent:</p> $N_{Sh} = \frac{0.25}{\epsilon} N_{Re}^{0.69} N_{Sc}^{1/3}$	<p>[E] Beds of spheres,</p> $N_{Re} = \frac{d_p v_{super} \rho}{\mu}$ <p>Deep beds.</p> $N_{Sh} = \frac{k'd_s}{D}$	<p>[91] p. 448</p> <p>[100] p. 195</p> <p>[151] p. 287 [166]</p>						

TABLE 5-27 Mass Transfer Correlations for Fixed and Fluidized Beds (Continued)

Situation	Correlation	Comments E = Empirical, S = Semiempirical, T = Theoretical	References*												
G. For liquids, fixed beds, Ohashi et al. correlation	$N_{Sh} = \frac{k'd_s}{D} = 2 + 0.51 \left(\frac{E^{1/3} d_p^{4/3} \rho}{\mu} \right)^{0.60} N_{Sc}^{1/3}$ <p>E = Energy dissipation rate per unit mass of fluid</p> $= 50(1 - \epsilon) \epsilon^2 C_{D0} \left(\frac{v_r^3}{d_p} \right), \text{ m}^2/\text{s}^3$ $= \left[\frac{50(1 - \epsilon) C_D}{\epsilon} \right] \left(\frac{v_{super}^3}{d_p} \right)$ <p>General form:</p> $N_{Sh} = 2 + K \left(\frac{E^{1/3} D_p^{4/3} \rho}{\mu} \right)^\alpha N_{Sc}^\beta$ <p>applies to single particles, packed beds, two-phase tube flow, suspended bubble columns, and stirred tanks with different definitions of E.</p>	<p>[S] Correlates large amount of published data. Compares number of correlations, v_r = relative velocity, m/s. In packed bed, $v_r = v_{super}/\epsilon$.</p> <p>C_{D0} = single particle drag coefficient at v_{super} calculated from $C_{D0} = AN_{Re}^{-m}$.</p> <table border="1" data-bbox="809 442 1138 529"> <thead> <tr> <th>N_{Re}</th> <th>A</th> <th>m</th> </tr> </thead> <tbody> <tr> <td>0 to 5.8</td> <td>24</td> <td>1.0</td> </tr> <tr> <td>5.8 to 500</td> <td>10</td> <td>0.5</td> </tr> <tr> <td>>500</td> <td>0.44</td> <td>0</td> </tr> </tbody> </table> <p>For packed bed: $0.001 < N_{Re} < 1000$ $505 < N_{Sc} < 70600$ $0.2 < \frac{E^{1/3} d_p^{4/3} \rho}{\mu} < 4600$</p> <p>Compares different situations versus general correlation. See also 5-24-F.</p>	N_{Re}	A	m	0 to 5.8	24	1.0	5.8 to 500	10	0.5	>500	0.44	0	[125]
N_{Re}	A	m													
0 to 5.8	24	1.0													
5.8 to 500	10	0.5													
>500	0.44	0													
H. For liquids, fixed and fluidized beds	$\epsilon j_D = \frac{1.1068}{N_{Re}^{0.72}}, 1.0 < N_{Re} \leq 10$ $\epsilon j_D = \frac{N_{Sh}}{N_{Re} N_{Sc}}, N_{Sh} = \frac{k'd_s}{D}$	<p>[E] Spheres:</p> $N_{Re} = \frac{d_p v_{super} \rho}{\mu}$	[84][91] p. 448												
I. For gases and liquids, fixed and fluidized beds, Dwivedi and Upadhyay correlation	$\epsilon j_D = \frac{0.765}{N_{Re}^{0.82}} + \frac{0.365}{N_{Re}^{0.386}}$ <p>Gases: $10 \leq N_{Re} \leq 15,000$. Liquids: $0.01 \leq N_{Re} \leq 15,000$.</p>	<p>[E] Deep beds of spheres,</p> $j_D = \frac{N_{Sh}}{N_{Re} N_{Sc}^{1/3}}$ $N_{Re} = \frac{d_p v_{super} \rho}{\mu}, N_{Sh} = \frac{k'd_s}{D}$ <p>Based on 20 gas studies and 17 liquid studies. Recommended instead of 5-27-D or F.</p>	[84][100] p. 196												
J. For gases and liquids, fixed bed	$j_D = 1.17 N_{Re}^{-0.415}, 10 \leq N_{Re} \leq 2500$ $j_D = \frac{k'}{v_{ac}} \frac{p_{BM}}{P} N_{Sc}^{2/3}$ <p>Comparison with other results are shown.</p>	<p>[E] Spheres:</p> $N_{Re} = \frac{d_p v_{super} \rho}{\mu}$ <p>Variation in packing that changes ϵ not allowed for. Extensive data referenced. $0.5 < N_{Sc} < 15,000$.</p>	[146] p. 241												
K. For liquids, fixed and fluidized beds, Rahman and Streat correlation	$N_{Sh} = \frac{0.86}{\epsilon} N_{Re} N_{Sc}^{1/3}, 2 \leq N_{Re} \leq 25$	<p>[E] Can be extrapolated to $N_{Re} = 2000$. $N_{Re} = d_p v_{super} \rho / \mu$. Done for neutralization of ion exchange resin.</p>	[134]												
L. For liquids and gases, Ranz and Marshall correlation	$N_{Sh} = \frac{k'd}{D} = 2.0 + 0.6 N_{Sc}^{1/3} N_{Re}^{1/2}$ $N_{Re} = \frac{d_p v_{super} \rho}{\mu}$	<p>[E] Based on freely falling, evaporating spheres (see 5-24-C). Has been applied to packed beds. Prediction is low compared to experimental data for packed beds. Limit of 2.0 at low N_{Re} is too high. Not corrected for axial dispersion.</p>	[135][141] p. 214 [163][168] p. 106												
M. For liquids and gases, Wakao and Funazkri correlation	$N_{Sh} = 2.0 + 1.1 N_{Sc}^{1/2} N_{Re}^{0.6}, 3 < N_{Re} < 10,000$ $N_{Sh} = \frac{k'_{film} d_p}{D} t$ <p>Graphical comparison with data shown by Refs. 141, p. 215, and 163.</p>	<p>[E] $N_{Re} = \frac{\rho_f v_{super} \rho}{\mu}$</p> <p>Correlate 20 gas studies and 16 liquid studies. Corrected for axial dispersion with:</p> $\frac{\epsilon D_{axial}}{D} = 10 + 0.5 N_{Sc} N_{Re}$ <p>D_{axial} is axial dispersion coefficient.</p>	[141] p. 214 [163] [165] p. 376 [168] p. 106												

TABLE 5-27 Mass Transfer Correlations for Fixed and Fluidized Beds (Concluded)

Situation	Correlation	Comments E = Empirical, S = Semiempirical, T = Theoretical	References ^o
N. Liquid fluidized beds	$N_{Sh} = \frac{2\xi/\epsilon^m + \left[\frac{(2\xi/\epsilon^m)(1-\epsilon)^{1/2}}{[1-(1-\epsilon)^{1/3}]^2} - 2 \right] \tan h(\xi/\epsilon^m)}{\frac{\xi/\epsilon^m}{1-(1-\epsilon)^{1/2}} - \tan h(\xi/\epsilon^m)}$ <p>where</p> $\xi = \left[\frac{1}{(1-\epsilon)^{1/3}} - 1 \right] \frac{\alpha}{2} N_{Sc}^{1/3} N_{Re}^{1/2}$ <p>This simplifies to:</p> $N_{Sh} = \frac{\epsilon^{1-2m}}{(1-\epsilon)^{1/3}} \left[\frac{1}{(1-\epsilon)^{1/3}} - 1 \right] \frac{\alpha^2}{2} N_{Re} N_{Sc}^{2/3} \quad (N_{Re} < 0.1)$	<p>[S] Modification of theory to fit experimental data. For spheres, $m = 1$, $N_{Re} > 2$.</p> $N_{Sh} = \frac{k'_L d_p}{D} \quad N_{Re} = \frac{V_{super} d_p \rho}{\mu}$ <p>$m = 1$ for $N_{Re} > 2$; $m = 0.5$ for $N_{Re} < 1.0$; $\epsilon =$ voidage; $\alpha =$ const. Best fit data is $\alpha = 0.7$. Comparison of theory and experimental ion exchange results in Ref. 113.</p>	[113, 123, 138]
O. Liquid fluidized beds	$N_{Sh} = 0.250 N_{Re}^{0.023} N_{Ga}^{0.306} \left(\frac{\rho_s - \rho}{\rho} \right)^{0.282} N_{Sc}^{0.410} \quad (\epsilon < 0.85)$ $N_{Sh} = 0.304 N_{Re}^{-0.057} N_{Ga}^{0.332} \left(\frac{\rho_s - \rho}{\rho} \right)^{0.297} N_{Sc}^{0.404} \quad (\epsilon > 0.85)$ <p>This can be simplified (with slight loss in accuracy at high ϵ) to</p> $N_{Sh} = 0.245 N_{Ga}^{0.323} \left(\frac{\rho_s - \rho}{\rho} \right)^{0.300} N_{Sc}^{0.400}$	<p>[E] Correlate amount of data from literature. Compare large number of published correlations.</p> $N_{Sh} = \frac{k'_L d_p}{D}, N_{Re} = \frac{d_p \rho v_{super}}{\mu}$ $N_{Ga} = \frac{d_p^3 \rho^2 g}{\mu^2}, N_{Sc} = \frac{\mu}{\rho D}$ <p>$1.6 < N_{Re} < 1320, 2470 < N_{Ga} < 4.42 \times 10^6$</p> <p>$0.27 < \frac{\rho_s - \rho}{\rho} < 1.114, 305 < N_{Sc} < 1595$</p> <p>Predicts very little dependence of N_{Sh} on velocity.</p>	[160]
P. Liquid film flowing over solid particles with air present, trickle bed reactors, fixed bed	$N_{Sh} = \frac{k_L}{aD} = 1.8 N_{Re}^{1/2} N_{Sc}^{1/3}, 0.013 < N_{Re} < 12.6$ <p>two-phases, liquid trickle, no forced flow of gas. $N_{Sh} = 0.8 N_{Re}^{1/2} N_{Sc}^{1/3}$, one-phase, liquid only.</p>	<p>[E] $N_{Re} = \frac{L}{a\mu}$</p> <p>$L =$ superficial liquid flow rate, $\text{kg/m}^2\text{s}$. $a =$ surface area/col. volume, m^2/m^3. Irregular granules of benzoic acid, $0.29 \leq d_p \leq 1.45$ cm.</p>	[142]
Q. Supercritical fluids in packed bed	$\frac{N_{Sh}}{(N_{Sc} N_{Gr})^{1/4}} = 0.1813 \left(\frac{N_{Re}^2 N_{Sc}^{1/3}}{N_{Gr}} \right)^{1/4} (N_{Re}^{1/2} N_{Sc}^{1/3})^{3/4}$ $+ 1.2149 \left[\left(\frac{N_{Re}^2 N_{Sc}^{1/3}}{N_{Gr}} \right)^{3/4} - 0.01649 \right]^{1/3}$	[E] Natural and forced convection, $4 < N_{Re} < 135$.	[119]
R. Supercritical fluids in packed bed	$\frac{N_{Sh}}{(N_{Sc} N_{Gr})^{1/4}} = 0.5265 \left(\frac{N_{Re}^{1/2} N_{Sc}^{1/3}}{(N_{Sc} N_{Gr})^{1/4}} \right)^{1.6808}$ $+ 2.48 \left[\left(\frac{N_{Re}^2 N_{Sc}^{1/3}}{N_{Gr}} \right)^{0.6439} - 0.8768 \right]^{1.553}$	[E] Natural and forced convection. $0.3 < N_{Re} < 135$. Improvement of correlation in Q.	[116]

NOTE: For $N_{Re} < 3$ convective contributions which are not included may become important. Use with logarithmic concentration difference (integrated form) or with arithmetic concentration difference (differential form).

^oSee pages 5-7 and 5-8 for references.

$$\phi = \hat{k}_L / \hat{k}_L^0 \geq 1 \quad (5-300)$$

where $\hat{k}_L =$ mass-transfer coefficient with reaction and $\hat{k}_L^0 =$ mass-transfer coefficient for pure physical absorption.

It is important to understand that when chemical reactions are involved, this definition of \hat{k}_L is based on the driving force defined as the difference between the concentration of unreacted solute gas at the interface and in the bulk of the liquid. A coefficient based on the total of both unreacted and reacted gas could have values smaller than the physical-absorption mass-transfer coefficient \hat{k}_L^0 .

When liquid-phase resistance is important, particular care should be taken in employing any given set of experimental data to ensure that the equilibrium data used conform with those employed by the original author in calculating values of \hat{k}_L or H_L . Extrapolation to widely different concentration ranges or operating conditions should

be made with caution, since the mass-transfer coefficient \hat{k}_L may vary in an unexpected fashion, owing to changes in the apparent chemical-reaction mechanism.

Generalized prediction methods for \hat{k}_L and H_L do not apply when chemical reaction occurs in the liquid phase, and therefore one must use actual operating data for the particular system in question. A discussion of the various factors to consider in designing gas absorbers and strippers when chemical reactions are involved is presented by Astarita, Savage, and Bisio, *Gas Treating with Chemical Solvents*, Wiley (1983) and by Kohl and Riesenfeld, *Gas Purification*, 4th ed., Gulf (1985).

Effective Interfacial Mass-Transfer Area a In a packed tower of constant cross-sectional area S the differential change in solute flow per unit time is given by

$$-d(G_M S y) = N_A a dV = N_A a S dh \quad (5-301)$$

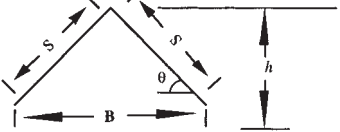
TABLE 5-28 Mass Transfer Correlations for Packed Two-Phase Contactors—Absorption, Distillation, Cooling Towers, and Extractors (Packing Is Inert)

Situation	Correlations	Comments E = Empirical, S = Semiempirical, T = Theoretical	References*																																																																																								
<p>A. Absorption, counter-current, liquid-phase coefficient H_L, Sherwood and Holloway correlation for random packings</p>	$H_L = a_L \left(\frac{L}{\mu_L} \right)^n N_{Sc,L}^{0.5}, L = \text{lb/hr ft}^2$ $H_L = \frac{L_M}{\hat{k}_L a}$ $L_M = \text{lbmoles/hr ft}^2, \hat{k}_L = \text{lbmoles/hr ft}^2, a = \text{ft}^2/\text{ft}^3, \mu_L \text{ in lb/(hr ft)}$ <hr/> <p style="text-align: center;">Ranges for 5-28-B (G and L)</p> <table border="1" style="width: 100%; border-collapse: collapse;"> <thead> <tr> <th>Packing</th> <th>a_C</th> <th>b</th> <th>c</th> <th>G</th> <th>L</th> <th>a_L</th> <th>n</th> </tr> </thead> <tbody> <tr> <td colspan="8" style="text-align: center;">Raschig rings</td> </tr> <tr> <td>3/8 inch</td> <td>2.32</td> <td>0.45</td> <td>0.47</td> <td>200–500</td> <td>500–1500</td> <td>0.00182</td> <td>0.46</td> </tr> <tr> <td>1</td> <td>7.00</td> <td>0.39</td> <td>0.58</td> <td>200–800</td> <td>400–500</td> <td>0.010</td> <td>0.22</td> </tr> <tr> <td>1</td> <td>6.41</td> <td>0.32</td> <td>0.51</td> <td>200–600</td> <td>500–4500</td> <td>—</td> <td>—</td> </tr> <tr> <td>2</td> <td>3.82</td> <td>0.41</td> <td>0.45</td> <td>200–800</td> <td>500–4500</td> <td>0.0125</td> <td>0.22</td> </tr> <tr> <td colspan="8" style="text-align: center;">Bertl saddles</td> </tr> <tr> <td>1/2 inch</td> <td>32.4</td> <td>0.30</td> <td>0.74</td> <td>200–700</td> <td>500–1500</td> <td>0.0067</td> <td>0.28</td> </tr> <tr> <td>1/2</td> <td>0.811</td> <td>0.30</td> <td>0.24</td> <td>200–800</td> <td>400–4500</td> <td>—</td> <td>—</td> </tr> <tr> <td>1</td> <td>1.97</td> <td>0.36</td> <td>0.40</td> <td>200–800</td> <td>400–4500</td> <td>0.0059</td> <td>0.28</td> </tr> <tr> <td>1.5</td> <td>5.05</td> <td>0.32</td> <td>0.45</td> <td>200–1000</td> <td>400–4500</td> <td>0.0062</td> <td>0.28</td> </tr> </tbody> </table> <p>Range for 5-28-A is $400 < L < 15,000 \text{ lb/hr ft}^2$</p>	Packing	a_C	b	c	G	L	a_L	n	Raschig rings								3/8 inch	2.32	0.45	0.47	200–500	500–1500	0.00182	0.46	1	7.00	0.39	0.58	200–800	400–500	0.010	0.22	1	6.41	0.32	0.51	200–600	500–4500	—	—	2	3.82	0.41	0.45	200–800	500–4500	0.0125	0.22	Bertl saddles								1/2 inch	32.4	0.30	0.74	200–700	500–1500	0.0067	0.28	1/2	0.811	0.30	0.24	200–800	400–4500	—	—	1	1.97	0.36	0.40	200–800	400–4500	0.0059	0.28	1.5	5.05	0.32	0.45	200–1000	400–4500	0.0062	0.28	<p>[E] From experiments on desorption of sparingly soluble gases from water. Graphs [Ref. 146], p. 606. Equation is dimensional. A typical value of n is 0.3 [Ref. 91] p. 633 has constants in kg, m, and s units for use in 5-28-A and B with \hat{k}_C in kgmole/s m^2 and \hat{k}_L in kgmole/s m^2 (kgmole/m^3). Constants for other packings are given by Refs. 121 p. 187 and 161, p. 239.</p>	<p>[121] p. 187 [122] p. 714 [146] p. 606 [164] p. 660</p>
Packing	a_C	b	c	G	L	a_L	n																																																																																				
Raschig rings																																																																																											
3/8 inch	2.32	0.45	0.47	200–500	500–1500	0.00182	0.46																																																																																				
1	7.00	0.39	0.58	200–800	400–500	0.010	0.22																																																																																				
1	6.41	0.32	0.51	200–600	500–4500	—	—																																																																																				
2	3.82	0.41	0.45	200–800	500–4500	0.0125	0.22																																																																																				
Bertl saddles																																																																																											
1/2 inch	32.4	0.30	0.74	200–700	500–1500	0.0067	0.28																																																																																				
1/2	0.811	0.30	0.24	200–800	400–4500	—	—																																																																																				
1	1.97	0.36	0.40	200–800	400–4500	0.0059	0.28																																																																																				
1.5	5.05	0.32	0.45	200–1000	400–4500	0.0062	0.28																																																																																				
<p>B. Absorption counter-current, gas-phase coefficient H_C, for random packing</p>	$H_C = \frac{a_C(G)^b N_{Sc,G}^{0.5}}{(L)^c}, G = \text{lb/hr ft}^2$ $H_C = \frac{G_M}{\hat{k}_C a}$ $G_M = \text{lbmoles/hr ft}^2, \hat{k}_C = \text{lbmoles/hr ft}^2$	<p>[E] Based on ammonia-water-air data in Feller's 1941 MIT thesis. Curves: Refs. 121, p. 186 and 146 p. 607. Constants given in 5-28-A. The equation is dimensional.</p>	<p>[91] p. 633 [121] p. 189 [146] p. 607 [164] p. 660</p>																																																																																								
<p>C. Absorption, counter-current, gas-liquid individual coefficients and interfacial area, Shulman data for random packings</p>	$\frac{k_G N_{Sc,G}^{2/3}}{G_M} = 1.195 \left[\frac{d_p G}{\mu_C (1 - \epsilon_{L_0})} \right]^{-0.36}$ $\frac{\hat{k}_L d_p}{D_L} = 25.1 \left(\frac{d_p L}{\mu_L} \right)^{0.45} N_{Sc,L}^{0.5}$ <p>Interfacial area a per volume given for Raschig rings and Bertl saddles in graphical form by Refs. 78 and 121 p. 178, and in equation form by Ref. 161, p. 205. Liquid holdups are given by Refs. 161 (p. 206), 148, or 121, p. 174.</p>	<p>[E] Compared naphthalene sublimation to aqueous absorption to obtain \hat{k}_C, a, and \hat{k}_L separately. Raschig rings and Bertl saddles. d_p = diameter of sphere with same surface area as packing piece. ϵ_{L_0} = operating void space = $\epsilon - \phi_{L_0}$, where ϵ = void fraction w/o liquid, and ϕ_{L_0} = liquid holdup. Same definition as 5-28-A and B. Onda et al. correlation (5-28-D) is preferred. $G = \rho_C v_{\text{super, gas}}$</p>	<p>[76][123] p. 174, 186 [151, 158] [161] p. 203</p>																																																																																								
<p>D. Absorption and distillation, counter-current, gas and liquid individual coefficients and wetted surface area, Onda et al. correlation for random packings</p>	$\frac{k'_C RT}{a_p D_C} = A \left(\frac{G}{a_p \mu_C} \right)^{0.7} N_{Sc,G}^{1/3} (a_p d_p')^{-2.0}$ <p>$A = 5.23$ for packing $\geq 1/2$ inch (0.012 m) $A = 2.0$ for packing $< 1/2$ inch (0.012 m) $k'_C = \text{lbmoles/hr ft}^2 \text{ atm} [\text{kg mol/s m}^2 (\text{N/m}^2)]$</p> $k'_L \left(\frac{\rho_L}{\mu_L g} \right)^{1/3} = 0.0051 \left(\frac{L}{a_w \mu_L} \right)^{2/3} N_{Sc,L}^{-1/2} (a_p d_p')^{0.4}$ $k'_L = \text{lbmoles/hr ft}^2 (\text{lbmoles/ft}^3) [\text{kgmoles/s m}^2 (\text{kgmoles/m}^3)]$ $\frac{a_w}{a_p} = 1 - \exp \left\{ \begin{aligned} & \left[-1.45 \left(\frac{\sigma_c}{\sigma} \right)^{0.75} \left(\frac{L}{a_p \mu_L} \right)^{0.1} \right] \\ & \times \left[\left(\frac{L^2 a_p}{\rho_L^2 g} \right)^{-0.05} \left(\frac{L}{\rho_L \sigma a_p} \right)^{0.2} \right] \end{aligned} \right\}$ <p>Critical surface tensions, $\sigma_C = 61$ (ceramic), 75 (steel), 33 (polyethylene), 40 (PVC), 56 (carbon) dynes/cm.</p> <p>Graphical comparison with data in Ref. 126.</p>	<p>[E] Gas absorption and desorption from water and organics plus vaporization of pure liquids for Raschig rings, saddles, spheres, and rods. d_p' = nominal packing size, a_p = dry packing surface area/volume. Equations are dimensionally consistent, so any set of consistent units can be used. σ = surface tension, dynes/cm.</p> <p>$4 < \frac{L}{a_w \mu_L} < 400$</p> <p>$5 < \frac{G}{a_p \mu_C} < 1000$</p> <p>Most data $\pm 20\%$ of correlation, some $\pm 50\%$.</p>	<p>[76][88] p. 399</p> <p>[111] p. 380</p> <p>[126][159] p. 355</p>																																																																																								

TABLE 5-28 Mass Transfer Correlations for Packed Two-Phase Contactors—Absorption, Distillation, Cooling Towers, and Extractors (Packing Is Inert) (Continued)

Situation	Correlations	Comments E = Empirical, S = Semiempirical, T = Theoretical	References ^o
<p>E. Distillation and absorption, counter-current, random packings, modification of Onda correlation, Bravo and Fair correlation</p>	<p>Use Onda's correlations (5-28-D) for k'_G and k'_L. Calculate:</p> $H_G = \frac{G}{k'_G a_p P M_G}, H_L = \frac{L}{k'_L a_p \rho_L}$ $H_{OG} = H_G + \lambda H_L$ <p>where</p> $\lambda = \frac{m}{L_M / G_M}$ <p>Using</p> $a_e = 0.498 a_p \left(\frac{\sigma^{0.5}}{Z^{0.4}} \right) (N_{Ca,L} N_{Re,G})^{0.392}$ <p>where</p> $N_{Re,G} = \frac{6G}{a_p \mu_G}$ $N_{Ca,L} = \frac{L \mu_L}{\rho_L \sigma_{eL}} \text{ (dimensionless)}$	<p>[E] Use's Bolles & Fair (Ref. 75) data base to determine new effective area a_e to use with Onda et al. (Ref. 126) correlation. Same definitions as 5-28-D. P = total pressure, atm; M_G = gas, molecular weight; m = local slope of equilibrium curve; L_M/G_M = slope operating line; Z = height of packing in feet. Equation for a_e is dimensional. Fit to data for effective area quite good for distillation. Good for absorption at low values of $(N_{Ca,L} \times N_{Re,G})$, but correlation is too high at higher values of $(N_{Ca,L} \times N_{Re,G})$.</p>	<p>[76]</p>
<p>F. Absorption, co-current downward flow, random packings</p>	<p>Air-oxygen-water results correlated by $k'_L a = 0.12 E_L^{0.5}$. Extended to other systems.</p> $k'_L a = 0.12 E_L^{0.5} \left(\frac{D_L}{2.4 \times 10^5} \right)^{0.5}$ $E_L = \left(\frac{\Delta p}{\Delta L} \right)_{2\text{-phase}} v_L$ $k'_L a = s^{-1}$ $D_L = \text{cm/s}$ $E_L = \text{ft, lbf/s ft}^3$ $v_L = \text{superficial liquid velocity, ft/s}$ $\frac{\Delta p}{\Delta L} = \text{pressure loss in two-phase flow} = \text{lbf/ft}^2 \text{ ft}$ $k'_G a = 2.0 + 0.91 E_G^{2/3} \text{ for NH}_3$ $E_G = \left(\frac{\Delta p}{\Delta L} \right)_{2\text{-phase}} v_g$ $v_g = \text{superficial gas velocity, ft/s}$	<p>[E] Based on oxygen transfer from water to air 77°F. Liquid film resistance controls. ($D_{\text{water}} @ 77^\circ\text{F} = 2.4 \times 10^{-5}$). Equation is dimensional. Data was for thin-walled polyethylene Raschig rings. Correlation also fit data for spheres. Fit $\pm 25\%$. See Reiss for graph.</p> <p>[E] Ammonia absorption into water from air at 70°F. Gas-film resistance controls. Thin-walled polyethylene Raschig rings and 1-inch Intalox saddles. Fit $\pm 25\%$. See Reiss for fit. Terms defined as above.</p>	<p>[136] [142] p. 217</p> <p>[136]</p>
<p>G. Absorption, stripping, distillation, counter-current, H_L, and H_G, random packings, Cornell et al. correlation, and Bolles and Fair correlation</p>	<p>For Raschig rings, Berl saddles, and spiral tie:</p> $H_L = \frac{\phi C_{\text{flood}}}{3.28} N_{Sc,L}^{0.5} \left(\frac{Z}{3.05} \right)^{0.15}$ <p>$C_{\text{flood}} = 1.0$ if below 40% flood—otherwise, use Fig. 5-28. ϕ shown in Fig. 5-29 for different packings and sizes. Range $0.02 < \phi < 0.300$.</p> $H_G = \frac{A \psi (d'_{col})^m Z^{0.33} N_{Sc,G}^{0.5}}{\left[\frac{L}{\mu_{\text{water}}} \right]^{0.16} \left(\frac{\rho_{\text{water}}}{\rho_L} \right)^{1.25} \left(\frac{\sigma_{\text{water}}}{\sigma_L} \right)^{0.8} }^n$ <p>$A = 0.017$ (rings) or 0.029 (saddles) d'_{col} = column diameter in m (if diameter > 0.6 m, use $d'_{col} = 0.6$) $m = 1.24$ (rings) or 1.11 (saddles) $n = 0.6$ (rings) or 0.5 (saddles) ψ is given in Fig. 5-30. Range: $25 < \psi < 190$ m.</p>	<p>[E] Z = packed height, m of each section with its own liquid distribution. The original work is reported in English units. Cornell et al. (Ref. 81) review early literature. Improved fit of Cornell's ϕ values given by Bolles and Fair (Refs. 74 and 75) and in Fig. 5-29.</p> <p>L = liquid rate, $\text{kg}/(\text{sm}^2)$, $\mu_{\text{water}} = 1.0 \text{ Pa} \cdot \text{s}$, $\rho_{\text{water}} = 1000 \text{ kg/m}^3$, $\sigma_{\text{water}} = 72.8 \text{ mN/m}$ (72.8 dynes/cm). H_G and H_L will vary from location to location. Design each section of packing separately.</p>	<p>[74, 75, 81] [100] p. 428 [111] p. 381 [151] p. 353 [164] p. 651</p>

TABLE 5-28 Mass Transfer Correlations for Packed Two-Phase Contactors—Absorption, Distillation, Cooling Towers, and Extractors (Packing Is Inert) (Concluded)

Situation	Correlations	Comments E = Empirical, S = Semiempirical, T = Theoretical	References*
H. Distillation and absorption. Counter-current flow. Structured packings. Gauze-type with triangular flow channels, Bravo, Rocha, and Fair correlation	Equivalent channel: $d_{eq} = Bh \left[\frac{1}{B + 2S} + \frac{1}{2S} \right]$  <p>Use modified correlation for wetted wall column (See 5-22-D)</p> $N_{Sh,v} = \frac{k'_l d_{eq}}{D_v} = 0.0338 N_{Re,v}^{0.8} N_{Sc,v}^{0.333}$ $N_{Re,v} = \frac{d_{eq} \rho_c (U_{v,eff} + U_{L,eff})}{\mu_v}$ <p>where effective velocities</p> $U_{v,eff} = \frac{U_{v,super}}{\epsilon \sin \theta}$ $U_{L,eff} = \frac{3\Gamma}{2\rho_L} \left(\frac{\rho_L^2 g}{3\mu_L \Gamma} \right)^{0.333}, \Gamma = \frac{L}{Per}$ $Per = \frac{Perimeter}{Area} = \frac{4S + 2B}{Bh}$ <p>Calculate k'_l from penetration model (use time for liquid to flow distance s).</p> $k'_l = 2(D_L U_{L,eff} / \pi S)^{1/2}$	<p>[T] Check of 132 data points showed average deviation 14.6% from theory. Johnstone and Pigford [Ref. 105] correlation (5-22-D) has exponent on N_{Re} rounded to 0.8. Assume gauze packing is completely wet. Thus, $a_{eff} = a_p$ to calculate H_G and H_L. Same approach may be used generally applicable to sheet-metal packings, but they will not be completely wet and need to estimate transfer area.</p> <p>L = liquid flux, kg/s m². G = vapor flux, kg/s m². Fit to data shown in Ref. 77.</p> $H_G = \frac{G}{k'_l a_p \rho_c}, H_L = \frac{L}{k'_l a_p \rho_L}$	[77] [87] p. 310, 326 [159] p. 356, 362
I. High-voidage packings, cooling towers, splash-grid packings	$\frac{(Ka)_H V_{tower}}{L} = 0.07 + A' N' \left(\frac{L}{G_a} \right)^{-n'}$ <p>A' and n' depend on deck type (Ref. 107), $0.060 \leq A' \leq 0.135$, $0.46 \leq n' \leq 0.62$. General form fits the graphical comparisons (Refs. 146 and 164).</p>	<p>[E] General form. G_a = lb dry air/hr ft². L = lb/h ft², N' = number of deck levels. $(Ka)_H$ = overall enthalpy transfer coefficient =</p> $\text{lb}/(\text{h})(\text{ft}^3) \left(\frac{\text{lb water}}{\text{lb dry air}} \right)$ <p>V_{tower} = tower volume, ft³/ft². If normal packings are used, use absorption mass-transfer correlations or Ref. 88, p. 452.</p>	[107][121] p. 220 [146] p. 286 [164] p. 681
J. Liquid-liquid extraction, packed towers	Use k values for drops (Table 5-25). Enhancement due to packing is at most 20%. Packing decreases drop size and increases interfacial area.	<p>[E]</p>	[156] p. 79
K. Liquid-liquid extraction in Rotating-disc contactor (RDC)	$\frac{k_{c,RDC}}{k_c} = 1.0 + 2.44 \left(\frac{N}{N_{Cr}} \right)^{2.5}$ $N_{Cr} = 7.6 \times 10^{-4} \left(\frac{\sigma}{d_{drop} \mu_c} \right) \left(\frac{H}{D_{tank}} \right)$ $\frac{k_{d,RDC}}{k_d} = 1.0 + 1.825 \left(\frac{N}{N_{Cr}} \right) \frac{H}{D_{tank}}$	<p>k_c, k_d are for drops (Table 5-25) N = impeller speed Breakage occurs when $N > N_{Cr}$. Maximum enhancement before breakage was factor of 2.0. H = compartment height, D_{tank} = tank diameter, σ = interfacial tension, N/m. Done in 0.152 and 0.600 m RDC.</p>	[70][156] p. 79
L. Liquid-liquid extraction, stirred tanks	See Table 5-26-F, G, H, and I.	<p>[E]</p>	

* See pages 5-7 and 5-8 for references.

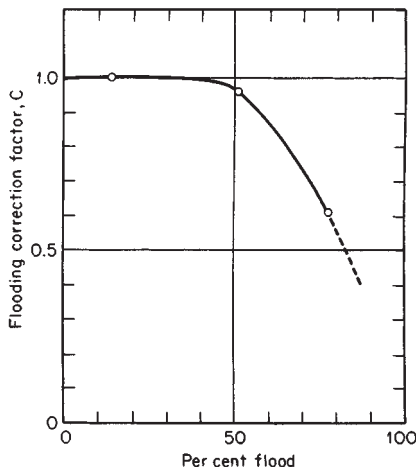


FIG. 5-28 Liquid-film correction factor (Table 5-28-C) for operation at high percent of flood. [Cornell et al., Chem. Eng. Prog., 56(8), 68 (1960).]

where a = interfacial area effective for mass transfer per unit of packed volume and V = packed volume. Owing to incomplete wetting of the packing surfaces and to the formation of areas of stagnation in the liquid film, the effective area normally is significantly less than the total external area of the packing pieces.

The effective interfacial area depends on a number of factors, as discussed in a review by Charpentier [Chem. Eng. J., 11, 161 (1976)]. Among these factors are (1) the shape and size of packing, (2) the packing material (for example, plastic generally gives smaller interfacial areas than either metal or ceramic), (3) the liquid mass velocity, and (4), for small-diameter towers, the column diameter.

Whereas the interfacial area generally increases with increasing liquid rate, it apparently is relatively independent of the superficial gas mass velocity below the flooding point. According to Charpentier's review, it appears valid to assume that the interfacial area is independent of the column height when specified in terms of unit packed volume (i.e., as a). Also, the existing data for chemically reacting gas-liquid systems (mostly aqueous electrolyte solutions) indicate that the interfacial area is independent of the chemical system. However, this situation may not hold true for systems involving large heats of reaction.

Rizzuti et al. [Chem. Eng. Sci., 36, 973 (1981)] examined the influence of solvent viscosity upon the effective interfacial area in packed columns and concluded that for the systems studied the effective interfacial area a was proportional to the kinematic viscosity raised to the 0.7 power. Thus, the hydrodynamic behavior of a packed absorber is strongly affected by viscosity effects. Surface-tension effects also are important, as expressed in the work of Onda et al. (see Table 5-28-D).

In developing correlations for the mass-transfer coefficients k_G and k_L , the various authors have assumed different but internally compatible correlations for the effective interfacial area a . It therefore would be inappropriate to mix the correlations of different authors unless it has been demonstrated that there is a valid area of overlap between them.

Volumetric Mass-Transfer Coefficients K'_{Ca} and K''_{La} Experimental determinations of the individual mass-transfer coefficients k_G and k_L and of the effective interfacial area a involve the use of extremely difficult techniques, and therefore such data are not plentiful. More often, column experimental data are reported in terms of overall volumetric coefficients, which normally are defined as follows:

$$K'_{Ca} = n_A / (h_T S p_T \Delta y_{1m}^\circ) \quad (5-302)$$

and
$$K''_{La} = n_A / (h_T S \Delta x_{1m}^\circ) \quad (5-303)$$

where K'_{Ca} = overall volumetric gas-phase mass-transfer coefficient, K''_{La} = overall volumetric liquid-phase mass-transfer coefficient, n_A =

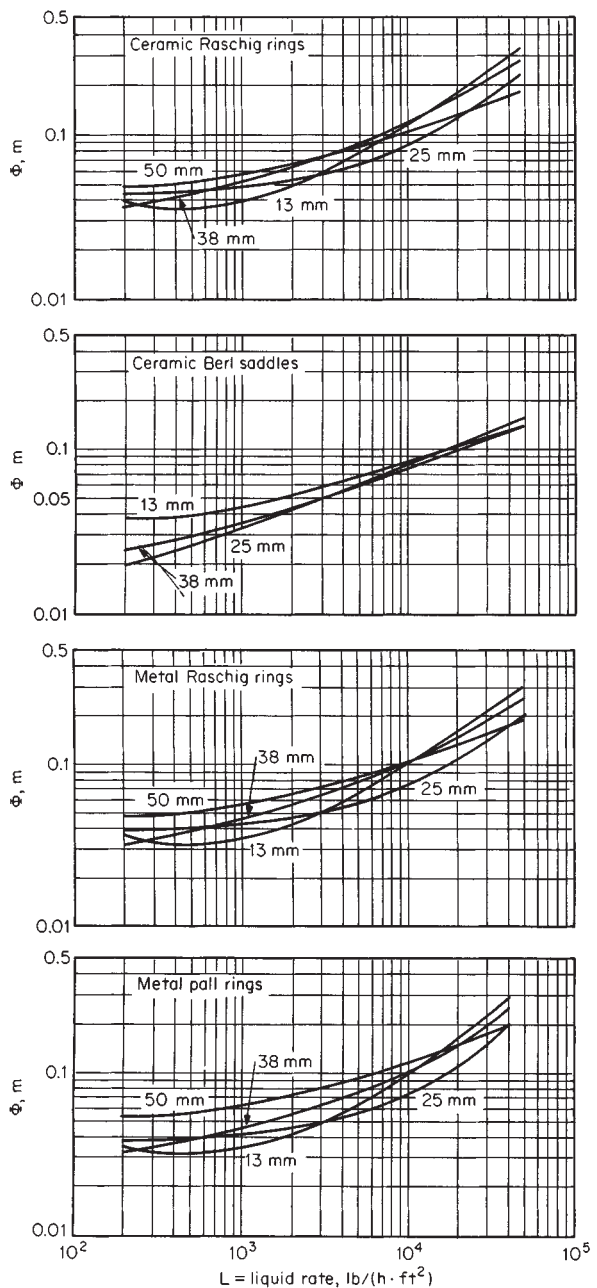


FIG. 5-29 H_1 correlation for various packings (Table 5-28-G). To convert meters to feet, multiply by 3.281; to convert pounds per hour-square foot to kilograms per second-square meter, multiply by 0.001356; and to convert millimeters to inches, multiply by 0.0394. [Bolles and Fair, Inst. Chem. Eng. Symp. Ser., no. 56, 3.3/35 (1969).]

overall rate of transfer of solute A, h_T = total packed depth in tower, S = tower cross-sectional area, p_T = total system pressure employed during the experiment, and Δx_{1m}° and Δy_{1m}° are defined as

$$\Delta y_{1m}^\circ = \frac{(y - y^\circ)_1 - (y - y^\circ)_2}{\ln [(y - y^\circ)_1 / (y - y^\circ)_2]} \quad (5-304)$$

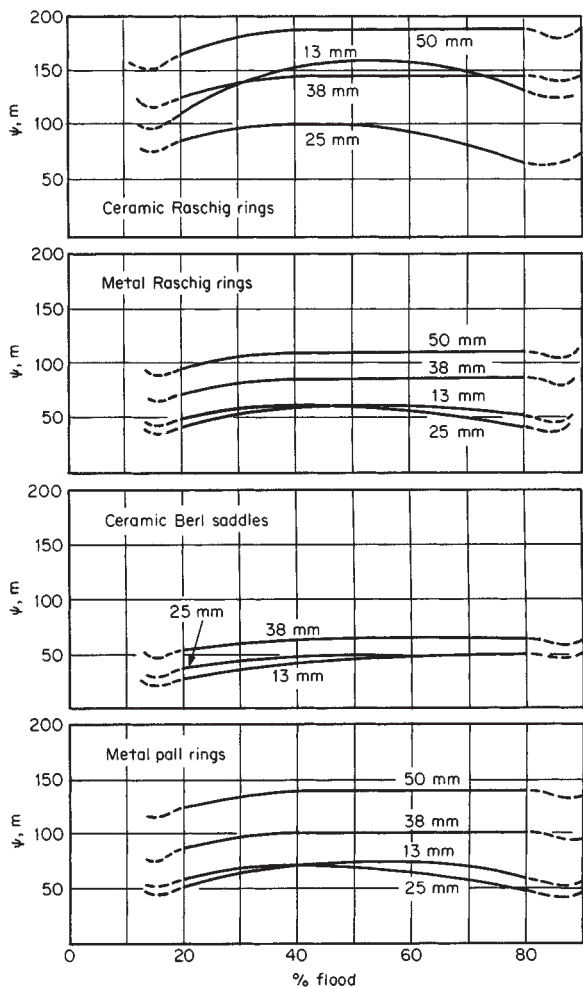


FIG. 5-30 H_g correlation for various packings (Table 5-28-G). To convert meters to feet, multiply by 3.281; to convert millimeters to inches, multiply by 0.03937. [Bolles and Fair, *Inst. Chem. Eng. Symp. Ser.*, no. 56, 3.3/35 (1979).]

and

$$\Delta x_{\text{lm}}^{\circ} = \frac{(x^{\circ} - x)_2 - (x^{\circ} - x)_1}{\ln [(x^{\circ} - x)_2 / (x^{\circ} - x)_1]} \quad (5-305)$$

where subscripts 1 and 2 refer to the bottom and top of the tower respectively.

Experimental $K'_c a$ and $K_l a$ data are available for most absorption and stripping operations of commercial interest (see Sec. 15). The solute concentrations employed in these experiments normally are very low, so that $K_l a \approx \bar{K}_l a$ and $K'_c a p_T \approx \bar{K}_c a$, where p_T is the total pressure employed in the actual experimental-test system. Unlike the individual gas-film coefficient $k_{c a}$, the overall coefficient $\bar{K}_c a$ will

vary with the total system pressure except when the liquid-phase resistance is negligible (i.e., when either $m = 0$, or $\bar{k}_{l a}$ is very large, or both).

Extrapolation of $K'_c a$ data for absorption and stripping to conditions other than those for which the original measurements were made can be extremely risky, especially in systems involving chemical reactions in the liquid phase. One therefore would be wise to restrict the use of overall volumetric mass-transfer-coefficient data to conditions not too far removed from those employed in the actual tests. The most reliable data for this purpose would be those obtained from an operating commercial unit of similar design.

Experimental values of H_{OG} and H_{OL} for a number of distillation systems of commercial interest are also readily available. Extrapolation of the data or the correlations to conditions that differ significantly from those used for the original experiments is risky. For example, pressure has a major effect on vapor density and thus can affect the hydrodynamics significantly. Changes in flow patterns affect both mass-transfer coefficients and interfacial area.

Chilton-Colburn Analogy When a fluid moves over either a liquid or a solid surface, the eddy motion that causes mass transfer also causes heat transfer and fluid friction owing to the transfer of thermal energy and momentum respectively. This close similarity among the mechanisms for the transfer of mass, heat, and momentum was brought out in the Reynolds analogy (see Table 5-23-T), which stated that the following dimensionless ratios are equal:

$$\bar{k}_c / G_M = h' / c_p G = f / 2 \quad (5-306)$$

where h' = heat-transfer coefficient, c_p = specific heat, G = mass flux, and f = friction factor.

Experimental data for mass transfer into gas streams agree approximately with Eq. (5-306) when the Schmidt number is close to unity and in smooth, straight tubes or along flat plates when the pressure drop is due entirely to skin friction against the surface. It does not, however, agree for cases involving "form" drag as well as skin friction. Also, it does not account for the mass-transfer resistance of the region of fluid near the liquid or solid boundary in which mass transfer occurs principally by molecular (as opposed to turbulent) motion.

Colburn [*Trans. Am. Inst. Chem. Eng.*, **29**, 174 (1933)] and Chilton and Colburn [*Ind. Eng. Chem.*, **26**, 1183 (1934)] showed empirically that the resistance of the laminar sublayer can be expressed by the following modification of the Reynolds analogy:

$$(\bar{k}_c / G_M) N_{\text{Sc}}^{2/3} = j_M = (h' / c_p G) N_{\text{Pr}}^{2/3} = j_H = f / 2 \quad (5-307)$$

for turbulent flow through straight tubes (see Table 5-23-U) and across plane surfaces (see Table 5-21-G), and

$$j_M = j_H \leq f / 2 \quad (5-308)$$

for turbulent flow around cylinders (see Table 5-24-I), where j_M = mass-transfer factor, j_H = heat-transfer factor, $N_{\text{Pr}} = c_p \mu / k$ = Prandtl number, and k = thermal conductivity; other symbols are as defined earlier.

On occasion one will find that heat-transfer-rate data are available for a system in which mass-transfer-rate data are not readily available. The Chilton-Colburn analogy provides a procedure for developing estimates of the mass-transfer rates based on heat-transfer data. Extrapolation of experimental j_M or j_H data obtained with gases to predict liquid systems (and vice versa) should be approached with caution, however. When pressure-drop or friction-factor data are available, one may be able to place an upper bound on the rates of heat and mass transfer, according to Eq. (5-308).